Technische Universität München

GSF-Forschungszentrum für Umwelt und Gesundheit
Institut für Entwicklungsgenetik
Abteilung Zebrafischneurogenetik

Towards a molecular understanding of midbrain-hindbrain neurogenesis and reward in zebrafish

Jovica Ninković

Vollständiger Abdruck der von der Fakultät Wissenschaftszentrum Weihstephan für Ernährung, Landnutzung und Umwelt der Technischen Universität München zur Erlangung des akademischen Grades eines

Doktors der Naturwissenschaften

genehmigten Dissertation.

Vorsitzender:	Univ.-Prof. Dr. Erwin Grill
Prüfer der Dissertation:	1. Univ.-Prof. Dr. Wolfgang Wurst
	2. Univ.-Prof. Dr. Kay H. Schneitz
	3. Univ.-Prof. Dr. Alfons Gierl

Die Dissertation wurde am 09.11.2005 bei der Technischen Universität München eingereicht und durch die Fakultät Wissenschaftszentrum Weihstephan für Ernährung, Landnutzung und Umwelt am 01.02.2006 angenommen.

Towards a molecular understanding of midbrain-hindbrain neurogenesis and reward in zebrafish

Kumulative Arbeit

Jovica Ninković

Abstract

The developmental functionality of neural networks involved in complex diseases, such as addiction, is an important determinant of adult behavior. Thus, understanding the principles of embryonic neurogenesis is of prime importance. To approach this issue, I focused on neurogenesis control in the midbrain-hindbrain domain, which contains a long-lasting progenitor pool, the Intervening zone (IZ). I identified the Hairy/E(Spl) factors Him and Her5 as the crucial determinants of IZ formation. The expression of these two factors at the end of gastrulation prefigures and later during development precisely delineates in space the IZ. The IZ is formed as a two-partite area (lateral (LIZ) and medial (MIZ)), these two domains differing with respect to their sensitivity to the "Him + Her5" inhibitory activity. Using single and double knockdowns of *him* and *her5*, as well as a *him + her5* deletion mutant background (*b404*), I demonstrated that Him and Her5 are equally necessary for MIZ formation, and that they act redundantly in LIZ formation *in vivo*. I showed that these processes do not involve cross-regulation between Him and Her5 expression or activities. Increasing the function of one factor when the other is depleted, I further showed that Him and Her5 are functionally interchangeable. My results are in agreement with a model where the global "Him + Her5" activity inhibits *ngn1* expression in a dose-dependent manner and through different sensitivity thresholds along the medio-lateral axis of the neural plate. I showed that this differential sensitivity of the MIZ and LIZ were based on graded Gli signaling along the medio-lateral neural plate axis at the level of the IZ, and that Gli1 activity in this process was regulated by the PKA/ GSK3β phosphorylation tandem. According to my results, Gli1 increases the threshold level for "Him + Her5" inhibitory activity in the MIZ and loss of Gli1 function render the MIZ into the LIZ in respect to "Him + Her5" inhibitory activity.

In parallel, to approach brain functionality, I developed a reliable conditioned place preference methodology to score addiction in zebrafish, including a number of crucial specificity controls, such as the assessment of the animal's stress, vision and memory, the measure of optimal drug doses, and a verification of the dose received into the animal's brain. Thanks to this methodology, I demonstrated that more than 95 % of wild-type zebrafish robustly experience the rewarding effects of the psychostimulant D-amphetamine. I next focused on the cholinergic system, a known modulator of dopaminergic transmission in mammals and demonstrated that *ache*/+ mutant adult zebrafish, which exhibit higher level of central acetylcholine (ACh) than wild-type individuals, are strongly resistant to the rewarding effects of D-amphetamine. This phenotype cannot be accounted for by alterations in the exploratory activity,

vision or memory of these mutants. Taken together, my results provide the first genetic arguments supporting manipulations of acetylcholinesterase (AChE) activity as a promising avenue towards limiting addiction behavior to psychostimulants. Second, they show that the rewarding potential of amphetamine, as well as the importance of the cholinergic system in modulating this effect, have been evolutionarily conserved in vertebrates, and thus validate the zebrafish as a reliable model to give insight into the molecular neurobiology of drug-induced reward in vertebrates. This is of crucial interest given the ease with which zebrafish can be used for to produce developmental mutants and run genetic or chemical screens. I conducted a large-scale screen aimed to recover dominant modifiers of addiction to D - amphetamine and recovered one mutation affecting the response to the rewarding effects of D - amphetamine. This mutation is currently being positionally cloned.

All together, my results set the stage for future forward genetics approaches of neurogenesis control and reward.

List of abbreviations

AC	anterior commissure
ACh	acetylcholine
AChE	acetylcholinesterase
AMPH	D - amphetamine
Anf	Anterior neural folds homolog
ANP	anterior neural plate
APC	Adenomatous Polyposis Coli
Av	aversion
Bf1	Brain factor 1
bHLH	basic helix-loop-helix
BMP	bone morphogenetic protein
BSR	brain stimulation reward
Ca	caudal reticulospinal neuron
CaP	caudal primary motorneuron
ChAT	choline acetyltransferase
Ci	Cubitus interruptus
CNS	central nervous system
CoPA	commissural primary ascending interneuron
Cos	Costal
CPP	conditioned place preference
DAT	dopamine transporter
des	deadly seven
Di	diencephalon
Dll	Distal-less
drc	dorso-rostral cluster
Dsh	disheveled
DVDT	dorsoventral diencephalic tract
e	epiphysis

E(Spl)	Enhancer of split
EAA	excitatory amino acid
Eng (En)	Engrailed
ENK	enkephalin
ENU	ethylnitrosourea
ep	epiphysial cluster
ERG	electroretinography
Esr6	Enhancer of split related epidermal protein-6
Fgf	fibroblast growth factor
GABA	gamma-aminobutyric acid
Gbx	Gastrulation and brain-specific homeobox protein
Gli	Glioblastoma
GSK3β	glycogen synthase kinase-3β
HADC	Histone deacetylase
Hairy/E(Spl)	Hairy and enhancer of split
Her5	Hairy-related 5
Hes	Hairy and enhancer of split
Hey	Hairy/E(spl)-related with YRPW motif
Him	Her5 image
Hox	Homeobox protein
hpf	hours-post-fertilization
hs	heat-shock
HuC	RNA-binding protein HuC
ICPC	intracranial place-conditioning
ICSA	intracranial self-administration
Id	Inhibitor of differentiation
in	spinal interneuron
Iro	Iroquis
IsO	isthmic organizer
IVSA	intravenous self-administration
IZ	intervening zone
LIZ	lateral intervening zone
LLF	lateral longitudinal commissure
LMA	locomotor activity
LSNI	longitudinal stripes of neurogenesis inhibition
M	Mauthner cell
mAChR	muscarinic acetylcholine receptor
MAPK	Mitogen-activated protein kinase
Math3	Mouse atonal homolog 3
MDMA	3,4 - methylenedioxymethamphetamine (ecstasy)
MEK	mitogen-activated protein kinase kinase
METH	methamphetamine

MH	midbrain-hindbrain
MHB	midbrain-hindbrain boundary
Mi	middle reticulospinal neuron
Mid	midbrain
mid-DA	midbrain dopamine-producing neuronal population
MiP	middle primary motorneuron
MIZ	medial intervening zone
MLF	medial longitudinal commissure
mn	spinal motorneuron
MPFC	medial prefrontal cortex
Ms	mesencephalon
Mt	metencephalon
MyoD	Myogenic differentiation protein
nAChR	nicotinic acetylcholine receptor
Ngn1	Neurogenin1
NIC	nicotinic receptor
NICD	intracellular domain of Notch
NIM	muscarinic receptor
NMDA	N-methyl-D-aspartate
nMLF	nucleus of medial longitudinal fascicle
nPC	nucleus of posterior commissure
NT	neurotensin
olf	olfactory placodes
Opl	Odd-paired-like
OTDZT	2,4-Dibenzyl-5-oxothiadiazolidine-3-thione
Otx	orthodenticle homolog
P	prosencephalon
p	prosomere
Pax	Paired box transcription factor
PKA	protein kinase A
PKA*	constitutively active protein kinase A
PMS	presomitic mesoderm
POC	post-optic commissure
PP	place preference
Ptp	Patched
r	rhombomere
r1	rhombomere 1
r2	rhombomere 2
r2LN	lateral neurons of rhombomere 2
r2MN	medial neurons of rhombomere 2
r4	rhombomere 4
r4LN	lateral neurons of rhombomere 4
r4MN	medial neurons of rhombomere 4

Ras	retrovirus-associated DNA sequences
RB	Rohon Beard neuron
Rhomb	rhombencephalon
RoL	rostral lateral reticulospinal neuron
RoM	rostral medial reticulospinal neuron
RoP	rostral primary motorneuron
rost-5HT	rostral hindbrain serotonin-producing neuronal population
Sef	Similar Expression to fibroblast growth factor
Shh	Sonic hedgehog
Smo	Smoothened
sn	spinal sensory neuron
SOT	supraoptic tract
Stra13	Stimulated by retinoic acid 13
Su(H)	Suppressor of Hairless
TCF	Thymocyte differentiation factor
Tel	telencephalon
tg	trigeminal ganglia
TH	tyrosine hydroxylase
THC	tract of habenular commissure
TLE	Transducin-like enhancer protein
TPC	tract of posterior commissure
TPOC	tract of postoptic commissure
V	fifth cranial nerve
vcc	ventro-caudal cluster
VII	seventh cranial nerve
VMAT	vesicular monoamine transporter
VP	ventral pallidum
vrc	ventro-rostral cluster
VTA	ventral tegmental area
Wnt	Wingless-type
WT	wild-type
Xash3	Xenopus achaete-scute homolog 3
Xdbx	Xenopus developing brain homeobox protein
Zic	zinc finger protein of the cerebellum

Index of definitions

Contents

Chapter 1

Introduction

The goals of my PhD project were to unravel some of the molecular mechanisms controlling neurogenesis in the vertebrate embryonic CNS, and to initiate the studies addressing the influence of embryonic neurogenesis on the functionality of complex neural networks.

The developmental functionality of neural networks involved in complex diseases, such as addiction is, as much as their activity at adulthood, a crucial determinant of adult behavior [1][2]. In addition, active adult neurogenesis is important in controlling different aspects of social behavior [3][4][5]. Thus, understanding the principle of embryonic neurogenesis is of prime importance. To address this issue, I focussed during my PhD on a specific pool of progenitor cells, the intervening zone (IZ), located at the midbrain - hindbrain boundary in the embryonic brain of all vertebrates. My model of choice was the zebrafish, because zebrafish embryos are produced in high number, develop externally and are optically clear, making it possible to combine genetic techniques (e.g. transgenic zebrafish) with embryonic manipulations (e.g. injections of RNA/DNA). To introduce these topics, I summarize below general features of neurogenesis in vertebrates (Section 1.1). Further, I describe two classes of bHLH transcription factors controlling neurogenesis: proneural bHLH factors and Hairy/E(Spl) transcription factors (see Section 1.2.2). Finally, because I studied, in more detail, factors controlling neurogenesis in the midbrain-hindbrain (MH) domain and therefore, I shortly describe MH domain development with respect to the isthmic organizer (IsO) activity and neuronal populations developing within the MH domain (Section 1.3).

The ultimate output of proper neurogenesis control is brain functionality, which results in appropriate behaviors. Among these, the brain reward system is a very important brain functional subunit involved in awarding both appropriate and inappropriate behavior. This strongly implies the brain reward system as a dominant determinant of animal's adaptation and evolution. Thus, the second goal of my PhD was to setup the basis for studying the functionality of the zebrafish reward system. To introduce this topic, I summarize current knowledge on the brain reward system, mainly obtained from studies in rodents (Section 1.4). The brain reward system is also a neuronal basis for many psychological diseases, including addiction. The molecular mechanisms of addiction to psychostimulants, the places of action of psychostimulants

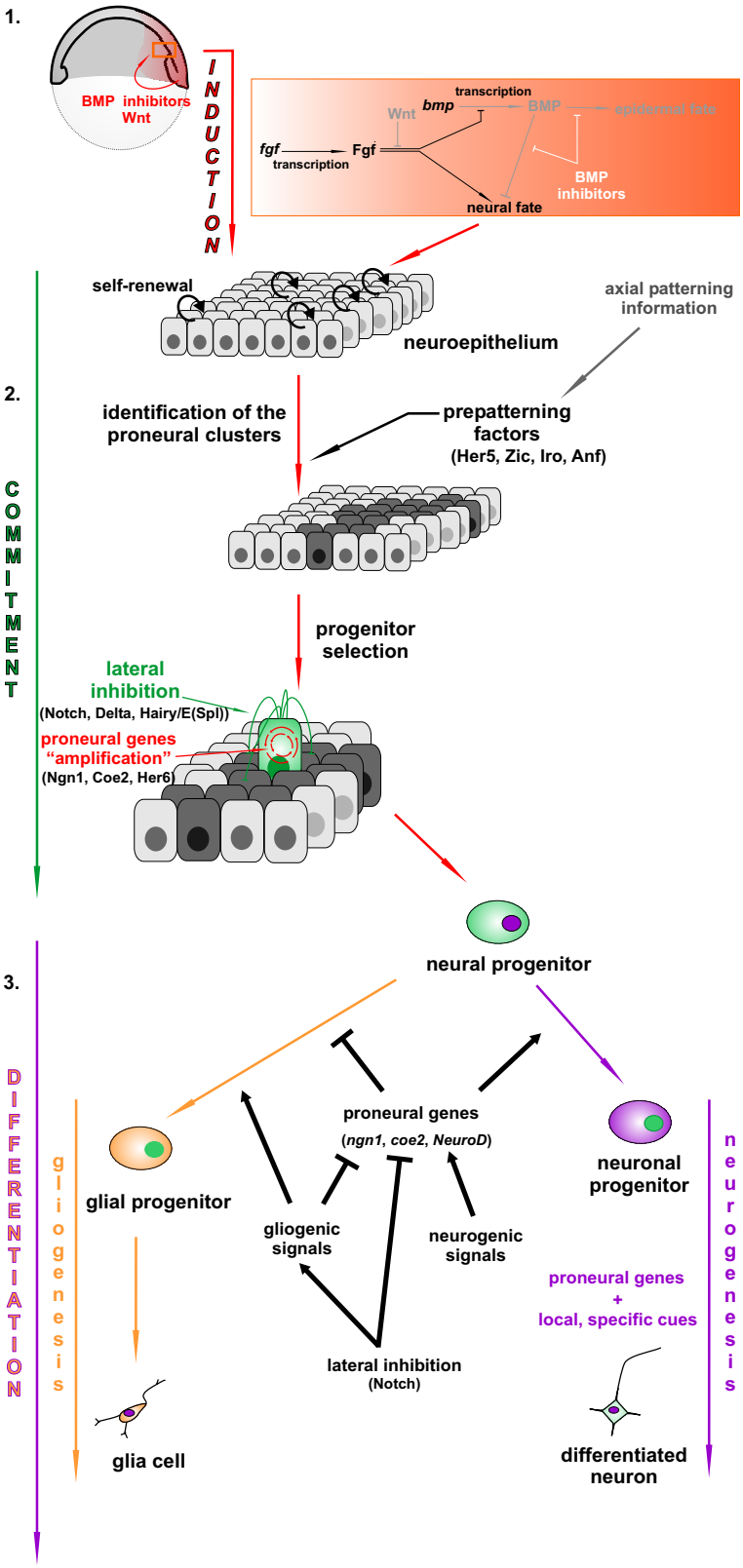
1.
BMP inhibitors
Wnt
INDUCTION
transcription
Wnt
bmp
BMP
epidermal fate
fgf
transcription
Fgf
BMP
inhibitors
neural fate
self-renewal
axial patterning
information
neuroepithelium
2.
COMMITMENT
identification of the
proneural clusters
prepatterning
factors
(Her5, Zic, Iro, Anf)
progenitor
selection
lateral
inhibition
(Notch, Delta, Hairy/E(Spl))
proneural genes
"amplification"
(Ngn1, Coe2, Her6)
neural progenitor
3.
DIFFERENTIATION
proneural genes
(ngn1, coe2, NeuroD)
gliogenesis
glial progenitor
gliogenic
signals
neurogenic
signals
neuronal
progenitor
neurogenesis
proneural genes
+
local, specific cues
lateral inhibition
(Notch)
glia cell
differentiated
neuron

and the experimental paradigms to study this disease in experimental animals will be presented in Section 1.5. Finally, in Section 1.5.2 I will present the structures in zebrafish brain that could be functional analogs of the brain reward system in mammals.

1.1 Neurogenesis

Building a vertebrate's nervous system involves the production of variety of neuronal and glial cell types at defined positions, in correct number and with appropriate connections during the process called *Neurogenesis*. In its broadest definition, neurogenesis is the multi-step process that brings from neural induction to the differentiation of functional neurons and glia [11]. It involves several successive steps, characterized by specific signaling events [6] and by the expression of different sets of transcription factors [12][13]. First, the neural plate is identified, this is the process of neural induction. During neural induction, competent ectodermal cells are endowed with the capacity to become neuronal precursors. Second, within the neural plate, neurogenesis-competent domains ("proneural clusters" or "proneural fields") are defined by the combinatorial action of neurogenesis activators ("proneural genes") and neurogenesis inhibitors.

Figure 1.1: **Neurogenesis in vertebrates involves several successive steps and specific signaling events.** 1. During gastrulation, the neural plate is identified through the process of neural induction (INDUCTION). The interaction between the three signaling pathways (Fgf, Wnt and Bmp) promotes neural and inhibits epidermal cell fate. In the most accepted model, the crucial role in promoting neural fate is assigned to Fgf signaling which both represses Bmp and activates an independent pathway necessary for progression towards the neural fate. Fgf signaling is modulated by Wnt from the embryonic margin. Other signals, independent from Fgf, but resulting in the same cell fate decision are Bmp inhibitors, originating from the embryonic primary organizer. Neural induction is beyond the scope of the work presented in this thesis and it will not be discussed in more details. For more detailed picture please see Wilson and Edlund, 2001 [6][7][8][9][10]. 2. (NEURAL COMMITMENT) Within the neural plate, proneural clusters where neurogenesis can take place are negatively defined by the activity of neurogenesis inhibitors (see section 1.1.3). A restricted number of neural progenitors from each cluster is further selected by the process of lateral inhibition (see section 1.1.5). As a consequence, the expression level of proneural genes in the selected progenitors is elevated, resulting in the final commitment to the neural linage. Committed progenitors can give rise to both neural and glial cells. 3. (DIFFERENTIATION) Generally, they first generate neurons and then glial cells. The switch from the neural to glial cell fate is controlled by both extrinsic and intrinsic cues. Proneural genes seems to be at least a part of the set of intrinsic determinants, and the response to extrinsic signals including Notch. It is likely that acquisition of different neuronal and glial identities is under control of local cues provided by the surrounding tissue.

Finally, neural progenitors are committed and differentiate to neurons or glia (Figure 1.1).

Neurogenesis in zebrafish, as in other lower vertebrates, occurs in two successive waves: primary and secondary neurogenesis [14]. Primary neurogenesis is initiated

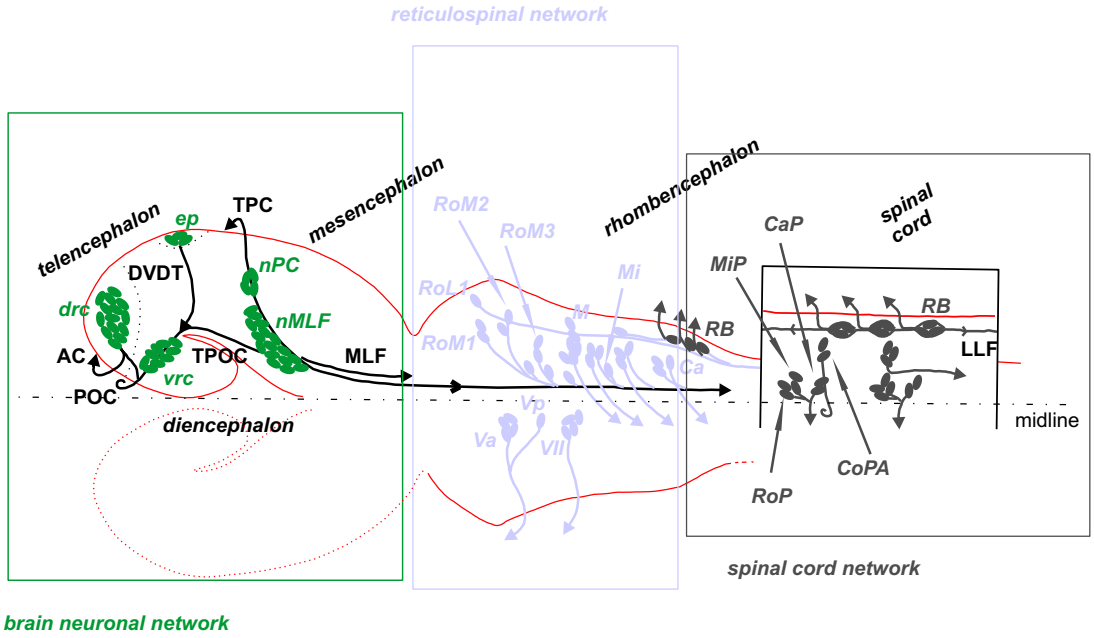

Figure 1.2: **The primary neuronal scaffold of the zebrafish embryo.** Schematized "open" preparation of the neural tube at ∼ 30 hpf, anterior to the left. Brain clusters in the tel-, di- and mesencephalon (drc, ep, nMLF, nPC and vrc) connected with the orthogonally oriented tracts (AC, DVDT, POC and TPC) build the embryonic brain neuronal network (green box). Three types of spinal cord primary motorneurons (RoP, MiP and CaP) together with primary sensory RB neurons constitute the spinal cord network (gray box). The reticulospinal network is built by rhombencephalic Ca, M, Mi and Ro neurons (light violet box). Abbreviations: **V**: fifth cranial nerve; **VII**: seventh cranial nerve, **AC**: anterior commissure; **Ca**: caudal reticulospinal neurons; **CaP**: caudal primary motorneurons; **CoPA**: commissural primary ascending interneuron; **drc**: dorso-rostral cluster; **DVDT**: dorsoventral diencephalic tract; **ep**: epiphyseal cluster; **LLF**: lateral longitudinal commissure; **M**: Mauthner cell; MLF: medial longitudinal commissure; **Mi**: middle reticulospinal neurons; **MiP**: middle primary motorneurons; **nMLF**: nucleus of the MLF; **nPC**: nucleus of the posterior commissure; **POC**: postoptic commissure; **RB**: Rohon Beard neurons; **RoL**: rostral lateral reticulospinal neurons; **RoM**: rostral medial reticulospinal neurons; **RoP**: rostral primary motorneurons; **TPC**: tract of posterior commissure; **TPOC**: tract of postoptic commissure; **vrc**: ventrorostral cluster. After Chapouton and Bally-Cuif, 2004 [15].

at late gastrulation and continues during embryogenesis to produce early-born big neurons such as the brain epiphyseal and post-optic clusters, Mauthner cells (M), Rohon-Beard (RB) sensory neurons and three types of primary spinal motorneurons (CaP, MiP and RoP) [16]. Between 14 and 24 hours-post-fertilization (hpf) these neurons form long axons and build the first functional embryonic and early larval neuronal scaffold, allowing the fish larva to move and feed [17]. Secondary neurogenesis starts at around 48 hpf at all rostro-caudal levels and at post-embryonic stages takes over functions of the primary system by a refined and increasingly complex network [18]. The mechanisms and factors controlling primary and secondary neurogenesis are not intrinsically different [15].

1.1.1 Neurogenesis is patterned in space and time

All cells of the neural plate adopt a neural fate during neural induction, but the progression towards neuronal differentiation does not occur homogenously and simultaneously throughout the neural plate. This results in the formation of neuronal clusters stereotypically distributed along the dorsoventral and anteroposterior axes in all vertebrates. Interconnected by long axons, these clusters form the primary neuronal scaffold.

The primary neuronal scaffold

The initiation of neural differentiation in the zebrafish embryo has traditionally been revealed using acetylcholinesterase (AChE) activity [19][20][21] or antibodies against acetylated tubulin [22] to visualize cell bodies, and antibodies against HNK1 [23] or DiI applications [24][25][26] to visualize axons. Using these techniques, three main neuronal networks can be seen within the primary neuronal scaffold of the zebrafish embryo:

- *the embryonic brain neuronal network* [20][25][26],
- *the reticulospinal network* [27][28] and
- *the spinal cord network* [29][30][31] (Figure 1.2).

Below, I will restrict myself to the formation of the embryonic brain neuronal network. Details about each specific network can be found in the publications cited.

The first neuronal clusters in the developing brain differentiate near the center of each neuromere. The earliest neuronal cluster observed in all vertebrates is the ventro-caudal cluster (vcc) which lies in the basal diencephalon and anterior midbrain (Figure 1.3). After 24 hpf the vcc separates into the nucleus of medial longitudinal fascicle (nMLF) and the nucleus of posterior commissure (nPC) (Figure 1.3). The formation of the vcc is followed by that of two forebrain clusters: first, the ventrorostral (vrc) and then the dorsorostral (drc) clusters (Figure 1.3). Finally, the dorsally positioned epiphyseal nucleus (ep) (Figure 1.3) is formed at 24 hpf. The nuclei of the embryonic brain neuronal network are subsequently connected with longitudinal and transversal axonal tracts (Figure 1.3). The schedule of appearance of these axonal tracts during early zebrafish development is summarized in Table 1.1.

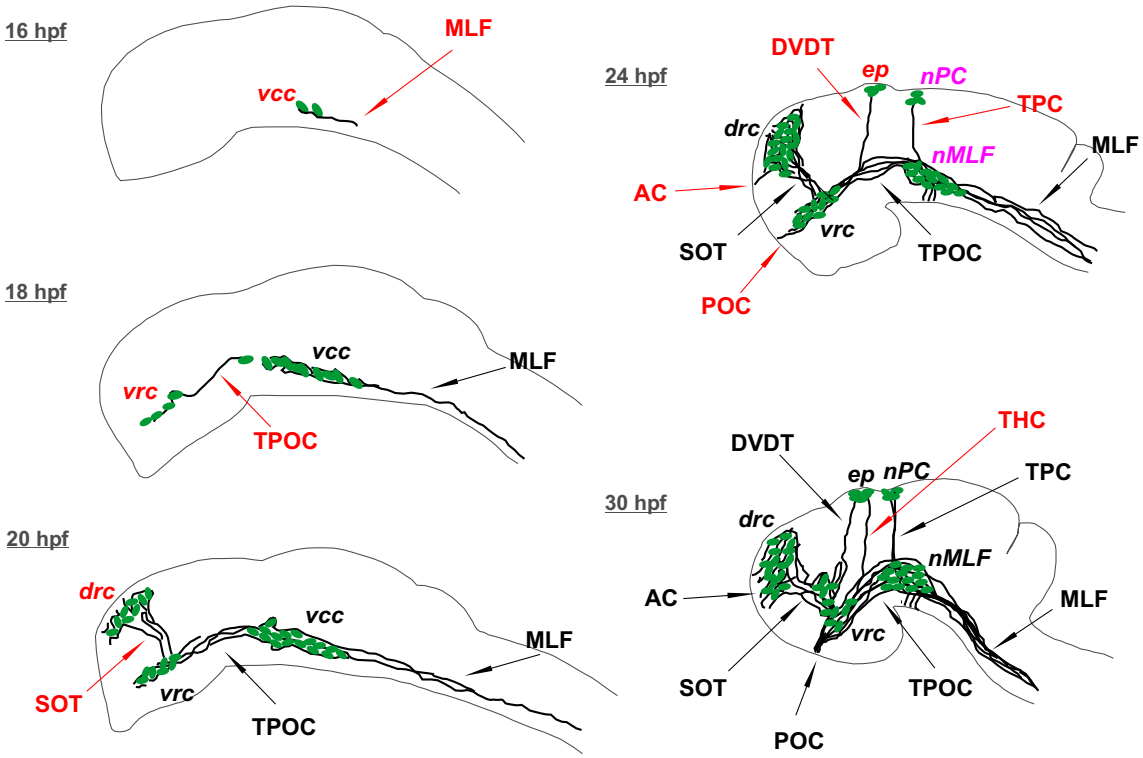

Figure 1.3: **Lateral views of the embryonic brain summarizing the progressive development of axonal tracts.** Axonal tracts: **AC**: anterior commissure; **DVDT**: dorsoventral diencephalic tract; **MLF**: medial longitudinal commissure; **POC**: post-optic commissure; **SOT**: supraoptic tract; **THC**: tract of habenular commissure; **TPC**: tract of posterior commissure; **TPOC**: tract of postoptic commissure;. Neural clusters: **drc**: dorso-rostral cluster; **ep**: epiphysial cluster; **nMLF**: nucleus of the medial longitudinal fascicle; **nPC**: nucleus of the posterior commissure; **vcc**: ventro-caudal cluster **vrc**: ventro-rostral cluster;. The moment of appearance of a given cluster or axonal tract is indicated with red color. After Ross *et al.*, 1992 [20].

1.1.2 Prepatterning of the neural plate

The stereotyped position of the neuronal clusters is a consequence of the "prepatterning" machinery that allows neurogenesis progression in only restricted regions of the neural plate, called proneural clusters. Prepattern factors are directly controlled by the early embryonic patterning machinery [32]. Thus, they link early patterning information to the definition of the first neurogenesis sites, in a manner analogous to the definition of proneural fields in Drosophila.

The proneural clusters can be revealed by the expression of proneural genes (see

axonal tract	abbreviation	appearance at
anterior commissure	AC	24 hpf
supraoptic tract	SOT	20 hpf
dorsoventral diencephalic tract	DVDT	24 hpf
medial longitudinal commissure	MLF	16 hpf
post-optic commissure	POC	24 hpf
tract of posterior commissure	TPC	24 hpf
tract of the post-optic commissure	TPOC	18 hpf
tract of the habenular commissure	THC	after 24 hpf

Table 1.1: **Appearance of early axonal tracts in developing zebrafish brain.** After Ross et al., 1992 [20] and Chapouton and Bally-Cuif, 2004 [15].

Section 1.2) such as *neurogenin1* (*ngn1*) at the 3-somite stage of the developing zebrafish embryo (Figure 1.4). Anteriorly, *ngn1* expression highlights the precursors of the rostral clusters, vcc and trigeminal ganglia. In the prospective spinal cord, *ngn1* expression indicates the position of the presumptive motor-, inter- and sensory neurons.

The proneural fields are separated by areas of delayed differentiation: the anterior neural plate (ANP), the midbrain-hindbrain boundary (MHB) and the longitudinal spinal cord stripes (Figure 1.4) in all vertebrates and the superficial ectoderm layer in the Xenopus neurula. These sites of delayed or absent differentiation are characterized by the expression of specific transcription factors of the Zic, Iro and Hairy/E(Spl) families, acting as neurogenesis inhibitors. In zebrafish, *opl*, *anf* and *bf1* are expressed in the anterior neural plate [33][34][35], *her5* [36][37] and *him* (see Article in Appendix A) expression label the midbrain-hindbrain boundary, and *zic3*, *her3* and *her9* highlight the posterior neural plate domains [38][39].

1.1.3 Definition of the proneural fields by inhibition

Following neural plate induction, the expression of several transcription factors promoting the neural fate can be observed. The most studied of these belong to the Sox, Gli, POU and Iroquois families and are initially expressed across broad domains of the neural plate [40][12]. At least some of these factors (Iro1, Iro7 and Pou2) are necessary and sufficient to induce ectopic *ngn1* expression within non-neural ectoderm [41][42]. Nevertheless, neurogenesis progression towards differentiation occurs only in restricted sites within the domains defined by these factors. This is because outside these sites, neurogenesis progression is blocked by the selective expression of transcription factors that actively inhibit the differentiation of neural precursors. The molecules mediating this block are site-specific, but it seems that the principles of neurogenesis inhibition are generally conserved. The main features of this neurogenesis inhibition process will be highlighted below.

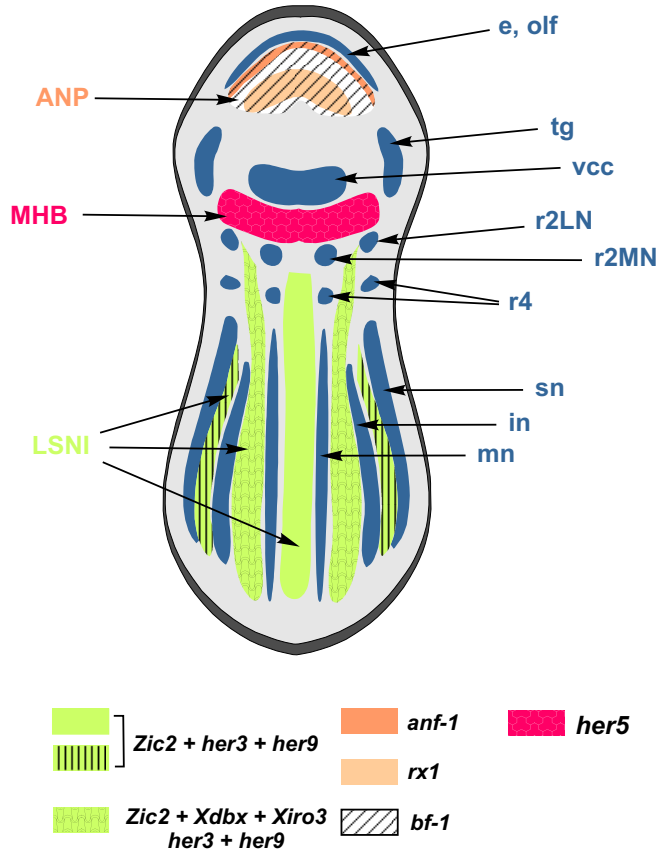

Figure 1.4: **The spatial pattern of neurogenesis in zebrafish.** Dorsal view of the zebrafish early neural plate, anterior to the top, with schematized neurogenesis foci (blue) and the expression of active neurogenesis inhibitors (colored patterns). Abbreviations: e, olf: epiphysis and olfactory placodes; tg: trigeminal placodes; vcc: ventro-caudal cluster; r2LN: lateral neurons of rhombomere 2; r2MN: motorneurons of rhombomere 2; r4: neurons of rhombomere 4; sn: spinal sensory neurons; mn: spinal motorneurons; in: spinal interneurons; ANP: anterior neural plate; MHB: midbrain-hindbrain boundary; LSNI: longitudinal stripes of neurogenesis inhibition. After Bally-Cuif and Hammerschmidt [12].

Establishment of inhibitory processes by early patterning

Inhibitory processes are established at an early developmental stage, which often precedes the expression of proneural genes, and the expression of the factors involved appears to be under control of the axial-patterning machinery. For example, *her5* expression starts at 75 % epiboly [36] well ahead the expression onset of the earliest proneural genes such as *ngn1* [43] or *coe2* [44]. Similarly, *Xanf1* marks the anterior

neural plate in Xenopus and its expression is one of the earliest responses of the ectoderm to Noggin and Chordin [45]. These findings indicate that the spatial pattern of neurogenesis is controlled by the general D/V- and A/P- patterning systems via the specific expression of the genes involved in neurogenesis inhibition.

The high redundancy of inhibitory processes secure progenitor pool maintenance

It has been shown that forced premature differentiation in the areas of neurogenesis inhibition seriously impairs the normal development of central nervous system structures. For example, premature differentiation of the ANP in Xenopus prevents expansion of the cerebral hemispheres [46][47], while early differentiation of the MHB prevents midbrain growth and the formation of some neural populations [48]. Therefore, neurogenesis inhibition appears to be crucial for the maintenance of progenitor pools that permit the expansion and diversification of the CNS. As described below, multiple functionally redundant pathways have been evolved to secure this process.

The superficial layer of the Xenopus neuroectoderm differentiates during the second wave of neurogenesis. During primary neurogenesis, the cells of this layer are exposed to a cell-autonomous inhibition of neural differentiation. The Hairy/E(Spl) bHLH transcription ESR6e, present in the zone of delayed neurogenesis, appears to be at least partially responsible for this inhibition, since it is able to inhibit neurogenesis when it is ectopically expressed in the neurogenic deep layer of the neural tube. However, loss of ESN6e function does not lead to the premature differentiation of superficial layer cells, indicating the involvement of additional and as yet unidentified factor(s) in preventing neurogenesis progression [49].

A similar redundancy is present in the systems blocking neural differentiation in the mouse MHB. At late stages in the mouse embryo, MHB integrity is maintained by the redundant action of two Hairy/E(Spl) bHLH transcription factors, Hes1 and Hes3 [48][50]. Ectopically expressed, these factors can inhibit neurogenesis *in vivo* [51][52], while the loss-of-function of both factors in double $Hes1^{-/-}$; $Hes3^{-/-}$ mutant results in premature neural differentiation preceded by the down-regulation of the expression of MHB identity markers [48].

In the posterior neural plate of lower vertebrates, longitudinal stripes of proneural gene expression are separated by interstripes of non-differentiating neural precursors expressing neurogenesis inhibitors. In Xenopus, the expression of *Zic1*, *Zic2*, *Xiro3* and *Xdbx* can be observed in the interstripes from late gastrulation onwards [53][54][55]. The ectopic activation of any of these factors results in posterior neural plate expansion and inhibition of neural differentiation [55]. In zebrafish, two *hairy/E(spl)* genes *her3* and *her9* are expressed in the posterior inter-proneural domains, and are required for its formation [39][56]. Inhibition of Her3 or Her9 led to ectopic expression of the proneural genes in part of the inter-proneural domains, while combined inhibition of Her3 and Her9 induced ubiquitous expression of proneural genes and abolished the formation of the inter-proneural domains [39], also suggesting the existence of parallel pathways securing neurogenesis inhibition in the posterior neural plate.

Neurogenesis inhibitors operate independently from the lateral inhibition pathway

Notch signaling and notch-activated E(Spl) factors are involved in limiting neurogenesis within the proneural clusters (see Section 1.1.5). However, the expression of

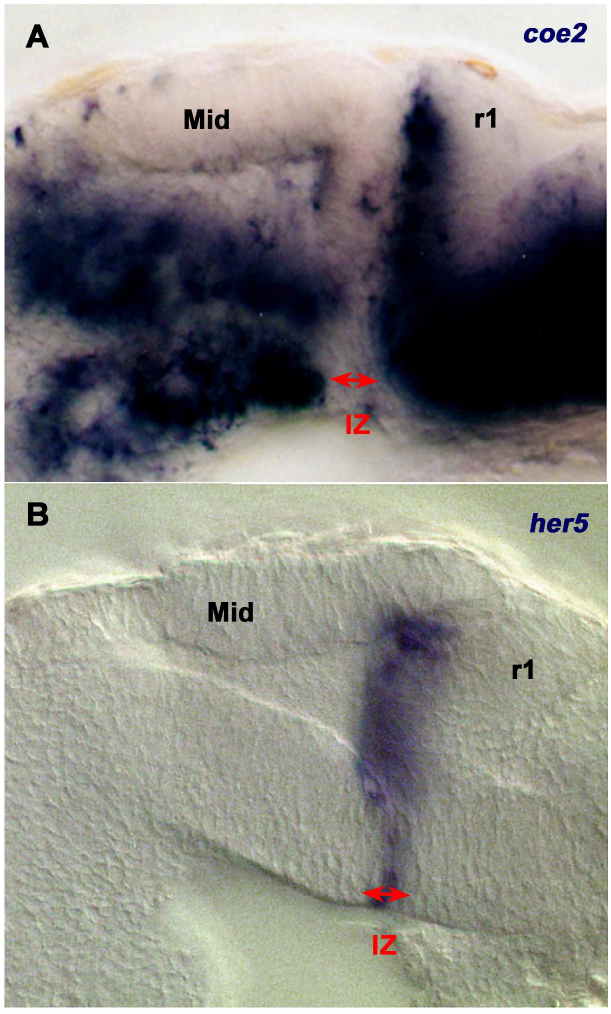

Figure 1.5: **Neurogenesis is delayed in the embryonic IZ.** Zebrafish embryo at 24 hpf stained with the proneural marker *coe2* (see Section 1.2) (**A**) and *hairy/E(Spl)* gene *her5* (**B**), anterior to the left. Note that the area referred to as the IZ zone is not expressing proneural genes, such as *coe2*, but does express genes encoding neurogenesis inhibitors, such as *her5*. Abbreviations: Mid: midbrain; r1: rhombomere 1; Rhomb: rhombencephalon. IZ: intervening zone

bHLH transcription factors involved in prepattern formation (e.g. *her5*, *her3*, *her9*,

ESR6) is not regulated by Notch signaling [49][57][39]. The activity of these factors in neurogenesis inhibition is also not under control of Notch signaling. Blocking or lowering Notch signaling in zebrafish using either *notch1a*-deficient embryos (*deadly seven* (*des*) mutation) or overexpression of the dominant $delta^{stu}$ does not induce neuronal differentiation within non-differentiation domains of the neural plate [57][58] [55][54][59]. This suggests that processes inhibiting neurogenesis progression outside of the proneural clusters do not rely on increased lateral inhibition through the Delta/Notch system. They are, rather, upstream of the lateral inhibition process and might use a specific subclass of E(Spl) factors.

Different mechanisms of proneural gene repression

Most systems that negatively define neurogenesis-competent domains across the neural plate act via inhibition of early proneural genes expression and/or action. However, their molecular mode of action might be factor- and site-specific. At present, several different molecular pathways resulting in neurogenesis inhibition are known.

Neurogenesis inhibition in the longitudinal interstripes of the posterior neural plate is achieved by direct competition of Zic factors with Gli2 and Gli3 for DNA-binding sites on the promoter of proneural genes [60][61][62]. A mechanism of active transcriptional repression is also likely to be used by Hairy/E(*Spl*) factors such as zebrafish Her5. Most likely, Her5 directly binds a "E-box" in the *ngn1* promoter and abolishes the activation of the neurogenic cascade (see Section 1.1.6) by inhibition of *ngn1* expression [57]. The ability of other Hairy/E(*Spl*) to directly bind to the promoter of proneural genes and repress their expression remains to be demonstrated.

Additionally to transcriptional repression, some neurogenesis inhibition systems also block the function of the proneural factors. In Xenopus, Zic2 and ENS6e block the ability of Ngnr1 to induce ectopic N-tubulin expression in co-injection experiments [60][49]. Similarly, Xiro3 and Xdbf abolish the proneural activity of Xash3 [55][54]. Finally, ectopic expression of Neurogenin, NeuroD or Delta in the superficial layer of the Xenopus neuroectoderm failed to push cells towards neuronal differentiation, suggesting the existence of multiple blocks acting in different steps of the neurogenic cascade (see Section 1.1.6). The factors and mechanisms of inhibition at all levels are mostly unknown, but existing data suggest that the inhibition might result from competition for transcriptional targets, direct repression, activation of reciprocal targets, and/or direct inhibitory protein-protein interactions. Although current evidence supports the existence of different systems of inhibition it of course remains possible that this only reflects our partial understanding of the processes involved.

1.1.4 The bHLH transcription factor Her5 and intervening zone formation in zebrafish

The intervening zone, spatially associated with the MHB (see Section 1.3), is one of the places within the neural plate characterized by delayed differentiation. It remains a source of neural precursors long after the differentiation of other neural domains [63][64][65], and most likely a zone of extensive growth. It has been shown that the embryonic IZ eventually gives rise to the entire midbrain-hindbrain region

[66]. Combining this evidence with the findings of Hirata et al. [48] emphasizes the importance of proper IZ formation for midbrain-hindbrain development.

The IZ can been seen as a neuron-free, transverse stripe that separates caudal mesencephalic and anterior rhombencephalic neurons (Figure 1.5). In zebrafish it has been shown that expression of the Hairy/E(Spl) transcription factor Her5 prefigures and then precisely delineates the IZ throughout embryonic development [36][37] (Figures 1.5 and 1.6 middle panel). Ubiquitous expression of *her5* driven by the zebrafish heat shock promoter [67][68] from the late gastrula stage onwards results in the strong down-regulation and in some cases abolishment of *ngn1* expression at the 3-somite stage in the regions surrounding the IZ, vcc and motorneurons of rhombomere 2 (Figure 1.6 right panel) [37]. This effect persists until much later stages and is followed by

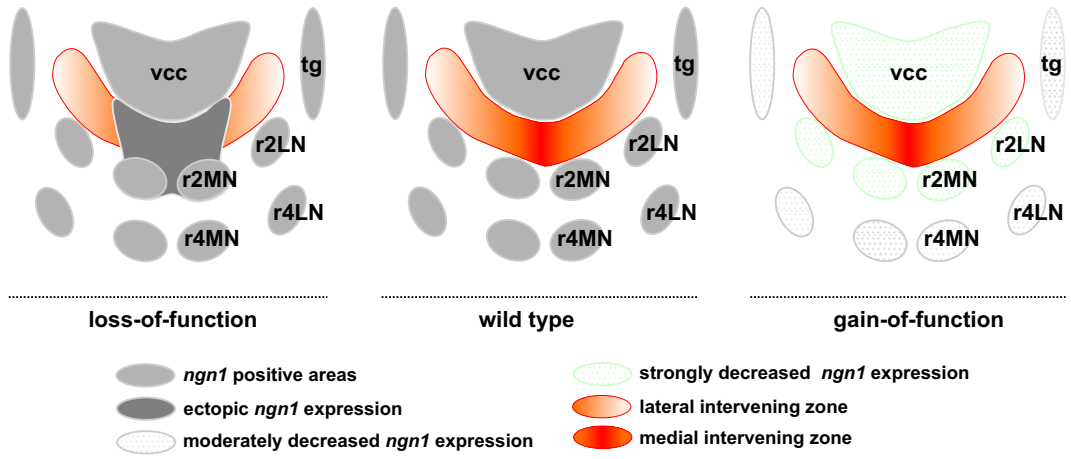

Figure 1.6: **Her5 is necessary and sufficient for medial IZ formation.** Dorsal view of the embryonic neural plate at the 3-somite stage, anterior up (the same view as in Figure 1.4) with focus on the midbrain-hindbrain area. Loss of Her5 function results in the generation of ectopic *ngn1* positive cells and triggering neurogenesis in the medial IZ, while its overexpression completely diminishes neurogenesis in the regions surrounding endogenous *her5* expression domain, the IZ. Abbreviations: vcc-ventral caudal cluster; tg-trigeminal ganglia; r2MN-medial neurons of rhombomere 2; r2LN-lateral neurons of rhombomere 2; r4MN-medial neurons of rhombomere 4 and r4LN-lateral neurons of rhombomere 4.

a lack of neuronal differentiation at 24 hpf, revealed with HuC immunoreactivity [37]. On the other hand, knocking-down *her5* translation by injecting a morpholino selective for endogenous *her5* mRNA results in ectopic *ngn1* expression across the medial part of IZ (later referred to as medial IZ) (Figure 1.6 left panel) and later on (24 hpf) in the differentiation of ectopic HuC positive, newborn neurons in this location [37]. Thus, gain- and loss-of-function experiments demonstrated that Her5 is necessary and sufficient for medial IZ development. Moreover, they showed that the IZ is composed

of two subdomains which differ in their requirement for Her5 function. Her5 is expressed across the entire IZ, but only the medial part is sensitive to the loss of Her5 function to undergo neurogenesis. The lateral parts of IZ (later referred to as lateral IZ) develop normally despite loss of Her5 function. When I started my PhD, the factor or factors controlling development of the lateral IZ in cooperation with Her5 were not known, but see Article in Appendix A. In addition to neurogenesis inhibition, Her5

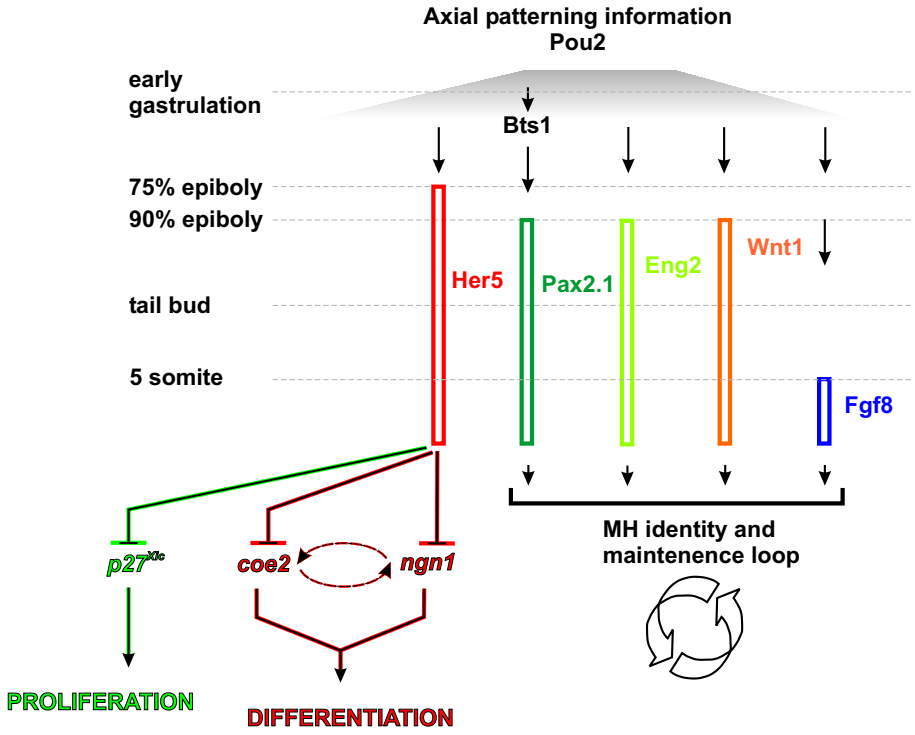

Figure 1.7: **Her5 controls both differentiation and proliferation at the MHB.** Simplified signaling events within the MHB at the onset of neurogenesis in zebrafish. Her5 prevents differentiation via blocking both *ngn1* and *coe2* expression and promotes proliferation via $p27^{Xic}$. Expression of the her5 is controlled by the axial patterning information and dependent of the MHB identity and maintenance loop (see Section 1.3.2), although Her5 is not part of it.

is involved in the promotion of cell proliferation, since loss of Her5 function results in severe down-regulation of $p27^{Xic}$ expression[1], at least in the medial IZ. Nevertheless, the functions in controlling neurogenesis and proliferation seem to be independent since blocking proliferation at the medial IZ did not result in ectopic neurogenesis [37]. Figure 1.7 summarizes the functions of Her5 in IZ development in the context of early signalling events positioning the MHB.

[1] $p27^{Xic}$ is a Cdk inhibitor encoding gene that inhibits cell proliferation.

1.1.5 Lateral inhibition mechanisms select neural progenitors within the proneural clusters

Prepatterning of the neural plate negatively defines proneural clusters, characterized by proneural genes expression. Each cell within the proneural cluster has the potential to adopt a neural fate and differentiate into a neuron or glia. Nevertheless, only a restricted number of cells will commit to the progenitor fate and differentiate further. The selection of these precursors relies on the process of lateral inhibition, which is initiated by the expression of Notch receptor ligands such as Delta (Figure 1.8) [69]. The expression of the ligand on the surface of the future progenitor cell triggers Notch signaling in neighboring cells. After binding Delta, the intracellular domain of Notch (NICD) translocates to the nucleus and activates transcription of the transcriptional repressors of the *Enhancer of split* ($E(Spl)$) family in Drosophila or their homologous *Hes/her/Ens* in vertebrates. These transcriptional repressors downregulate proneural genes expression and block differentiation.

In parallel, cells initially expressing a higher level of ligand maintain proneural gene expression and ligand transcription. Thus, through the process of lateral inhibition, initial stochastic differences in *Delta* expression are amplified, restricting the expression and/or activity of proneural genes to a small number of cells that will enter the neuronal-differentiation pathway [70][71][72]. The lateral inhibition process is reiterated throughout the period of neurogenesis, allowing transformation of neuroepithelial cells of one proneural cluster into a collection of individual progenitors. These are generated at different time points during neurogenesis and likely as a result adopt different fates [72][73]. The direct and dose-dependent transcriptional activation of the Notch receptor ligand Delta by proneural genes is crucial for lateral inhibition in Drosophila [74][75][76]. In vertebrates, Notch ligands Delta and Jagged are similarly regulated by Mash1 and Ngns [77][78][79][80][71].

Following lateral inhibition, committed progenitors express increased level of Delta and proneural genes, and positive feedback mechanisms are further required to increase and/or maintain the high level of proneural genes in selected progenitors. The initially increased level of proneural genes induces expression of a second set of proneural genes (e.g. *senseless* in Drosophila [81] or *xcoe2* [82] and *Hes6* in vertebrates [83][84]), which, in turn, upregulate proneural gene expression. This is achieved either by repression of E(Spl) genes and Notch signaling inhibition [81] or through the interference at post-transcriptional levels with the inhibitory activity of the bHLH factors activated by Notch signaling [83].

1.1.6 A cascade of neuronal-differentiation genes executes the neuronal differentiation program

The expression of proneural genes in individual neuronal progenitors is transient. In vertebrates, proneural genes are down-regulated before the progenitor cell exits the proliferative zone and begins to differentiate [80][86][87]. Therefore, neurogenesis progression must rely on the ability of proneural genes to induce downstream regulatory factors, so called neuronal-differentiation genes. The best studied neuronal-differentiation genes in vertebrates belong to the Ngn and NeuroD families. These

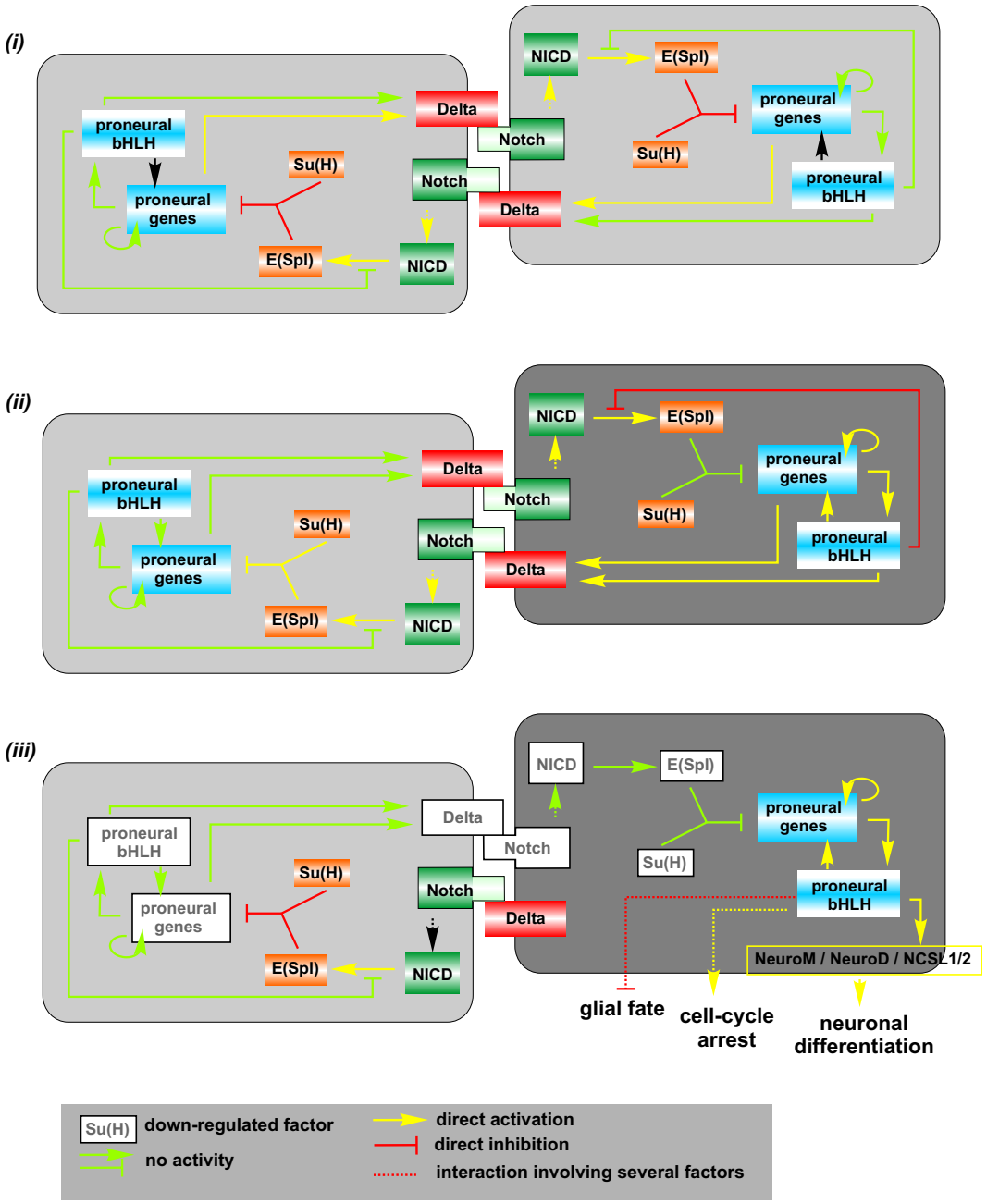

Figure 1.8: **Lateral inhibition mechanisms select neuronal progenitors within the proneural cluster.** Precursors selection within the proneural clusters occurs in three steps. Cells within the proneural clusters initially express proneural genes, Notch and the Notch ligand Delta at a similar, low level *(i)*. During the second phase, there is reinforcement of stochastic differences in the expression of proneural genes between adjacent cells by Notch-Delta interactions *(ii)*. Initial differences are further increased leading to the strong up-regulation of proneural bHLH transcription factors and Delta ligand in the neural progenitor (dark gray) and down-regulation of Delta and proneural genes in the neighboring cells (light gray) by Notch signaling. Elevated level of proneural factors activity that induces expression of several HLH factors implicated in the promotion of neuronal differentiation, cell cycle arrest and repression of gliogenesis *(iii)*.

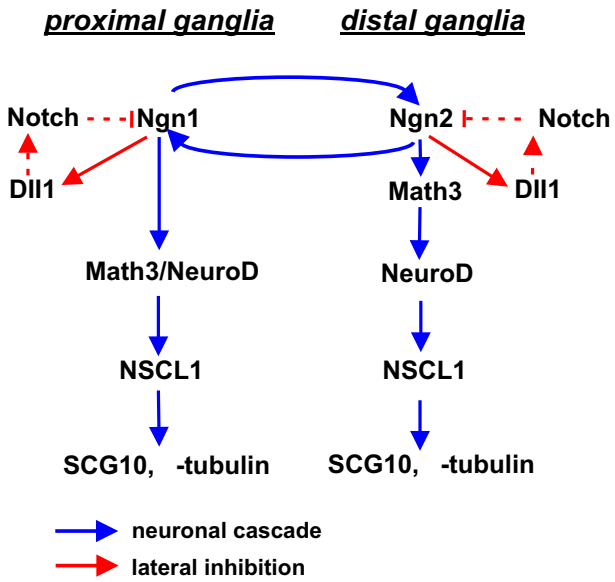

Figure 1.9: **A Cascade of proneural genes controls the development of mouse cranial sensory neurons.** The cascade of proneural genes is triggered by Ngn1 or Ngn2 in the proximal and distal ganglia, respectively. The two *ngn* genes exhibit positive cross-regulatory interactions that cause a lower level of expression of each gene in the other's principal domain. Activation of the *ngn*s triggers expression of bHLH factors including *NeuroD*, *Math3* and *NSCL1* and finally markers of the differentiated neurons: *SCG10* and *β-tubulin*. After Ma *et al.* 1998 [85].

genes are not expressed in self-renewing neuroepithelial cells, but they have the capacity to promote neuronal differentiation within the competent domain when they are ectopically expressed [88]. Additionally, gain-of-function experiments in Xenopus and loss-of-function experiments in mice have shown the epistatic relationships between proneural and neuronal-differentiation genes [80][89]. Thus, distinct bHLH genes likely act in a cascade to underly the sequential steps of cell determination and differentiation [90][91].

For example, the sequential expression of *Math3* and *NeuroD* is controlled by Ngn1 and Ngn2 in the mouse cranial sensory neurons (see Figure 1.9) [79][85], while *Mash1* acts upstream of the *Ngn1* and *NeuroD* in the olfactory sensory epithelium [78].

1.2 The basic helix-loop-helix transcription factors in neurogenesis

The family of basic helix-loop-helix (bHLH) transcription factors encompasses a variety of heterogenous proteins involved in a wide array of developmental processes in different organisms ranging from yeasts to mammals. They are involved in the regulation of a number of developmental processes such as neurogenesis, myogenesis, cell proliferation and differentiation, cell lineage commitment and sex determination [92][93][94][95]. Additionally, bHLH factors regulate several important metabolic processes including phospholipid metabolism and phosphate uptake [96][97][98].

A number of bHLH transcription factors have been implicated in the control of

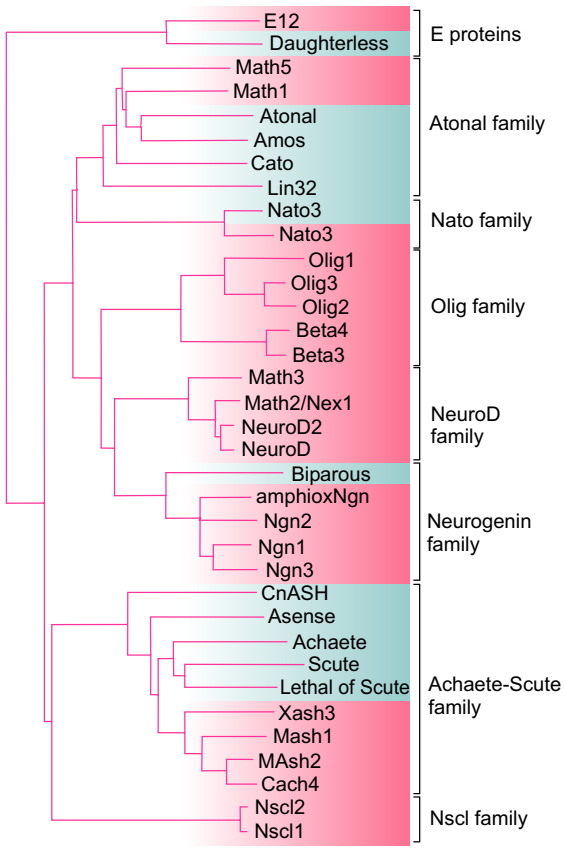

Figure 1.10: **Dendrogram of the invertebrate (blue) and vertebrate (red) neural genes based on the sequence of their basic helix-loop-helix domain.** After Bertrand *et al.*, 2002 [13].

vertebrate neurogenesis. During neurogenesis they can act either as transcriptional activators promoting neurogenesis (e.g all proneural genes (Figure 1.10)) or as transcriptional repressors important for prepattern formation and lateral inhibition (Hairy and Enhancer of split proteins, Id proteins (see Section 1.2.2)).

The main structural and functional features of bHLH transcription factors in respect to neurogenesis will be summarized in the following sections.

1.2.1 Molecular structure and classification of the bHLH factor family

bHLH transcription factors are characterized by a highly conserved bipartite domain for protein-protein interactions and DNA binding. The protein interaction domain (HLH) is composed of two conserved, hydrophobic α-helices separated by a non-conserved loop of variable length [99]. This domain allows bHLH proteins to interact and form homo- and/or heterodimers [100]. Immediately N-terminal to the first helix is located the conserved basic domain. The basic domain recognizes consensus hexanucleotide E-boxes or/and N-boxes and is required for DNA binding by bHLH proteins [101].

There are several classifications of bHLH transcription factors according to their structural features, biochemical characteristics and biochemical functions [102][32][103] [104][13][105].

A phylogenetic analysis based on the sequence of the bHLH domain has lead to a subdivision of the bHLH family into four monophyletic groups of proteins named A, B, C and D [32][104] (Table 1.2).

Group A includes bHLH proteins that bind hexameric DNA sequences referred to as "E Boxes" (CANNTG) [100][106][107]. It comprises several tissue-specific members (MyoD, Achaete-Scute proteins) [108] as well as the ubiquitously distributed E12/Daughterless-type bHLH proteins [109] that make heterodimers. Binding of the heterodimers to an E-box of the target gene leads to its transcriptional activation [110][106].

The second group (B) can be divided into two subgroups according to the presence or absence of an additional functional domain known as Leucine Zipper domain, involved in protein dimerization. These factors bind an E-box and act as transcriptional repressors [111][112][113]. The second subgroup includes proteins related to the Drosophila Hairy and Enhancer of split bHLH proteins [107][102]. These proteins will be described in more detail in the next section.

bHLH factors belonging to group C are characterized by a PAS domain involved in dimerization between PAS proteins, the binding of small molecules (e.g. dioxin) and interactions with non-PAS proteins [114]. These proteins are involved in the control of a variety of developmental processes, including neurogenesis, but their biochemical activity is still unknown.

Group D corresponds to HLH proteins that lack a basic domain and are hence unable to bind DNA. They have a high affinity for bHLH proteins from group A and form with these proteins heterodimers unable to bind DNA [115][116]. Therefore, they act as functional antagonists of group A proteins.

Group	Structural features	Biochemical activity	Examples	DNA binding site
A	bHLH	transcriptional activators	MyoD, Mash	E-box *(CANNTG)*
B	bHLH leucine zipper	transcriptional repressors	Myc, Max	E-box *(CANNTG)*
	conserved proline in basic domain	transcriptional repressors	Hairy and E(*Spl*) Hes, Esr, Her	E-box *(CANNTG)* N-box *(CACNAG)*
C	bHLH-PAS	unknown	Sim, ARNT	*(ACGTG)* *(GCGTG)*
D	HLH	antagonists of group A	Id, Emc	no DNA binding

Table 1.2: **Subdivision of the bHLH family in monophyletic groups and their function.** After Fisher and Caudy, 1998 [32].

1.2.2 The Hairy and Enhancer of split (Hairy/E(Spl)) family

Over the past decade, numerous vertebrate proteins structurally related to the Drosophila Hairy and Enhancer of split bHLH proteins have been identified. They function as transcriptional repressors and regulate a variety of biological processes. Hairy/E(*Spl*) proteins are involved in the control of differentiation [32][117], anterio-posterior segmentation in both vertebrates and invertebrates [118][119][120] and sex determination in flies [121][122].

Comparison of full-length protein sequences suggests the existence of four major subfamilies within the Hairy/E(Spl) family. They are named : Hairy, E(Spl), Hey and Stra13 according to the name of prototype protein for each of these subfamilies (Figure 1.11). All Hairy/E(Spl) proteins are transcriptional repressors, but differences in primary structure between proteins belonging to the different subfamilies imply that members of different subfamilies can be differently regulated at the post-translational level and/or have a distinct mode of action [123].

Although there are differences in the primary structure of Hairy/E(Spl) proteins, several structural features have been conserved among the family members (Figure 1.12).

All members of Hairy/E(Spl) family contain a conserved amino acid sequence known as the Orange domain [124] or helix III/IV domain [125] just C-terminal to the bHLH domain. At present, the molecular function of the Orange domain is unclear. There is evidence that this domain is responsible for the specificity of Hairy for *scute* inhibition in Drosophila [124]. In vertebrates, the Hes1 Orange domain is necessary for Hes1 to inhibit the activation of the *p27* promoter by Mash/E47 complex *in vitro* [126].

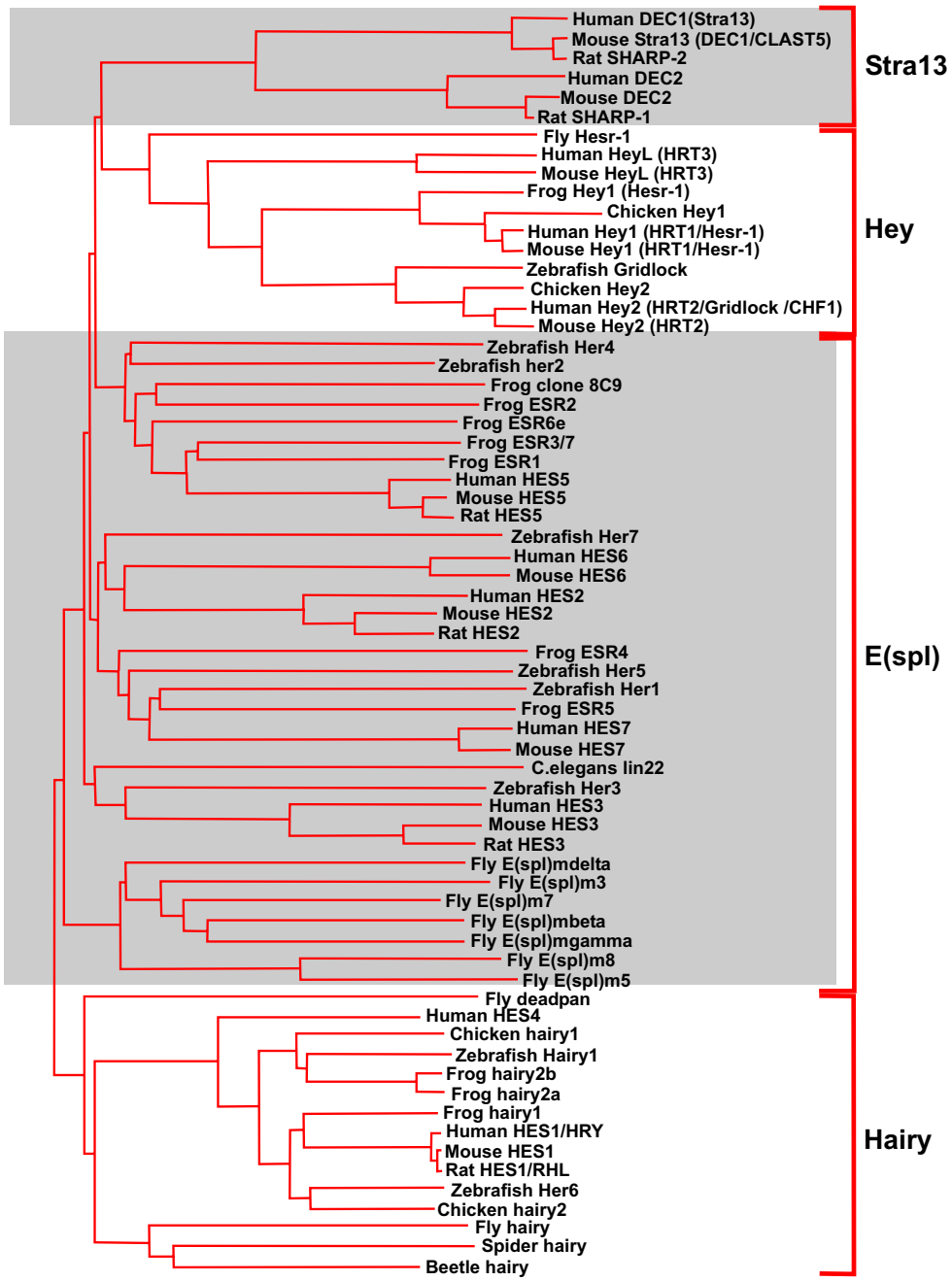

Figure 1.11: **Phylogenetic tree for the Hairy/E(Spl) family.** After Davis and Turner, 2001 [123].

The conserved relationship of the Orange domain with the bHLH domain resembles the relationship between the PAS and bHLH domains in group C bHLH proteins,where the PAS domain acts as an additional dimerization domain [127]. Therefore, the role of the Orange domain could be in the dimerization of Hairy/E(Spl) proteins [128].

Hairy/E(Spl) proteins can bind both E- and N-boxes in the promoter of their target gene with different affinity, which is factor-specific. For example, Hes1 and Hes5 bind to a N-box [129][130][131], while Hes2 proteins preferentially bind to an E-box although they can bind to a N-box with low affinity [132][133]. DNA-binding is mediated by the basic domain. The basic domain of Hairy and E(Spl) proteins differs from other bHLH proteins by the presence of a proline at a conserved position. Hey proteins harbor a glycine residue at the same position, while the basic region of the Stra13 proteins has a proline at a different place (Figure 1.12). The functional significance of these conserved residues is not entirely clear.

Except for the Stra13 proteins, all Hairy/E(Spl) proteins have a conserved C - terminal tetrapeptide motif, either WRPW for the Hairy and E(Spl) subfamilies [134] [135][125], or YXXW for the Hey family (Figure 1.12). This conserved tetrapeptide domain allows recruitment of the transcriptional corepressor Groucho [32] or its vertebrate homologs TLEs.

At present, more than 16 *hairy/E(Spl)*-related genes have been predicted in zebrafish by *in silico* searches [136], of which 10 proved to encode expressed transcripts. Her1, Her4, Her6, Him (Her11) and Her7 are involved in somite formation [137][138] [139][140] [136][141], but only Her1 and Her7 are cycling and both are critically expressed in the presomitic mesoderm (PMS) [138][142]. Her3, Her4, Her5, Her6, Him (Her11) and Her9 are expressed in the developing nervous system [56][143] [36][144] [140][136]. Additionally, Her5 is expressed in the endoderm [66]. Based on the full-length protein sequence, Her6 and Her9 belong to the Hairy subfamily and all others are members of the E(Spl) subfamily [145]. In Drosophila, Hairy proteins control patterning and act upstream of Notch, while members of E(Spl) subfamily act as downstream effectors of Notch in the lateral inhibition process. In vertebrates this distinction has not been conserved. In zebrafish, *her* genes acting downstream of Notch are *her1* and *her7* in the somite development [146][143] and *her4* in neurogenesis [146].

1.2.3 Repression mechanisms by the Hairy/E(Spl) proteins

Biochemical and genetic studies lead to postulating three possible mechanisms of repression by Hairy/E(*Spl*) proteins (Figure 1.13). The first mechanism is DNA binding-dependent transcriptional repression, also known as active repression [117][147]. According to this mechanism, Hairy/E(*Spl*) homo- or heterodimers bound to the DNA-consensus site recruit the corepressor Groucho or its mammalian homolog TLE via the WRPW domain [148][149][150]. Groucho then recruits the histone deacetylase (Rpd3 in Drosophila or HADC in vertebrates) which may repress transcription by altering local chromatin structure [151].

The second mechanism is passive repression [130][152] involving protein sequestration. Hairy/E(*Spl*) proteins utilizing this mechanism form non-functional heterodimers with other bHLH factors normally functioning as common partners of tissue specific

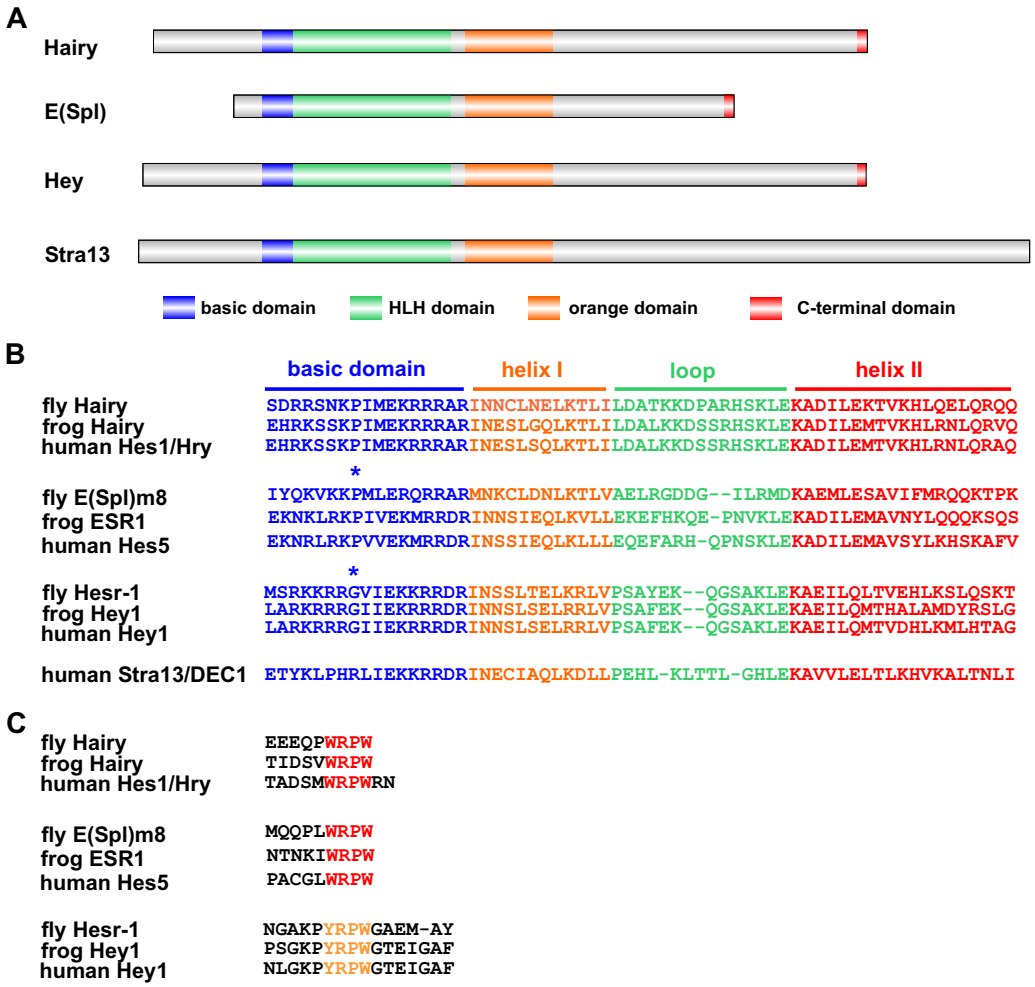

Figure 1.12: **Hairy/E(Spl) proteins share main structural features.** **(A)** Schematic representation of the conserved domains within the Hairy/E(Spl) family. The bHLH and Orange domains are present in all family members, while the C-terminal domain is missing in the Stra13 subfamily. Conserved domains are color-coded. Light gray labeled domains are not generally conserved, but might contain one or a few motifs shared within a subfamily. Alignment of the bHLH **(B)** and C-terminal **(C)** domains of selected Hairy/E(Spl) factors. The asterisk indicates the conserved proline found in Hairy and E(Spl) subfamilies, and the conserved glycine at the same position in the Hey subfamily. Most of the Hairy and E(Spl) proteins end with WRPW, but a small subset (human Hes1, zebrafish Her7, mouse and human Hes7, etc.) ends with additional less conserved amino acids. The C-terminal domain of all Hey-like proteins contains a YRPW motif, with a generally conserved 6-10 amino acid extension. After Davis and Turner, 2001 [123].

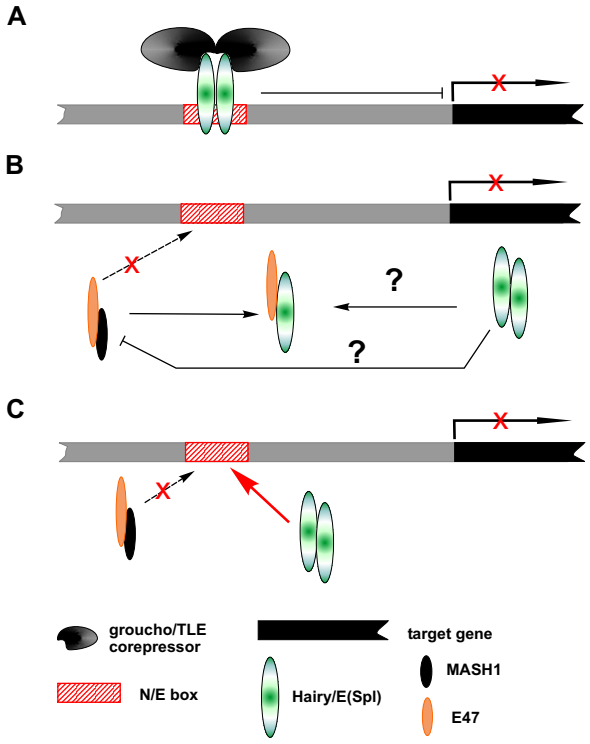

Figure 1.13: **Repression mechanisms of the Hairy/E(Spl) proteins.** Three possible mechanisms have been postulated: binding DNA dependent transcriptional repression (**A**), protein sequestration (**B**) and the Orange domain based repression (**C**).

bHLH factors, such as E47. Therefore, they disrupt formation of the functional heterodimers such as MyoD-E47 in the muscle tissue or Mash-E47 in the neural tube.

The third mechanism is mediated by the Orange domain and is based on the ability of the Hes1 Orange domain to repress both the *hes1* and $p27^{WAF}$ promoters [126].

1.3 Development of the MH domain - the role of the MHB -

As described above, the embryonic MHB is the source of a crucial progenitor pool, controlled by Her5 expression in zebrafish. Strikingly, the MHB also hosts a "secondary neural plate organizer", the isthmic organizer (IsO). The IsO is necessary [153][154] and sufficient [155][156][157] for the development of mesencephalic and metencephalic structures. It lies at the junction between the midbrain and hindbrain,

called midbrain-hindbrain boundary (MHB). Because IsO activity might impinge on Her5 function and/or neurogenesis control, I will summarize below current knowledge on IsO formation and function. For a more comprehensive and detailed picture the reader is referred to the recent reviews [158][159][160].

1.3.1 Induction of the IsO at the MHB

Transplantation experiments in the avian embryo revealed IsO activity for the first time. Ectopic transplantation of tissue encompassing the MHB into other locations, such as diencephalon, resulted in the ectopic induction of genes specific for the midbrain-hindbrain (MH) around the graft [156][157] [161][162][163], and in a corresponding fate change in the host territories: the tissue in contact with the graft adopted a MH fate at the expense of its natural (for example diencephalic) identity. Conversely, prosencephalic tissue grafted to the isthmus region acquired MH gene expression patterns and fate [155][164][165]. Interestingly, the induced MH tissue was always polarized, like its endogenous counterparts, such that the caudal portion of the ectopically induced mesencephalon and the rostral side of the ectopically induced metencephalon were in contact with the isthmic graft in all experiments [156] [157] [161][163][165]. Additionally, ablation experiments showed that complete removal of the isthmus results in the loss of the entire mesencephalon and metencephalon [153][154][166]. Therefore, IsO activity is necessary and sufficient for the development of the entire MH domain, controlling both the growth and the ordered rostrocaudal specification of the MH domain.

These results, later refined by mutant analyses in the mouse and zebrafish (recently reviewed in [159][158][160]), indicate that positioning of the IsO is a crucial event in the development of the entire MH domain. The spatio-temporal sequence of the molecular events involved in IsO positioning and maintenance seems to be conserved throughout evolution. Nevertheless, subtle differences have been noticed among different species, mainly in the relative onset of expression of different genes.

The rostral epiblast becomes polarized during gastrulation (end of gastrulation in the mouse at embryonic stage E7.5 and 65 % epiboly in zebrafish) according to the largely complementary expression of two homeobox containing genes, *Otx2* and *Gbx2* (in zebrafish *gbx1*) (Figure 1.14A). *Otx2* is expressed within the presumptive forebrain and midbrain region, with its posterior border adjacent to the anterior border of *Gbx2* expression, defining the anterior hindbrain [168][169]. The meeting point of the territories expressing these two genes, which is still fuzzy at this stage, seems to identify the future position of the MHB and IsO [170]. Indeed, series of loss-of-function [168][171][172] and gain-of-function experiments [173][174][175] revealed that the relative doses of Otx2 and Gbx2 proteins control the induction and positioning of the IsO and therefore the development of midbrain versus anterior hindbrain fates (Figure 1.15).

Following *Otx2*/*Gbx2* expression, the transcription factor Pax2 (*pax2.1* in zebrafish) and the secreted glycoprotein Wnt1 are expressed in broad, overlapping domains at the onset of somitogenesis (embryonic stage E8) in the mouse or at the end of gastrulation in zebrafish (Figure 1.14B). *Wnt1* expression is largely restricted to the

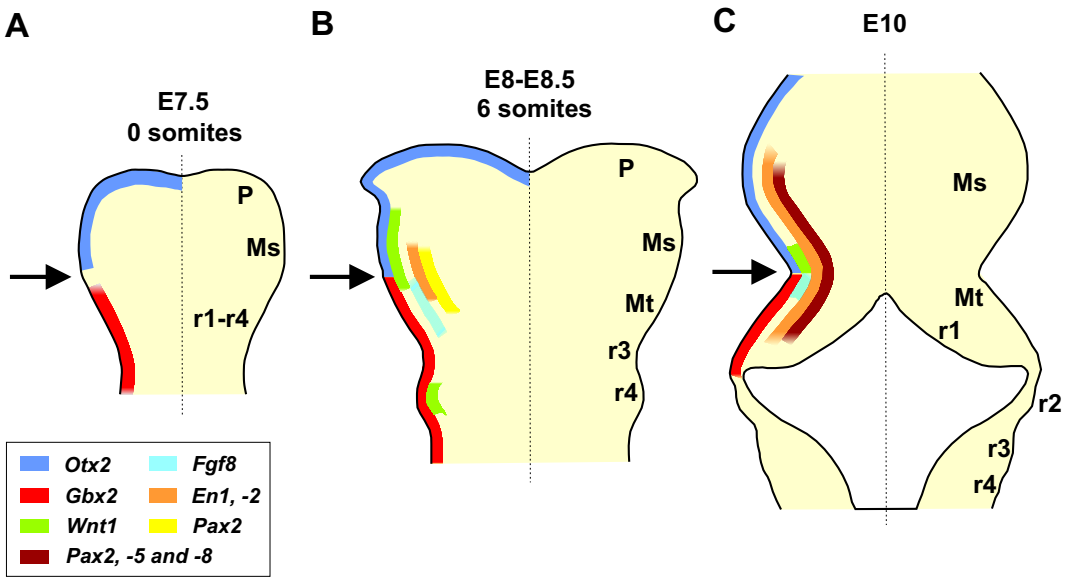

Figure 1.14: **Dynamics of gene expression patterns at the midbrain-hindbrain junction.** Dorsal views of the mouse embryonic neural plate at **(A)** the 0 - somite stage, **(B)** 6 - somite stage and **(C)** E10 stage, anterior to the top. At the end of gastrulation **(A)**, the neural plate is subdivided into the anterior part, expressing *Otx2* and posterior part, expressing *Gbx2*. Expression of the two genes meet at the future MHB position and form decreasing gradients in opposite directions. At this stage, the border between *Otx2*- and *Gbx2*-expression domain is still fuzzy. At 6 somites **(B)**, this border becomes sharp. *Wnt1* expression is initiated in the mesencephalon, and *En1* followed by *En2* and *Pax2* are turned on across the *Otx2*/*Gbx2* border. Slightly later, *Fgf8* expression is initiated caudally to the future MHB. **(C)** At the E10 stage, the expression domains of *Wnt1* and *Fgf8* become restricted to narrow rings rostral and caudal to the MHB, respectively. The expression domains of *En1* and *Pax2* narrow as well, but still cross the MHB. On the other hand, *En2*, *Pax5* and *Pax8* are expressed across most of the midbrain-hindbrain domain. An arrow indicates the position of the MHB. Abbreviations: Ms: mesencephalon; Mt: metencephalon; P: prosencephalon; r: rhombomeres. After Wurst and Bally-Cuif, 2001 [159].

Otx2-positive territory [176], while *Pax2* crosses the *Otx2*/*Gbx2* border [176]. Shortly after, the transcription factors *En1* (at the 1-somite stage), *En2* (at the 3-5-somite stage) [177][178] and *Pax5* (at the 3-5-somite stage) [159] become expressed across the future MHB. Finally, expression of the fibroblast growth factor 8 (Fgf8) gene is initiated simultaneously with *Pax5* and *En2* and confined to the rostral part of the *Gbx2* positive area (Figure 1.14B) [179].

These results indicate that the boundary between the midbrain and hindbrain

is roughly positioned during late gastrulation, but progressively refined during early somitogenesis.

1.3.2 Feedback loops maintain the MHB

During the establishment phase *Otx2*, *Wnt1*, *Gbx2*, *Fgf8*, *En* and *Pax* expression domains are mainly formed independently, since the induction of expression of other genes is generally not perturbed in the mutants harboring mutation in any of above mentioned genes. Expression domains of these genes are established in response to

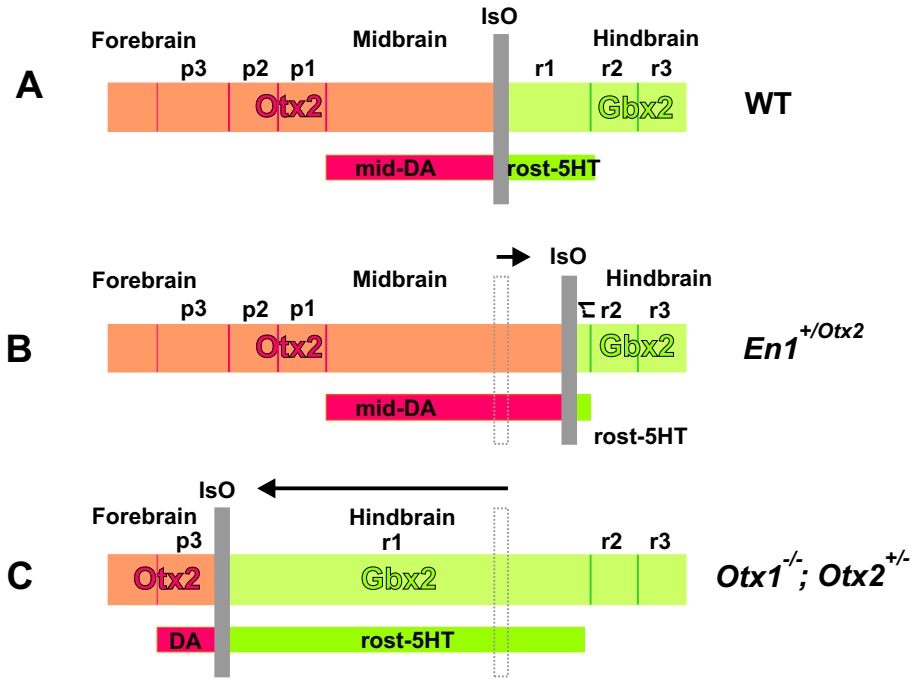

Figure 1.15: **The position of the IsO controls the size and location of the midbrain dopamine-producing (mid-DA) and rostral hindbrain serotonin-producing (rost-5HT) neuronal populations.** **(A)** In wild-type (WT), mid-DA neurons are generated in the ventral midbrain rostral to the IsO within the *Otx2* expression domain, whereas rost-5HT neurons develop in the ventro-rostral hindbrain, caudal to the IsO within a *Gbx2*-positive territory. **(B)** Shifting of the *Otx2*-positive domain and IsO caudally in $En1^{+/Otx2}$ mice induces expansion of the mid-DA population at the expense of the rost-5HT cell population. **(C)** Reduced Otx dosage in $Otx1^{-/-}$; $Otx2^{+/-}$ mice results in the repositioning of the IsO in the forebrain. mid-DA neurons are still formed rostral to the IsO at new ectopic position, but in smaller number. The rost-5HT cell population is expanded to the new caudal border of the IsO. Abbreviations used: p: prosomere; r: rhombomere, IsO: isthmic organizer. From Brodski *et al.*, 2003 [167].

different developmental cues. For example, the axial mesoderm provides signals necessary for maintenance of the *Otx2* expression, Fgf4 is important for *En* expression while posteriorly expressed Wnts, Fgfs and retinoic acid might be involved in *Gbx2* induction. Soon after the initiation phase, expression of these factors become interdependent via a series of positive and negative interactions necessary to maintain the MHB and its organizing activity. Positive interactions between Fgf8, En1, Wnt1 and Gbx2 maintain their own expression, whereas the sharp posterior border of *Otx2* expression is a result of the negative reciprocal interactions between Otx2 and Gbx2 or Fgf8 [180].

It has been shown that the complete or partial knock-out of Wnt1 [181] or Fgf8 [182] in mouse (equivalent results have been obtained with zebrafish mutants *ace* or Df^{w5} lacking functional Fgf8 [63] or Wnt1 and Wnt10 [183]proteins, respectively) lead to the gradual disappearance of both mesencephalic and metencephalic structures, indicating that these genes might be involved in the maintenance or activity of the IsO. On the other hand, beads that are soaked with Fgf8 and implanted into the diencephalon or rhombencephalon triggered the ectopic expression of the mes-metencephalic markers such as En1, En2, Pax2, Pax5 and Pax8 [184][185][186]. As *Fgf8* is normally expressed after the onset of *Pax* and *En* expression, the effect of the beads most likely does not correspond to role of Fgf8 in IsO in induction, but rather in the maintenance of the organizer after its induction by activating a positive feed-back loop that involves Fgf8, Wnt1, En and Pax (Figure 1.16). These experiments also highlight Fgf8 as the crucial factor for the maintenance but not the initiation of marker genes expression at the MHB [63][187][188].

Negative feed-back regulatory loops also take place in the MH domain in order to constrain the development of mesencephalic and metencephalic fates to the MH. There are two sources of negative influence at the MHB, located within the MH itself or in adjacent territories (Figure 1.16).

Within the MH domain, the negative feedback loops are initiated by IsO activity. Fgf8 triggers expression of the Fgf signaling inhibitors of the Sprouty family in the MH domain, which then suppress the influence of Fgf8 under a certain threshold of Fgf8 protein [189]. Similarly, Fgf8 positively regulate Sef proteins, which then antagonize Ras/Raf/MEK/MAPK-mediated Fgf signaling [190]. Thus, Sef and Sproutys function synergistically to restrict IsO activity [191]. In addition, the transcriptional inhibitor Grg4, expressed across the MH domain, can down-regulate *En* expression and activity and antagonize Pax5 activity. At the same time it induces *Pax6* activity and promotes diencephalic development (Figure 1.16) [192].

Outside of the MH domain, Pax6 blocks expression of En and Pax2 to position the mesencephalic-diencephalic boundary anteriorly [193][194][195], and the homeobox containing protein Hoxa2 in rhombomere 2 also inhibits these factors to prevent caudal expansion of the cerebellar primordium [186][196].

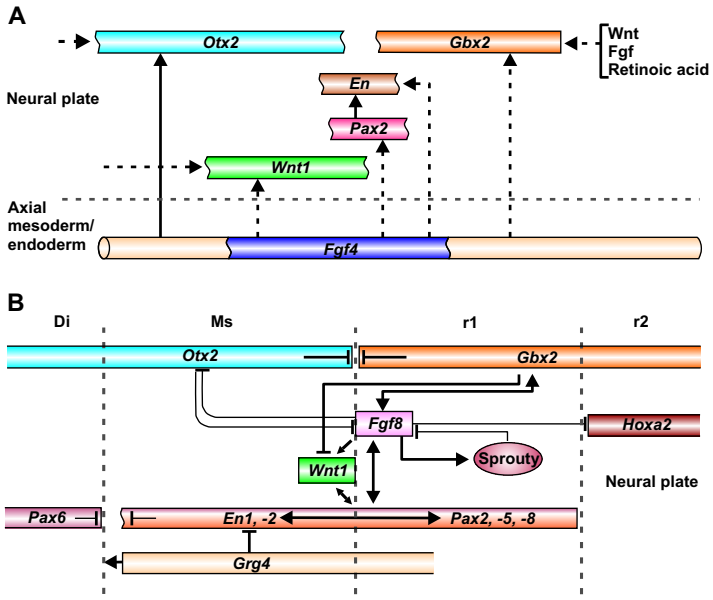

Figure 1.16: **Genetic interactions of midbrain-hindbrain induction and maintenance. (A)** Gene expression patterns in the neural plate (top) or the underlying axial meso/endoderm (bottom), anterior to the left. Vertical arrows represent vertical interactions, horizontal arrows depict planar interactions, and hatched arrows are hypothetical. During gastrulation, the anterior mesoderm is necessary to maintain *Otx2* expression in the anterior neural plate. The mechanisms that regulate *Gbx2* expression are unknown, but posteriorizing influences via Wnt, Fgf or retinoic acid might be involved. *Fgf4* expressed by the axial mesoderm might directly or indirectly induce *En* expression. *En* expression is also dependent on *Pax2* function. **(B)** Gene expression patterns within the neural plate during early somitogenesis, anterior to the left. After the initiation phase, *Gbx2* expression maintains *Fgf8* expression, whereas *Otx2* and *Gbx2*/*Fgf8* regulate each other negatively, leading to the establishment and maintenance of sharp expression borders. Concomitantly, the expression territories of *Fgf8*, *Wnt1*, *En1*, *En2*, *Pax2*, *-5* and *-8* become interdependent and establish a positive regulatory loop that is necessary to maintain midbrain-hindbrain identity. At least two negative feedback mechanisms that involve Sprouty and *Grg4* restrict the expansion of the positive regulatory loop along the anteroposterior axis. The mid-diencephalic border is positioned in parallel by negative cross-regulations of *En1*, *-2*/ *Pax2*, *-5*, *-8* and *Pax6*, whereas *Fgf8* exerts a negative influence on the caudal expression of Hox genes, positioning the border between rhombomeres 1 and 2. Abbreviations used: Di: diencephalon; Ms: mesencephalon; r1: rhombomere 1; r2: rhombomere2. After Wurst and Bally-Cuif, 2001 [159].

1.3.3 MHB development and neuronal differentiation in the MH domain

Early neuronal populations in the MH domain

Several neuronal types with distinct roles [197][198] develop within the mesmetencephalic territory in stereotyped locations along the anteroposterior and dorsoventral axes. The motorneurons of cranial nerve III and the dopaminergic neurons of the

substantia nigra develop in the ventral tegmental area[2] of the mesencephalon in mouse [199], but not in zebrafish, rostral to the MHB and IsO. Caudal to the MHB, motorneurons of cranial nerve IV and serotonergic neurons of the raphe nuclei appear in the basal plate of the metencephalon [197]. Finally, noradrenergic neurons of the locus coeruleus are formed in the metencephalic alar plate (Figure 1.17).

Motorneurons, midbrain dopaminergic neurons and serotonergic neurons of the raphe nuclei are induced close to the floor plate and it has been shown that this induction is dependent on floor plate-derived signals, which can be mimicked by graded doses of Shh [201][202][203] [200][204][205]. Since *Shh* is expressed along the entire floor plate, other factors have to be involved in the positioning of these neural populations along the anteroposterior axis. Indeed, experiments where IsO was shifted rostral or caudal from its original position revealed the importance of the IsO in controlling the location and size of the mesencephalic dopaminergic and rostral hindbrain serotonergic cell populations (Figure 1.15) [167]. Fgf8 coming from the IsO is likely to be one local factor involved in the development of the midbrain dopaminergic neurons [200].

Nevertheless, Shh and Fgf8 alone are not able to induce dopaminergic neurons, suggesting that the proper induction of these neurones requires integration of anteroposterior and dorsoventral signalling. One hypothesis could be that the crucial factor to be associated with Fgf8 and Shh is ventral Wnt. The argument supporting this hypothesis is that, in zebrafish, expression of Wnt is restricted to the MHB and dorsal midline and can not be seen in the ventral part of the midbrain. Therefore, the combination of factors necessary for induction of dopaminergic neurons is not achieved and this neural population is missing in the fish midbrain.

The maintenance of IsO activity requires an undifferentiated state of the MHB

The conditional inactivation of *Otx2* [206] and *Gbx2* [207] at later developmental stages highlighted the involvement of IsO activity in refining restricted compartments within the MH domain, to give rise to the complex cellular organization of the mature brain. Therefore, IsO activity has to be long-lasting. The MHB maintenance loop including Fgf8, Wnt1, Pax and En proteins certainly has a central role in the maintenance of IsO activity, but recent experiments pointed to some additional factors necessary for long-lasting of IsO maintenance. These factors are not part of the MHB maintenance loop, but rather dependent on it. Among these are Hairy/E(Spl) transcription factors present at the MHB in the mouse (Hes1 and Hes3) [48] and in zebrafish (Her5 and Him) [36][140]. The lack of both *Hes1* and *Hes3* genes in compound mouse mutants results in severe patterning defects in the MH domain, with the deletion of midbrain and anterior hindbrain structure [48]. This might be the consequence of a premature termination of IsO activity, and of the premature differentiation of the proliferating MHB neural precursor cells into neurons [48]. Similarly, in zebrafish forced neuronal differentiation induced by ectopic *ngn1* overexpression results in the late loss of MHB integrity [37]. The functional relationship between *Hes* genes and MHB maintenance

[2]Along the dorsoventral axis, the mesencephalon is divided into tegmentum (basal region) and tectum (alar region).

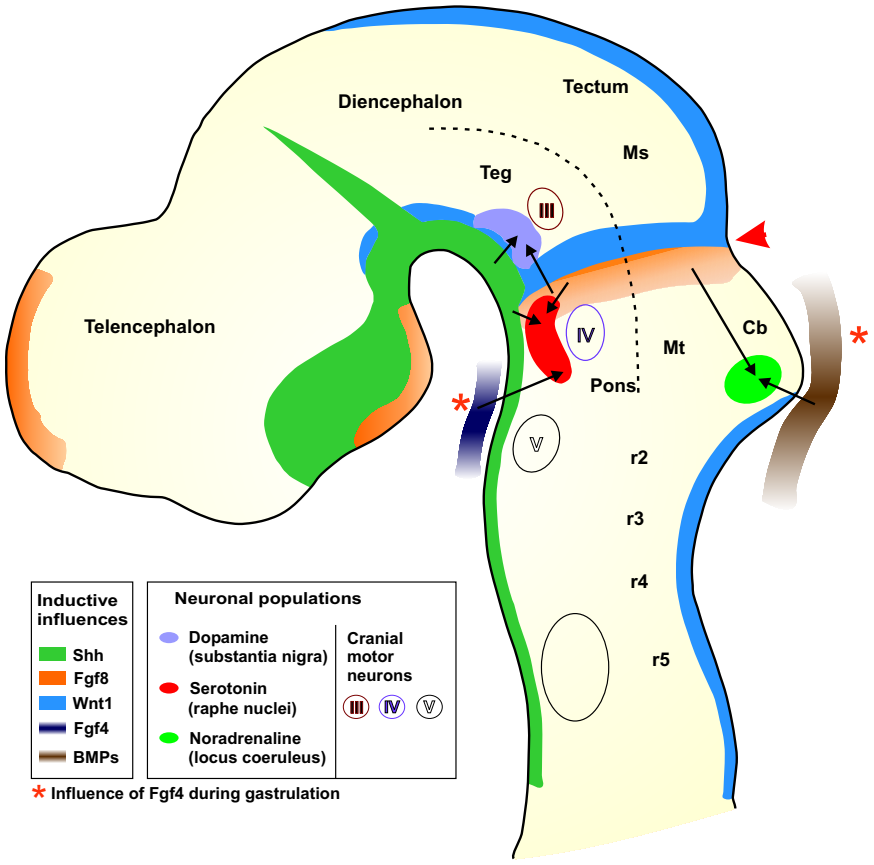

Figure 1.17: **IsO activity is necessary for the proper specification of midbrain-hindbrain neuronal populations.** A sagittal view of a mouse neural tube at E11 is shown, anterior to the left. The MHB is indicated with a red arrowhead. Inductive signals, indicated with the arrows, shown to control neuronal identity originate from the neural plate at the MHB (Fgf8 and Wnt1), the floor plate (Shh) and from non-neural tissues (Fgf4 from the anterior mesoderm, and members of the BMP family from the non-neural, dorsal ectoderm [200]). The combination of Fgf8 and Shh provides inductive information for midbrain dopamine-producing neurons, while these factors together with Fgf4 specify serotonin-producing neurons in the rostral hindbrain. Noradrenergic neurons of the *locus coeruleus* are induced by the combination of Fgf8 from the MHB and bone morphogenetic proteins (BMPs) secreted from the adjacent non-neural dorsal ectoderm during gastrulation. Abbreviations used: Ms: mesencephalon; Mt: metencephalon; Cb: cerebellum; r: rhombomere. After Wurst and Bally-Cuif, 2000 [159].

loop genes has not been studied, but in zebrafish expression of *her* genes at the MHB is downstream of the IsO genes during the maintenance phase. Thus, keeping the MHB

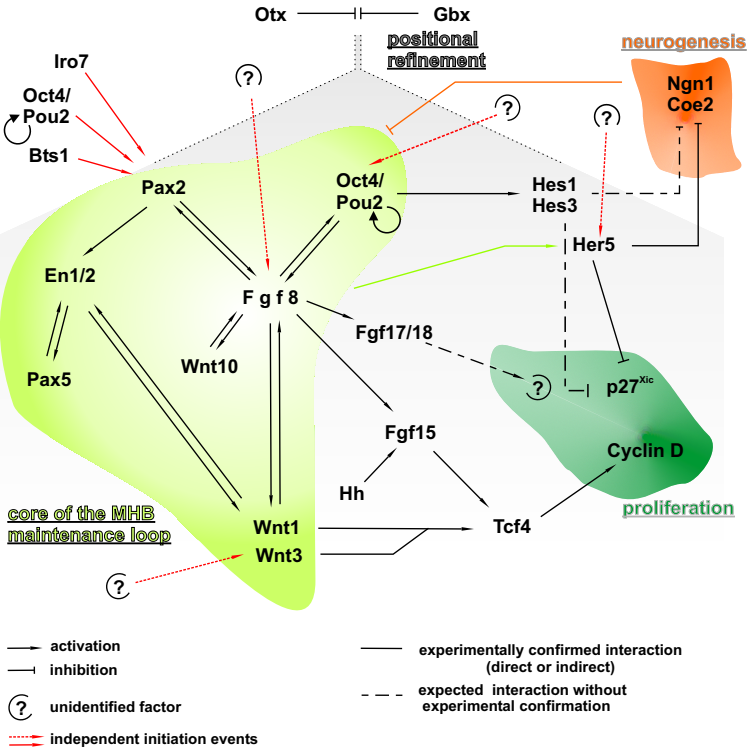

Figure 1.18: Factors involved in the synchronization of patterning signals, neurogenesis and proliferation at the MHB

undifferentiated is crucial not only to permit the development of the full complement of neurons, but also to permit late IsO function.

Synchronization of patterning signals, neurogenesis and proliferation at the MHB

Transplantation experiments in chicken as well as loss- and gain-of-function experiments in mouse and zebrafish suggest that the specification and patterning of the MH domain is a highly complex process, requiring the spatiotemporally coordinated interaction of signals located in the neuroectoderm, but also in the non-neural tissue along the A/P and D/V axes of the developing embryo. Signaling molecules originating from these centers and their effectors in the MH area establish and control a complex molecular network the underlying specification of divergent, but ordered midbrain-hindbrain structures in the mature brain.

The high interdependence between the factors implicated in the A/P or D/V patterning, proliferation and neurogenesis control is demonstrated by the following

findings:

- The expression of neurogenesis inhibitors (e.g. *her5*) is influenced by the IsO [37].
- Both *her5* and IsO factors (e.g. Wnt1, Wnt3, Wnt11, Fgf15, Fgf8, Fgf17) control proliferation [208][209][210][211].
- In addition to promoting proliferation, IsO activity is also involved in the control of neural differentiation [206][212][213][214].

A synopsis of the most prominent factors identified in chicken, mouse and zebrafish, as well as their interactions in controlling MH patterning, neurogenesis and proliferation is shown in Figure 1.18.

1.4 The brain reward system

Animal behavior results from the activity of three large brain functional systems controlling arousal, reward and cognition. The close interaction of these systems is necessary for the proper functioning of the organism and its interaction with the environment.

The reward system is involved in awarding positive feelings (e.g. for pleasurable or good actions) as well as negative feelings (e.g. for the punishment of wrong action). A reward system has been evidenced in many vertebrates (goldfish, guinea-pig, dogs, cats, rats, dolphins, monkeys and humans) and its functionality is classically revealed through stimulation experiments. In humans, electrical stimulation of the sites evoking pleasure elicit general feelings of bliss, happiness and unusual well-being, while stimulation of aversive sites cause a feeling of anxiety, approaching danger, isolation and abandonment. The pleasure centers are connected with the ascending projection of mesencephalic dopaminergic neurons in the median forebrain bundle [215] and their terminals in the prefrontal cortex [216]. On the other hand, aversive centers are located in the periventricular system and they receive modulatory inputs from GABA-ergic and serotonergic neurons of the anterior *raphe nuclei*. Thus, two neural populations deriving from the embryonic MH domain in higher vertebrates, the mesencephalic dopaminergic population and the serotonergic population of raphe nuclei located in the hindbrain, play a key role in the brain reward system.

The following sections will review the brain reward system and the roles of the dopaminergic and serotonergic systems in more detail. Additionally, the most common disease of the brain reward system, addiction, will be described.

1.4.1 Dopaminergic neurons play a central role in the brain reward pathway

At present, it is unquestionable that dopamine plays the key role in motivational behavior and consequently in addiction. The dopaminergic theory of reward is principally based on findings showing that the structures involved in feeling pleasure are also

sensitive to dopamine [217]. According to this theory, the mesencephalic dopaminergic system of the ventral tegmental area (VTA) is the anatomical basis of the reward system [218]. Dopaminergic neurons of the VTA project to the limbic system structures, especially to the shell of the nucleus accumbens and prefrontal cortex [218]. In response to pleasurable activities such as feeding, drinking, sexual activity or the consumption of drugs of abuse, dopaminergic transmission in the nucleus accumbens septi is increased. Recent studies showed that the main increase in dopaminergic transmission occurs at the beginning of the pleasurable activities, when pleasurable experience is anticipated [219]. According to Di Chiara and North [220], reward consists of two successive phases: the incentive phase, in which a pleasure is anticipated, and the consummatory phase, that is the experience of the pleasurable stimulus. It appears that dopamine contribution dominates in the first phase. However, low pleasure during the consummatory phase causes a reduction of the dopamine signal if the incentive phase is repeated. This suggests that response of mesencephalic dopaminergic neurons is subject to learning, taking into account an anticipated error in the expectation of a reward [221].

However, dopamine is not the only neurotransmitter engaged in rewarding behavior. Indeed, dopamine-transporter knock-out mice, whose synaptic dopamine level is much higher than in normal animals, can still activate a reward system and get addicted to cocaine [222]. As cocaine also influences the serotonin transporter, the serotonergic system is likely also involved in the reward pathway.

1.5 Addiction

Drug addiction should be considered as a complex disease of the central nervous system, characterized by the compulsive, uncontrolled craving for drug, its seeking and striving to get it at all costs, and its use despite obvious, serious health- and life-threatening consequences. Addiction is utilizing the components of the brain reward system and it can be assumed as a disease of this system.

1.5.1 Anatomical targets of addictive substances

The reward system comprises a number of brain structures involved in feeling both pleasure and aversion [223]. Nevertheless, an essential role in addiction has been ascribed to the mesocorticolimbic system, which encompasses the ventral tegmental area, the nucleus accumbens, the prefrontal cortex, the hippocampus and the pedunculopontine nucleus. Despite the fact that the final rewarding effect is connected with an elevation of dopamine release in the nucleus accumbens [224], different parts of the limbic system seem to be targets of particular drugs of abuse.

Addictive effects localized in the ventral tegmental area

The VTA is the place where some rewarding effects of morphine are localized [225][226]. Both μ- and δ-opioid receptor agonists exert their reinforcing effect via this

region [227][228]. μ-receptor agonist block GABA receptors on dopaminergic neurons and cause their disinhibition and the subsequent release of dopamine [229].

The VTA is also associated with nicotine addiction. Nicotine receptors located on the dopaminergic neurons in the VTA induce dopamine neuron firing and the release of dopamine after ligand binding [230][231]. Additionally, VTA neurons form synapses with cholinergic neurons of the laterodorsal tegmental nucleus and the pedunculopontine nucleus, believed to be involved in nicotine addiction.

Addictive effects localized in the nucleus accumbens

The nucleus accumbens is a heterogenous structure composed of two functionally distinct parts: a ventromedial shell and a laterally and dorsally located core. The cells of the shell, believed to be an extended part of the amygdala, project to the VTA and contribute to the brain reward system. Thus, these cells are the biological substrate for the action of drugs acting at the nucleus accumbens level. Neurons of the core are projecting more strongly to the zona compacta of the substantia nigra and they are involved in the control of locomotor systems [232].

The shell of the nucleus accumbens is the structure where the action of addictive psychostimulants such as cocaine and amphetamine are localized. After peripheral administration of these drugs, dopamine levels are elevated in this brain region [233][234][235]. Dopamine is released in the shell of the nucleus accumbens in response to cocaine or amphetamine administration during both the incentive phase and the consummatory phase of reward [236][237][238][239]. Although, it is believed that cocaine and amphetamine have similar mechanisms of action, they differ with respect to the targets for their addiction-evoked action. Rats readily self-administrate amphetamine into the nucleus accumbens [240][241], while cocaine self-administration can be obtained only with significantly higher doses received over a long time period [242].

Additionally to cocaine and amphetamine, the shell of the nucleus accumbens also seems to be a place of action for morphine and met-enkephalin [243][244]. In contrast to psychostimulants, morphine and met-enkephalin action is independent of the effects in the VTA [243].

Addictive effects in the prefrontal cortex

The prefrontal cortex responds to cocaine action. Rats readily self-administrate cocaine into the medial region of the prefrontal cortex, even if the doses used are significantly smaller than those evoking addiction in the shell of the nucleus accumbens [245].

The prefrontal cortex is also the key structure in developing sensitization to psychostimulants. Behavioral sensitization is the augmented motor-stimulant response that occurs with repeated, intermittent exposure to cocaine and amphetamine [246][219]. The prefrontal cortex is a terminal region of the mesocorticolimbic dopamine system and changes in both dopamine and serotonin transmission in this region are likely to be responsible for sensitization in response to repeated drug administration. Repeated cocaine and amphetamine administrations decrease dopamine overflow in the prefrontal

cortex [247][248][249][250], and this decrease is associated with an increased capacity to clear dopamine via the dopamine transporters [251][252]. Further, reports indicate that acute amphetamine and cocaine administration decrease serotonin transmission in the prefrontal cortex due to the an increased number of serotonin transporters in the prefrontal cortex and an increase in autoreceptor-mediated inhibition of dorsal raphe serotonin neurons [253]. Thus, sensitization to cocaine and amphetamine may be associated with decreased serotonin and dopamine transmission in the prefrontal cortex, most likely due to permanent changes in the level of their transporters.

Addictive effects in the hippocampus

The hippocampal formation has been linked with memory processes rather than addiction, but opioids, morphine and α-dynorphin are readily self-administrated by rats into the CA3 region of the hippocampus [254][255].

Addictive drug effects in the pedunculopontine nucleus

The addictive action of morphine and amphetamine are also associated with the pedunculopontine nucleus, since lesions of this brain structure inhibits morphine- and amphetamine induced place preference [256]. In addiction, cholinergic neurons of these nuclei activate nicotinic receptors on dopaminergic neurons in the VTA and induce dopamine release within the brain reward system [257][258].

The centers involved in drug addiction in higher vertebrates are presented in Figure 1.22

1.5.2 Neural basis for addiction in zebrafish

The reward pathway and addiction have been extensively studied in mammals, in particular in rodents. Sections 1.4.1 and 1.5.1 shortly summarize the current knowledge obtained in these studies. Recent experiments have convincingly shown a functional conservation of the reward pathway among not only the amniotes but all vertebrates [259][260]. For example, amphibians do have separate clusters of dopaminergic neurons in the basal midbrain and diencephalon which project to the striatum proper (mesostriatal system) and to the nucleus accumbens (mesolimbic system), respectively [259][260].

Identification of the functionally analogous structures in teleosts, including zebrafish, has been difficult due to several reasons: (*i*) dopaminergic cells are missing in the teleost midbrain, (*ii*) the nucleus accumbens or an analogous structure has not been identified in zebrafish and finally (*iii*) the telencephalic hemispheres are everted in zebrafish and the location of the lateral subpallium is not clear. Nevertheless, tyrosine hydroxylase (TH)-positive cells can be seen in the rostral part of the posterior tubercle in zebrafish, similarly to amphibians [259][260]. These cells project to the ventral telencephalon and therefore might represent the meso-striatal and meso-limbic systems in teleosts [261].

Additionally, there are some improvements with regard to recognizing the teleostean basal ganglia. Namely, the dorsal nucleus of area ventralis telencephali receives direct

ascending spinal projections in zebrafish [262], reminiscent of such a projections to the nucleus accumbens in various mammals [263][264]. This projections together with high levels of D_1 dopamine receptor [265] and glutamate decarboxylase expression [266] would be expected features of striatal structures when compared to the situation in mammals.

Finally, TH immunoreactive cell bodies of the posterior tuberal nucleus project to the pallium in goldfish [267] and zebrafish [261], suggesting that posterior tuberal nucleus may represent the meso-cortical system in zebrafish.

Thus, these anatomical studies in zebrafish as well as the functional studies performed in other teleost [268][269] suggest that the ascending dopaminergic system of zebrafish could be considered as homologous to the ascending dopaminergic system in mammals despite the difference in location in the adult midbrain and forebrain. Therefore, I postulate the existence of the neural network necessary to activate the reward pathway in zebrafish, and the formal proof for this hypothesis is presented in the Article in Appendix B.

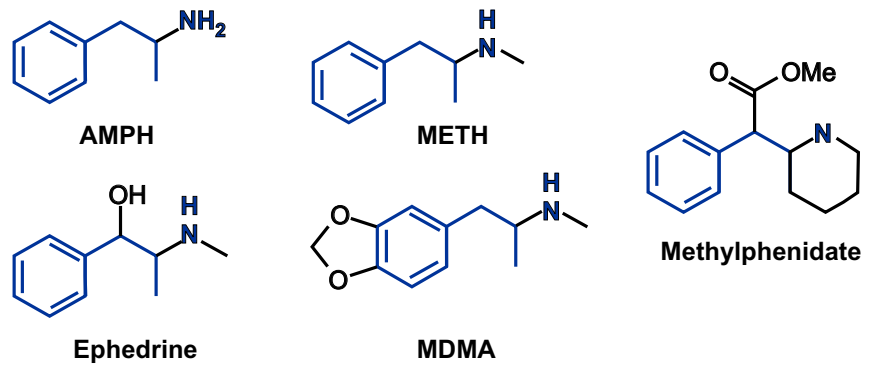

Figure 1.19: **The chemical structure of the most commonly used amphetamines.** The common structural features are highlighted in blue. Abbreviations: AMPH: amphetamine; METH: methamphetamine; MDMA: 3,4 - methylenedioxymethamphetamine (ecstasy)

1.5.3 Amphetamines - structural characteristics

Amphetamine and substituted amphetamines, including methamphetamine, methylphenidate (Ritalin), methylenendioxymethamphetamine (ecstasy), and the herbs khat and ephedra, encompass the widely administrated class of drugs that predominantly release neurotransmitters, mainly catecholamines, by a non-exocytic mechanism. The main structural features of the amphetamines are: an unsubstituted phenyl ring, a two-carbon side chain between the phenyl ring and nitrogen, an α-methyl group and a primary amino group (see Figure 1.19) [270].

The most commonly used compounds within the amphetamine class are amphetamine and methamphetamine. Although they have a different chemical structure, these two drugs show no differences in terms of eliciting dopamine release, in their elimination rates or other pharmacokinetic properties [271]. Additionally, the two drugs induce indistinguishable behavior in humans [272].

1.5.4 Mode of action of amphetamines

As mentioned above, dopaminergic transmission plays an important role in the brain reward system and addiction development. The synaptic event characterizing dopaminergic transmission can vary depending on the amount of released dopamine, the sensitivity of dopamine receptors, and the length of time dopamine spends in the synaptic space. Thus, regulation of dopamine trafficking at the level of the presynaptic membrane, mainly via the dopamine transporter (DAT), crucially influences the brain reward system. DAT is also the site of action of many drugs, including the psychostimulants amphetamine and cocaine [273][274][275].

Dopamine transporter - function in dopamine trafficking

The key mechanism regulating the level of extracellular dopamine is its reuptake into the cytosol [276], mediated by the DAT (Figure 1.20).

DAT is crucial for the clearance rate of dopamine within the terminal fields, although it is equally distributed between the synaptic bouton, the axon, soma and dendrites [277][278]. DAT knock-out mice are characterized by a 300-fold increase in the persistence of extracellular dopamine within the striatum, followed by a decrease in dopamine tissue content, desensitization and down-regulation of both presynaptic and postsynaptic dopamine receptors, and a decrease in the magnitude of quantal exocytotic dopamine release [279][280]. These findings confirmed the importance of DAT not only for terminating dopamine transmission, but also for synaptic homeostasis as a whole.

DAT belongs to the class of active transporters that utilize the energy stored in the ionic gradients (Na^+/Cl^- in the case of DAT) to reuptake the ligand [276]. Therefore, dopamine influx generates depolarization of the membrane mediated by Cl^- ions. The physiological significance of this depolarization is not clear, but it might increase neural excitability and hence exocytotic amine release during tonic firing [281].

In contrast to the normal inward movement of dopamine, transport mediated by DAT can be reversed and cause the non-exocytotic efflux of dopamine into the perineuronal space. The ability of different compounds to induce reversal transport seems related to their ability to induce current flow as described above [282]. Reversal transport is voltage-dependent and regulated by intracellular Na^+ [282] and Ca^+ [283] concentrations.

Modulation of DAT function by amphetamine

The pharmacological agents that interact with DAT function can be divided into two classes: those that compete for dopamine uptake, and those that prevent

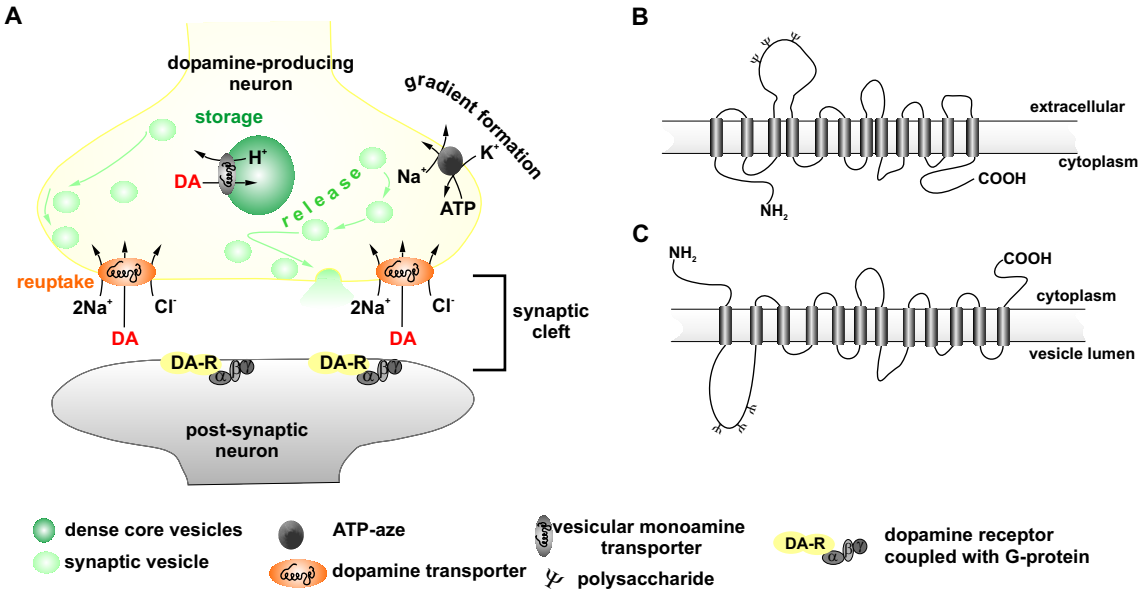

Figure 1.20: **Transporter proteins involved in the uptake of dopamine. (A)** Dopamine trafficking at the synaptic cleft. Exocytotic release of intracellular dopamine increases dopamine concentration in the synaptic cleft. Released dopamine diffuses across the synaptic cleft to bind to its receptor (DA-R). Both diffusion and transporters-mediated transport act to decrease the extracellular concentration of neurotransmitters, thus limiting the stimulation of receptors. Active dopamine reuptake is mediated by the dopamine transporter (DAT), utilizing the energy stored in the sodium gradient generated across the plasma membrane by the Na^+/ K^+-ATP-ase. Once dopamine is transported back into the cell, it can be taken up into vesicles by vesicular monoamine transporters (VMAT), present on both large dense core vesiculaes and on small synaptic vesicles. VMATs energetically couple dopamine transport to the proton electrochemical gradient across the vesicular membrane. The proposed topology and structural features of DAT **(B)** and VMAT **(C)** are based on hydrophobicity analysis of the predicted protein sequences.

dopamine uptake. Amphetamine-like substances belong to the first class and, in addition to interfering with dopamine uptake, also induce DAT-mediated dopamine efflux [273][274].

Several models are used to explain the elevation of extracellular dopamine levels upon amphetamine treatment. According to the *weak base* or *vesicle depletion model*, amphetamine enters the cells as a lipophilic substance and interact with vesicular monoamine transporter (VMAT) on dopamine storage vesicles. This interaction induces dopamine release from the storage place, increase of the cytoplasmical dopamine concentration and alteration of the dopamine gradient across the plasma membrane. This increased gradient would be responsible for dopamine efflux [284][285].

Thus, in this model, dopamine efflux is completely independent from the interaction amphetamine-DAT [285]. In contrast, the *facilitated exchange diffusion model* suggests that dopamine efflux is a consequence of amphetamine translocation into the cell. This model predicts that amphetamine's movement through the transporter would increase the rate of reverse transport by increasing the availability of intracellular-facing DAT to bind dopamine [286][273]. Recent data support the second model, showing that reserpine-like compounds, which displace dopamine from the vesicles into the cytosol, do not cause dopamine efflux [287].

However, the facilitated exchange diffusion model alone cannot explain newer experimental data showing that dopamine efflux is dependent on protein kinase C [288] and on the intracellular concentration of Ca^{2+} [288] and Na^{+} [289][283]. It appeared that an increase in the intracellular Na^{+} concentration is extraordinarily important to revert the DAT cycle and induce dopamine efflux [289][283][290][282]. Thus, according to the *modified facilitated exchange diffusion model*, amphetamine transport via DAT into the cell stimulates DAT-mediated inward Na current, and increases intracellular Na^{+}, which is then essential for amphetamine-stimulated dopamine efflux [283].

Additional mechanisms may also allow the extracellular dopamine concentration to remain elevated upon amphetamine administration. For instance, amphetamine is able to regulate DAT dynamics and functionality. Indeed, in response to acute

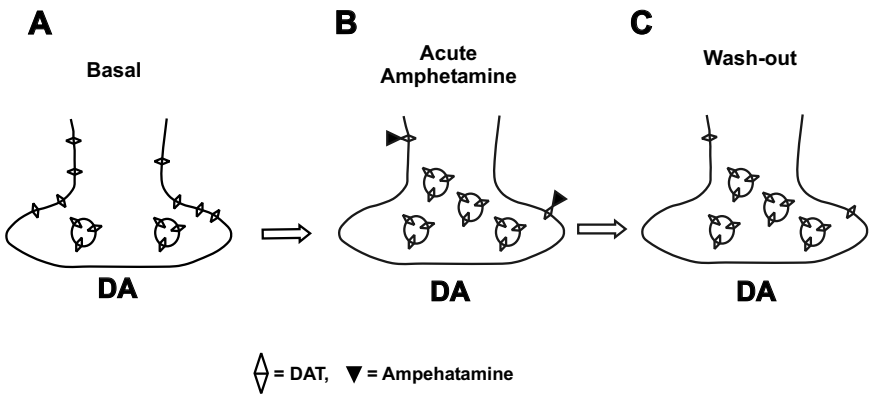

Figure 1.21: **A model for the regulation of dopamine transport capacity by acute D - amphetamine exposure.** **(A)** Under basal conditions, DAT is expressed on both cell surface and intracellular membranes. **(B)** The DAT substrate amphetamine competes with dopamine for uptake and reduces transporter cell surface expression. **(C)** Following amphetamine wash-out, DATs remain located at the intracellular membranes and the extracellular dopamine concentration could remain elevated due to the reduction in transport capacity.

amphetamine application, DAT is redistributed from the plasma membrane to the cytosol (Figure 1.21) [291]. As a consequence the ability of cells to transport dopamine

is significantly lower and dopamine clearance from the synaptic cleft is slower [292][293]. It remains to be determined if DAT undergoes functional modifications prior to its surface redistribution or simply leaves the plasma membrane as an active transporter. Amphetamine-induced DAT redistribution seems to be irreversible [291]. Thus, after amphetamine removal, the reduced transporter capacity of the system would allow extracellular dopamine levels to remain elevated.

1.5.5 Neuronal networks involved in drug addiction

The main nuclei involved in reward have been presented in Section 1.5.1 and, the major component of the drug-reward circuit are midbrain dopamine-producing neurons located in the ventral tegmental area (A10 group). These neurons release dopamine with nerve impulses from axonal varicosities in the striatum, nucleus accumbens and prefrontal cortex [294][295][296] [219][297][298]. Most dopamine neurons show activations after primary rewards (food, water, sex, drugs of abuse, etc.) or conditioned, reward-predicting visual, olfactory and auditory stimuli. Thus, dopaminergic neurons label environmental stimuli with appetitive value, predict and detect rewards and signal alerting and motivating events. The function of the dopaminergic system is supplemented by the activity of numerous neurons producing different excitatory and inhibitory neurotransmitters in the striatum, prefrontal cortex, ventral pallium, amygdala, hippocampus and brain stem, which process specific reward information and regulate the excitability of dopamine-producing neurons but do not emit alerting signals about reward existence (Figure 1.22).

Intracranial self-administration (ICSA) and intracranial place-conditioning (ICPC) studies have shown that the cell bodies of dopaminergic neurons in the ventral tegmental area contain $GABA_A$[3], $GABA_B$[4], nicotinic, muscarinic receptors and receptors binding neurotensin [299][300] [301][302][303]. Therefore, these neurons are receiving both inhibitory imputs via GABA-producing neurons and excitatory imputs via acetylcholine-, neurotensin- and glutamate-producing neurons. The activity of the GABA-producing neurons is regulated via NMDA, $GABA_A$, excitatory amino acid (EAA) and mu-opioid receptors (Figure 1.23A) [303][301] [302] [299] [304][299] [305][306] [307][308]. The existence of these receptors is extremely important for coupling specific information about the reward signal from the associative visual cortex, medial prefrontal cortex, ventral striatum and pars reticulata with the activity of VTA dopaminergic neurons [309].

Activation of the VTA dopamine-producing neurons increases the extracellular concentration of dopamine in the nucleus accumbens. This increase results in the inhibition of the spiny GABA neurons within the shell of the nucleus accumbens, via activation of D_1 and D_2 dopamine receptors (Figure 1.23B) [310][311][312]. The inhibition of the spiny GABA neurons results in the activation of a reinforcement process, presumably due to the disinhibition of downstream circuits that are innervated by the nucleus accumbens. The final output, i.e. the inhibition of the spiny GABA neurons, can be modified at the level of the dopamine-producing neuron as well as at the level

[3] anterior located cell bodies
[4] posterior located cell bodies

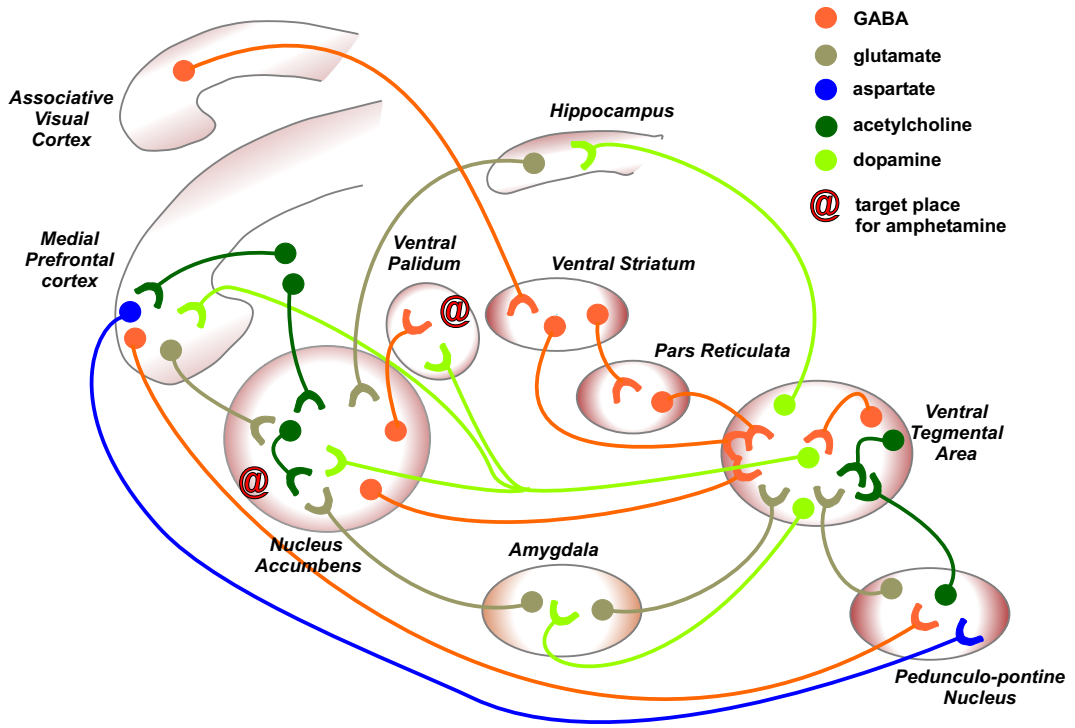

Figure 1.22: **Neuronal networks involved in the brain reward system.** The neuronal network controlling the brain reward system and underlying drug addiction is complex, and many possible sites are involved in the initiation and maintenance of drug reinforcement. Amphetamine produces reinforcing effects in the nucleus accumbens and ventral pallidum (sites labelled with @) and in both places dopamine appears to mediate the action of the amphetamine.

of the target GABA-producing neurons. The activity of dopaminergic neurons is positively regulated by acetylcholine via muscarinic receptors [313], while repression can be achieved by the activity of GABA interneurons activating $GABA_A$ receptor [300]. The spiny GABA neurons contain mu-opioid [243][314] and EAA receptors [315][310] additionally to D_1/D_2, receptors and therefore can be regulated by enkephalin-producing neurons and glutamatergic neurons originating from the amygdala, hippocampus and prefrontal cortex [300].

Neuroanatomical studies indicate that the ventral pallidum (VP) receives a major input from the nucleus accumbens [316][317]. It has been proposed that the VP processes the rewarding actions of drugs of abuse [317][318]. In addition to processing information from the nucleus accumbens, the VP receives a direct DA projection from the VTA (Figure 1.23) [317][319][320], suggesting that this mesopallidal dopamine pathway may provide reward independently from the mesolimbic system. Indeed, bilateral injection of amphetamine and cocaine into the rostral VP produced conditioned

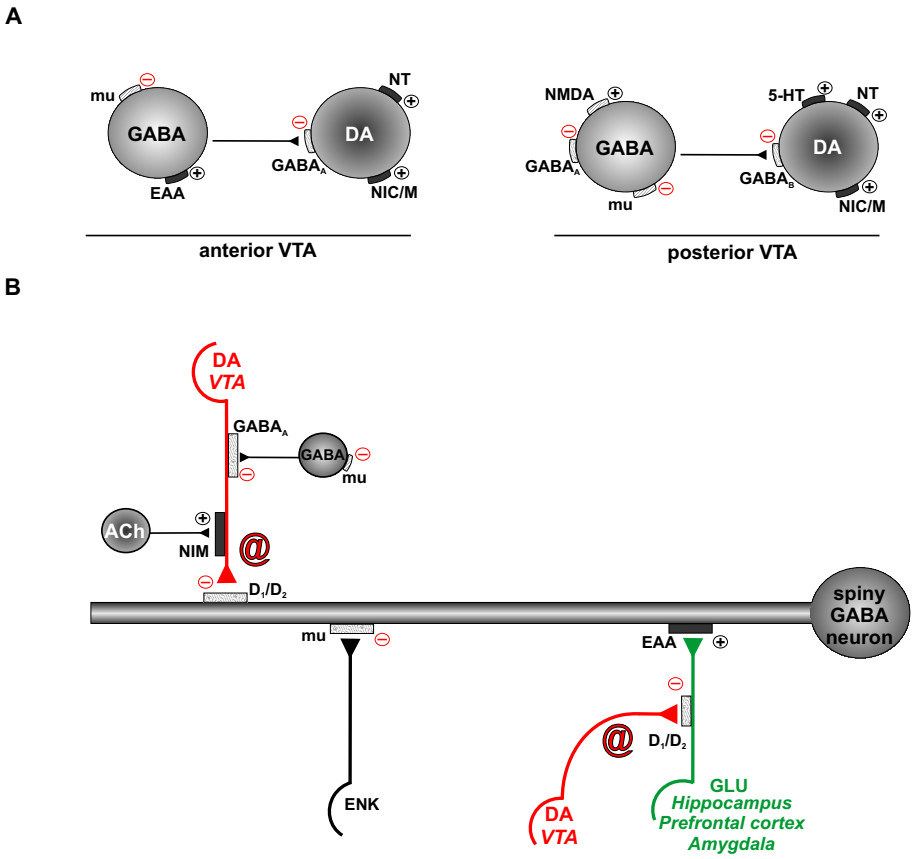

Figure 1.23: **The activity of dopamine-producing neurons in the VTA and NAc is controlled through multiple excitatory and inhibitory interactions.** Hypothetical simplified circuits within the VTA mediating reinforcement **(A)**. In the anterior portion of the VTA, activating mu-receptors on GABA interneurons, or activating neurotensin (NT), nicotinic (NIC) or muscarinic (NIM) acetylcholine receptors on DA neurons result in increased firing rate of VTA DA neurons and initiate the reinforcing process. Similarly, blocking excitatory amino acid (EAA) receptors on GABA interneurons or $GABA_A$ receptors on the DA neurons reduces tonic inhibition on the DA neurons and increases their firing rate. In the posterior VTA, tonic inhibition of dopamine-producing neurons is mediated by $GABA_B$ receptors. Additionally, DA neurons are positively regulated via 5-TH_3 receptors. The activity of GABA neurons in the posterior VTA can be modified via NMDA, $GABA_A$ and mu-opioid receptors. Hypothetical simplified circuits within the NAc mediating reinforcement **(B)**. Within the nucleus accumbens, activating D_1 and D_2 receptors on spiny GABA neurons projecting to the ventral pallidum reduce firing rates and initiate the reinforcing process. In addition, activating D_1 and D_2 receptors on EAA input to the spiny GABA neurons reduces this excitation. Alternatively, activating inhibitory opioid receptors with enkephalin (ENK) on GABA interneurons, locally regulating DA input activity, can result in enhanced DA release, activation of DA receptors, and increasing reinforcing effects. In a similar fashion, activating excitatory cholinergic (ACh) muscarinic receptors on DA afferents can also result in enhanced DA release and increased reinforcing effects. Amphetamine is reinforcing in the NAc because it increases the extracellular levels of DA which results in activation of D_1 and D_2 receptors. @ indicates a potential place of amphetamine actions.

place preference [321], suggesting that the VTA dopaminergic pathway projecting to the rostral VP can be involved in the reward pathway, at least for psychostimulants.

Similarly, the medial prefrontal cortex (MPFC) receives direct dopaminergic input from the VTA [316], suggesting a role of the MPFC in the brain mechanisms mediating drug reward. ICSA studies have shown the involvement of cortical dopaminergic mechanisms in cocaine, but not in amphetamine reinforcement [242][245] [322][243][323]. The ICSA of cocaine into the MPFC also significantly increased dopamine turnover in the NAC [322] , suggesting a link between the MPFC and the mesolimbic dopamine system in mediating cocaine reward.

Cholinergic neurons play an important role in the modulation of the brain reward system

ICSA and ICPC studies using specific agonists or antagonists of either muscarinic or nicotinic cholinergic receptors suggested a cholinergic role in the brain reward system (see Section 1.23) [300][306][305]. According to this model, cholinergic neurons could modulate dopaminergic transmission in the nucleus accumbens and VTA. Recent experiments using more specific pharmacological agents, genetic and ablation studies support this model. Namely, specific blocking of muscarinic cholinergic transmission in rodents increases the response to psychostimulants in the self-administration or conditioned place preference tests [324][325], paradigms classically applied to evaluate addictive behavior (see Section 1.5.6). Further, the activity of the cholinergic neurons innervating the nucleus accumbens is decreased by dopamine release [326] and their ablation increases the sensitivity to psychostimulants and the reinforcing effects of cocaine [327]. Additionally, other components of the cholinergic system, like M5 muscarinic receptors on VTA DA neurons or nicotinic ACh receptors on dopamine terminals in the striatum, are implicated in the regulation of addictive behavior [328]. Using pharmacological inhibitors, Hikida *et al.* [327] suggested that inhibiting acetylcholinesterase activity, which terminates ACh action at the synapse, can block cocaine- and morphine-induced CPP in the mouse. Therefore, the cholinergic system can be considered as a promising target for the drug addiction therapy, although the specific components to target within this cholinergic system remain to be determined.

1.5.6 Experimental methods used to study drug addiction

Although human drug addiction is highly complex, animal models of addictive behavior have long been useful in exploring the underlying neuropharmacological and molecular mechanisms of drug addiction as well as in predicting the abuse liability of different compounds. A number of experimental procedures have been developed to study the biological bases of drug addiction in laboratory animals, mainly rodents. The majority of these procedures directly or indirectly measure the reinforcing effects of drug administration. Drug reinforcement refers to the ability of some drugs to motivate the individual to engage in behaviors leading to further drug administration that is, in the development of addiction.

The methods used to study drug addiction in laboratory animals can be divided into two groups: methods employing *choice testing*, which do not require any operant

activity of the animal to receive the drug; and methods employing *self-administration*, which require operant activity in order to activate the brain reward pathway. Conditioned place preference and measuring locomotor activity belong to the first class, while intravenous self-administration and brain stimulation reward interactions encompass the second class.

Intravenous self-administration (IVSA)

Intravenous self-administration is the most direct method of determining drug reinforcing potential in experimental animals, and was initially developed to address the reinforcing properties of different drugs in rats [329]. Later on, modifications of IVSA have successfully been applied to different model organisms: the rhesus monkey [330][331], the squirrel monkey [332][333], the dog [334], the pig [335], the baboon [336][337], the cat [338] and the mouse [339].

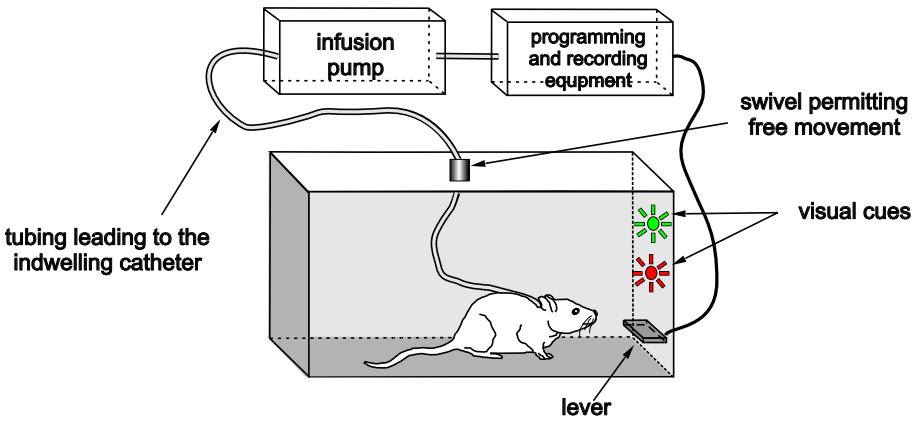

Figure 1.24: **Drug self-administration apparatus.** Pressing the lever in response to appropriate visual cue according to a predetermined schedule provides the delivery of drug or vehicle into a vein (intravenous self-administration) or into discrete brain areas (intracranial self-administration).

In this method, the behavioral response (animal action, usually a lever press) is followed by intravenous drug administration through a catheter implanted into the animal vein (Figure 1.24), and the ability of drug injection to directly reinforce behavior is determined [329]. Generally, it is concluded that drug is self-administrated if the rate of lever pressing is greater in animals receiving the drug than in uninjected animals or animals receiving the saline or vehicle solution [340][341]. The drug is acting as a reinforcer if the rate of behavioral response (a lever pressing) is maintained for some time after the drug is not delivered in response to a lever pressing. Even more, an increase in rate of operant behavior following drug cessation should be seen [342][329][343].

The largest advantage of the IVSA technique is that the principles of operant conditioning can be directly applied to the study of drug reinforcement. IVSA can control behavior in much the same manner as traditional reinforcers such as food and water in hungry or thirsty animals [344][345]. Second, the persistence of drug-seeking behavior as well as relapse, can directly be studied by examining the extinction patterns of the response [346]. Finally, choice procedures (cross substitution procedures) have been developed where the animal chooses between several drug injections. This way, the reinforcing properties of different doses of the same compound, or reinforcing properties of the different compounds can be tested in the same animal [345].

The main disadvantage of the IVSA procedure is its technical complexity. Namely, the intravenous preparation is relatively difficult to maintain, and cases of blocked or leaky catheters and illness of the animal are frequent[5]. Additionally, although animals learn to self-administrate some drugs, a long time period is often required for the response pattern and drug intake-levels to stabilize [349]. When the cross substitution procedure is used, drug interactions and learning variables can have a significant influence on the results obtained.

1.5.7 Brain stimulation reward (BSR)

The brain stimulation reward method rely on the ability of addictive drugs to enhance or facilitate an already existing reward mechanism [350]. Animals are trained to press levers to receive brief pulses of electrical stimulation via surgically implanted electrodes in the brain regions where electrical stimulation is directly reinforcing. The facilitation effect of the drug can be seen either as an increased rate of lever pressing for a fixed intensity of the stimulating current [351], or as a lowering of the current threshold necessary for successful brain stimulation [352] upon drug administration.

This technique offers numerous advantage compared to the IVSA. It is technically less demanding, the surgical procedure is simpler and the animals are easy to maintain. Drug effect is assessed against an already established behavior and learning effects are not important. The initial drug dose tested is not critical, because the animal is working for the reward effects of the electrical stimulation and the behavior will be not extinguished with subrewarding drug doses [353]. Finally, repeated drug testing does not disturb animal's behavior, making this method ideal for dose-response experiments. Nevertheless, the fact that BSR does not directly measure drug reinforcement is a serious limitation of this methodology compared to the IVSA.

Conditioned place preference (CPP)

The conditioned place preference procedure is based on the ability of animals to develop an association between the subjective state produced by a drug (e.g. reward comparable to mood elevation and euphoria in humans) and specific environmental cues in several conditioning trials [354]. During these conditioning trials, the animal is injected with the drug and placed in a specific compartment of the testing apparatus

[5]To overcome the problem of intravenous drug administration, different alternative procedures such as oral, intragastric and intracranial self-administration have been developed [347][348].

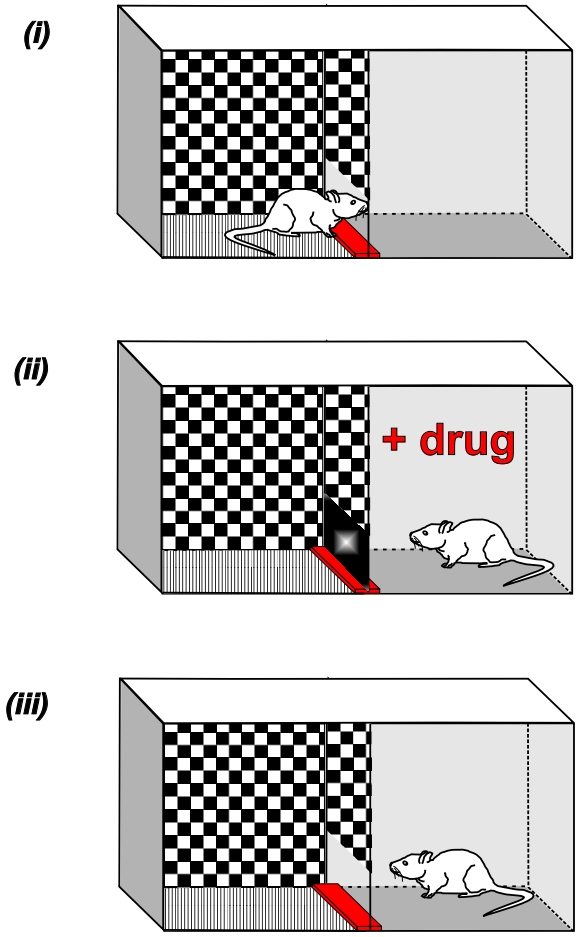

Figure 1.25: **The scheme for CPP assay.** The apparatus consists of two compartments that vary along several sensory dimensions, including the pattern or color of the floor and walls. The experiment is composed of three phases: monitoring of time spent in left vs. right compartment prior to drug exposure *(i)*, exposure to the drug in left or right compartment *(ii)* monitoring of time spent in left vs. right compartment after the drug exposure, in a drug-free condition (*iii)*. If the drug has reinforcing properties, the time spent in the drug-associated compartment should increase compared to the initial measurement.

containing various cues (visual, tactile, olfactory, etc.) for a defined time period. When this animal is afterwards tested in the drug-free state, in an experimental apparatus offering the drug-related environmental cues in one compartment, and neutral cues in another, it voluntarily moves towards the compartment containing the drug-related

cues if conditioning is developed (Figure 1.5.7). The ability of a drug to induce conditioning (i.e. the association of the drug and environmental cues) is an indication that the drug has reinforcing properties [346][355].

The CPP method appears to be quick and easy. It does not require special equipment or special surgical preparation of animals. Therefore, a high number of animals and different compounds can be tested within a reasonably short time period. Additionally, CPP can be used on animals that are not experimentally amenable to IVSA or BSR, e.g. fish. The huge advantage of CPP is that animals are tested in the drug-free state, excluding any influence of drug-induced motoric effects, aversion or toxicity on the observed conditioning [356]. The main disadvantage of the CPP paradigm is that it does not directly measure drug reinforcement. However, there is a considerable concordance between CPP and IVSA. A wide variety of drugs that are addictive in humans induce CPP, and nonaddictive drugs do not produce a place preference in experimental animals [346]. The characteristics discussed above make the CPP method indispensable in the initial screening for either a new, potential drug of addict or its antagonists, or for the molecular players underlying addiction.

1.5.8 Locomotor activity (LMA)

The main mechanisms mediating drug addiction are associated with normal behaviors such as exploratory behavior or locomotor activity, at least at the level of the nucleus accumbens. Therefore, these processes are very often affected by the drugs of abuse, but they are not measures of drug reinforcement. Because LMA is easy to measure, this behavioral test is frequently used for the preliminary determination of experimental manipulations that may affect drug addiction.

Chapter 2

Aims and achievements

The two main goals of my PhD project were to:
(*i*) understand the molecular mechanisms controlling neurogenesis in the zebrafish MH domain, and
(*ii*) setup the bases to analyze a potential contribution of embryonic neurogenesis to the functionality of the adult neuronal networks controlling complex behaviors, such as drug addiction.

To approach the molecular mechanisms controlling neurogenesis in the MH domain I analyzed the maintenance of the progenitor pool at the MHB (intervening zone, IZ). It had been shown that the Hairy/E(Spl) transcription factor Her5 plays a crucial role in medial IZ formation [37], but the lateral parts of the IZ (LIZ) are formed in absence of Her5 function. Therefore, I performed a systematic search for Hairy/E(Spl) transcription factors that would control formation of the LIZ in cooperation with Her5. This search resulted in the identification of a new Hairy/E(Spl) transcription factor encoding gene, *him*, in near proximity to *her5*. In loss-of-function experiments, I showed that Him and Her5 control formation of the entire IZ and that the IZ is composed of two different domains differing in their requirement for Hairy/E(Spl) inhibitory activity. This work is presented in Section 3.1 and Appendix A.

The IZ is composed of two domains with different sensitivity to neurogenesis. To assess how this differential sensitivity arises, I analyzed the role of Wnt and Shh signaling pathways that exhibit graded activities along the medio-lateral axis at the level of the forming MHB. This analysis revealed that the medio-lateral difference in the propensity of IZ cells to undergo neurogenesis forms at the end of gastrulation (75 % - 90 % epiboly) and in response to Gli signaling pathway, but independently of the smoothened coreceptor. Data supporting these conclusions are presented in Section 3.1.2.

As a broad approach to gain insight into the molecular mechanisms controlling the brain reward system, I decided to run a large-scale genetic screen in zebrafish to recover dominant mutations affecting addiction to D - amphetamine, using the conditioned place preference (CPP) paradigm.

The first task was to develop a reliable CPP methodology for zebrafish, since the CPP paradigm had been successfully applied only in higher vertebrates (see section 1.5.6). The development of this methodology, including crucial specificity controls,

is reported in Section 3.2 and Appendix B. Thanks to the developed methodology, I demonstrated that more than 95 % of wild-type zebrafish robustly experience the rewarding effects of the psychostimulant D - amphetamine.

Further, I analyzed zebrafish *ache*/+ mutant fish, deficient for cholinergic neuronal transmission throughout life, and found that these mutants are strongly resistent to the rewarding effects of D - amphetamine. These findings suggest that the rewarding potential of amphetamine, as well as the importance of the cholinergic system in modulating this effect, have been evolutionary conserved in vertebrates. They also show that the developed methodology can be used to reveal dominant modifiers of drug addiction, such as the $ache^{sb55}$ mutation impairing cholinergic transmission in *ache*/+ fish. Experiments addressing addiction of *ache*/+ fish to D - amphetamine are presented in Section 3.2.3 and Appendix C.

The development of appropriate assays and the evolutionary conservation of the brain reward system enabled me to run genetic screens in zebrafish, aimed at recovering dominant mutations affecting drug addiction in vertebrates. I performed two genetic screens and up to date recovered one family with the searched mutant phenotype. The organization and preliminary results of the two genetic screens are presented in Section 3.2.4 and Appendix B.

Chapter 3

Results

3.1 Molecular control of neurogenesis at the zebrafish MHB

Article Appendix A

3.1.1 Inhibition of neurogenesis in the IZ by the combined and dose-dependent activity of Him/ Her5 pair

The maintenance of the progenitor pool located at the MHB is crucial for MH development. Indeed, premature differentiation of the proliferating MHB neural precursor cells into neurons results in a late loss of MHB integrity [37][48] and a loss of MH neuronal populations [48]. The molecular events controlling the generation or maintenance of neural progenitor pools remain largely hypothetical. Recent experiments showed that the Hairy/E(Spl) transcription factor Her5 precisely delineates the IZ at all embryonic stages [36][37] and is necessary and sufficient for medial IZ formation [37]. In the absence of Her5 function, premature differentiation occurs in the medial (future basal) part of the IZ, while the lateral (future alar) domain forms, despite the absence of Her5 function [37].

I reasoned that other Hairy/E(spl) factors might be expressed within this domain and act redundantly with Her5. Because there are examples of physically linked *E(spl)* genes in Drosophila (*E(spl)* complex) [357][125] and zebrafish (*her1* and *her7*) [358], and because linked genes are more likely to share spatiotemporal characteristics of expression, I searched for new *Hairy/E(spl)* genes in the vicinity of the *her5* locus. Sequencing of a *her5*-containing PAC [66] revealed the presence of an open reading frame encoding a new Hairy/E(spl) factor, Him, located 3.3 kb upstream of *her5* and in a head-to-head orientation, reminiscent of the genomic organization of *her7-her1* [358].

The Him protein, translated from my full-length cDNA sequence, consists of 297 amino acids and exhibits all structural features of an Hairy/E(Spl) bHLH factor acting as transcriptional repressor [123]: a conserved proline residue in the basic domain, an "orange domain" [124] and a WRPW tetrapeptide in the C-terminus [149] (see Appendix A).

him expression within the presumptive MH is identical to *her5* and marks the intervening zone

I analyzed *him* expression by RT-PCR and *in situ* hybridization. *him*, like *her5*, is maternally expressed. Early zygotic *him* expression is ubiquitous but rapidly resolves in a first, transient, profile within the presumptive dorsal endoderm and mesoderm. From mid-gastrulation onwards (70 % epiboly), *him* becomes transcribed in the anterior neural plate, in a V-shaped domain interrupted at the midline. At the three-somite stage, this expression fuses medially and, by anatomical landmarks, is clearly located within the presumptive MH domain, like *her5*. Detailed expression profile of *him* during zebrafish development is shown in Figure 2 in Appendix A.

Him activity is crucial for the formation of the MIZ at early neurogenesis stages

Because *him* has a similar expression to *her5* and encodes a related Hairy/E(Spl) factor, I explored a potential involvement of Him in IZ formation. I tested a requirement for Him in IZ formation in loss-of-function experiments where *him* mRNA translation was blocked by specific antisense GripNAs. *him*GripNAs-injected embryos displayed a complete lack of the MIZ, with bridging of the vcc and r2MN clusters by ectopic *ngn1*-expressing cells at the 3-somite stage. Ectopic *ngn1* expression is followed by premature differentiation across the basal MHB at later stages. This phenotype is in all respects similar to that triggered by the loss of Her5 function (see Appendix A) [37]. Thus, loss-of-function of either Her5 or Him results in the same failure to form and maintain the MIZ.

The above results are compatible with a simple model where Him and/or Her5 would act in a common regulatory cascade. Thus, loss of Him function would cause loss of *her5* expression, or the reverse. Alternatively, Him and Her5 might be independently necessary for MIZ formation. To address this question, I studied *him* and *her5* expression in embryos where Her5 or Him activity, respectively, was blocked. *him* expression was unchanged in Her5 morphants under conditions where *ngn1* expression was strongly induced in place of the MIZ, suggesting that *him* expression is not under immediate control of Her5. Likewise, loss of Him function did not alter either *her5* transcription or translation of *her5* mRNA (Figure 4 in Appendix A). I conclude that Him and Her5 do not act in a simple cascade of cross-regulation of expression. Rather, the two genes are expressed independently of each other and are both essential to MIZ formation.

The crucial determinant of MIZ formation is the total dose of "Him + Her5" inhibitory activities

Several hypotheses could account for the above results. First, Him and Her5 might both be required for MIZ formation because they need to heterodimerize with each other to be active. Alternatively, these factors do not have unique essential activities, but rather are required to reach together a threshold level of Hairy/E(spl) activity necessary to prevent proneural gene expression. Finally, both factors might

exert distinct and/or complementary functions necessary for MIZ formation.

Using a yeast two-hybrid system, I found that Her5 can homodimerize as well as form heterodimers with Him. Thus, the requirement for Him and Her5 for MIZ formation *in vivo* might indeed be explained by the necessity for these factors to heterodimerize.

Nevertheless, my finding that Her5 can homodimerize, as well as reports of functional bHLH oligomers [359][360][361], suggested that Her5 and/or Him alone could permit MIZ formation, provided the dose of this factor is sufficient. To test this hypothesis, I analyzed MIZ formation in a context where the dose of Him is increased across the IZ. Interestingly, I observed that an increased dose of Him permits formation of the MIZ although Her5 function is blocked by *her5*MO injections (Figure 5 in Appendix A). Thus Him, when present in sufficient amount is capable of replacing Her5 activity to prevent neurogenesis across the MIZ.

I conclude from these observations that the crucial component of MIZ formation and maintenance is a threshold level of "Him + Her5" inhibitory activity, achieved by either Her5-Him heterodimers or homodimers and/or by oligomers from each factor separately (Figure 3.1).

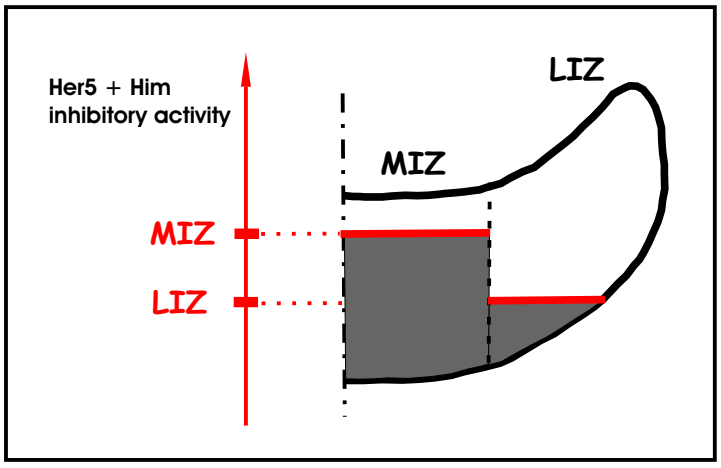

Figure 3.1: **IZ formation relies on "Him + Her5" activity.** Schematic representation of one half IZ (black line) (dorsal view, anterior up) and the thresholds of "Him + Her5" activity necessary for neurogenesis inhibition in the MIZ and LIZ. *ngn1* expression (gray) replaces the MIZ when the dose of "Him + Her5" is below the MIZ threshold (upper red line), and the LIZ when "Him + Her5" drops below the LIZ threshold (lower red line).

Formation of the LIZ also relies on the level of "Him + Her5" activity but with a lower threshold than the MIZ

The LIZ is preserved in both *her5* and *him* single knockdown embryos, suggesting that it might require other factors than Him and Her5 for its formation. Alternatively, the LIZ might primarily differ from the MIZ in requiring a lower threshold of "Him + Her5" activity, the endogenous level of one factor alone (two doses) being sufficient to block neurogenesis in this location. To address these hypotheses, I assayed for *ngn1* expression in double knockdown embryos. Strikingly, I observed that the simultaneous interference with both Her5 and Him activities results in ectopic *ngn1* expression in place of the entire IZ, i.e. including the LIZ (Figure 6 in Appendix A).

In addition, I found that Him and Her5 are equally potent neurogenesis inhibitors in the LIZ and that only one dose of any of these two factors is sufficient to inhibit neurogenesis in the LIZ (Figure 7 in Appendix A). Therefore, I propose that a crucial determinant of LIZ formation is the threshold of "Him + Her5" activities rather than the specific presence of both factors (Figure 3.1).

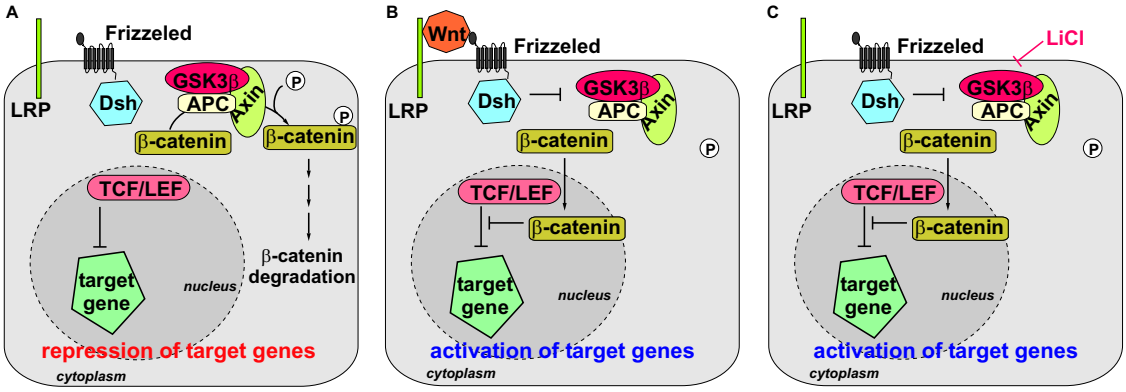

Figure 3.2: **Simplified schematics of Wnt signaling components.** (A) Wnt proteins interact with transmembrane receptors of the Frizzled family of proteins and activate Disheveled (Dsh). Once the Dsh protein is activated, it inhibits the activity of the glycogen synthase kinase-3β (GSK3β) enzyme. When GSK3β is inhibited , β-catenin can dissociate from the APC protein and enter the nucleus. Once inside the nucleus, it can form a heterodimer with an LEF or TCF DNA-binding protein. This complex activates the Wnt-responsive genes. (B) In the absence of Wnt ligand, β-catenin is phosphorylated by GSK3β and tagged for degradation. Depletion of β-catenin leads to repression of the Wnt-responsive genes. (C) LiCl inhibits GSK3β and mimics the effect of a Wnt ligand.

3.1.2 Formation of a differential sensitivity to neurogenesis inhibitors across the IZ

Manuscript in preparation

As discussed in Section 3.1 both the MIZ and LIZ respond to "Him+Her5", but the MIZ requires a higher level of this inhibitory activity than the LIZ for its maintenance. To elucidate the mechanisms accounting for this differential sensitivity, I tested the role of (*i*) two secreted factors exhibiting graded activities along the medio-lateral axis of the neural plate at the level of the IZ: Wnt and Shh, and (*ii*) signaling pathways triggered by these two molecules. Since I assumed that the medio-lateral gradient of morphogen activity is involved in the formation of this differential sensitivity , I analyzed the response of the MIZ and LIZ to "Him + Her5" in contexts where the Wnt and Shh pathways were perturbed, using different approaches summarized in the following section.

GSK3β activity is necessary for the proper formation of the MIZ

Wnt1 is the most prominent candidate to mediate Wnt signaling at the level of the IZ during its formation (late gastrulation in zebrafish). Wnt1 is expressed from the future dorsal midline and lateral IZ with a medial to lateral increasing gradient (not shown). Endogenous levels of canonical Wnt signaling can be modified via several intracellular components of the Wnt cascade in the target cell (Figure 3.2) [362][363]. One of the critical complexes in the regulation of Wnt signaling is a GSK3β functional complex that phosphorylates β-catenin, targeting it for degradation [364][365][366], and thereby limiting the amount of β-catenin available to activate Wnt target genes. Therefore, inhibiting GSK3β activity results in activation of Wnt target genes (Figure 3.2). In zebrafish, the functionality of the GSK3β complex can be abolished using GSK3β inhibitor LiCl (Figure 3.2C). Thus, to assess the involvement of GSK3β in the formation of the differential sensitivity across the IZ, I applied 0.3 M LiCl at 80 % epiboly. Surprisingly, LiCl applied at 80 % epiboly triggered *ngn1* expression in place of the MIZ, but not LIZ (Figure 3.3) (83.3 % of cases, n=60). This suggests that inhibition of GSK3β increases the threshold level for Him- and Her5-dependent inhibition, and that in this context two doses of both factors are not sufficient to secure MIZ formation. Moreover, applications of LiCl at different time points during embryo gastrulation revealed that the formation of the MIZ is sensitive to GSK3β activity during a narrow time window, between 75 and 90 % epiboly (Figure 3.4 and not shown). Outside of this window, LiCl induced just a few ectopic *ngn1*-positive cells (Figure 3.4A and C) (90 % of cases, n=50 for 60 % epiboly; 87.5 % of cases, n=56 for 90 % epiboly). Application of 0.3 M LiCl at 60 % epiboly induced an enlargement of the IZ (compare the size of the red bars indicating the IZ in Figure 3.4A and D) that is related to the requirement for a functional GSK3β complex to regulate head size during the gastrulation process [367]. Nevertheless, only scattered *ngn1*-positive cells can be observed across the MIZ (Figure 3.4A, red arrowheads).

The finding that a functional GSK3β complex is necessary for the formation of the MIZ pointed to the possibility that Wnt signaling plays an important role in IZ

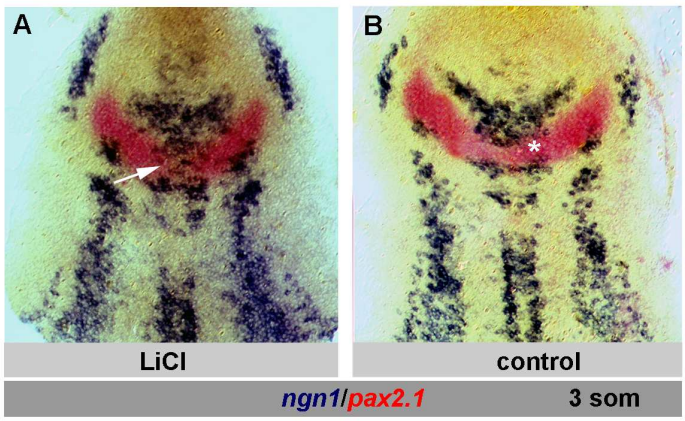

Figure 3.3: **LiCl induces ectopic neurogenesis in the MIZ.** Whole-mount in situ hybridizations on 3-som stage embryos (anterior to the top) probed for *ngn1*. The IZ is highlighted with *pax2.1* expression in red. LiCl treatment triggers ectopic neurogenesis in the MIZ (white arrow in A) after application at 80 % epiboly. Untreated embryos develop the IZ normally, as indicated with white asterisk on B.

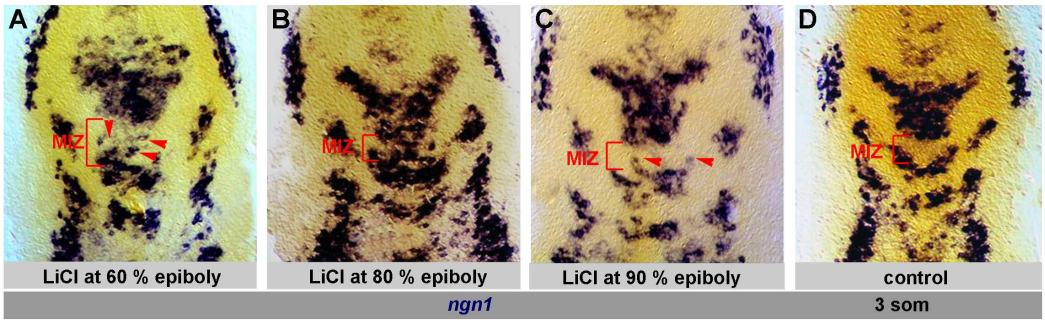

Figure 3.4: **Sensitivity of the MIZ to neurogenesis is established between 75 % and 90 % epiboly.** Whole-mount in situ hybridizations on 3-somite stage embryos (anterior to the top) probed for *ngn1* after treatment with 0.3 M LiCl at gastrulation stages as indicated at the bottom of each panel. The position and the size of the IZ is indicated with red lines. Note that a complete bridging of the MIZ with ectopic *ngn1*-positive cells is achieved only when LiCl is applied at 80 % epiboly (D), while the application of LiCl at 60 % (C) and 90 % (E) epiboly causes only scattered *ngn1*-positive cells across the MIZ (red arrowheads).

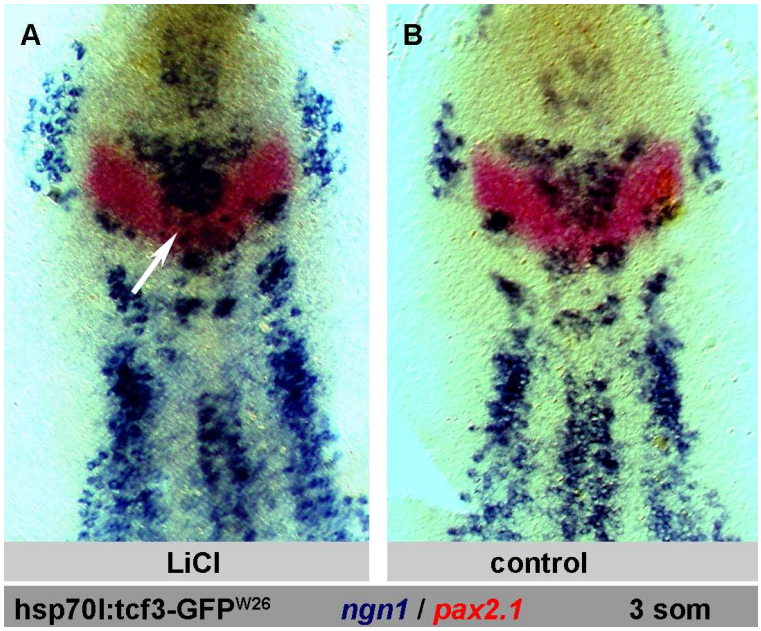

Figure 3.5: **Canonical Wnt signaling is not involved in the formation of the MIZ.** The inhibition of GSK3β activity, using LiCl, triggers ectopic neurogenesis (white arrow) in place of the MIZ after induction of a sufficient amount of ΔTcf in *hsp70l:tcf-GFP*^{w26} embryos (dorsal views of the MH region in flat-mounted embryos at the three-somite stage, anterior to the top). ΔTcf itself, produced by heat shock treatment in the heat-shock *hsp70l:tcf-GFP*^{w26} line, does not influence either the formation of the IZ or neurogenesis (B). Embryos are probed for *ngn1* (blue) and *pax2.1* (red) expression following appropriate treatment.

formation. To test whether the GSK3β complex controlled MIZ formation as part of the Wnt signaling pathway, I analyzed the requirement for a functional GSK3β complex in a context where Wnt signaling was blocked downstream of GSK3β, at the level of Tcf (Figure 3.5). I used a zebrafish line *hsp70l:tcf-GFP*^{w26} [368] that is transgenic for an heat-shock (hs) inducible dominant negative form of *tcf3* (ΔTcf) and that can be used to inhibit endogenous Wnt/β-catenin signaling at discrete time points during development [368].

Two hours after activation of *hs-ΔTcf*, the amount of dominant negative form of Tcf is sufficient to repress transcription of Wnt targets *in vivo*, based on a Wnt-responsive reporter transgenic line [369] that contains a destabilized variant of GFP under the control of four Tcf binding sites (data not shown).

To assess the effect of ΔTcf on GSK3β-regulated formation of the MIZ, I exposed *hsp70l:tcf-GFP*^{w26} transgenic embryos at 50 % epiboly to heat shock for 15 min at 42 ^{0}C and 2 hours later (80 % epiboly) to 0.3 M LiCl treatment. Treated and control

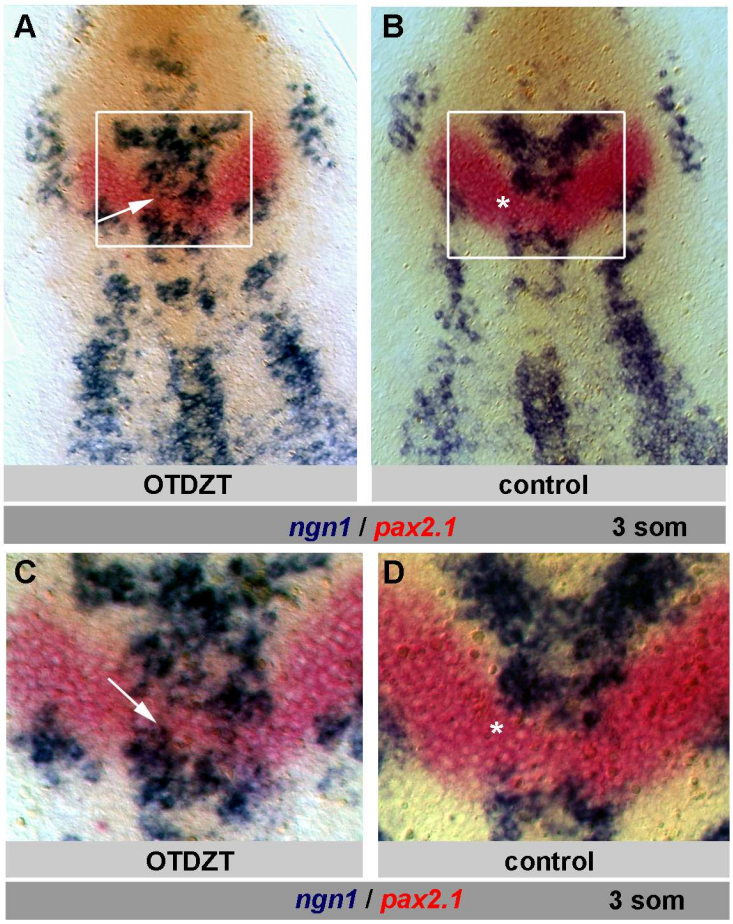

Figure 3.6: **The activity of GSK3β is necessary for normal formation of the MIZ *in vivo*.** The inhibition of GSK3β activity, using a GSK3β-specific inhibitor (OTDZT), triggers ectopic neurogenesis (white arrow) in place of the MIZ (dorsal views of the MH region in flat-mounted embryos at the three-somite stage, anterior to the top). Embryos are probed for *ngn1* (blue) and *pax2.1* (red) expression following appropriate treatment. Higher magnifications of the IZ in inhibitor-treated and untreated embryos (white boxes on A and B) are shown in panels C and D, respectively.

embryos are further assessed for *ngn1* expression at 3-somite stage. Strikingly, LiCl was able to increase the threshold level for "Him + Her5" inhibitory activity and induce ectopic *ngn1* expression in heat shock-treated embryos (Figure 3.5A) (83.3 % of cases, n=42). Thus, although GSK3β likely plays a role, Wnt/β-catenin signaling is not involved in the formation of the differential sensitivity to Him and Her5 across the IZ in zebrafish.

At least two hypotheses could account for the above results. First, LiCl might

inhibit other enzymes than GSK3β, such as inositol monophosphatase [370][371], that are not involved in Wnt/β-catenin signaling and that control formation of the MIZ. Second, GSK3β activity might act on neurogenesis via other signaling pathways present at the zebrafish MHB, such as Fgf or Shh signaling.

To find out whether LiCl impairs IZ formation by blocking GSK3β, I analyzed IZ formation in embryos where GSK3β activity is specifically blocked by OTDZT (2,4-Dibenzyl-5-oxothiadiazolidine-3-thione) [372] from 80 % epiboly onwards. Importantly, OTDZT - treated embryos assayed at the three-somite stage for *ngn1* expression displayed a complete lack of the MIZ, with bridging of the vcc and r2MN clusters by ectopic *ngn1*-expressing cells (Figure 3.6A and C, white arrows) (86.8 % of cases, n=38). This phenotype is in all respects similar to that triggered by LiCl treatment (Figure 3.3A).

Taken together, my results showed that the sensitivity of the MIZ to undergo neurogenesis is established during late gastrulation and regulated by GSK3β activity independently from the activation or inhibition of Wnt/β-catenin target genes.

Gli1 is a crucial determinant of IZ formation

According to a second hypothesis GSK3β might be involved in neurogenesis control via other signaling pathways than Wnt/β-catenin, acting at the zebrafish MHB. For instance, GSK3β might be involved in Shh signaling originating from the ventral midline and specifically active at the MHB [373][374]. Recent publications showed that GSK3β phosphorylates Ci proteins in Drosophila [375][376], and that this phosphorylation plays an important role in the regulation of the equilibrium between Ci-155 (activator form) and Ci-75 (repressor form) by targeting Ci-155 for proteolysis. Proteolysis from Ci-155 to Ci-75 keeps the Shh pathway silent [376].

In zebrafish, there are four Ci orthologs: Gli1 [377], Gli2 [377], Gli3 [378] and Gli2b [379]. To elucidate whether these factors can be targets of GSK3β in the IZ, I first analyzed the expression patterns of *gli* genes with a focus on the MH domain.

These expression analyses pointed to *gli1* as a promising target of GSK3β involved in the formation of the different sensitivity to neurogenesis inhibitors of the MIZ versus LIZ. First, *gli1* is expressed in the anterior neural plate during late gastrulation (Figure 3.7), that is during the time window crucial for the establishment of the differential sensitivity (see Figure 3.4) and second, the expression levels of *gli1* show a medio-lateral gradient, decreasing towards the LIZ (Figure 3.7). Thus, Gli1 could regulate the differential sensitivity of the MIZ versus LIZ by increasing the threshold level for "Him + Her5" activity in the MIZ. If this hypothesis is true, loss of Gli1 function would decrease the threshold level in the MIZ and render it "LIZ-like" with respect to its requirement for "Him + Her5" function. To address this hypothesis, I analyzed the requirement for Her5 function in MIZ formation in embryos lacking Gli1 activity. In WT embryos, loss of Her5 function resulted in ectopic neurogenesis in place of the MIZ and bridging of the vcc and r2MN clusters with ectopic *ngn1*-positive cells (Figure 3.8A, red arrow) (97.5 % of cases, n=30). Importantly, however loss of Her5 function did not induce ectopic neurogenesis in the Gli1 morphants (Figure 3.8C, white arrow) (81.6 % of cases, n=60), while blocking Gli1 function alone had

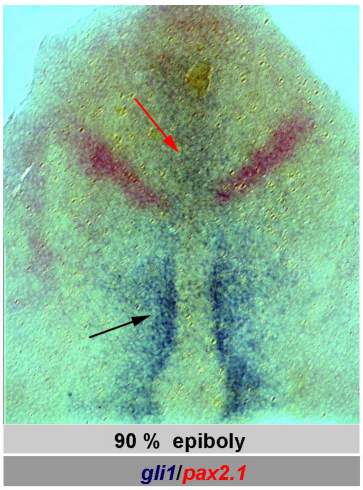

Figure 3.7: **Gli1 is expressed in a graded manner across the IZ.** Dorsal view of the flat-mounted embryo (anterior to the top) at late gastrulation probed for *gli1* expression. Gli1 expression (blue staining) is observed in both the neural plate (red arrow) and adaxial cells (black arrow). *gli1* expression level in the neural plate is the highest at the midline and decreases laterally. The IZ is highlighted by *pax2.1* expression stained in red.

no visible effects, suggesting that loss of Gli1 function decreased the threshold level for "Him + Her5" activity. Therefore, Him activity is sufficient to prevent neurogenesis in place of the MIZ in Her5 morphants.

Similarly, inhibition of GSK3β activity in Gli1 morphants did not induce ectopic neurogenesis in place of the MIZ (not shown), suggesting that GSK3β is involved in MIZ formation via regulation of the equilibrium between the activator and repressor form of Gli1 (Figure 3.10).

In Drosophila, protein kinase A (PKA) together with GSK3β regulate the propensity of Gli proteins to undergo proteolysis and repress target genes in the absence of Shh [376]. To elucidate whether the GSK3β/ PKA tandem has any role in the regulation of the Gli equilibrium during IZ formation, I analyzed the sensitivity of the MIZ to the loss of Her5 function in the context where PKA was constitutively active (PKA*) [380]. PKA* continuously phosphorylates Gli proteins and therefore depletes the Gli activator pool (Figure 3.10). Loss of Her5 activity did not induce ectopic neurogenesis in place of the MIZ when *her5*gripNA was coinjected with 20 ng/μl of PKA* mRNA (Figure 3.9C, white asterisk) (66 % of cases, n=50), while injecting *her5*gripNA at the same dose induced ectopic neurogenesis (Figure 3.9A) (92.3 % of cases, n=26). Thus, depletion of the Gli1 activator pool by PKA* activity decreases the threshold level for "Him + Her5" activity.

I demonstrated above that Gli1 activity is a crucial determinant of the sensitivity

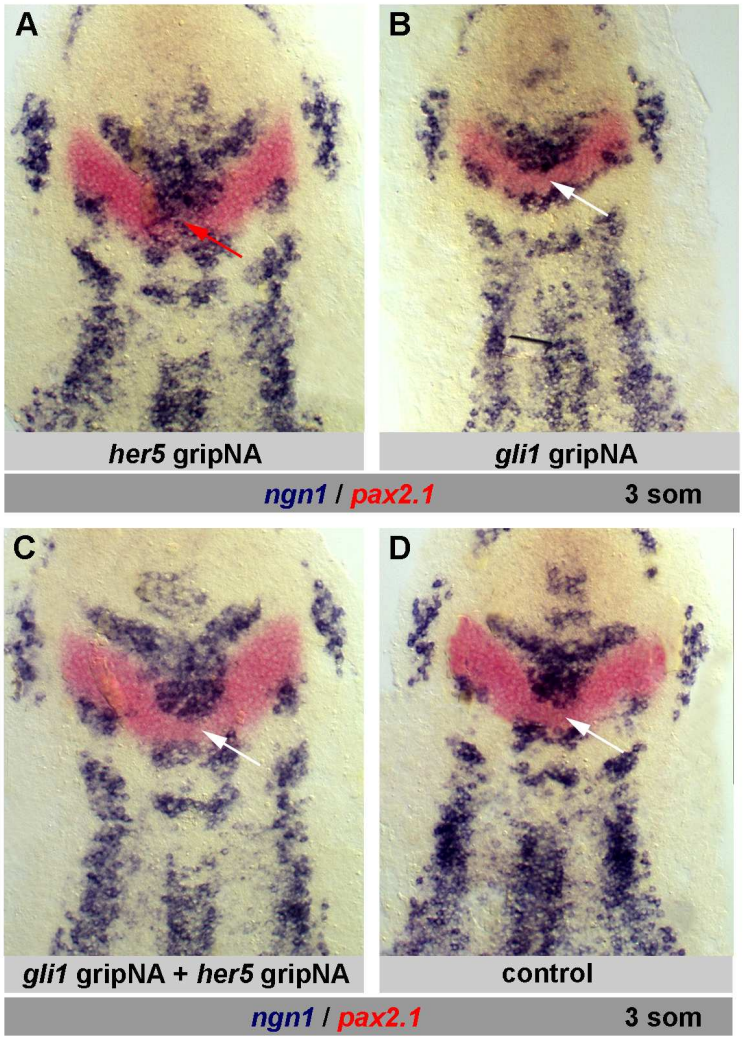

Figure 3.8: **Effects of the Gli1 activity on the formation of the medio-lateral gradient of sensitivity to "Him + Her5".** Dorsal views of the flat-mounted embryos probed for *ngn1* (blue) and *pax2.1* (red) following injection of *her5*GripNA (A), *gli1*gripNA (B), coinjection of *her5*gripNA and *gli1*gripNA (C), compared to a non-injected WT control embryo (D). Note that the loss of Her5 function is not sufficient to induce the ectopic *ngn1*-positive cells across the IZ (red arrow in A) in the context where Gli1 function is blocked (white arrow in C). Gli1 morphant (B) is indistinguishable from control embryo (D) in respect to *ngn1* expression.

to "Him + Her5" inhibitory activity of the MIZ and that the Gli1 activator pool can be regulated by PKA and GSK3β. However, these experiments did not address

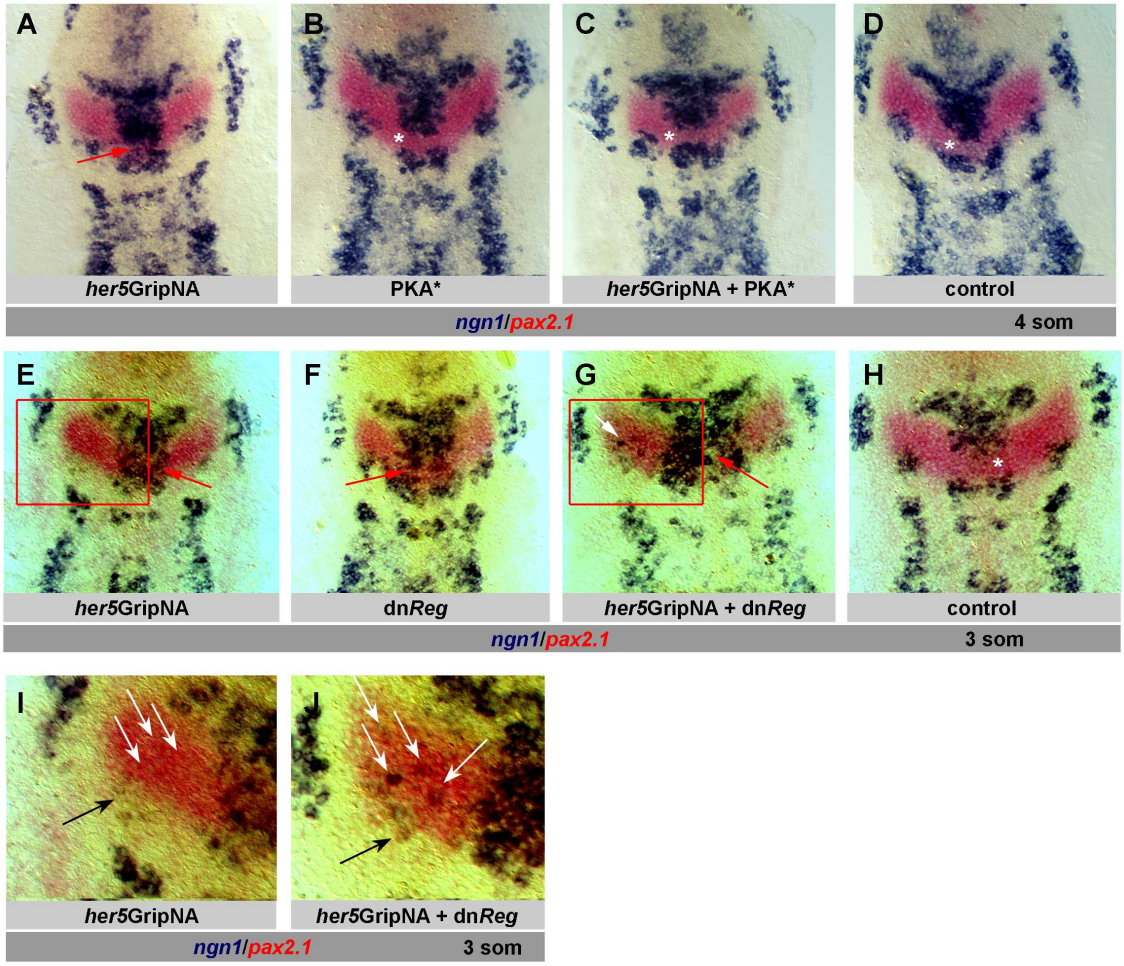

Figure 3.9: **Effects of PKA activity on IZ formation.** Constitutively active PKA increases the threshold for "Him + Her5" inhibitory activity in the MIZ (A-D). Constitutively active PKA (PKA*) prevented the loss of Her5 function to induce ectopic neurogenesis across the MIZ (compare A and C). Nevertheless, constitutively active PKA does not influence normal neurogenesis in the MH domain (compare B and D). Normal formation of the MIZ is indicated with white asterisks, while red arrows indicate ectopic *ngn1* expression. All panels show dorsal views of flat-mounted embryos at the 3-somite stage probed for *ngn1* (blue) and *pax2.1* (red), anterior to the top. Dominant negative PKA (dn*Reg*) decreases the threshold for "Him + Her5" inhibitory activity in both the MIZ and LIZ (E-J). Dorsal views of flat-mounted embryos at the 3-somite stage probed for *ngn1* (blue) and *pax2.1* (red), anterior to the top, following injection of *her5*GripNA (E, I), dn*Reg* (F), coinjection of *her5*Grip and dn*Reg* (G, J), compared to a non-injected control embryo (H). Note that loss of function of Her5 and PKA results in a very similar phenotype, namely ectopic *ngn1*-positive cells in place of the MIZ (compare E and F (red arrows) to H (white asterisk)). Loss of function of both Her5 and PKA in the same embryo induces *ngn1* expression in the LIZ (white arrows in G and J) in addition to its expression in the MIZ (red arrows). Panels I and J are higher magnifications of the area boxed in red in panels E and G, respectively. Black arrows indicate lateral motorneurons of rhombomere 2.

the relative contribution of Gli signaling to the formation of the LIZ. According to my model for formation of the IZ in response to "Him + Her5" activity, the LIZ is characterized by a lower threshold level (see Figure 3.1). To determine whether this threshold level can be modified by Gli1 function, I analyzed the requirement for Her5 inhibitory activity in embryos with an enriched activator Gli1 pool. Enrichment of the activator pool is achieved by inhibiting PKA activity with a dominant negative form of this enzyme (dn*Reg*) [381]. Injection of 50 ng/μl of dn*Reg* induced ectopic neurogenesis across the MIZ (Figure 3.9F, red arrow) (84 % of cases, n=50), similar to the ectopic neurogenesis induced by inhibiting GSK3β activity (Figure 3.3A and Figure 3.6A). In addition, loss of Her5 function in these embryos resulted in ectopic neurogenesis

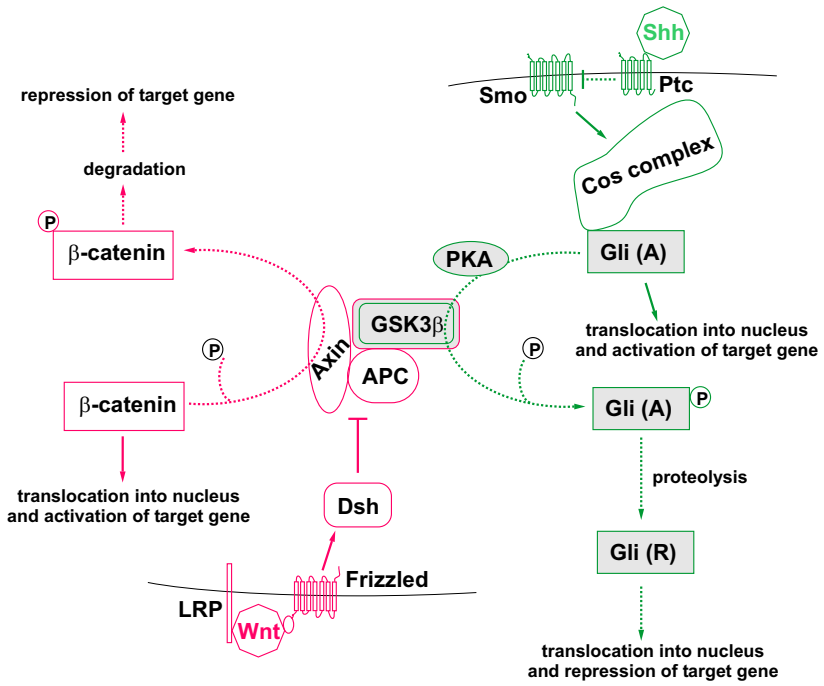

Figure 3.10: **Wnt signaling (red line) and Shh signaling (green line) crosstalk via GSK3β.** GSK3β regulates the amount of effector molecules for both Wnt ($\beta - catenin$) and Shh (Gli) signaling. Parts of the signaling pathways that are inactive in the presence of the ligand are indicated with dotted line. Factors involved in the regulation of the threshold level for the "Him+Her5" inhibitory activity are highlighted in gray. Abbreviations: GSK3β: glycogen synthase kinase-3β; PKA: protein kinase A; Smo: Smoothened; Ptc: Patched; Shh: Sonic hedgehog; Cos: Costal; Dsh: Disheveled; APC: Adenomatous Polyposis Coli.

in both the MIZ (Figure 3.9G and J, red arrows) and the LIZ (Figure 3.9G and J, white arrows) (85.7 % of cases, n=35), a result never observed in embryos lacking

Her5 function alone (Figure 3.9E and I) (90 % of cases, n=30). Thus, LIZ cells, like MIZ cells, respond to Gli1 activity by decreasing their sensitivity to Him and Her5. The accumulation of the activator Gli1 form increases the threshold level in the LIZ and two functional copies of Him are no longer enough to secure the formation of the LIZ. I conclude that *in vivo* the lower threshold level for "Him + Her5" activity in the LIZ is a consequence of the smaller amount of available activator Gli1 form.

Taken together, my data suggest that the graded activity of Gli1 accounts for the differential sensitivity to "Him + Her5" across the IZ. Moreover, this sensitivity is likely regulated by the equilibrium between activator and repressor forms of Gli1, where the activator form increases the threshold level for "Him + Her5", since it is sensitive to PKA/ GSK3β function.

Gli1 activity is not regulated by Shh activity

The above findings that factors involved in Shh signaling (Gli1, PKA and GSK3β) (Figure 3.10) are responsible for the differential sensitivity of the MIZ versus LIZ, and the expression of *shh* at the embryonic midline, suggested that Shh is the signal inducing graded Gli1 activity across the IZ and therefore differential sensitivity across the IZ. To test if Shh signaling is required for the formation of the MIZ and Gli1 activity, I examined the sensitivity of the MIZ to Her5 activity and *gli1* expression in embryos treated with 100 μM cyclopamine. Cyclopamine is thought to completely block Hh signaling at the level of Smoothened (Smo)[382] (Figure 3.10) and to affect the formation of the structures depending on Hh signaling. Indeed, applying cyclopamine onto zebrafish embryos at 50 % epiboly impaired the formation of both somites and adaxial cells , as revealed by *myoD* staining (Figure 3.11E and F, white arrowheads) (97.5 % of cases, n=40). Surprisingly, cyclopamine treatment however did not interfere with the induction of ectopic neurogenesis across the IZ after loss of Her5 function (compare Figure 3.11A (red arrow) and C (white arrow)) (100 % of cases, n=45 for *her5*GripNA; 100 % of cases, n=65 for *her5*GripNA+cyclopamine). In addition, *gli1* expression in cyclopamine - treated embryos was identical to that in non-treated controls (not shown), suggesting that Smoothened-mediated Hh signaling is not necessary to initiate *gli1* expression and regulate its function via PKA and GSK3β during IZ formation.

3.1.3 Conclusions

Maintaining a progenitor pool at the embryonic MHB is crucial to MH growth and IsO maintenance, and I reported here a new molecular player and its associated mechanism preventing neurogenesis in this territory. My arguments are as follows:

1. I identified a new gene encoding for Hairy/E(Spl) transcription factor, *him*, physically linked to *her5* and divergently transcribed, which shares with *her5* expression across the IZ.

2. I demonstrated that blocking either Her5 or Him function results in the same failure to form and maintain the MIZ, and that interfering concomitantly with the function of both factors prevents formation of the LIZ.

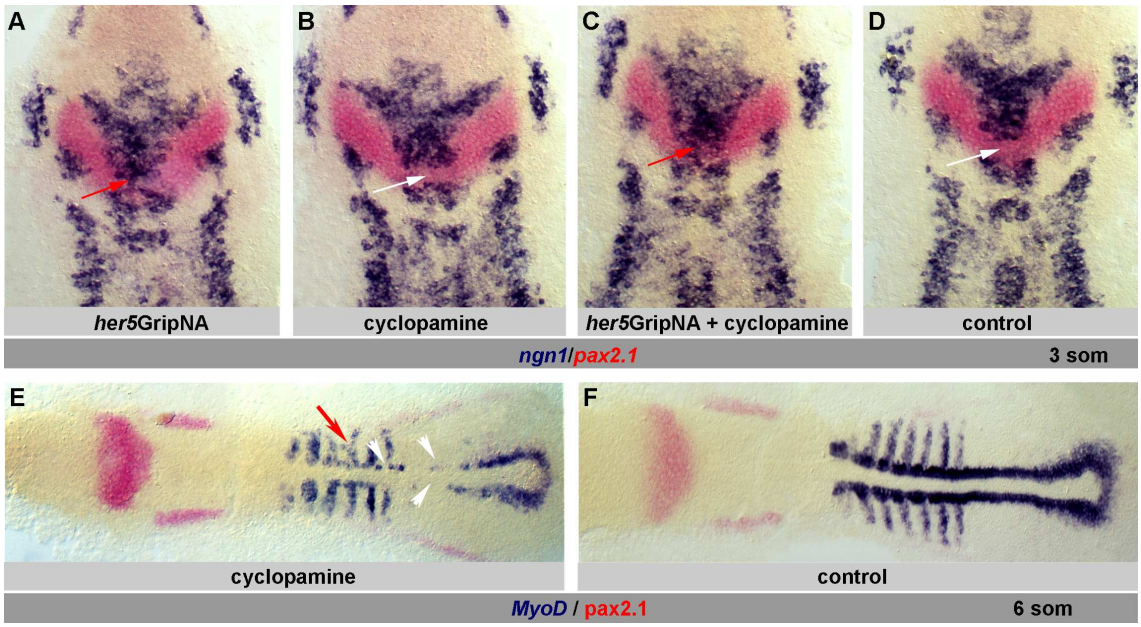

Figure 3.11: **Differential sensitivity of the IZ to "Him + Her5" does not depend on the Shh signaling.** (A-D) Dorsal views of the flat-mounted embryos at 3-somite stage probed for *ngn1* (blue) and *pax2.1* (red) following injection of *her5*GripNA (A), cyclopamine treatment (B), injection of *her5*gripNA combined with cyclopamine treatment (C), compared to an untreated WT, control embryo (D). Note that the embryo unable to receive Shh signal (cyclopamine treated embryo) develop the IZ (compare B and D, white arrow), with the sensitivity to "Him + Her5" activity undistinguishable from WT embryo (compare A and C, red arrow). The dose of cyclopamine insufficient to change sensitivity of the MIZ to "Him + Her5" activity blocks Shh signaling in the mesoderm and impair with formation of both somites and adaxial cells (E, F). Dorsal view of the flat-mounted embryos at 6-somite stage probed for *myoD* (blue) and *pax2.1* (red) following cyclopamine treatment (E), compared to an untreated WT, control embryo (F). *myoD* expression disappears in the adaxial cells (white arrowheads) and decreases in the forming somites (red arrow) upon cyclopamine treatment (E) compared to an untreated embryo (F).

3. Further, I showed that sufficient levels of one factor alone are sufficient to compensate for the lack of the other.

Together, my results are most compatible with a model where the molecular basis of IZ formation is the total "Him + Her5" inhibitory activity.

More recently, I demonstrated that the mechanisms accounting for the differential sensitivity of the MIZ and LIZ were based on graded Gli signaling along the mediolateral neural plate axis at the level of the IZ, and that Gli1 activity in this process was regulated by the PKA/GSK3β3 phosphorylation tandem (Figure 3.10). My arguments

are as follows:

1. I showed that PKA and GSK3β were crucial components of the signaling pathway accounting for the medio-lateral difference across the IZ.

2. Loss of Gli1 function experiments directly implicated the Gli signaling pathway in controlling neurogenesis control.

3.2 Molecular control of addiction

Articles in Appendix B and Appendix C

The best way to study brain functionality is to assess its behavioral output. Studding complex behaviors, such as addiction or anxiety, has two main implications: it provides knowledge and tools to tackle these social illnesses and it offers an excellent opportunity to reveal linkage between genes, neuronal circuitry and elucidated behavior, existing not only at adulthood but also during development.

Most of our knowledge on social behavior comes from studies conducted on laboratory animals, mainly rodents. Although these studies have being performed over more than 40 years, the molecular control of addiction and anxiety remains largely unknown. The main reasons are the complexity of the disorders, which involve environmental factors, and the limited candidate genes. The candidate gene approach, used in mammals, has two main disadvantages: (*i*) it requires that the genes of interest are known and very well characterized and (*ii*) the production of adequate sample size is costly. On the contrary, methods of forward genetics where the genome is mutagenized, the resulting phenotypes characterized and the affected gene subsequently cloned give opportunity to detect both new and known genes controlling the behavior of interest.

In order to gain insight into the molecular control of addiction, I decided to perform genetic screens for dominant mutations affecting addiction to D - amphetamine at adulthood[1], using conditioned place preference (CPP) (see Section 1.5.7) as the experimental assay. I have chosen D - amphetamine because of two reasons: first, all vertebrates tested so far got rapidly addicted to this psychostimulant and second, studies in rodents showed that D - amphetamine affects dopamine uptake, storage in the cytoplasmical vesicles and DAT trafficking (see Section 1.5.4). Therefore, I expected a broad spectrum of molecular networks to be affected and result in altered CPP to D - amphetamine.

In order to conduct genetic screens to detect dominant modifiers of addiction to D - amphetamine, I first setup a CPP paradigm for zebrafish, since this methodology had been developed only for mammals. Further, I performed parametric analyses to make the CPP assay more robust and high throughput for the purpose of large-scale screening. I validated the developed methodology by applying it to fish deficient for cholinergic neural activity. Finally, I developed two additional tests: a test for cognitive

[1]I consider that fish is an adult when it is reproductively mature and all fish used were between 3 and 6 months old.

capacities and a test for anxiety of zebrafish, in order to exclude phenotypes detected in CPP paradigm which are not related to addiction mechanisms *per se*. The development of all three assays, the parametric analyses and the organization and the preliminary results of the two genetic screens will be summarized in the following sections and the reader is referred to the original publications in Appendix B and Appendix C for more detail.

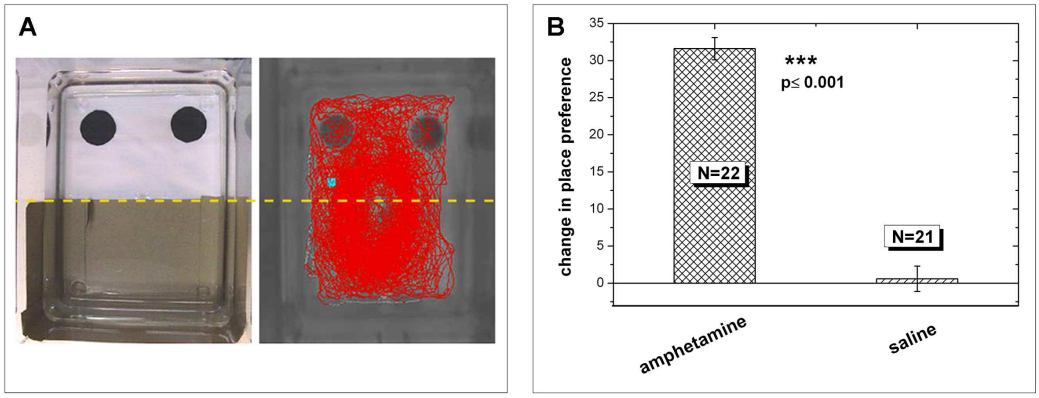

Figure 3.12: **Addiction of adult zebrafish to D - amphetamine measured in CPP paradigm.** **A:** Place Preference measurement setup (left panel, viewed from top) and representative video-recorded route followed by a wild-type fish in this setup (right panel, example with 58 % of the time spent in the preferred compartment). **B:** Change in place preference induced by the intraperitoneal administration of 40 μg/g of D - amphetamine (left) associated with the non-preferred compartment, compared to the administration of saline (right) in identical conditions. The "change in place preference" (Y axis) is measured as the relative difference in time spent in the preferred (non-amphetamine-associated) compartment before (PP_i) and after (PP_f) drug exposure (in percentage of PP_i). This change was compared between N amphetamine-treated and control fish using independent samples Student t-test followed by *arcsine* transformation (see Appendix B for more detail). Standard errors are indicated. Note that amphetamine-injected fish significantly revert their place preference to choose the amphetamine-associated compartment after drug exposure, while fish injected with saline do not revert their preference.

3.2.1 Development of assays for complex behavior in zebrafish

I first developed a reliable place preference test using a two-compartment experimental box. Distinct visual cues divide the experimental tank into two halves: a dark half colored in brown and a bright half colored in white with two frightening, black spots placed at the bottom of the tank (see Figure 3.12A). In this setup, most (95 %, N > 50) wild-type AB adults spend significantly higher (55-75 %) time in the

attractive compartment. The attractive compartment is defined as the compartment in which a fish spends more time during the 1^{st} measuring session and the place preference (PP) is calculated as the percentage of time that the fish spends in the preferred compartment.

To measure addiction to psychostimulants, I developed a conditioned version of the PP test (CPP) where the initially repulsive compartment is associated with the intraperitoneal administration of an optimal dose of D - amphetamine. After conditioning sessions with amphetamine, most (95 %, N > 500) wild-type AB adults reverse their PP, while control fish, injected with saline only, fail to do so (see Figure 3.12B). Unlike observed in mammals, I found that D - amphetamine does not influence zebrafish locomotor activity.

If no significant change in place preference is observed after conditioning with D - amphetamine, one however cannot directly conclude to an absence of positive reinforcing by D - amphetamine. Indeed, there are at least three parameters unrelated to reinforcing *per se*, which might artificially bias the CPP response: (*i*) the degree of aversion to the initially non-preferred compartment, which may interfere with conditioning, (*ii*) the capacity of the animal tested to learn and remember which compartment was associated with the drug, and (*iii*) the capacity of the animal tested to appreciate the visual cues identifying the drug-paired compartment. To rule out an involvement of these factors in the cases where only a low change in PP is detected, I have developed appropriate setups to estimate the basal levels of aversion and the cognitive capacities of adult zebrafish.

The aversion of each fish for the non-preferred compartment was calculated as the difference in the time spent in the preferred versus the non-preferred compartment as follows: $Av = PP_i - ta$, where Av represents the aversion, PP_i is the percentage of time spent in the preferred compartment and ta is the percentage of time in the non-preferred compartment. Tests for the basal levels of aversion have been successfully applied on different zebrafish strains (see Appendix B and Appendix C).

The ability of zebrafish to learn and remember is assessed in a T-maze, where the fish have to find the deep compartment containing food (more detail about the setup design can be found in Appendix D). Each fish was tested once a day and the time needed to reach the deep compartment is scored. I consider that a fish has learned the task when its time to find the target compartment is decreased by more than 50 % compared to the initial value and varies of less than 10 % upon consecutive trials. Analyses conducted on AB fish showed that AB fish need 6 trials to learn the task (see Figure 4C in Appendix B and supplementary material on CD). Therefore, I consider that a muatgenized family where both a lowered CPP and a significant lengthening from baseline learning value are detected rather carries mutation(s) affecting the cognitive abilities of the fish than affecting D - amphetamine - induced reward.

3.2.2 The parametric analysis

In order to improve reproducibility and reliability of CPP and to shorten the time necessary for assay conduction and therefore make CPP appropriate for high throughput large-scale screens, I analyzed several important parameters:

- experimental tank design,
- habituation,
- optimal measuring interval,
- drug administration and
- dose-response.

More details on this parametric analysis can be found in Appendix B.

Following this analysis, I optimized the experimental protocol and obtained a rapid, robust and reproducible assay for addiction to D - amphetamine in zebrafish. This protocol can further be applied in the large-scale screens. The complete experimental protocol is shown in Appendix D.

3.2.3 Genetic identification of AChE as a positive modulator of addiction to D - amphetamine

In mammals, lowered brain ACh signaling has been associated with an increased propensity to get addicted to psychostimulants [324][325]. To determine whether the cholinergic system was involved in a similar regulatory pathway in zebrafish and whether I could reveal modulatory a role of ACh signaling, I measured the sensitivity of zebrafish with genetically impaired ACh metabolism towards the rewarding effects of D - amphetamine.

The *ache*^{sb55} mutation causes increased ACh levels in the brain of *ache*^{sb55}/+ fish

Zebrafish *ache*^{sb55} mutants harbor a point mutation in the AChE-encoding gene, resulting in the production of a non-functional AChE enzyme [383]. Because AChE is the only ACh-degrading enzyme in zebrafish, *ache*^{sb55}/*ache*^{sb55} homozygous embryos are completely deficient in ACh hydrolysis and die of progressive paralysis at early larval stages [383]. *ache*^{sb55}/+ heterozygotes, however, reach adulthood without obvious locomotor or any morphological defects and they do not suffer from grossly abnormal neuroanatomy. I found that AChE activity was decreased by nearly 50 % in the brain of *ache*^{sb55}/+ heterozygotes compared to their wild-type siblings or our AB control strain (see Figure 2A in Appendix C), resulting in a 1.4-fold increase in their level of brain ACh (see Figure 2B in Appendix C). These results suggest that *ache*^{sb55}/+ mutants are a valuable genetic model to test the effects of increased brain levels of ACh.

Amphetamine-induced CPP is reduced in zebrafish AChE mutants

To measure the impact of lowered AChE activity on drug-induced addiction, I assessed the behavior of *ache*^{sb55}/+ adults upon administration of amphetamine in the CPP paradigm. I found that *ache*^{sb55}/+ heterozygotes exhibit a significantly lowered change in place preference compared to their wild-type siblings, which do not

differ from controls of the wild-type AB strain (see Figure 3.13 and Appendix C). Additionally, a dose-response analysis showed that *ache*^{sb55}/+ fish respond with a significantly lower CPP than their siblings over a range of doses reaching at least 60 μg/g. Thus, I concluded that the cholinergic system strongly modulates addictive behavior in zebrafish.

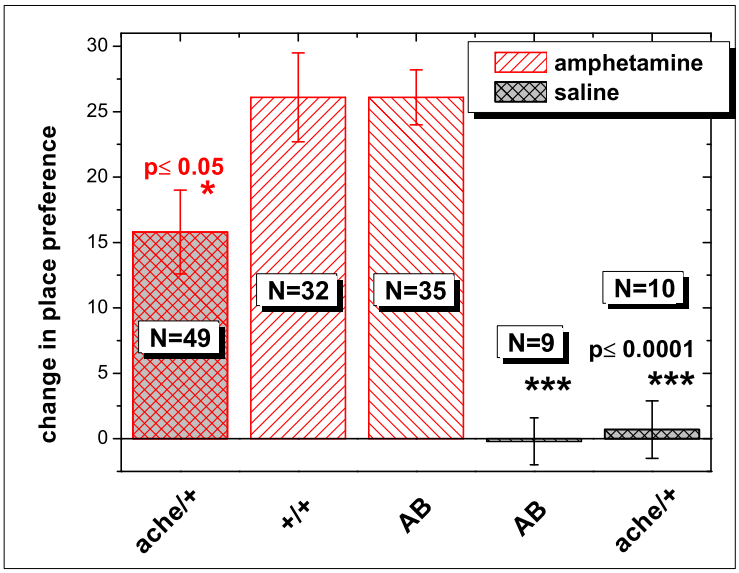

Figure 3.13: **Lowered amphetamine-induced CPP in *ache*^{sb55}/+ heterozygotes.** Amphetamine-induced change in place preference in *ache*^{sb55}/+ heterozygotes (red, left), their wild-type siblings (+/+, red, middle) and AB controls (red, right), also compared to the effect of saline injections in *ache*^{sb55}/+ (black, right) and AB (black, left). The change in place preference (Y axis) is measured and statistically evaluated as in Figure 3.12, and each value is an average of N fish. Amphetamine-induced change in place preference is significantly decreased (1.6 times) in *ache*^{sb55}/+ heterozygotes compared to their wild-type siblings, which do not differ from AB controls. Saline injections have no effect in any of the two populations analyzed.

Genetic impairment of AChE function is not associated with an abnormally high initial place preference (aversion), with lowered memory or with vision defects

To rule out an involvement of factors unrelated to addiction mechanisms *per se* (see Section 3.2.1 and Appendix B) on the lowered CPP response of *ache*^{sb55}/+ heterozygotes, I assessed their basal level of place preference, their memory and their visual performance.

Analysis of the initial place preference in the *ache*^{sb55}/+ fish population revealed

that most *ache*^{sb55}/+ heterozygotes still prefer the brown side (like wild-type fish), but I found that their preference for this compartment is significantly decreased compared to that of their wild-type siblings or AB controls (see Figure 3A in Appendix C). Thus, the reduced change in place preference of *ache*^{sb55}/+ fish following amphetamine administration cannot be due to a strong PP_i preventing conditioning. Further, I more generally showed that the absolute change in place preference does not depend on the PP_i over a range of values tested (see Appendix C). These results support my conclusion that the lowered change in place preference of *ache*^{sb55}/+ fish upon amphetamine injection is not related to their basal preference levels.

I next assessed the learning capacities of *ache*^{sb55}/+ heterozygotes in a simple T-maze assay (see Section 3.2.1, Appendix B and Appendix C). I observed that *ache*^{sb55}/+ fish perform better in the T-maze than their wild-type siblings or AB fish (see Figure 3D and E in Appendix B and Supplemental Movies 2 and 3 on CD). Thus, the reduced CPP of *ache*^{sb55}/+ fish is unlikely to result from an inability to learn and remember.

Finally, in collaboration, the visual performance of *ache*^{sb55}/+ fish was assessed by electroretinography (ERG). The results of ERG tests together with the T-maze assay suggested that vision defects are unlikely to account for the reduced CPP in *ache*^{sb55}/+.

3.2.4 Large-scale screens for mutations affecting D -amphetamine - induced reward

As a broader approach towards gaining insight into the mechanisms controlling reward, I undertook large-scale ENU[2] screens to recover dominant mutations affecting the response to D - amphetamine.

I have conducted two screens (see Appendix D for the scheme of screening procedure) aimed to recover these mutations using the optimized experimental protocol (see Appendix D).

In the first screen, Screen I[3], I have tested 396 F_1 AB adults, corresponding to 396 mutagenized genomes, for their CPP (see Table 3.1). Among these, 21 fish did not show response to D - amphetamine, although all displayed a normal amphetamine content in the brain after intraperitoneal injection.

I have crossed these fish to AB wild-type siblings and raised F_2 generations to confirm the transmissibility of mutant phenotype. So far, I have tested 4 families and in one case I observed transmission of the mutant phenotype (see Figure 3.14) over 5 generations following the typical 50 % mutant/50 % WT ratio expected for a dominant mutation. In addition, I was able to detect the mutant phenotype in the polymorphic mapping background (see Appendix B) and positional cloning of the mutation is in progress.

The second screen, Screen II[4], was done in the Tü background[5]. In this screen,

[2]ENU (ethylnitrosourea) induces point mutations upon repeated administration.
[3]Mutagenesis rate was 1/650, tested against the pigmentation locus *golden*.
[4]A specific mutagenesis rate was not tested.
[5]The fish strain frequently used by number of labs and polymorphic to AB strain.

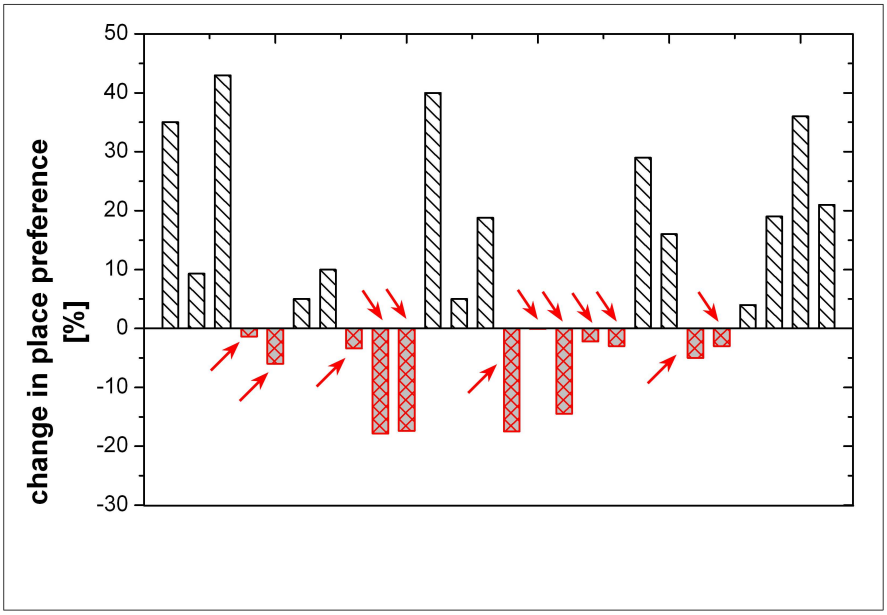

Figure 3.14: **Response to D - amphetamine in the family with mutant phenotype.** Change in PP after D - amphetamine administration in the family with mutant phenotype in the F_2 generation calculated in the same way as in Figure 3.12B. If the change in PP is positive there is a response to the drug, while negative value or no change at all corresponds to the absence of response (mutant phenotype, red arrows in the graph). Note that around 50 % of the fish tested did not respond to D - amphetamine administration measured in CPP paradigm, as expected for a dominant mutation.

I have screened families in the F_2 generation ("multiple animals approach") in order to reduce the problem of false-positives faced in the first screen ("single animal approach"). I have screened 366 families, corresponding to 732 mutagenized genomes, and I detected a mutant phenotype in 25 families[6] (see Table 3.1). Fish from these families were crossed with WT Tü fish to generate the next generation and I am currently checking the transmissibility of phenotype detected in F_2 generation.

3.2.5 Conclusions

The second project of my PhD studies was to set the bases for an investigation of the potential role of neurogenesis control on adult behavior. Within this project I developed a reliable methodology to assess drug-induced reward in zebrafish, involving a number of crucial specificity controls, such as the assessment of the animal's stress,

[6] A family is considered as caring a mutation if $\sim$ 50 % of the fish do not develop addiction to D - amphetamine, as expected for a dominant heritable mutation.

	number of families screened in			number of families with mutant phenotype in			frequency of mutant phenotype		
	F_1	F_2	F_3	F_1	F_2	F_3	F_1	F_2	F_3
Screen I	396	21	1	4	1	1	0.053	0.25	1
Screen II	ND	366	ND	ND	25	ND	ND	0.068	ND

Table 3.1: **Screen statistics.** I performed two screens with the independent ENU - mutagenesis. In Screen I, I screened F_1 generation by testing single animals. Animals which did not develop addiction to D - amphetamine were used for the generation of F_2 families. These families were then screened to confirm transmission of the detected phenotype. In Screen II, I screened families in the F_2 generation. 20 fish per family were analyzed, and families with around 50 % of the fish developing no addiction to D - amphetamine were considered as carrying potential mutations affecting the reward pathway. I concluded that a fish does not develop addiction to D - amphetamine when its PP shift has smaller than 2 % upon three D - amphetamine conditioning sessions.

vision and memory, the measure of optimal drug doses, and a verification of the dose received into the animal's brain.

Thanks to this methodology, I demonstrated the following:

1. more than 95 % of wild-type zebrafish adults robustly experience the rewarding effects of the psychostimulant D - amphetamine,

2. *ache*/+ mutant adult zebrafish, deficient for acetylcholinesterase activity, are strongly resistant to the rewarding effects of D - amphetamine. This phenotype cannot be accounted for by alterations in the exploratory activity, vision or memory of these mutants.

My results provide the first genetic arguments supporting manipulations of AChE activity as a promising avenue towards limiting addiction behavior to psychostimulants.

Based on these results, I have conducted two genetic screens and identified one family carrying a mutation that affects the ability of D - amphetamine to induce reward. This mutation is currently being positionally cloned.

Chapter 4

Discussion and perspectives

The IZ is located at the MHB, present in all vertebrates and characterized by delayed differentiation. Non-differentiation zones, acting as embryonic signaling centers, have been reported in different species and in different embryonic structures, such as the Drosophila wing margin, the dorsal and ventral midlines of the neural tube [384] and inter-rhombomeric boundaries [385]. These signaling centers are involved in the progressive building and patterning of their adjacent territories, and the maintenance of their integrity necessitates their remaining undifferentiated. An undifferentiated state is achieved by Notch signaling at the wing margin and inter-rhombomeric boundaries, and by Shh signaling along the neural tube ventral midline, while the factors involved along the dorsal midline probably involve Wnt and BMP signaling. My findings identify a new developmental strategy to build and maintain signaling centers, namely the differential response of MHB cells to the combined inhibitory activity of two twin and co-regulated Hairy/E(Spl)-like factors, independently of Notch.

I have shown that Him and Her5 play an equally important role in MIZ formation, since an exactly identical phenotype is triggered by lack of either Him or Her5 activity (see Appendix A and [37]). I propose that the crucial determinant of MIZ formation is a total level of "Him + Her5" inhibitory activity, because the regulation of *him* and *her5* function are not interdependent and because increased levels of Him alone to three doses (as in *her5PAC::egfp/+* heterozygote transgenic embryos injected with *her5*MO; Figure 5E in Appendix A) can compensate for the lack of Her5 function within the MIZ. Above a threshold of "Him + Her5", *ngn1* expression is prevented medially and the MIZ is formed, while *ngn1* expression is induced below this threshold (see Figure 3.1). Because the same factors Him and Her5 account for LIZ formation, and can functionally replace each other in this domain as well, a parsimonious interpretation of my findings is to implicate the same dose-dependent mechanism within the LIZ, albeit with a lower threshold level (see Figure 3.1). Together, my results thus lead to a unified model where the maintenance of a pool of progenitor cells at the MHB is orchestrated by a variable dose-dependency to the Him/Her5 pair.

Because of the high redundancy and similar sequence of Him and Her5, it is likely that both factors act together on common targets controlling neurogenesis and . Both factors act upstream of Notch to inhibit expression of *ngn1* and *coe2*, but I failed to show a direct inhibition. The other early proneural genes such as *asha*, *ashb* and

ato3 are not controlled by the Her5/Him pair. To achieve a more comprehensive picture of the cascade connecting Her5 and Him with the proneural genes, such as *ngn1*, or genes involved in control, such as *p27*, it would be interesting to compare the expression profile of wild-type embryos versus embryos lacking Him and Her5 function to identify downstream targets of these two factors. Differentially expressed genes should be analyzed functionally using gain- and loss-of-function approaches, and epigenetic studies conducted to spatio-temporally position these putative factors within the molecular network controlling IZ formation.

Further, it will be important to determine whether the molecular cascade(s) and mechanisms downstream of Her5 and Him are conserved in the MIZ and LIZ. Compared to the MIZ, the LIZ exhibits an additional block, still molecularly unknown, that prevents neurogenesis downstream of Ngn1 activity [37]. Whether Him and Her5 also take part in this second block remains to be tested.

Even in the absence of Him and Her5, I failed to induce *ngn1* expression within a small intermediate field located between the MIZ and LIZ (Figure 7F, and grey triangle in Figure 8 in Appendix A). In this domain, an additional (as yet unknown) factor might increase the total inhibitory activity and/or prevent neurogenesis in addition to Him and Her5. I failed to recover additional IZ-expressed E(Spl) genes following my search through the zebrafish genome and expression studies. Because the intermediate field is aligned with the longitudinal domains of non-differentiation in the hindbrain and spinal cord, it is perhaps more likely that this factor is expressed along the AP axis of the neural plate, like other known neurogenesis inhibitors [12]. A good candidate could be *her3* that is expressed in the longitudinal stripes of non-differentiation and overlaps with the area that stays undifferentiated after loss of Him and Her5 function [56]. It is possible that *her3* contributes to the repression of proneural genes in the LIZ and increases the total inhibitory activity above the threshold level in the small intermediate field, resulting in the inhibition of *ngn1* expression. *him*, *her5* and *her3* might redundantly function in this region, as the inhibition of Her3 function does not lead to ectopic *ngn1* expression at the place of the LIZ [39]. The relative contribution of Her3 to the total inhibitory activity in the IZ remains to be determined.

Redundant factors are generally viewed as "safety" locks, and the biological significance of the Him/Her5 couple might be to secure IZ formation. In the mouse, IZ formation also relies on the two redundant bHLH factors Hes1 and Hes3 [48]. In that case, however, Hes1 and Hes3 are not genetically linked and their expression profiles are clearly distinct, overlapping only at the MHB [386][387], suggesting that mouse and zebrafish have independently evolved a strategy for the redundant expression and function of Hairy/E(Spl) factors at the MHB. A dose dependency and the spatial details of IZ formation in the mouse have not been explored. The fact that one dose of each factor Him and Her5 suffices to maintain the MIZ in zebrafish, while two doses of each single factor do not, probably explains the maintenance of the two genes *him* and *her5* in zebrafish. Linked genes sharing sequence similarity have been reported for a variety of genetic functions in several organisms [388][389][390] [391][392] [125][393]. Duplication events resulting in linked arrays of related genes generate copies that often share cis-acting regulatory sequences. Whether *him* and *her5* expression across the IZ is

coregulated remains to be directly demonstrated but is highly likely, given that the enhancer driving MH expression of *her5* extends into the *him* locus [66]. In addition, *him* and *her5* differ in some aspects of their expression profiles (in the shield and presomitic mesoderm, versus presumptive pharyngeal endoderm, respectively). The regulatory elements controlling endodermal expression of *her5* are located closer to the *her5* ATG than the MH expression elements [66]. Thus expression of the *him*/*her5* pair may be controlled by a combination of proximal, gene-specific elements (accounting for the differential expression sites of the two genes), and distal, probably common elements (driving IZ expression). Detailed dissection of the promoter region will not only answer this coregulation issue, but can also permit the identification of potential inducers of *him* and/or *her5* expression. While the maintenance of *him* and *her5* expression in the MHB involves Pax2.1, En2/3 and Fgf8 (see Figure 3 in Appendix A and [37]), the mechanism that induces the expression of both genes is not clear. The identification of the *him* and *her5* inducers would be an important step in understanding molecular mechanisms linking positional patterning and neurogenesis, since Him and Her5 are both the earliest markers of the MHB (Appendix A) [37][66] and active neurogenesis inhibitors at the MHB (Appendix A) [37].

To further gain insight into the prepatterning of IZ formation it is necessary to identify the cues controlling the differential sensitivity of the MIZ versus LIZ to "Him + Her5", and their functional significance. A priori, there are at least three different mechanisms that can account for this observed differential sensitivity: first, the MIZ may exhibit more cells in M phase than the LIZ, as suggested by antiphosphoH3 immunostaining at 3-somite stage [37], and this difference between MIZ and LIZ cell cycle properties might influence the sensitivity to Her5 and Him; second, initially higher expression levels of *wnt1* in the LIZ than MIZ might enhance cell sensitivity to neurogenesis inhibitors in the LIZ; third, Shh signaling from the ventral midline [374][373] could increase "neurogenic competence". The first two mechanisms are unlikely, given the observations that impairing the cell cycle does not interfere with the sensitivity to neurogenesis inhibition [37] and that disturbing the Wnt medio-lateral gradient does not change the differential sensitivity of the LIZ versus MIZ (see Section 3.1.2 and J. Ninković, unpublished data). I propose that the crucial determinant of the differential sensitivity across the IZ is the Gli network, because Gli1 is expressed in a graded manner across the IZ with a gradient decreasing laterally, and, because after loss of Gli1 function, the MIZ adopts the sensitivity to Hairy/E(Spl) inhibition characteristic for the LIZ (see Figure 3.8). Thus, using a knock-down approach, I showed that Gli proteins are important for the progenitor pool maintenance in addition to their function in neural tube patterning [60][394][395] and primary neurons induction of the [396]. Strikingly, it appears that the role of Gli proteins in neurogenesis is a characteristic of primary neurogenesis in lower vertebrates, since loss of Gli function in mouse does not impair induction of the spinal cord neurons [397], while in Xenopus it abolishes neurogenesis [396]. The role of the Gli network in the maintenance of the progenitor pool at the mouse MHB has not been studied.

Gli proteins act at two levels during neurogenesis: first, they determinate the sites of neural differentiation in combination with neurogenesis inhibitors from the Zic family [60] and second, they regulate neurogenic bHLH genes [60][396]. Several

mechanisms have been postulated to explain how Gli proteins regulate bHLH protein function in both neurogenesis inhibition (Zic proteins) and promotion of neurogenesis (proneural and neural bHLH factors): (*i*) Gli proteins might affect co-factors or additional proteins, such as Id [398] or homeodomain proteins [399][55] or (*ii*) Gli proteins might interact with multiple bHLH proteins. My data suggest that Gli1 proteins do not regulate proneural genes such as *ngn1* downstream of Her5/Him, since loss of Gli1 function does not affect *ngn1* expression. Rather, it reduces the efficiency of Her5 and Him to inhibit neurogenesis. Whether this requires direct interaction with Him and Her5 proteins or specific co-factors remains to be determined.

Knock-down of *gli1* resulted in a change of sensitivity of the MIZ to the "Him + Her5" inhibition, suggesting a specific and functionally relevant role of Gli1 protein in the formation of the IZ. Nevertheless, the findings that the interplay of three frog Gli proteins form dynamic, functional network controlling primary neurogenesis [396], and the expression profiles of the three *gli* genes (*gli1*, *gli2* and *gli2b*) in zebrafish [377][378][379] (J. Ninković, unpublished) indicate the possibility that a network of Gli proteins also controls formation of the progenitor pool at the MHB. In this network, either Gli1 has a dominant regulatory function, or the IZ sensitivity to neurogenesis inhibition is dependent on the dose of total Gli activity which is modified by manipulating Gli1. To discriminate between these two hypotheses, it would be necessary to perform gain-of-function and loss-of-function analyses of other Gli factors, alone or in combination.

Previous work has shown that Gli1 can be induced by Shh signaling and that it can mediate some of the effects of Shh. This together with the existence of a medio-lateral gradient of Shh across the IZ raised the possibility that graded expression and activity of Gli1 is induced and regulated by Shh signaling. Strikingly, inhibition of Shh signaling at the level of coreceptor smoothened (*smo*) by either cyclopeamine application (Figure 3.11) or *smo* specific morpholino knock-down (J. Ninković, unpublished data) did not change either *gli1* expression or the differential sensitivity to neurogenesis inhibitors of the MIZ versus the LIZ. These findings suggest that other unknown factor(s) rather than Shh regulate Gli1 expression or function. The finding that Gli2 participates in A-P patterning as a part of a Fgf-brachyury regulatory loop [400] suggest possibility that Gli1 expression and/or activity is regulated by Fgf signaling at the MHB.

The embryonic MHB progenitor pool serves several vital functions. It generates the large majority of MH neurons and glia, as demonstrated in lineage tracing experiments [66] and genetic or surgical ablation [154][48]. MH neurons form crucial integration centers involved in visual, auditory and motor control and social behavior. Since it has been shown that the developmental functionality of the neurons controlling complex behavior, rather than their activity at adulthood, is the crucial determinant of adult behavior [1][2], I reasoned that addressing complex behaviors, such as drug addiction, will improve not only our knowledge on the mechanisms controlling the brain reward system, but also provide us with more information about the involvement of embryonic events of neurogenesis control in the behavioral output at adulthood.

Zebrafish appears as an ideal model to elucidate these questions, because of its powerful genetics and of the ease with which it can be used to produce developmental

mutants. Prior to the work presented here, two studies had been conducted in zebrafish adults to approach the neurogenetics of drug addiction [401][402]. Importantly, these studies are missing several important controls regarding drug administration, habituation phase and conditioning, thus failing to be reproducible. In contrast, the method I have developed solves the reproducibility problem and in addition includes several specificity controls. Specificity controls are crucial to eliminate scoring behaviors unrelated to the reward pathway *per se*, but rather reflecting changes in the stress status of the tested individual, or impaired drug uptake or transport to the brain.

The methodology developed allowed me to analyze addiction to D - amphetamine in the context of increased cholinergic activity using the zebrafish mutant $ache^{sb55}$ (see Appendix C). I found that a 1.4 fold increased ACh content in the fish brain decreases the rewarding properties of amphetamine and increases cognitive capacities in zebrafish. Because this parallels the situation in mammals, my results provide the first validation of the zebrafish model for studying the neurotransmitter and molecular pathways that underlie the process of addiction in vertebrates.

A number of molecular components of the zebrafish cholinergic system have been identified [403][404], but outside choline acetyltransferase (ChAT, the ACh synthesizing enzyme) and AChE [405][406], their spatial distribution in the adult brain has not been established. The latter reports agree on the presence of ChAT immunoreactive nuclei and fibers in the diencephalon and on AChE activity in most of the forebrain, while Mueller et al. [406] describe in addition an intense cholinergic innervation and cell bodies in the subpallium (striatum). Because the *ache* mutation is likely to affect ACh amounts at all brain levels, my results do not permit to point to the specific cholinergic pathways and developmental time points involved in modulating reward, exploratory activity or learning in zebrafish. These results do not necessarily contrast with previous targeted studies performed in mammals where, although the cholinergic system was initially locally perturbed e.g. by targeted neuron ablation, a widespread adaptative regulation of cholinergic transmission was noted [407].

In my model however, because the genetic impairment of AChE function is operating since the earliest developmental stages, a permanent increase in cholinergic activity is operating to modulate behavior. This may suggest a role for desensitization of AChR rather than an acute inhibition of AChE. In mammals, DA terminals projecting to the NAc harbor nAChR that are highly prone to desensitization [408]. A zebrafish functional equivalent to the NAc remains to be identified, but it is possible that a similar mechanism is at play in the zebrafish subpallium. In addition, in mammals, desensitization of the mAChR present on DA cell bodies projecting to the NAc might also limit the reinforcing effect of amphetamine triggered by ACh on these neurons [409][410]. It will be important to determine whether DA neurons of the posterior tuberculum, the likely zebrafish equivalent of the mammalian VTA [261], receive cholinergic innervation via mAChR.

An alternative scenario to explain the observed phenotype relies on the finding that AChE function is necessary for neuronal development in the zebrafish embryo [383]. According to this model, decreased AChE activity in $ache^{sb55}/+$ animals could impair neuronal survival and/or establishment of proper synapses causing, alterations at adulthood. To test this hypothesis, it would be necessary to rescue the full AChE

activity at different developmental stages and at adulthood and score for the addiction phenotype. However, it is unlikely that neuronal survival accounts for the observed phenotype, since I failed to detect obvious neuroanatomical or neurotransmitter expression failures in the brain of $ache^{sb55}/+$ adults by immunocytochemistry.

Although the central modulatory role of ACh in the CNS and in particular in the control of central DA transmission is well documented, a universal and directly accessible target of this system for drug addiction therapy has been lacking. I demonstrate here that lowering the central activity of AChE by two fold is sufficient to reduce the rewarding effect of amphetamine. In line with this study, a recent report pointed to the pharmacological inhibition of AChE activity by intraperitoneal injection of donepezil in the mouse as a potential means of decreasing the addictive response elicited by cocaine and morphine [327]. It is likely that such injections also globally affect AChE levels, like in zebrafish $ache^{sb55}/+$ mutants, further suggesting that targeting AChE at the organismal level might be effective over a broad range of drugs. Importantly, $ache^{sb55}/+$ zebrafish survive the general modification of AChE and ACh levels over their entire life span without deleterious effects. Together, my findings suggests that a treatment moderately lowering AChE activity could be envisaged in a systemic manner over an extended period of the individual's life with a significant improvement of his resistance to addiction. The zebrafish model itself might be used to select anti-AChE compounds that exhibit minimal side effects [411].

Finally, an important implication of the study conducted in $ache^{sb55}/+$ fish is the demonstration that zebrafish adults can be used to screen for the effect of developmental mutations on adult reward-related behavior and to identify dominant modulators of behavior related to addiction, as I here identify AChE. In ENU mutant screens (see Appendix C), I scored 1128 mutagenized zebrafish genomes and recovered one family with transmission of mutant phenotype over several generations. Although I did not have time to positionally clone the mutations causing the scored phenotypes and to elucidate their developmental significance, the results presented in this thesis provide the fundamental basis for future systematic searches for genetic or pharmacological modifiers of drug-induced reward. These searches should provide crucial and unbiased information not only on the molecular biology of drug addiction but also on the neuronal and molecular networks underlying natural reward learning and memory in vertebrates.

Bibliography

[1] C. Gross, X. Zhuang, K. Stark, S. Ramboz, R. Oosting, L. Kirby, L. Santarelli, S. Beck, and R. Hen. Serotonin1A receptor acts during development to establish normal anxiety-like behaviour in the adult. *Nature*, 416(6879):396–400, 2002.

[2] T.J. Hendricks, D.V. Fyodorov, L.J. Wegman, N.B. Lelutiu, E.A. Pehek, B. Yamamoto, J. Silver, E.J. Weeber, J.D. Sweatt, and E.S. Deneris. Pet-1 ETS gene plays a critical role in 5-HT neuron development and is required for normal anxiety-like and aggressive behavior. *Neuron*, 37(2):233–47, 2003.

[3] L. Santarelli, M. Saxe, C. Gross, A. Surget, F. Battaglia, S. Dulawa, N. Weisstaub, J. Lee, R. Duman, O. Arancio, C. Belzung, and R. Hen. Requirement of hippocampal neurogenesis for the behavioral effects of antidepressants. *Science*, 301(5634):805–9, 2003.

[4] A.B. Vojtek, J. Taylor, S.L. DeRuiter, J.Y. Yu, C. Figueroa, R.P. Kwok, and D.L. Turner. Akt regulates basic helix-loop-helix transcription factor-coactivator complex formation and activity during neuronal differentiation. *Mol Cell Biol*, 23(13):4417–27, 2003.

[5] J.M. Brezun and A. Daszuta. Depletion in serotonin decreases neurogenesis in the dentate gyrus and the subventricular zone of adult rats. *Neuroscience*, 89(4):999–1002, 1999.

[6] S.I. Wilson and T. Edlund. Neural induction: toward a unifying mechanism. *Nat Neurosci*, 4 Suppl:1161–8, 2001.

[7] A. C. Streit and C. D. Stern. Competence for neural induction: HGF/SF, HGF1/MSP and the c-Met receptor. *Ciba Found Symp.*, 212:155–65, 1997.

[8] A. C. Streit, A. J. Berliner, C. Papanayotou, A. Sirulnik, and C. D. Stern. Initiation of neural induction by FGF signalling before gastrulation. *Nature*, 406:74–78, 2000.

[9] A.C. Streit and C.D. Stern. Establishment and maintenance of the border of the neural plate in the chick: involvement of FGF and BMP activity. *Mech Dev.*, 82(1-2):51–66, 1999.

[10] A.C. Streit and C.D. Stern. Neural induction. A bird's eye view. *Trends Genet.*, 15(1):20–4, 1999.

[11] B. Appel and A. Chitnis. Neurogenesis and specification of neuronal identity. *Results Probl Cell Differ*, 40:237–51, 2002.

[12] L. Bally-Cuif and M. Hammerschmidt. Induction and patterning of neuronal development, and its connection to cell cycle control. *Curr Opin Neurobiol*, 13(1):16–25, 2003.

[13] N. Bertrand, D.S. Castro, and F. Guillemot. Proneural genes and the specification of neural cell types. *Nat Rev Neurosci*, 3(7):517–30, 2002.

[14] C.B. Kimmel. Patterning the brain of the zebrafish embryo. *Annu Rev Neurosci*, 16:707–32, 1993.

[15] P. Chapouton and L. Bally-Cuif. Neurogenesis. *Methods Cell Biol*, 76:163–206, 2004.

[16] C.B. Kimmel and M. Westerfield. *Primary neurons of the zebrafish*, pages 561–588. 1990.

[17] S.S. Jr. Easter, J. Burrill, R.C. Marcus, L.S. Ross, J.S. Taylor, and S.W. Wilson. Initial tract formation in the vertebrate brain. *Prog Brain Res*, 102:79–93, 1994.

[18] T. Mueller and M.F. Wullimann. Anatomy of neurogenesis in the early zebrafish brain. *Brain Res Dev Brain Res*, 140(1):137–55, 2003.

[19] E. Hanneman and M. Westerfield. Early expression of acetylcholinesterase activity in functionally distinct neurons of the zebrafish. *J Comp Neurol*, 284(3):350–61, 1989.

[20] L.S. Ross, T. Parrett, and S.S. Jr. Easter. Axonogenesis and morphogenesis in the embryonic zebrafish brain. *J. Neurosci.*, 12(2):467–482, 1992.

[21] S.W. Wilson, L.S. Ross, T. Parrett, and S.S. Jr. Easter. The development of a simple scaffold of axon tracts in the brain of the embryonic zebrafish, Brachydanio rerio. *Development*, 108(1):121–45, 1990.

[22] A.B. Chitnis and J.Y. Kuwada. Axonogenesis in the brain of zebrafish embryos. *J Neurosci*, 10(6):1892–905, 1990.

[23] W.K. Metcalfe, P.Z. Myers, B. Trevarrow, M.B. Bass, and C.B. Kimmel. Primary neurons that express the L2/HNK-1 carbohydrate during early development in the zebrafish. *Development*, 110(2):491–504, 1990.

[24] P.Z. Myers, J.S. Eisen, and M. Westerfield. Development and axonal outgrowth of identified motoneurons in the zebrafish. *J Neurosci*, 6(8):2278–89, 1986.

[25] S.W. Wilson and S.S. Jr. Easter. A pioneering growth cone in the embryonic zebrafish brain. *Proc Natl Acad Sci U S A*, 88(6):2293–6, 1991.

[26] S.W. Wilson and S.S. Jr. Easter. Stereotyped pathway selection by growth cones of early epiphysial neurons in the embryonic zebrafish. *Development*, 112(3):723–46, 1991.

[27] B. Mendelson. Development of reticulospinal neurons of the zebrafish. II. Early axonal outgrowth and cell body position. *J Comp Neurol*, 251(2):172–84, 1986.

[28] B. Mendelson. Development of reticulospinal neurons of the zebrafish. I. Time of origin. *J Comp Neurol*, 251(2):160–71, 1986.

[29] R.R. Bernhardt, A.B. Chitnis, L. Lindamer, and J.Y. Kuwada. Identification of spinal neurons in the embryonic and larval zebrafish. *J Comp Neurol*, 302(3):603–16, 1990.

[30] J.S. Eisen, S.H. Pike, and B. Romancier. An identified motoneuron with variable fates in embryonic zebrafish. *J Neurosci*, 10(1):34–43, 1990.

[31] J.Y. Kuwada, R.R. Bernhardt, and A.B. Chitnis. Pathfinding by identified growth cones in the spinal cord of zebrafish embryos. *J Neurosci*, 10(4):1299–308, 1990.

[32] A. Fisher and M. Caudy. The function of hairy-related bHLH repressor proteins in cell fate decisions. *Bioessays*, 20(4):298–306, 1998.

[33] Y. Grinblat, J. Gamse, M. Patel, and H. Sive. Determination of the zebrafish forebrain: induction and patterning. *Development*, 125:4403–4416, 1998.

[34] O.V. Kazanskaya, E.A. Severtzova, K.A. Barth, G.V. Ermakova, S.A. Lukyanov, A.O. Benyumov, M. Pannese, E. Boncinelli, S.W. Wilson, and A.G. Zaraisky. Anf: a novel class of vertebrate homeobox genes expressed at the anterior end of the main embryonic axis. *Gene*, 200:25–34, 1997.

[35] H. Toresson, J.P. Martinez-Barbera, A. Bardsley, X. Caubit, and S. Krauss. Conservation of BF-1 expression in amphioxus and zebrafish suggests evolutionary ancestry of anterior cell types that contribute to the vertebrate telencephalon. *Dev. Genes Evol.*, 208:431–439, 1998.

[36] M. Muller, E. v Weizsacker, and J.A. Campos-Ortega. Expression domains of a zebrafish homologue of the Drosophila pair-rule gene hairy correspond to primordia of alternating somites. *Development*, 122(7):2071–8, 1996.

[37] A. Geling, M. Itoh, A. Tallafuss, P. Chapouton, B. Tannhauser, J.Y. Kuwada, A.B. Chitnis, and L. Bally-Cuif. bHLH transcription factor Her5 links patterning to regional inhibition of neurogenesis at the midbrain-hindbrain boundary. *Development*, 130(8):1591–604, 2003.

[38] Y. Grinblat and H. Sive. zic gene expression marks anteroposterior pattern in the presumptive neurectoderm of the zebrafish gastrula. *Dev. Dyn.*, 222(4):688–693, 2001.

[39] Y.K. Bae, T. Shimizu, and M. Hibi. Patterning of proneuronal and inter-proneuronal domains by hairy- and enhancer of split-related genes in zebrafish neuroectoderm. *Development*, 132(6):1375–85, 2005.

[40] J.J. Bainter, A. Boos, and K.L. Kroll. Neural induction takes a transcriptional twist. *Dev Dyn*, 222(3):315–27, 2001.

[41] H.G. Belting, G. Hauptmann, D. Meyer, S. Abdelilah-Seyfried, A. Chitnis, C. Eschbach, I. Soll, C. Thisse, B. Thisse, K.B. Artinger, K. Lunde, and W. Driever. Spiel ohne Grenzen/pou2 is required during establishment of the zebrafish midbrain-hindbrain boundary organizer. *Development*, 128(21):4165–76, 2001.

[42] M. Itoh, T. Kudoh, M. Dedekian, C.H. Kim, and A.B. Chitnis. A role for iro1 and iro7 in the establishment of an anteroposterior compartment of the ectoderm adjacent to the midbrain-hindbrain boundary. *Development*, 129(10):2317–27, 2002.

[43] V. Korzh, I. Sleptsova, J. Liao, J. He, and Z. Gong. Expression of zebrafish bHLH genes ngn1 and nrd defines distinct stages of neural differentiation. *Dev Dyn*, 213(1):92–104, 1998.

[44] L. Bally-Cuif, L. Dubois, and A. Vincent. Molecular cloning of Zcoe2, the zebrafish homolog of Xenopus Xcoe2 and mouse EBF-2, and its expression during primary neurogenesis. *Mech Dev*, 77(1):85–90, 1998.

[45] A.G. Zaraisky, S.A. Lukyanov, O.L. Vasiliev, Y.V. Smirnov, A.V. Belyavsky, and O.V. Kazanskaya. A novel homeobox gene expressed in the anterior neural plate of the Xenopus embryo. *Dev Biol*, 152(2):373–82, 1992.

[46] G.V. Ermakova, E.M. Alexandrova, O.V. Kazanskaya, O.L. Vasiliev, M.W. Smith, and A.G. Zaraisky. The homeobox gene, Xanf-1, can control both neural differentiation and patterning in the presumptive anterior neurectoderm of the Xenopus laevis embryo. *Development*, 126(20):4513–23, 1999.

[47] M.T. Dattani, J.P. Martinez-Barbera, P.Q. Thomas, J.M. Brickman, R. Gupta, I.L. Martensson, H. Toresson, M. Fox, J.K. Wales, P.C. Hindmarsh, S. Krauss, R.S. Beddington, and I.C. Robinson. Mutations in the homeobox gene HESX1/Hesx1 associated with septo-optic dysplasia in human and mouse. *Nat Genet*, 19(2):125–33, 1998.

[48] H. Hirata, K. Tomita, Y. Bessho, and R. Kageyama. Hes1 and Hes3 regulate maintenance of the isthmic organizer and development of the mid/hindbrain. *Embo J*, 20(16):4454–66, 2001.

[49] A.D. Chalmers, D. Welchman, and N. Papalopulu. Intrinsic differences between the superficial and deep layers of the Xenopus ectoderm control primary neuronal differentiation. *Dev Cell*, 2(2):171–82, 2002.

[50] M. Ishibashi, S.L. Ang, K. Shiota, S. Nakanishi, R. Kageyama, and F. Guillemot. Targeted disruption of mammalian hairy and Enhancer of split homolog-1 (HES-1) leads to up-regulation of neural helix-loop-helix factors, premature neurogenesis, and severe neural tube defects. *Genes Dev*, 9(24):3136–48, 1995.

[51] M. Ishibashi, K. Moriyoshi, Y. Sasai, K. Shiota, S. Nakanishi, and R. Kageyama. Persistent expression of helix-loop-helix factor HES-1 prevents mammalian neural differentiation in the central nervous system. *Embo J*, 13(8):1799–805, 1994.

[52] T. Ohtsuka, M. Ishibashi, G. Gradwohl, S. Nakanishi, F. Guillemot, and R. Kageyama. Hes1 and Hes5 as notch effectors in mammalian neuronal differentiation. *Embo J*, 18(8):2196–207, 1999.

[53] K. Nakata, T. Nagai, J. Aruga, and K. Mikoshiba. Xenopus Zic family and its role in neural and neural crest development. *Mech Dev*, 75(1-2):43–51, 1998.

[54] E.J. Bellefroid, A. Kobbe, P. Gruss, T. Pieler, J.B. Gurdon, and N. Papalopulu. Xiro3 encodes a Xenopus homolog of the Drosophila Iroquois genes and functions in neural specification. *Embo J*, 17(1):191–203, 1998.

[55] A.A. Gershon, J. Rudnick, L. Kalam, and K. Zimmerman. The homeodomain-containing gene Xdbx inhibits neuronal differentiation in the developing embryo. *Development*, 127(13):2945–54, 2000.

[56] S. Hans, N. Scheer, I. Riedl, E. v Weizsacker, P. Blader, and J.A. Campos-Ortega. her3, a zebrafish member of the hairy-E(spl) family, is repressed by Notch signalling. *Development*, 131(12):2957–69, 2004.

[57] A. Geling, C. Plessy, S. Rastegar, U. Strahle, and L. Bally-Cuif. Her5 acts as a prepattern factor that blocks neurogenin1 and coe2 expression upstream of Notch to inhibit neurogenesis at the midbrain-hindbrain boundary. *Development*, 131(9):1993–2006, 2004.

[58] C. Bourguignon, J. Li, and N. Papalopulu. XBF-1, a winged helix transcription factor with dual activity, has a role in positioning neurogenesis in Xenopus competent ectoderm. *Development*, 125(24):4889–900, 1998.

[59] A. Pierani, S. Brenner-Morton, C. Chiang, and T.M. Jessell. A sonic hedgehog-independent, retinoid-activated pathway of neurogenesis in the ventral spinal cord. *Cell*, 97(7):903–15, 1999.

[60] R. Brewster, J. Lee, and A. Ruiz i Altaba. Gli/Zic factors pattern the neural plate by defining domains of cell differentiation. *Nature*, 393(6685):579–83, 1998.

[61] Y. Koyabu, K. Nakata, K. Mizugishi, J. Aruga, and K. Mikoshiba. Physical and functional interactions between Zic and Gli proteins. *J Biol Chem*, 276(10):6889–92, 2001.

[62] K. Mizugishi, J. Aruga, K. Nakata, and K. Mikoshiba. Molecular properties of Zic proteins as transcriptional regulators and their relationship to GLI proteins. *J Biol Chem*, 276(3):2180–8, 2001.

[63] F. Reifers, H. Bohli, E.C. Walsh, P.H. Crossley, D.Y. Stainier, and M. Brand. Fgf8 is mutated in zebrafish acerebellar (ace) mutants and is required for maintenance of midbrain-hindbrain boundary development and somitogenesis. *Development*, 125(13):2381–95, 1998.

[64] G. Reim and M. Brand. Spiel-ohne-Grenzen/pou2 mediates regional competence to respond to Fgf8 during zebrafish early neural development. *Development*, 129(4):917–33, 2002.

[65] K. Lun and M. Brand. A series of no isthmus (noi) alleles of the zebrafish pax2.1 gene reveals multiple signaling events in development of the midbrain- hindbrain boundary. *Development*, 125:3049–3062, 1998.

[66] A. Tallafuss and L. Bally-Cuif. Tracing of her5 progeny in zebrafish transgenics reveals the dynamics of midbrain-hindbrain neurogenesis and maintenance. *Development*, 130(18):4307–23, 2003.

[67] W. Shoji, C.S. Yee, and J.Y. Kuwada. Zebrafish semaphorin Z1a collapses specific growth cones and alters their pathway in vivo. *Development*, 125(7):1275–83, 1996.

[68] M.C. Halloran, M. Sato-Maeda, J.T. Warren, F. Su, Z. Lele, P.H. Krone, J.Y. Kuwada, and W. Shoji. Laser-induced gene expression in specific cells of transgenic zebrafish. *Development*, 125(9):1953–60, 2000.

[69] P. Simpson. Notch signalling in development: on equivalence groups and asymmetric developmental potential. *Curr Opin Genet Dev*, 7(4):537–42, 1997.

[70] S. Artavanis-Tsakonas, M.D. Rand, and R.J. Lake. Notch signaling: cell fate control and signal integration in development. *Science*, 284(5415):770–6, 1999.

[71] A. Chitnis and C. Kintner. Sensitivity of proneural genes to lateral inhibition affects the pattern of primary neurons in Xenopus embryos. *Development*, 122(7):2295–301, 1996.

[72] J. Lewis. Notch signalling and the control of cell fate choices in vertebrates. *Semin Cell Dev Biol*, 9(6):583–9, 1998.

[73] M. Perron and W.A. Harris. Determination of vertebrate retinal progenitor cell fate by the Notch pathway and basic helix-loop-helix transcription factors. *Cell Mol Life Sci*, 57(2):215–23, 2000.

[74] P. Heitzler, M. Bourouis, L. Ruel, C. Carteret, and P. Simpson. Genes of the Enhancer of split and achaete-scute complexes are required for a regulatory loop between Notch and Delta during lateral signalling in Drosophila. *Development*, 122(1):161–71, 1996.

[75] U. Hinz, B. Giebel, and J.A. Campos-Ortega. The basic-helix-loop-helix domain of Drosophila lethal of scute protein is sufficient for proneural function and activates neurogenic genes. *Cell*, 76(1):77–87, 1994.

[76] M. Kunisch, M. Haenlin, and J.A. Campos-Ortega. Lateral inhibition mediated by the Drosophila neurogenic gene delta is enhanced by proneural proteins. *Proc Natl Acad Sci U S A*, 91(21):10139–43, 1994.

[77] S. Casarosa, C. Fode, and F. Guillemot. Mash1 regulates neurogenesis in the ventral telencephalon. *Development*, 126(3):525–34, 1999.

[78] E. Cau, S. Casarosa, and F. Guillemot. Mash1 and Ngn1 control distinct steps of determination and differentiation in the olfactory sensory neuron lineage. *Development*, 129(8):1871–80, 2002.

[79] C. Fode, G. Gradwohl, X. Morin, A. Dierich, M. LeMeur, C. Goridis, and F. Guillemot. The bHLH protein NEUROGENIN 2 is a determination factor for epibranchial placode-derived sensory neurons. *Neuron*, 20(3):483–94, 1998.

[80] Q. Ma, C. Kintner, and D.J. Anderson. Identification of neurogenin, a vertebrate neuronal determination gene. *Cell*, 87(1):43–52, 1996.

[81] R. Nolo, L.A. Abbott, and H.J. Bellen. Senseless, a Zn finger transcription factor, is necessary and sufficient for sensory organ development in Drosophila. *Cell*, 102(3):349–62, 2000.

[82] L. Dubois, L. Bally-Cuif, M. Crozatier, J. Moreau, L. Paquereau, and A. Vincent. XCoe2, a transcription factor of the Col/Olf-1/EBF family involved in the specification of primary neurons in Xenopus. *Curr Biol*, 8(4):199–209, 1998.

[83] S. Bae, Y. Bessho, M. Hojo, and R. Kageyama. The bHLH gene Hes6, an inhibitor of Hes1, promotes neuronal differentiation. *Development*, 127(13):2933–43, 2000.

[84] N. Koyano-Nakagawa, J. Kim, D. Anderson, and C. Kintner. Hes6 acts in a positive feedback loop with the neurogenins to promote neuronal differentiation. *Development*, 127(19):4203–16, 2000.

[85] Q. Ma, Z. Chen, I. del Barco Barrantes, J.L. de la Pompa, and D.J. Anderson. neurogenin1 is essential for the determination of neuronal precursors for proximal cranial sensory ganglia. *Neuron*, 20(3):469–82, 1998.

[86] N. Ben-Arie, A.E. McCall, S. Berkman, G. Eichele, H.J. Bellen, and H.Y. Zoghbi. Evolutionary conservation of sequence and expression of the bHLH protein Atonal suggests a conserved role in neurogenesis. *Hum Mol Genet*, 5(9):1207–16, 1996.

[87] G. Gradwohl, C. Fode, and F. Guillemot. Restricted expression of a novel murine atonal-related bHLH protein in undifferentiated neural precursors. *Dev Biol*, 180(1):227–41, 1996.

[88] M.H. Farah, J.M. Olson, H.B. Sucic, R.I. Hume, S.J. Tapscott, and D.L. Turner. Generation of neurons by transient expression of neural bHLH proteins in mammalian cells. *Development*, 127(4):693–702, 2000.

[89] M. Perron, K. Opdecamp, K. Butler, W.A. Harris, and E.J. Bellefroid. X-ngnr-1 and Xath3 promote ectopic expression of sensory neuron markers in the neurula ectoderm and have distinct inducing properties in the retina. *Proc Natl Acad Sci U S A*, 96(26):14996–5001, 1999.

[90] J.E. Lee. Basic helix-loop-helix genes in neural development. *Curr Opin Neurobiol*, 7(1):13–20, 1997.

[91] C. Kintner. Neurogenesis in embryos and in adult neural stem cells. *J Neurosci*, 22(3):639–43, 2002.

[92] G. Bain, E.C. Maandag, D.J. Izon, D. Amsen, A.M. Kruisbeek, B.C. Weintraub, I. Krop, M.S. Schlissel, A.J. Feeney, and M. van Roon. E2A proteins are required for proper B cell development and initiation of immunoglobulin gene rearrangements. *Cell*, 79(5):885–92, 1994.

[93] J.E. Lee, S.M. Hollenberg, L. Snider, D.L. Turner, N. Lipnick, and H. Weintraub. Conversion of Xenopus ectoderm into neurons by NeuroD, a basic helix-loop-helix protein. *Science*, 268(5212):836–44, 1995.

[94] C. Porcher, W. Swat, K. Rockwell, Y. Fujiwara, F.W. Alt, and S.H. Orkin. The T cell leukemia oncoprotein SCL/tal-1 is essential for development of all hematopoietic lineages. *Cell*, 86(1):47–57, 1996.

[95] Y. Zhuang, P. Soriano, and H. Weintraub. The helix-loop-helix gene E2A is required for B cell formation. *Cell*, 79(5):875–84, 1994.

[96] D.M. Nikoloff, P. McGraw, and S.A. Henry. The INO2 gene of Saccharomyces cerevisiae encodes a helix-loop-helix protein that is required for activation of phospholipid synthesis. *Nucleic Acids Res*, 20(12):3253, 1992.

[97] D.K. Hoshizaki, J.E. Hill, and S.A. Henry. The Saccharomyces cerevisiae INO4 gene encodes a small, highly basic protein required for derepression of phospholipid biosynthetic enzymes. *J Biol Chem*, 265(8):4736–45, 1990.

[98] G. Berben, M. Legrain, V. Gilliquet, and F. Hilger. The yeast regulatory gene PHO4 encodes a helix-loop-helix motif. *Yeast*, 6(5):451–4, 1990.

[99] A.R. Ferre-D'Amare, G.C. Prendergast, E.B. Ziff, and S.K. Burley. Recognition by Max of its cognate DNA through a dimeric b/HLH/Z domain. *Nature*, 363(6424):38–45, 1993.

[100] C. Murre, P.S. McCaw, H. Vaessin, M. Caudy, L.Y. Jan, Y.N. Jan, C.V. Cabrera, J.N. Buskin, S.D. Hauschka, and A.B. Lassar. Interactions between heterologous helix-loop-helix proteins generate complexes that bind specifically to a common DNA sequence. *Cell*, 58(3):537–44, 1989.

[101] A. Voronova and D. Baltimore. Mutations that disrupt DNA binding and dimer formation in the E47 helix-loop-helix protein map to distinct domains. *Proc Natl Acad Sci U S A*, 87(12):4722–6, 1990.

[102] W.R. Atchley and W.M. Fitch. A natural classification of the basic helix-loop-helix class of transcription factors. *Proc Natl Acad Sci U S A*, 94(10):5172–6, 1997.

[103] M.E. Massari and C. Murre. Helix-loop-helix proteins: regulators of transcription in eucaryotic organisms. *Mol Cell Biol*, 20(2):429–40, 2000.

[104] V. Ledent and M. Vervoort. The basic helix-loop-helix protein family: comparative genomics and phylogenetic analysis. *Genome Res*, 11(5):754–70, 2001.

[105] T. Iso, L. Kedes, and Y. Hamamori. HES and HERP families: multiple effectors of the Notch signaling pathway. *J Cell Physiol*, 194(3):237–55, 2003.

[106] M. Van Doren, P.A. Powell, D. Pasternak, A. Singson, and J.W. Posakony. Spatial regulation of proneural gene activity: auto- and cross-activation of achaete is antagonized by extramacrochaetae. *Genes Dev*, 6(12B):2592–605, 1992.

[107] C.V. Dang, C. Dolde, M.L. Gillison, and G.J. Kato. Discrimination between related DNA sites by a single amino acid residue of Myc-related basic-helix-loop-helix proteins. *Proc Natl Acad Sci U S A*, 89(2):599–602, 1992.

[108] B.A. Hassan and H.J. Bellen. Doing the MATH: is the mouse a good model for fly development? *Genes Dev*, 14(15):1852–65, 2000.

[109] C. Murre, P.S. McCaw, and D. Baltimore. A new DNA binding and dimerization motif in immunoglobulin enhancer binding, daughterless, MyoD, and myc proteins. *Cell*, 56(5):777–83, 1989.

[110] C.V. Cabrera and M.C. Alonso. Transcriptional activation by heterodimers of the achaete-scute and daughterless gene products of Drosophila. *Embo J*, 10(10):2965–73, 1991.

[111] M. Henriksson and B. Luscher. Proteins of the Myc network: essential regulators of cell growth and differentiation. *Adv Cancer Res*, 68:109–82, 1996.

[112] L.M. Facchini and L.Z. Penn. The molecular role of Myc in growth and transformation: recent discoveries lead to new insights. *Faseb J*, 12(9):633–51, 1998.

[113] C.R. Goding. Mitf from neural crest to melanoma: signal transduction and transcription in the melanocyte lineage. *Genes Dev*, 14(14):1712–28, 2000.

[114] S.T. Crews. Control of cell lineage-specific development and transcription by bHLH-PAS proteins. *Genes Dev*, 12(5):607–20, 1998.

[115] R. Benezra, R.L. Davis, D. Lockshon, D.L. Turner, and H. Weintraub. The protein Id: a negative regulator of helix-loop-helix DNA binding proteins. *Cell*, 61(1):49–59, 1990.

[116] H.M. Ellis, D.R. Spann, and J.W. Posakony. Extramacrochaetae, a negative regulator of sensory organ development in Drosophila, defines a new class of helix-loop-helix proteins. *Cell*, 61(1):27–38, 1990.

[117] R. Kageyama and S. Nakanishi. Helix-loop-helix factors in growth and differentiation of the vertebrate nervous system. *Curr Opin Genet Dev*, 7(5):659–65, 1997.

[118] I. Palmeirim, D. Henrique, D. Ish-Horowicz, and O. Pourquie. Avian hairy gene expression identifies a molecular clock linked to vertebrate segmentation and somitogenesis. *Cell*, 91(5):639–48, 1997.

[119] W.C. Jen, V. Gawantka, N. Pollet, C. Niehrs, and C. Kintner. Periodic repression of Notch pathway genes governs the segmentation of Xenopus embryos. *Genes Dev*, 13(11):1486–99, 1999.

[120] W.G. Damen, M. Weller, and D. Tautz. Expression patterns of hairy, even-skipped, and runt in the spider Cupiennius salei imply that these genes were segmentation genes in a basal arthropod. *Proc Natl Acad Sci U S A*, 97(9):4515–9, 2000.

[121] S.M. Parkhurst, D. Bopp, and D. Ish-Horowicz. X:A ratio, the primary sex-determining signal in Drosophila, is transduced by helix-loop-helix proteins. *Cell*, 63(6):1179–91, 1990.

[122] S. Younger-Shepherd, H. Vaessin, E. Bier, L.Y. Jan, and Y.N. Jan. deadpan, an essential pan-neural gene encoding an HLH protein, acts as a denominator in Drosophila sex determination. *Cell*, 70(6):911–22, 1992.

[123] R.L. Davis and D.L. Turner. Vertebrate hairy and Enhancer of split related proteins: transcriptional repressors regulating cellular differentiation and embryonic patterning. *Oncogene*, 20(58):8342–57, 2001.

[124] S.R. Dawson, D.L. Turner, H. Weintraub, and S.M. Parkhurst. Specificity for the hairy/enhancer of split basic helix-loop-helix (bHLH) proteins maps outside the bHLH domain and suggests two separable modes of transcriptional repression. *Mol Cell Biol*, 15(12):6923–31, 1995.

[125] E. Knust, H. Schrons, F. Grawe, and J.A. Campos-Ortega. Seven genes of the Enhancer of split complex of Drosophila melanogaster encode helix-loop-helix proteins. *Genetics*, 132(2):505–18, 1992.

[126] P. Castella, S. Sawai, K. Nakao, J.A. Wagner, and M. Caudy. HES-1 repression of differentiation and proliferation in PC12 cells: role for the helix 3-helix 4 domain in transcription repression. *Mol Cell Biol*, 20(16):6170–83, 2000.

[127] S.T. Crews and C.M. Fan. Remembrance of things PAS: regulation of development by bHLH-PAS proteins. *Curr Opin Genet Dev*, 9(5):580–7, 1999.

[128] C. Leimeister, K. Dale, A. Fischer, B. Klamt, M. Hrabe de Angelis, F. Radtke, M.J. McGrew, O. Pourquie, and M. Gessler. Oscillating expression of c-Hey2 in the presomitic mesoderm suggests that the segmentation clock may use combinatorial signaling through multiple interacting bHLH factors. *Dev Biol*, 227(1):91–103, 2000.

[129] C. Akazawa, Y. Sasai, S. Nakanishi, and R. Kageyama. Molecular characterization of a rat negative regulator with a basic helix-loop-helix structure predominantly expressed in the developing nervous system. *J Biol Chem*, 267(30):21879–85, 1992.

[130] Y. Sasai, R. Kageyama, Y. Tagawa, R. Shigemoto, and S. Nakanishi. Two mammalian helix-loop-helix factors structurally related to Drosophila hairy and Enhancer of split. *Genes Dev*, 6(12B):2620–34, 1992.

[131] K. Tietze, N. Oellers, and E. Knust. Enhancer of splitD, a dominant mutation of Drosophila, and its use in the study of functional domains of a helix-loop-helix protein. *Proc Natl Acad Sci U S A*, 89(13):6152–6, 1992.

[132] M. Ishibashi, Y. Sasai, S. Nakanishi, and R. Kageyama. Molecular characterization of HES-2, a mammalian helix-loop-helix factor structurally related to Drosophila hairy and Enhancer of split. *Eur J Biochem*, 215(3):645–52, 1993.

[133] B.H. Jennings, D.M. Tyler, and S.J. Bray. Target specificities of Drosophila enhancer of split basic helix-loop-helix proteins. *Mol Cell Biol*, 19(7):4600–10, 1999.

[134] C.A. Rushlow, A. Hogan, S.M. Pinchin, K.M. Howe, M. Lardelli, and D. Ish-Horowicz. The Drosophila hairy protein acts in both segmentation and bristle patterning and shows homology to N-myc. *Embo J*, 8(10):3095–103, 1989.

[135] E. Bier, H. Vaessin, S. Younger-Shepherd, L.Y. Jan, and Y.N. Jan. deadpan, an essential pan-neural gene in Drosophila, encodes a helix-loop-helix protein similar to the hairy gene product. *Genes Dev*, 6(11):2137–51, 1992.

[136] D. Sieger, D. Tautz, and M. Gajewski. her11 is involved in the somitogenesis clock in zebrafish. *Dev Genes Evol*, 214(8):393–406, 2004.

[137] C. Takke and J.A. Campos-Ortega. her1, a zebrafish pair-rule like gene, acts downstream of notch signalling to control somite development. *Development*, 126(13):3005–14, 1999.

[138] S.A. Holley, D. Julich, G.J. Rauch, R. Geisler, and C. Nusslein-Volhard. her1 and the notch pathway function within the oscillator mechanism that regulates zebrafish somitogenesis. *Development*, 129(5):1175–83, 2002.

[139] H.L. Stickney, M.J. Barresi, and S.H. Devoto. Somite development in zebrafish. *Dev Dyn*, 219(3):287–303, 2000.

[140] J. Ninkovic, A. Tallafuss, C. Leucht, J. Topczewski, B. Tannhauser, L. Solnica-Krezel, and L. Bally-Cuif. Inhibition of neurogenesis at the zebrafish midbrain-hindbrain boundary by the combined and dose-dependent activity of a new hairy/E(spl) gene pair. *Development*, 132(1):75–88, 2005.

[141] C. Leve, M. Gajewski, K.B. Rohr, and D. Tautz. Homologues of c-hairy1 (her9) and lunatic fringe in zebrafish are expressed in the developing central nervous system, but not in the presomitic mesoderm. *Dev Genes Evol*, 211(10):493–500, 2001.

[142] A. Sawada, A. Fritz, Y.J. Jiang, A. Yamamoto, K. Yamasu, A. Kuroiwa, Y. Saga, and H. Takeda. Zebrafish Mesp family genes, mesp-a and mesp-b are segmentally expressed in the presomitic mesoderm, and Mesp-b confers the anterior identity to the developing somites. *Development*, 127(8):1691–702, 2000.

[143] C. Takke, P. Dornseifer, E. v Weizsacker, and J.A. Campos-Ortega. her4, a zebrafish homologue of the Drosophila neurogenic gene E(spl), is a target of NOTCH signalling. *Development*, 126(9):1811–21, 1999.

[144] A. Pasini, D. Henrique, and D.G. Wilkinson. The zebrafish Hairy/Enhancer-of-split-related gene her6 is segmentally expressed during the early development of hindbrain and somites. *Mech Dev*, 100(2):317–21, 2001.

[145] M. Gajewski and C. Voolstra. Comparative analysis of somitogenesis related genes of the hairy/Enhancer of split class in Fugu and zebrafish. *BMC Genomics*, 3(1):21, 2002.

[146] A. Pasini, Y.J. Jiang, and D.G. Wilkinson. Two zebrafish Notch-dependent hairy/Enhancer-of-split-related genes, her6 and her4, are required to maintain the coordination of cyclic gene expression in the presomitic mesoderm. *Development*, 131(7):1529–41, 2004.

[147] R. Kageyama, T. Ohtsuka, and K. Tomita. The bHLH gene Hes1 regulates differentiation of multiple cell types. *Mol Cells*, 10(1):1–7, 2000.

[148] Z. Paroush, R.L. Jr. Finley, T. Kidd, S.M. Wainwright, P.W. Ingham, R. Brent, and D. Ish-Horowicz. Groucho is required for Drosophila neurogenesis, segmentation, and sex determination and interacts directly with hairy-related bHLH proteins. *Cell*, 79(5):805–15, 1994.

[149] A.L. Fisher, S. Ohsako, and M. Caudy. The WRPW motif of the hairy-related basic helix-loop-helix repressor proteins acts as a 4-amino-acid transcription repression and protein-protein interaction domain. *Mol Cell Biol*, 16(6):2670–7, 1996.

[150] D. Grbavec and S. Stifani. Molecular interaction between TLE1 and the carboxyl-terminal domain of HES-1 containing the WRPW motif. *Biochem Biophys Res Commun*, 223(3):701–5, 1996.

[151] G. Chen, J. Fernandez, S. Mische, and A.J. Courey. A functional interaction between the histone deacetylase Rpd3 and the corepressor groucho in Drosophila development. *Genes Dev*, 13(17):2218–30, 1999.

[152] H. Hirata, T. Ohtsuka, Y. Bessho, and R. Kageyama. Generation of structurally and functionally distinct factors from the basic helix-loop-helix gene Hes3 by alternative first exons. *J Biol Chem*, 275(25):19083–9, 2000.

[153] P.D. Nieuwkoop. The successive steps in the pattern formation of the amphibian central nervous system. *Dev. Growth. Diff.*, 30:717–725, 1989.

[154] W.M. Cowan and T.E. Finger. in Neural Development. *(ed. Spitzer, N.C.)*, pages 377–415, 1982.

[155] C.A. Gardner and K.F. Barald. The cellular environment controls the expression of engrailed-like protein in the cranial neuroepithelium of quail-chick chimeric embryos. *Development*, 113(3):1037–48, 1991.

[156] R.M. Alvarado-Mallart, S. Martinez, and C.C. Lance-Jones. Pluripotentiality of the 2-day-old avian germinative neuroepithelium. *Dev Biol*, 139(1):75–88, 1990.

[157] S. Martinez, M. Wassef, and R.M. Alvarado-Mallart. Induction of a mesencephalic phenotype in the 2-day-old chick prosencephalon is preceded by the early expression of the homeobox gene en. *Neuron*, 6(6):971–81, 1991.

[158] N. Prakash and W. Wurst. Specification of midbrain territory. *Cell Tissue Res*, 318(1):5–14, 2004.

[159] W. Wurst and L. Bally-Cuif. Neural plate patterning: upstream and downstream of the isthmic organizer. *Nat Rev Neurosci*, 2(2):99–108, 2001.

[160] F. Raible and M. Brand. Divide et Impera–the midbrain-hindbrain boundary and its organizer. *Trends Neurosci*, 27(12):727–34, 2004.

[161] F. Marin and L. Puelles. Patterning of the embryonic avian midbrain after experimental inversions: a polarizing activity from the isthmus. *Dev Biol*, 163(1):19–37, 1994.

[162] S. Martinez and R.M. Alvarado-Mallart. Expression of the homeobox Chick-en gene in chick/quail chimeras with inverted mes-metencephalic grafts. *Dev Biol*, 139(2):432–6, 1990.

[163] S. Martinez, F. Marin, M.A. Nieto, and L. Puelles. Induction of ectopic engrailed expression and fate change in avian rhombomeres: intersegmental boundaries as barriers. *Mech Dev*, 51(2-3):289–303, 1995.

[164] H. Nakamura, K.E. Nakano, H.H. Igawa, S. Takagi, and H. Fujisawa. Plasticity and rigidity of differentiation of brain vesicles studied in quail-chick chimeras. *Cell Differ*, 19(3):187–93, 1986.

[165] E. Bloch-Gallego, S. Millet, and R.M. Alvarado-Mallart. Further observations on the susceptibility of diencephalic prosomeres to En-2 induction and on the resulting histogenetic capabilities. *Mech Dev*, 58(1-2):51–63, 1996.

[166] C. Irving and I. Mason. Regeneration of isthmic tissue is the result of a specific and direct interaction between rhombomere 1 and midbrain. *Development*, 126(18):3981–9, 1999.

[167] C. Brodski, D.M. Weisenhorn, M. Signore, I. Sillaber, M. Oesterheld, V. Broccoli, D. Acampora, A. Simeone, and W. Wurst. Location and size of dopaminergic and serotonergic cell populations are controlled by the position of the midbrain-hindbrain organizer. *J Neurosci*, 23(10):4199–207, 2003.

[168] K.M. Wassarman, M. Lewandoski, K. Campbell, A.L. Joyner, J.L. Rubenstein, S. Martinez, and G.R. Martin. Specification of the anterior hindbrain and establishment of a normal mid/hindbrain organizer is dependent on Gbx2 gene function. *Development*, 124(15):2923–34, 1997.

[169] A. Simeone, D. Acampora, M. Gulisano, A. Stornaiuolo, and E. Boncinelli. Nested expression domains of four homeobox genes in developing rostral brain. *Nature*, 358(6388):687–90, 1992.

[170] Z.M. Varga, J. Wegner, and M. Westerfield. Anterior movement of ventral diencephalic precursors separates the primordial eye field in the neural plate and requires cyclops. *Development*, 126(24):5533–46, 1999.

[171] D. Acampora, V. Avantaggiato, F. Tuorto, and A. Simeone. Genetic control of brain morphogenesis through Otx gene dosage requirement. *Development*, 124(18):3639–50, 1997.

[172] Y. Suda, I. Matsuo, and S. Aizawa. Cooperation between Otx1 and Otx2 genes in developmental patterning of rostral brain. *Mech Dev*, 69(1-2):125–41, 1997.

[173] V. Broccoli, E. Boncinelli, and W. Wurst. The caudal limit of Otx2 expression positions the isthmic organizer. *Nature*, 401(6749):164–8, 1999.

[174] S. Millet, K. Campbell, D.J. Epstein, K. Losos, E. Harris, and A.L. Joyner. A role for Gbx2 in repression of Otx2 and positioning the mid/hindbrain organizer. *Nature*, 401(6749):161–4, 1999.

[175] T. Katahira, T. Sato, S. Sugiyama, T. Okafuji, I. Araki, J. Funahashi, and H. Nakamura. Interaction between Otx2 and Gbx2 defines the organizing center for the optic tectum. *Mech Dev*, 91(1-2):43–52, 2000.

[176] D.H. Rowitch and A.P. McMahon. Pax-2 expression in the murine neural plate precedes and encompasses the expression domains of Wnt-1 and En-1. *Mech Dev*, 52(1):3–8, 1997.

[177] C.A. Davis and A.L. Joyner. Expression patterns of the homeo box-containing genes En-1 and En-2 and the proto-oncogene int-1 diverge during mouse development. *Genes Dev*, 2(12B):1736–44, 1988.

[178] C.A. Davis, S.E. Noble-Topham, J. Rossant, and A.L. Joyner. Expression of the homeo box-containing gene En-2 delineates a specific region of the developing mouse brain. *Genes Dev*, 2(3):361–71, 1988.

[179] P.H. Crossley and G.R. Martin. The mouse Fgf8 gene encodes a family of polypeptides and is expressed in regions that direct outgrowth and patterning in the developing embryo. *Development*, 121(2):439–51, 1995.

[180] A. Simeone. Positioning the isthmic organizer where Otx2 and Gbx2meet. *Trends Genet*, 16(6):237–40, 2000.

[181] A.P. McMahon, A.L. Joyner, A. Bradley, and J.A. McMahon. The midbrain-hindbrain phenotype of Wnt-1-/Wnt-1- mice results from stepwise deletion of engrailed-expressing cells by 9.5 days postcoitum. *Cell*, 69(4):581–95, 1992.

[182] X. Sun, E.N. Meyers, M. Lewandoski, and G.R. Martin. Targeted disruption of Fgf8 causes failure of cell migration in the gastrulating mouse embryo. *Genes Dev*, 13(14):1834–46, 1999.

[183] A.C. Lekven, G.R. Buckles, N. Kostakis, and R.T. Moon. Wnt1 and wnt10b function redundantly at the zebrafish midbrain-hindbrain boundary. *Dev Biol*, 254(2):172–87, 2003.

[184] P.H. Crossley, S. Martinez, and G.R. Martin. Midbrain development induced by FGF8 in the chick embryo. *Nature*, 380(6569):66–8, 1996.

[185] S. Martinez, P.H. Crossley, I. Cobos, J.L. Rubenstein, and G.R. Martin. FGF8 induces formation of an ectopic isthmic organizer and isthmocerebellar development via a repressive effect on Otx2 expression. *Development*, 126(6):1189–200, 1999.

[186] C. Irving and I. Mason. Signalling by FGF8 from the isthmus patterns anterior hindbrain and establishes the anterior limit of Hox gene expression. *Development*, 127(1):177–86, 2000.

[187] M. Rhinn and M. Brand. The midbrain–hindbrain boundary organizer. *Curr Opin Neurobiol*, 11(1):34–42, 2001.

[188] W. Wurst, A.B. Auerbach, and A.L. Joyner. Multiple developmental defects in Engrailed-1 mutant mice: an early mid-hindbrain deletion and patterning defects in forelimbs and sternum. *Development*, 120(7):2065–75, 1994.

[189] G. Minowada, L.A. Jarvis, C.L. Chi, A. Neubuser, X. Sun, N. Hacohen, M.A. Krasnow, and G.R. Martin. Vertebrate Sprouty genes are induced by FGF signaling and can cause chondrodysplasia when overexpressed. *Development*, 126(20):4465–75, 1999.

[190] M. Furthauer, W. Lin, S. L. Ang, B. Thisse, and C. Thisse. Sef is a feedback-induced antagonist of Ras/MAPK-mediated FGF signalling. *Nat Cell Biol.*, 4(2):170–4, 2002.

[191] W. Lin, N. Jing, M. A. Basson, A. Dierich, J. Licht, and S.L. Ang. Synergistic activity of Sef and Sprouty proteins in regulating the expression of Gbx2 in the mid-hindbrain region. *Genesis*, 41(3):110–5, 2005.

[192] S. Sugiyama, J. Funahashi, and H. Nakamura. Antagonizing activity of chick Grg4 against tectum-organizing activity. *Dev Biol*, 221(1):168–80, 2000.

[193] I. Araki and H. Nakamura. Engrailed defines the position of dorsal di-mesencephalic boundary by repressing diencephalic fate. *Development*, 126(22):5127–35, 1999.

[194] F. Ristoratore, M. Carl, K. Deschet, L. Richard-Parpaillon, D. Boujard, J. Wittbrodt, D. Chourrout, F. Bourrat, and J.S. Joly. The midbrain-hindbrain boundary genetic cascade is activated ectopically in the diencephalon in response to the widespread expression of one of its components, the medaka gene Ol-eng2. *Development*, 126(17):3769–79, 1999.

[195] E. Matsunaga, I. Araki, and H. Nakamura. Pax6 defines the di-mesencephalic boundary by repressing En1 and Pax2. *Development*, 127(11):2357–65, 2000.

[196] A. Gavalas, M. Davenne, A. Lumsden, P. Chambon, and F.M. Rijli. Role of Hoxa-2 in axon pathfinding and rostral hindbrain patterning. *Development*, 124(19):3693–702, 1997.

[197] B. Fritzsch and R.G. Northcutt. Origin and migration of trochlear, oculomotor and abducent motor neurons in Petromyzon marinus L. *Brain Res Dev Brain Res*, 74(1):122–6, 1993.

[198] J. Mallet, R. Meloni, and C. Laurent. Catecholamine metabolism and psychiatric or behavioral disorders. *Curr Opin Genet Dev*, 4(3):419–26, 1994.

[199] J. Altman and S.A. Bayer. Development of the brain stem in the rat. V. Thymidine-radiographic study of the time of origin of neurons in the midbrain tegmentum. *J Comp Neurol*, 198(4):677–716, 1981.

[200] W. Ye, K. Shimamura, J.L. Rubenstein, M.A. Hynes, and A. Rosenthal. FGF and Shh signals control dopaminergic and serotonergic cell fate in the anterior neural plate. *Cell*, 93(5):755–66, 1998.

[201] M. Hynes, J.A. Porter, C. Chiang, D. Chang, M. Tessier-Lavigne, P.A. Beachy, and A. Rosenthal. Induction of midbrain dopaminergic neurons by Sonic hedgehog. *Neuron*, 15(1):35–44, 1995.

[202] M. Hynes, K. Poulsen, M. Tessier-Lavigne, and A. Rosenthal. Control of neuronal diversity by the floor plate: contact-mediated induction of midbrain dopaminergic neurons. *Cell*, 80(1):95–101, 1995.

[203] M.Z. Wang, P. Jin, D.A. Bumcrot, V. Marigo, A.P. McMahon, E.A. Wang, T. Woolf, and K. Pang. Induction of dopaminergic neuron phenotype in the midbrain by Sonic hedgehog protein. *Nat Med*, 1(11):1184–8, 1995.

[204] T. Yamada, M. Placzek, H. Tanaka, J. Dodd, and T.M. Jessell. Control of cell pattern in the developing nervous system: polarizing activity of the floor plate and notochord. *Cell*, 64(3):635–47, 1991.

[205] Y. Watanabe and H. Nakamura. Control of chick tectum territory along dorsoventral axis by Sonic hedgehog. *Development*, 127(5):1131–40, 2000.

[206] E. Puelles, A. Annino, F. Tuorto, A. Usiello, D. Acampora, T. Czerny, C. Brodski, S.L. Ang, W. Wurst, and A. Simeone. Otx2 regulates the extent, identity and fate of neuronal progenitor domains in the ventral midbrain. *Development*, 131(9):2037–48, 2004.

[207] J.Y. Li, Z. Lao, and A.L. Joyner. Changing requirements for Gbx2 in development of the cerebellum and maintenance of the mid/hindbrain organizer. *Neuron*, 36(1):31–43, 2002.

[208] S.G. Megason and A.P. McMahon. A mitogen gradient of dorsal midline Wnts organizes growth in the CNS. *Development*, 129(9):2087–98, 2002.

[209] M. Ishibashi and A.P. McMahon. A sonic hedgehog-dependent signaling relay regulates growth of diencephalic and mesencephalic primordia in the early mouse embryo. *Development*, 129(20):4807–19, 2002.

[210] M. Panhuysen, D.M. Vogt-Weisenhorn, V. Blanquet, C. Brodski, U. Heinzmann, W. Beisker, and W. Wurst. Effects of Wnt1 signaling on proliferation in the developing mid-/hindbrain region. *Mol Cell Neurosci*, 26(1):101–11, 2004.

[211] J. Xu, Z. Liu, and D.M. Ornitz. Temporal and spatial gradients of Fgf8 and Fgf17 regulate proliferation and differentiation of midline cerebellar structures. *Development*, 127(9):1833–43, 2000.

[212] E. Puelles, D. Acampora, E. Lacroix, M. Signore, A. Annino, F. Tuorto, S. Filosa, G. Corte, W. Wurst, S.L. Ang, and A. Simeone. Otx dose-dependent integrated control of antero-posterior and dorso-ventral patterning of midbrain. *Nat Neurosci.*, 6(5):453–60, 2003.

[213] W.H. Norton, M. Mangoli, Z. Lele, H.M. Pogoda, B. Diamond, S. Mercurio, C. Russell, H. Teraoka, H.L. Stickney, G.J. Rauch, C.P. Heisenberg, C. Houart, T.F. Schilling, H.G. Frohnhoefer, S. Rastegar, C.J. Neumann, R.M. Gardiner, U. Strahle, R. Geisler, M. Rees, W.S. Talbot, and S.W. Wilson. Monorail/Foxa2 regulates floorplate differentiation and specification of oligodendrocytes, serotonergic raphe neurones and cranial motoneurones. *Development*, 132(4):645–58, 2005.

[214] A. Chandrasekhar, H.E. Schauerte, P. Haffter, and J.Y. Kuwada. The zebrafish detour gene is essential for cranial but not spinal motor neuron induction. *Development*, 126(12):2727–37, 1999.

[215] C.R. Gallistel. The role of the dopaminergic projections in MFB self-stimulation. *Behav. Brain Res.*, 22:97–105, 1986.

[216] F. Mora and J.M. Ferrer. Neurotransmitters, pathways and circuits as the neural substrates of self-stimulation of the prefrontal cortex: facts and speculations. *Behav. Brain Res.*, 22:127–140, 1986.

[217] R.D. Hall, F.E. Bloom, and J. Olds. Neuronal and neurochemical substrates of reinforcement. *Neurosci. Res. Program Bull.*, 15:131–134, 1977.

[218] R.A. Wise and P.P. Rompre. Brain dopamine and reward. *Annu. Rev. Psychol.*, 40:191–225, 1989.

[219] T.E. Robinson and K.C. Berridge. The neural basis for drug craving: an incentive-sensitization theory of addiction. *Brain Res. Rev*, 18:247–291, 1993.

[220] G. Di Chiara and R.A. North. Neurobiology of opiate abuse. *Trends Pharmacol. Sci.*, 13:185–193, 1992.

[221] J.R. Hollerman and W. Schultz. Dopamine neurons report an error in the temporal prediction of reward during learning. *Nat. Neurosci.*, 1:304–309, 1998.

[222] B.A. Rocha, F. Fumagalli, R.R. Gainetdinov, S.R. Jones, R. Ator, B. Giros, G.W. Miller, and M.G. Caron. Cocaine self-administration in dopamine-transporter knockout mice. *Nat. Neurosci.*, 1:132–137, 1998.

[223] M.E. Olds and J.L. Fobes. The central basis of motivation: intracranial self-stimulation studies. *Annu. Rev. Psychol.*, 32:523–574, 1981.

[224] Kostowski W. Involvement of dopamine in reward mechanisms and development of addictions: facts and hypotheses (Polish). *Alkohol. Narkoman.*, 13:9–32, 2000.

[225] M.A. Bozarth and R.A. Wise. Intracranial self-administration of morphine into the ventral tegmental area in rats. *Life Sci.*, 28:551–555, 1981.

[226] A.G. Phillips and F.G. LePiane. Reinforcing effects of morphine microinjection into the ventral tegmental area. *Pharmacol. Biochem. Behav.*, 12:965–968, 1980.

[227] R. Bals-Kubik, A. Ableitner, A. Herz, and T.S. Shippenberg. Neuroanatomical sites mediating the motivational effects of opioids as mapped by the conditioned place preference paradigm in rats. *J. Pharmacol. Exp. Ther.*, 264:489–495, 1993.

[228] D.P. Devine, P. Leone, D. Pocock, and R.A. Wise. Differential involvement of ventral tegmental mu, delta, and kappa opioid receptors in modulation of basal mesolimbic dopamine release: in vivo microdialysis studies. *J. Pharmacol. Exp. Ther.*, 266:1236–1246, 1993.

[229] S.W. Johnson and R.A. North. Opioids excite dopamineneurons by hyperpolarization of local interneurons. *J. Neurosci.*, 12:483–488, 1992.

[230] P.B.S. Clarke and A. Pert. Autoradiographic evidence for nicotine receptors on nigrostriatal and mesolimbic dopaminergic neurons. *Brain Res.*, 348:355–358, 1985.

[231] G. Mereu, K-W.P. Yoon, V. Boi, G.L. Gessa, L. Naes, and T.C. Westfall. Preferential stimulation of ventral tegmental area dopaminergic neurons by nicotine. *Eur. J. Pharmacol.*, 141:395–400, 1987.

[232] E.R. Larson and M.A. Ariano. D3 and D2 dopamine receptors: visualization of cellular expression patterns in motor and limbic structures. *Synapse*, 20:325–337, 1995.

[233] J.L. Hurd, F. Weiss, G.F. Koob, N-E. Andén, and U. Ungerstedt. Cocaine reinforcement and extracellular dopamine overflow in rat nucleus accumbens: an in vivo microdialysis study. *Brain Res.*, 498:199–203, 1989.

[234] H.O. Pettit and J.B. Justice. Dopamine in the nucleus accumbens during cocaine self-administration as studied by in vivo microdialysis. *Pharmacol. Biochem. Behav.*, 34:899–904, 1989.

[235] R. Ranaldi, D. Pocock, R. Zereik, and R.A. Wise. Dopamine fluctuations in the nucleus accumbens during maintenance, extinction, and reinstatement of intravenous D-amphetamine self-administration. *J. Neurosci.*, 19:4102–4109, 1999.

[236] R.M. Carelli and S.A. Deadwyler. A comparison of nucleus accumbens neuronal firing patterns during cocaine self-administration and water reinforcement in rats. *J. Neurosci.*, 14:7735–7746, 1994.

[237] R.M. Carelli, V.C. King, R.E. Hampson, and S.A. Deadwyler. Firing patterns of nucleus accumbens neurons during cocaine self-administration in rats. *Brain Res.*, 626:14–22, 1993.

[238] J.Y. Chang, S.F. Sawyer, R.S. Lee, and D.J. Woodward. Electrophysiological and pharmacological evidence for the role of the nucleus accumbens in cocaine selfadministration in freely moving rats. *J. Neurosci.*, 14:1224–1244, 1994.

[239] W. Schultz, P. Apicella, and T. Ljungberg. Responses of monkey dopamine neurons to reward and conditioned stimuli during successive steps of learning a delayed response task. *J. Neurosci.*, 13:900–913, 1993.

[240] B.G. Hoebel, A.P. Monaco, L. Hernandez, E.F. Aulisi, B.G. Stanley, and Lenard L. Self-injection of amphetamine directly into the brain. *Psychopharmacology*, 81:158–163, 1983.

[241] G.D. Phillips, T.W. Robbins, and B.J. Everitt. Bilateral intra-accumbens self-administration of D-amphetamine: antagonism with intra-accumbens SCH-23390 and sulpiride. *Psychopharmacology*, 114:477–485, 1994.

[242] N.E. Goeders and J.E. Smith. Cortical dopaminergic involvement in cocaine reinforcement. *Science*, 221:773–775, 1983.

[243] N.E. Goeders, J.D. Lane, and J.E. Smith. Self-administration of methionine enkephalin into the nucleus accumbens. *Pharmacol. Biochem. Behav.*, 20:451–455, 1984.

[244] R.E. Hinson and S. Siegel. Anticipatory hyperexcitability and tolerance to the narcotizing effect of morphine in the rat. *Behav. Neurosci.*, 97:759–767, 1983.

[245] N.E. Goeders and J.E. Smith. Reinforcing properties of cocaine in the medial prefrontal cortex: primary action on presynaptic dopaminergic terminals. *Pharmacol. Biochem. Behav.*, 25:191–199, 1986.

[246] P.W. Kalivas, R.C. Pierce, J. Cornish, and B.A. Sorg. A role for sensitization in craving and relapse in cocaine addiction. *J. Psychopharmacol.*, 12:49–53, 1998.

[247] B. Moghaddam and B.S. Bunney. Differential effect of cocaine on extracellular dopamine levels in rat medial prefrontal cortex and nucleus accumbens: comparison to amphetamine. *Synapse*, 4:156–161, 1989.

[248] E.A. Pehek and Y.M. Bi. Ritanserin administration potentiates amphetamine-stimulated dopamine release in the rat prefrontal cortex. *Prog. Neuropsychopharmacol. Biol. Psych.*, 21:671–682, 1997.

[249] B.A. Sorg, D.L. Davidson, P.W. Kalivas, and B.M. Prasad. Repeated daily cocaine alters subsequent cocaine-induced increase of extracellular dopamine in the medial prefrontal cortex. *J. Pharmacol. Exp. Ther.*, 281:54–61, 1997.

[250] B.A. Sorg and P.W. Kalivas. Effects of cocaine and footshock stress on extracellular dopamine levels in the medial prefrontal cortex. *Neuroscience*, 53:695–703, 1993.

[251] V.I. Chefer, J.A. Moron, B. Hope, W. Rea, and T.S. Shippenberg. Kappa-opioid receptor activation prevents alterations in mesocortical dopamine neurotransmission that occur during abstinence from cocaine. *Neuroscience*, 101:619–627, 2000.

[252] S.M. Meiergerd, J.O. Schenk, and B.A. Sorg. Repeated cocaine and stress increase dopamine clearance in the rat medial prefrontal cortex. *Brain Res.*, 773:203–207, 1997.

[253] K.A. Cunningham, J.M. Paris, and N.E. Goeders. Chronic cocaine enhances serotonin autoregulation and serotonin uptake binding. *Synapse*, 11:112–123, 1992.

[254] D.W. Self and L. Stein. Pertussis toxin attenuates intracranial morphine self-administration. *Pharmacol. Biochem. Behav.*, 46:689–695, 1993.

[255] K.E. Stevens, G. Shiotsu, and L. Stein. Hippocampal-receptors mediate opioid reinforcement in the CA3 region. *Brain Res.*, 545:8–16, 1991.

[256] A. Bechara and D. Van der Kooy. The tegmental pedunculopontine nucleus: a brainstem output of the limbic system critical for the conditioned place preferences produced by morphine and amphetamine. *J. Neurosci.*, 9:3400–3409, 1989.

[257] C.D. Blaha, L.F. Allen, S. Das, W.L. Inglis, M.P. Latimer, S.R. Vincent, and P. Winn. Modulation of dopamine efflux in the nucleus accumbens after cholinergic stimulation of the ventral tegmental area in intact, pedunculopontine tegmental nucleus-lesioned, and laterodorsal tegmental nucleus-lesioned rats. *J. Neurosci.*, 16:714–722, 1996.

[258] A.J. Lanca, K.L. Adamson, K.M. Coen, B.L. Chow, and W.A. Corrigall. The pedunculopontine tegmental nucleus and the role of cholinergic neurons in nicotine self-administration in the rat: a correlative neuroanatomical and behavioral study. *Neuroscience*, 96:735–742, 2000.

[259] O. Marín, A. González, and W.J.A.J. Smeets. Evidence for a mesolimbic pathway in anuran amphibians: a combined trct-tracing/immunohistochemical study. *Neurosci. Lett.*, 190:183–186, 1995.

[260] O. Marín, W.J.A.J. Smeets, and A. González. Basal ganglia organization in amphibians: evidence for a common pattern in tetrapods. *Prog. Neurobiol.*, 55:363–397, 1998.

[261] E. Rink and M.F. Wullimann. The teleostean (zebrafish) dopaminergic system ascending to the subpallium (striatum) is located in the basal diencephalon (posterior tuberculum). *Brain Res.*, 889:316–330, 2001.

[262] T. Becker, M.F. Wullimann, C.G. Becker, R.R. Bernhardt, and M. Schachner. Axonal regrowth after spinal cord transection in adult zebrafish. *J. Comp. Neurol.*, 377:577–595, 1997.

[263] R. Burstein, K.D. Cliffer, and G.J. Giesler. Direct somatosensory projections from the spinal cord to the hypothalamus and telencephalon. *J. Neurosci.*, 7:4159–4164, 1987.

[264] H.M. Newman and R.T. Stevens. Direct spinal projections to limbic and striatal areas: anterograde transport studies from the upper cervical spinal cord and the cervical enlargement in squirrel monkey and rat. *J.Comp.Neurol.*, 365:640–658, 1996.

[265] M. Kapsimali, B. Vidal, A. González, S. Dufour, and P. Vernier. Distribution of the mRNA encoding the four dopamine D1 receptor subtypes in the brain of the european eel (Anguilla anguilla): comparative approach to the function of D1 receptors in vertebrates. *J. Comp. Neurol.*, 419:320–343, 2000.

[266] I. Anglade, D. Mazurais, V. Douard, C. Le Jossic-Corcos, E.L. Mañanos, D. Michel, and O. Kah. Distribution of glutamic acid decarboxylase mRNA in the forebrain of the rainbow trout as studied by in situ hybridization. *J. Comp. Neurol.*, 410:277–289, 1999.

[267] M.F. Wullimann and D.L. Meyer. Possible multiple evolution of indirect telencephalocerebellar pathways in teleosts: Studies in Carassius auratus and Pantodon buchholzi. *Cell Tissue Res*, 274:447–455, 1993.

[268] E.Y.M. Mok and A.D. Munro. Effects of dopaminergic drugs on locomotor activity in teleost fish of genus Oreochromis (Cichlidae): involvement of the telencephalon. *Physiol. Behav.*, 64:227–234, 1998.

[269] G. Goping, H.B. Pollard, O.M. Adeyemo, and G.A.J. Kuijpers. Effect of MPTP on dopaminergic neurons in the goldfish brain: a light and electron microscope study. *Brain Res.*, 687:35–52, 1995.

[270] J.H. Biel and B.A. Bopp. Amphetamines: structure–activity relationships. In: L.L. Iversen, S.D. Iversen and S.H. Snyder, Editors. *Handbook of Psychopharmacology: Stimulants, Plenum, New York*, page 1–40, 1978.

[271] W.P. Melega, A.E. Williams, D.A. Schmitz, E.W. DiStefano, and A.K. Cho. Pharmacokinetic and pharmacodynamic analysis of the actions of D-amphetamine and D-methamphetamine on the dopamine terminal. *J. Pharmacol. Exp. Ther.*, 274:90–96, 1995.

[272] R.J. Lamb and J.E. Henningfield. Human D-amphetamine drug discrimination: methamphetamine and hydromorphone. *J. Exp. Anal. Behav.*, 61:169–180, 1994.

[273] J.F. Fischer and A.K. Cho. Chemical release of dopamine from striatal homogenates: evidence for an exchange diffusion model. *J Pharmacol Exp Ther*, 208(2):203–9, 1979.

[274] R.C. Pierce and P.W. Kalivas. Repeated cocaine modifies the mechanism by which amphetamine releases dopamine. *J Neurosci*, 17(9):3254–61, 1997.

[275] G.F. Koob and F.E. Bloom. Cellular and molecular mechanisms of drug dependence. *Science*, 242(4879):715–23, 1988.

[276] B. Giros, M. Jaber, S.R. Jones, R.M. Wightman, and M.G. Caron. Hyperlocomotion and indifference to cocaine and amphetamine in mice lacking the dopamine transporter. *Nature*, 379(6566):606–12, 1996.

[277] M.J. Nirenberg, J. Chan, A. Pohorille, R.A. Vaughan, G.R. Uhl, M.J. Kuhar, and V.M. Pickel. The dopamine transporter: comparative ultrastructure of dopaminergic axons in limbic and motor compartments of the nucleus accumbens. *J Neurosci*, 17(18):6899–907, 1997.

[278] V.M. Pickel and J. Chan. Ultrastructural localization of the serotonin transporter in limbic and motor compartments of the nucleus accumbens. *J Neurosci*, 19(17):7356–66, 1999.

[279] R.R. Gainetdinov and M.G. Caron. Monoamine transporters: from genes to behavior. *Annu Rev Pharmacol Toxicol*, 43:261–84, 2003.

[280] G.E. Torres, R.R. Gainetdinov, and M.G. Caron. Plasma membrane monoamine transporters: structure, regulation and function. *Nat Rev Neurosci*, 4(1):13–25, 2003.

[281] D. Sulzer and A. Galli. Dopamine transport currents are promoted from curiosity to physiology. *Trends Neurosci*, 26(4):173–6, 2003.

[282] H.H. Sitte, S. Huck, H. Reither, S. Boehm, E.A. Singer, and C. Pifl. Carrier-mediated release, transport rates, and charge transfer induced by amphetamine, tyramine, and dopamine in mammalian cells transfected with the human dopamine transporter. *J Neurochem*, 71(3):1289–97, 1998.

[283] H. Khoshbouei, H. Wang, J.D. Lechleiter, J.A. Javitch, and A. Galli. Amphetamine-induced dopamine efflux. A voltage-sensitive and intracellular Na+-dependent mechanism. *J Biol Chem*, 278(14):12070–7, 2003.

[284] D. Sulzer and S. Rayport. Amphetamine and other psychostimulants reduce pH gradients in midbrain dopaminergic neurons and chromaffin granules: a mechanism of action. *Neuron*, 5(6):797–808, 1990.

[285] D. Sulzer, E. Pothos, H.M. Sung, N.T. Maidment, B.G. Hoebel, and S. Rayport. Weak base model of amphetamine action. *Ann N Y Acad Sci*, 654:525–8, 1992.

[286] W.B. Burnette, M.D. Bailey, S. Kukoyi, R.D. Blakely, C.G. Trowbridge, and J.B. Jr. Justice. Human norepinephrine transporter kinetics using rotating disk electrode voltammetry. *Anal Chem*, 68(17):2932–8, 1996.

[287] S.R. Jones, R.R. Gainetdinov, R.M. Wightman, and M.G. Caron. Mechanisms of amphetamine action revealed in mice lacking the dopamine transporter. *J Neurosci*, 18(6):1979–86, 1998.

[288] L. Kantor, G.H. Hewlett, Y.H. Park, S.M. Richardson-Burns, M.J. Mellon, and M.E. Gnegy. Protein kinase C and intracellular calcium are required for amphetamine-mediated dopamine release via the norepinephrine transporter in undifferentiated PC12 cells. *J Pharmacol Exp Ther*, 297(3):1016–24, 2001.

[289] N. Chen, C.G. Trowbridge, and J.B. Jr. Justice. Voltammetric studies on mechanisms of dopamine efflux in the presence of substrates and cocaine from cells expressing human norepinephrine transporter. *J Neurochem*, 71(2):653–65, 1998.

[290] C. Pifl, E. Agneter, H. Drobny, H.H. Sitte, and E.A. Singer. Amphetamine reverses or blocks the operation of the human noradrenaline transporter depending on its concentration: superfusion studies on transfected cells. *Neuropharmacology*, 38(1):157–65, 1999.

[291] C. Saunders, J.V. Ferrer, L. Shi, J. Chen, G. Merrill, M.E. Lamb, L.M. Leeb-Lundberg, L. Carvelli, J.A. Javitch, and A. Galli. Amphetamine-induced loss of human dopamine transporter activity: an internalization-dependent and cocaine-sensitive mechanism. *Proc Natl Acad Sci U S A*, 97(12):6850–5, 2000.

[292] K.Y. Little, L.W. Elmer, H. Zhong, J.O. Scheys, and L. Zhang. Cocaine induction of dopamine transporter trafficking to the plasma membrane. *Mol Pharmacol*, 61(2):436–45, 2002.

[293] J.M. Gulley, S. Doolen, and N.R. Zahniser. Brief, repeated exposure to substrates downregulates dopamine transporter function in Xenopus oocytes in vitro and rat dorsal striatum in vivo. *J Neurochem*, 83(2):400–11, 2002.

[294] H.C. Fibiger and A.G. Phillips. Reward, motivation, cognition, psychobiology of mesotelencephalic dopamine systems. *Handbook of Physiology—The Nervous System IV, Williams and Wilkins, Baltimore*, page 647–675, 1986.

[295] A.G.M. Canavan, R.E. Passingham, C.D. Marsden, N. Quinn, M. Wyke, and C.E. Polkey. The performance on learning tasks of patients in the early stages of Parkinson's disease. *Neuropsychologia*, 27:141–156, 1989.

[296] R.A. Wise and D.C. Hoffman. Localization of drug reward mechanisms by intracranial injections. *Synapse*, 10:247–263, 1992.

[297] B.J. Knowlton, J.A. Mangels, and L.R. Squire. A neostriatal habit learning system in humans. *Science*, 273:1399–1402, 1996.

[298] T.W. Robbins and B.J. Everitt. Neurobehavioural mechanisms of reward and motivation. *Curr. Opin. Neurobiol*, 6:228–236, 1996.

[299] P.W. Glimcher, D.M. Margolin, A.A. Giovino, and B.G. Hoebel. Neurotensin: a new 'reward peptide'. *Brain Res.*, 291:119–124, 1984.

[300] P.W. Kalivas. Neurotransmitter regulation of dopamine neurons in the ventral tegmental area. *Brain Res. Rev.*, 18:75–113, 1993.

[301] S. Ikemoto, J.M. Murphy, and W.J. McBride. Self-infusion of GABAA antagonists directly into the ventral tegmental area and adjacent regions. *Behav. Neurosci.*, 111:369–380, 1997.

[302] S. Ikemoto, J.M. Murphy, and W.J. McBride. Regional differences within the rat ventral tegmental area for muscimol self-infusions. *Pharmacol. Biochem. Behav.*, 61:87–92, 1998.

[303] V. David, T.P. Durkin, and P. Cazala. Self administration of the GABAA antagonist bicuculline into the ventral tegmental area in mice: dependence on D2 dopaminergic mechanisms. *Psychopharmacology*, 130:85–90, 1997.

[304] V. David, T.P. Durkin, and P. Cazala. Rewarding effects elicited by the microinjection of either AMPA or NMDA glutamatergic antagonists into the ventral tegmental area revealed by an intracranial self-administration paradigm in mice. *Eur. J. Neurosci*, 10:1394–1402, 1998.

[305] M.G. Lacy, P. Calabresi, and R.A. North. Muscarine depolarizes rat substantia nigra zona compacta and ventral tegmental neurons in vitro through M1-like receptors. *J. Pharmacol. Exp. Ther.*, 253:395–400, 1990.

[306] E. Museo and R.A. Wise. Place preference conditioning with ventral tegmental injections of cytisine. *Life. Sci.*, 55:1179–1186, 1994.

[307] M. Karreman, B.H.C. Westerink, and B. Moghaddam. Excitatory amino acid receptors in the ventral tegmental area regulate dopamine release in the ventral striatum. *J. Neurochem.*, 67:601–607, 1996.

[308] B.H.C. Westerink, H.F. Kwint, and J.B. deVries. The pharmacology of mesolimbic dopamine neurons: a dual-probe microdialysis study in the ventral tegmental area and the nucleus accumbens of the rat brain. *J. Neurosci.*, 16:2605–2611, 1996.

[309] W. Schultz. Predictive reward signal of dopamine neurons. *The American Physiological Society*, pages 1–27, 1998.

[310] W.A. Carlezon and R.A. Wise. Rewarding actions of phencyclidine and related drugs in nucleus accumbens shell and frontal cortex. *J. Neurosci.*, 16:3112–3122, 1996.

[311] W.A. Carlezon, D.P. Devine, and R.A. Wise. Habit-forming actions of nomifensine in nucleus accumbens. *Psychopharmacology*, 122:194–197, 1995.

[312] S. Ikemoto, B.S. Glazier, J.M. Murphy, and W.J. McBride. Role of dopamine D1 and D2 receptors in the nucleus accumbens in mediating reward. *J. Neurosci*, 122:8580–8587, 1997.

[313] C.R. Gerfen. Substance P (neurokinin-1) receptor mRNA is selectively expressed in cholinergic neurons in the striatum and basal forebrain. *Brain Res.*, 556:165–170, 1991.

[314] D. Van der Kooy, R.F. Mucha, M. O'Shaughessy, and P. Bucenieks. Reinforcing effects of brain microinjection of morphine revealed by conditioned place preference. *Brain Res.*, 243:107–117, 1982.

[315] E. Carboni, A. Imperato, L. Perezzani, and G. DiChiara. Amphetamine, cocaine, phencyclidine and nomifensine increase extracellular dopamine concentrations preferentially in the nucleus accumbens of freely moving rats. *Neuroscience*, 28:653–661, 1989.

[316] G.F. Alheid and L. Heimer. New perspectives in basal forebrain organization of special relevance for neuropsychiatric disorders: the striatopallidal, amygdaloid, and corticopetal components of substantia inominata. *Neuroscience*, 27:1–39, 1988.

[317] P.W. Kalivas, L. Churchill, and M.A. Klitenick. The circuitry mediating the translation of motivational stimuli into adaptive motor responses. *Neuroscience*, page 237–287, 1993.

[318] G.F. Koob. Drugs of abuse: anatomy, pharmacology and function of reward pathways. *Trends Pharmacol. Sci.*, 13:177–184, 1992.

[319] M.A. Klitenick, A.Y. Deutch, L. Churchill, and P.W. Kalivas. Topography and functional role of dopaminergic projection from the ventral mesencephallic tegmentum to the ventral pallidum. *Neuroscience*, 50:371–386, 1992.

[320] G.F. Koob and N.R. Swerdlow. Functional output of the mesolimbic dopamine system. *Ann. New York Acad. Sci.*, 537:216–227, 1988.

[321] W.H. Gong, D. Neill, and J.B. Justice. Conditioned place preference and locomotor activation produced by injection of psychostimulants into ventral pallidum. *Brain Res.*, 707:64–74, 1996.

[322] N.E. Goeders and J.E. Smith. Intracranial cocaine self-administration into the medial prefrontal cortex increases dopamine turnover in the nucleus accumbens. *J. Pharmacol. Exp. Ther.*, 265:592–600, 1993.

[323] G.D. Carr and N.M. White. Conditioned place preference from intra-accumbens but not intra-caudate amphetamine injections. *Life Sci.*, 33:2551–2557, 1983.

[324] D. Gerber, T. Sotnikova, R. Gainetdinov, S. Huang, M. Caron, and S. Tonegawa. Hyperactivity, elevated dopaminergic transmission, and response to amphetamine in M1 muscarinic acetylcholine receptor-deficient mice. *Proc. Natl. Acad. Sci. USA*, 98:14312–15317, 2001.

[325] J. Ichikawa, Y. Chung, Z. Li, J. Dai, and H. Meltzer. Cholinergic modulation of basal and amphetamine-induced dopamine release in rat medial prefrontal cortex and nucleus accumbens. *Brain Res.*, 958:176–184, 2002.

[326] A. Alcantara, V. Chen, B. Herring, J. Mendenhall, and M. Berlanga. Localization of dopamine D2 receptors on cholinergic interneurons of the dorsal striatum and nucleus accumbens of the rat. *Brain Res.*, 986:22–29, 2003.

[327] T. Hikida, Y. Kitabatake, I. Pastan, and S. Nakanishi. Acetylcholine enhancement in the nucleus accumbens prevents addictive behaviors of cocaine and morphine. *Proc. Natl. Acad. Sci. USA*, 100:6169–6173, 2003.

[328] T. Tzschentke. Measuring reward with the conditioned place preference paradigm: a comprehensive review of drug effects, recent progress and new issues. *Prog. Neurobiol.*, 56:613–672, 1998.

[329] J.R. Weeks. Experimental morphine addiction: Method for automatic intravenous injections in unrestrained rats. *Science*, 138:143–144, 1962.

[330] G. Deneau, T. Yanagita, and M.H. Seevers. Self-administration of psychoactive substances by the monkey. *Psychopharmacologia*, 16:30–48, 1969.

[331] T. Thompson and C.R. Schuster. Morphine self-administration, food reinforced, and avoidance behaviors in rhesus monkey. *Psychopharmacologia*, 5:87–94, 1964.

[332] S.R. Goldberg. Comparable behavior maintained under fixed-ratio and second-order schedules of food presentation, cocaine injection or D-amphetamine injection in the squirrel monkey. *Journal of Pharmacology and Experimental Therapeutics*, 186:18–30, 1973.

[333] R. Stretch and G.J. Gerber. A method for chronic intravenous drug administration in squirrel monkeys. *Canadian Journal of Physiology and Pharmacology*, 48:575–581, 1970.

[334] B.E. Jones and J.A. Prada. Relapse to morphine use in dog. *Psychopharmacologia*, 30:1–12, 1973.

[335] J.A. Bedford. Drug self-administration in the pig. *Dissertation Abstracts International*, 34:1767–B, 1973.

[336] R.R. Griffiths, J.D. Findley, J.V. Brady, K. Dolan-Gutcher, and W.W. Robinson. Comparison of progressive-ratio performance maintained by cocaine, methylphenidate and secobarbital. *Psychopharmacologia*, 43:81–83, 1975.

[337] S.E. Lukas, R.R. Griffiths, L.D. Bradford, J.V. Brady, L. Daley, and R. Delorenzo. A tethering system for intravenous and intragastric drug administration in the baboon. *Pharmacology Biochemistry Behavior*, 17:823–829, 1982.

[338] R.L. Balster, M.M. Kilbey, and E.H. Ellinwood. Methamphetamine self-administration in the cat. *Psychopharmacologia*, 46:229–233, 1976.

[339] H.E. Criswell and A. Ridings. Intravenous self-administration of morphine by naive mice. *Pharmacology Biochemistry Behavior*, 18:467–470, 1983.

[340] J.D. Davis and N.E. Miller. Fear and pain: Their effect on self-injection of amobarbital sodium by rats. *Science*, 141:1286–1287, 1963.

[341] R. Pickens, R. Meisch, and L.E. McGuire. Methamphetamine reinforcement in rats. *Psychonomic Science*, 8:371–372, 1967.

[342] R. Pickens and W.C. Harris. Self-administration of D-amphetamine by rats. *Psychopharmacologia*, 12:158–163, 1968.

[343] R. Pickens and T. Thompson. Cocaine-reinforced behavior in rats: Effects of reinforcement magnitude and fixed-ratio size. *Journal of Pharmacology and Experimental Therapeutics*, 161:122–129, 1968.

[344] R.D. Spealman and S.R. Goldberg. Drug self-administration by laboratory animals: Control by schedules of reinforcement. *Annual Reviews of Pharmacology and Toxicology*, 18:313–339, 1978.

[345] J.L. Katz and S.R. Goldberg. Second-order schedules of drug reinforcement. *Methods of Assessing the Reinforcing Properties of Abused Drugs*, 1:105–115, 1987.

[346] J. Stewart and H. de Wit. Reinstatement of drug-taking behavior as a method of assessing incentive motivational properties of drugs. *Methods of Assessing the Reinforcing Properties of Abused Drugs*, 1:211–227, 1987.

[347] R.A. Meisch and M.E. Carroll. Oral drug self-administration: Drugs as reinforcers. *Methods of Assessing the Reinforcing Properties of Abused Drugs*, 1:143–160, 1987.

[348] M.A. Bozarth. Intracranial self-administration procedures for the assessment of drug reinforcement. *Methods of Assessing the Reinforcing Properties of Abused Drugs*, 1:173–187, 1987.

[349] R.A. Wise. Intravenous drug self-administration: A special case of positive reinforcement. *Methods of Assessing the Reinforcing Properties of Abused Drugs*, 1:117–141, 1987.

[350] C.L.E. Broekkamp. Combined microinjection and brain stimulation reward methodology for the localization of reinforcing drug effects. *Methods of Assessing the Reinforcing Properties of Abused Drugs*, 1:479–488, 1987.

[351] L.D. Reid and M.A. Bozarth. Addictive agents and pressing for intracranial stimulation (ICS): The effects of various opioids on pressing for ICS. *Problems of Drug Dependence*, pages 729–741, 1978.

[352] R. Esposito and C. Kornetsky. Opioids and rewarding brain stimulation. *Neuroscience and Biobehavioral Reviews*, 2:115–122, 1978.

[353] J. Atalay and R.A. Wise. Time course of pimozide effects on brain stimulation reward. *Pharmacology Biochemistry and Behavior*, 18:655–658, 1983.

[354] D. van der Kooy. Place conditioning: A simple and effective method for assessing the motivational properties of drugs. *Methods of Assessing the Reinforcing Properties of Abused Drugs*, 1:229–240, 1987.

[355] W.M. Davis and S.G. Smith. Conditioned reinforcement as a measure of the rewarding properties of drugs. *Methods of Assessing the Reinforcing Properties of Abused Drugs*, 1:199–210, 1987.

[356] M.A. Bozarth. Conditioned place preference: A parametric analysis using systemic heroin injections. *Methods of Assessing the Reinforcing Properties of Abused Drugs*, 1:241–273, 1987.

[357] C. Klambt, E. Knust, K. Tietze, and J.A. Campos-Ortega. Closely related transcripts encoded by the neurogenic gene complex enhancer of split of Drosophila melanogaster. *EMBO J*, 8:203 –210, 1989.

[358] C.A. Henry, M.K. Urban, K.K. Dill, J.P. Merlie, M.F. Page, C.B. Kimmel, and S.L. Amacher. Two linked hairy/Enhancer of split-related zebrafish genes, her1 and her7, function together to refine alternating somite boundaries. *Development*, 129:3693 –3704, 2002.

[359] B.A. Firulli, D.B. Hadzic, J.R. McDaid, and A.B. Firulli. The basic helix-loop-helix transcription factors dHAND and eHAND exhibit dimerization characteristics that suggest complex regulation of function. *J. Biol. Chem*, 275:33567 –33573, 2000.

[360] T. Iso, V. Sartorelli, C. Poizat, S. Iezzi, H.Y. Wu, G. Chung, L. Kedes, and Y. Hamamori. THERP, a novel heterodimer partner of HES/E(spl) in Notch signaling. *Mol. Cell. Biol*, 21:6080 –6089, 2001.

[361] S.M. Wainwright and D. Ish-Horowicz. Point mutations in the Drosophila hairy gene demonstrate in vivo requirements for basic, helix-loop-helix, and WRPW domains. *Mol. Cell. Biol*, 12:2475 –2483, 1992.

[362] J.D. Brown and R.T. Moon. Wnt signaling: Why is everything so negative? *Curr. Opin. Cell Biol*, 10:182–187, 1998.

[363] A. Wodarz and R. Nusse. Mechanisms of Wnt signaling in development. *Annu. Rev. Cell. Dev. Biol*, 14:59–88, 1998.

[364] H. Aberle, A. Bauer, J. Stappert, A. Kispert, and R. Kemler. Beta-catenin is a target for the ubiquitin-proteasome pathway. *EMBO J.*, 16:3797–3804, 1997.

[365] S. Ikeda, S. Kishida, H. Yamamoto, H. Murai, S. Koyama, and A. Kikuchi. Axin, a negative regulator of the Wnt signaling pathway, forms a complex with GSK-3beta and beta-catenin and promotes GSK-3beta-dependent phosphorylation of beta-catenin. *EMBO J.*, 17:1371–1384, 1998.

[366] S. Kishida, H. Yamamoto, S. Hino, S. Ikeda, M. Kishida, and A. Kikuchi. DIX domains of Dvl and axin are necessary for protein interactions and their ability to regulate beta-catenin stability. *Mol. Cell. Biol*, 19:4414–4422, 1999.

[367] C.P. Heisenberg, C. Houart, M. Take-Uchi, G.J. Rauch, N. Young, P. Coutinho, I. Masai, L. Caneparo, M.L. Concha, R. Geisler, T.C. Dale, S.W. Wilson, and D.L. Stemple. A mutation in the Gsk3-binding domain of zebrafish Masterblind/Axin1 leads to a fate transformation of telencephalon and eyes to diencephalon. *Genes Dev*, 15(11):1427–34, 2001.

[368] J.L. Lewis, J. Bonner, M. Modrell, J.W. Ragland, R.T. Moon, R.I. Dorsky, and D.W. Raible. Reiterated Wnt signaling during zebrafish neural crest development. *Development*, 131(6):1299–308, 2004.

[369] R.I. Dorsky, L.C. Sheldahl, and R.T. Moon. A transgenic Lef1/beta-catenin-dependent reporter is expressed in spatially restricted domains throughout zebrafish development. *Dev. Biol*, 241:229 –237, 2002.

[370] M.J. Berridge, C.P. Downes, and M.R. Hanley. Neural and developmental actions of lithium: a unifying hypothesis. *Cell*, 59(3):411–419, 1989.

[371] L.M. Hallcher and W.R. Sherman. The effects of lithium ion and other agents on the activity of myo-inositol-1-phosphatase from bovine brain. *J Biol Chem*, 255(22):10896–901, 1980.

[372] A. Martinez, M. Alonso, A. Castro, C. Perez, and F.J. Moreno. First non-ATP competitive glycogen synthase kinase 3 beta (GSK-3beta) inhibitors: thiadiazolidinones (TDZD) as potential drugs for the treatment of Alzheimer's disease. *J Med Chem*, 45(6):1292–9, 2002.

[373] M. Carl and J. Wittbrodt. Graded interference with FGF signalling reveals its dorsoventral asymmetry at the mid-hindbrain boundary. *Development*, 126:5659 –5667, 1999.

[374] R. Koster, R. Stick, F. Loosli, and J. Wittbrodt. Medaka spalt acts as a target gene of hedgehog signaling. *Development*, 124:3147 –3156, 1997.

[375] J. Jia, K. Amanai, G. Wang, J. Tang, B. Wang, and J. Jiang. Shaggy/GSK3 antagonizes Hedgehog signalling by regulating Cubitus interruptus. *Nature*, 416(6880):548–52, 2002.

[376] M.A. Price and D. Kalderon. Proteolysis of the Hedgehog signaling effector Cubitus interruptus requires phosphorylation by Glycogen Synthase Kinase 3 and Casein Kinase 1. *Cell*, 108(6):823–35, 2002.

[377] R.O. Karlstrom, O.V. Tyurina, A. Kawakami, N. Nishioka, W.S. Talbot, H. Sasaki, and A.F. Schier. Genetic analysis of zebrafish gli1 and gli2 reveals divergent requirements for gli genes in vertebrate development. *Development*, 130(8):1549–64, 2003.

[378] O.V. Tyurina, B. Guner, E. Popova, J. Feng, A.F. Schier, J.D. Kohtz, and R.O. Karlstrom. Zebrafish Gli3 functions as both an activator and a repressor in Hedgehog signaling. *Dev Biol*, 277(2):537–56, 2005.

[379] Z. Ke, A. Emelyanov, S.E. Lim, V. Korzh, and Z. Gong. Expression of a novel zebrafish zinc finger gene, gli2b, is affected in Hedgehog and Notch signaling related mutants during embryonic development. *Dev Dyn*, 232(2):479–86, 2005.

[380] M. Hammerschmidt, M.J. Bitgood, and A.P. McMahon. Protein kinase A is a common negative regulator of Hedgehog signaling in the vertebrate embryo. *Genes Dev*, 10(6):647–58, 1996.

[381] U. Strahle, N. Fischer, and P. Blader. Expression and regulation of a netrin homologue in the zebrafish embryo. *Mech Dev*, 62(2):147–60, 1997.

[382] J. Taipale, J.K. Chen, M.K. Cooper, B. Wang, R.K. Mann, L. Milenkovic, M.P. Scott, and P.A. Beachy. Effects of oncogenic mutations in Smoothened and Patched can be reversed by cyclopamine. *Nature*, 406:1005 –1009, 2000.

[383] M. Behra, X. Cousin, C. Bertrand, J.L. Vonesch, D. Biellmann, A. Chatonnet, and U. Strahle. Acetylcholinesterase is required for neuronal and muscular development in the zebrafish embryo. *Nat Neurosci*, 5:111–118, 2002.

[384] P. Alexandre and M. Wassef. The isthmic organizer links anteroposterior and dorsoventral patterning in the mid/hindbrain by generating roof plate structures. *Development*, 130:5331 –5338, 2003.

[385] Y.C. Cheng, M. Amoyel, X. Qiu, Y.J. Jiang, Q. Xu, and D.G. Wilkinson. Notch activation regulates the segregation and differentiation of rhombomere boundary cells in the zebrafish hindbrain. *Dev. Cell*, 6:539 –550, 2004.

[386] T. Allen and C.G. Lobe. A comparison of Notch, Hes and Grg expression during murine embryonic and post-natal development. *Cell Mol Biol*, 45(5):687–708, 1999.

[387] C.G. Lobe. Expression of the helix-loop-helix factor, Hes3, during embryo development suggests a role in early midbrain-hindbrain patterning. *Mech Dev.*, 62(2):227–37, 1997.

[388] M. Akam. Hox and HOM: homologous gene clusters in insects and vertebrates. *Cell*, 57:347 –349, 1989.

[389] M.C. Alonso and C.V. Cabrera. The achaete-scute gene complex of Drosophila melanogaster comprises four homologous genes. *EMBO J.*, 7:2585 –2591, 1988.

[390] E. Bober, C. Baum, T. Braun, and H.H. Arnold. A novel NK-related mouse homeobox gene: expression in central and peripheral nervous structures during embryonic development. *Dev. Biol.*, 162:288 –303, 1994.

[391] K.G. Coleman, S.J. Poole, M.P. Weir, W.C. Soeller, and T. Kornberg. The invected gene of Drosophila: sequence analysis and expression studies reveal a close kinship to the engrailed gene. *Genes Dev.*, 1:19–28, 1987.

[392] M. Kmita and D. Duboule. Organizing axes in time and space; 25 years of colinear tinkering. *Science*, 301:331 –333, 2003.

[393] S. Stein, K. Niss, and M. Kessel. Differential activation of the clustered homeobox genes CNOT2 and CNOT1 during notogenesis in the chick. *Dev. Biol.*, 180:519 –533, 1996.

[394] A. Ruiz i Altaba. Catching a Gli-mpse of Hedgehog. *Cell*, 90(2):193–6, 1997.

[395] A. Ruiz i Altaba. Combinatorial Gli gene function in floor plate and neuronal inductions by Sonic hedgehog. *Development*, 125(12):2203–12, 1998.

[396] V. Nguyen, A.L. Chokas, B. Stecca, and A. Ruiz i Altaba. Cooperative requirement of the Gli proteins in neurogenesis. *Development*, 132(14):3267–79, 2005.

[397] C.B. Bai, D. Stephen, and A.L. Joyner. All mouse ventral spinal cord patterning by hedgehog is Gli dependent and involves an activator function of Gli3. *Dev Cell*, 6(1):103–15, 2004.

[398] K.J. Liu and R.M. Harland. Cloning and characterization of Xenopus Id4 reveals differing roles for Id genes. *Dev. Biol*, 264:339 –351, 2003.

[399] J. Briscoe, A. Pierani, T.M. Jessell, and J. Ericson. A homeodomain protein code specifies progenitor cell identity and neuronal fate in the ventral neural tube. *Cell*, 101:435 –445, 2000.

[400] R. Brewster, J.L. Mullor, and A. Ruiz i Altaba. Gli2 functions in FGF signaling during antero-posterior patterning. *Development*, 127:4395 –4405, 2000.

[401] T. Darland and J.E. Dowling. Behavioral screening for cocaine sensitivity in mutagenized zebrafish. *Proc Natl Acad Sci U S A*, 98:11691–11696, 2001.

[402] R. Gerlai, M. Lahav, S. Guo, and A. Rosenthal. Drinks like a fish: zebra fish (Danio rerio) as a behavior genetic model to study alcohol effects. *Pharmacol Biochem Behav*, 67:773–782, 2000.

[403] J. Zirger, C. Beattie, D. McKay, and R. Thomas Boyd. Cloning and expression of zebrafish neuronal nicotinic acetylcholine receptors. *Gene Expr. Patterns*, 3:747–754, 2003.

[404] F. Williams and W.J. Messer. Muscarinic acetylcholine receptors in the brain of the zebrafish (Danio rerio) measured by radioligand binding techniques. *Comp. Biochem. Psysiol*, 137:349–353, 2004.

[405] D. Clemente, A. Porteros, E. Weruaga, J. Alonso, F. Arenzana, J. Aijon, and R. Arevalo. Cholinergic elements in the zebrafish central nervous system: histochemical and immunohistochemical analysis. *J. Comp. Neurol*, 474:75–107, 2004.

[406] T. Mueller, P. Vernier, and M. Wullimann. The adult central nervous cholinergic system of a neurogenetic model animal, the zebrafish Danio rerio. *Brain Res*, 1011:156–169, 2004.

[407] Y. Kitabatake, T. Hikida, D. Watanabe, I. Pastan, and S. Nakanishi. Impairment of reward-related learning by cholinergic cell ablation in the striatum. *Proc Natl Acad Sci U S A*, 100:7965 –7970, 2003.

[408] F-M. Zhou, Y. Liang, and J. Dani. Endogenous nicotinic cholinergic activity regulates dopamine release in the striatum. *Nat. Neurosc*, 4:1224–1229, 2001.

[409] C.D. Fiorillo and J.T. Williams. Cholinergic inhibition of ventral midbrain dopamine neurons. *J Neurosci*, 20:7855–7860, 2000.

[410] A. Fink-Jensen, I. Fedorova, G. Wortwein, D. Woldbye, T. Rasmussen, M. Thomsen, T. Bolwig, K. Knitowski, D. McKinzie, M. Yamada, J. Wess, and A. Basile. Role for M5 muscarinic acetylcholine receptors in cocaine addiction. *J. Neurosc. Res*, 74:91–96, 2003.

[411] M. Behra, C. Etard, X. Cousin, and U. Straehle. The use of zebrafish mutants to identify secondary target effects of acetycholinesterase inhibitors. *Toxicol. Sci*, 77:325–333, 2004.

Appendix A

Article in *Development*

Inhibition of neurogenesis at the zebrafish midbrain-hindbrain boundary by the combined and dose-dependent activity of a new hairy/ E(spl)gene pair,

Jovica Ninković, Alexandra Tallafuss, Christoph Leucht, Jacek Topczewski, Birgit Tannhäuser, Lilianna Solnica-Krezel and Laure Bally-Cuif

Development (2005), 132, 75-88

Inhibition of neurogenesis at the zebrafish midbrain-hindbrain boundary by the combined and dose-dependent activity of a new *hairy/E(spl)* gene pair

Jovica Ninkovic[1,2,‡,§], Alexandra Tallafuss[1,2,*,‡], Christoph Leucht[1,2], Jacek Topczewski[3,†], Birgit Tannhäuser[1,2], Lilianna Solnica-Krezel[3] and Laure Bally-Cuif[1,2,§]

[1]Zebrafish Neurogenetics Junior Research Group, Institute of Virology, Technical University-Munich, Trogerstrasse 4b, D-81675 Munich, Germany
[2]GSF-National Research Center for Environment and Health, Institute of Developmental Genetics, Ingolstaedter Landstrasse 1, D-85764 Neuherberg, Germany
[3]Department of Biological Sciences, Vanderbilt University, Nashville, TN 37235 USA
*Present address: Institute of Neuroscience, University of Oregon, Eugene, OR 97403, USA
†Present address: Children's Memorial Institute for Education and Research, Northwestern University Feinberg School of Medicine, Chicago, IL 60614, USA
‡These two authors contributed equally to this work
§Authors for correspondence (e-mail: ninkovic@gsf.de and bally@gsf.de)

Accepted 6 October 2004

Development 132, 75-88
Published by The Company of Biologists 2005
doi:10.1242/dev.01525

Summary

The intervening zone (IZ) is a pool of progenitor cells located at the midbrain-hindbrain boundary (MHB) and important for MHB maintenance, midbrain-hindbrain growth and the generation of midbrain-hindbrain neurons. Recently, we implicated the Hairy/E(spl) transcription factor Her5 in the formation of the medial (most basal) part of the IZ (MIZ) in zebrafish; the molecular bases for lateral IZ (LIZ) formation, however, remain unknown. We now demonstrate that *her5* is physically linked to a new family member, *him*, displaying an identical MHB expression pattern. Using single and double knockdowns of *him* and *her5*, as well as a *him+her5* deletion mutant background (*b404*), we demonstrate that Him and Her5 are equally necessary for MIZ formation, and that they act redundantly in LIZ formation in vivo. We show that these processes do not involve cross-regulation between Him and Her5 expression or activities, although Him and Her5 can heterodimerize with high affinity. Increasing the function of one factor when the other is depleted further shows that Him and Her5 are functionally interchangeable. Together, our results demonstrate that patterning and neurogenesis are integrated by the *her5-him* gene pair to maintain a progenitor pool at the embryonic MHB. We propose a molecular mechanism for this process where the global 'Him+Her5' activity inhibits *ngn1* expression in a dose-dependent manner and through different sensitivity thresholds along the medio-lateral axis of the neural plate.

Key words: Hairy, E(spl), *her5*, *him*, Midbrain-hindbrain, MHB, Neurogenesis, Zebrafish

Introduction

Development of the vertebrate central nervous system (CNS) is a complex process that needs to connect patterning and neurogenesis. Crucial to this process are local events of neurogenesis inhibition, which maintain pools of progenitors in defined locations of the neural tube. The delayed differentiation of these progenitor zones permits the generation of large as well as spatiotemporally patterned structures, such as the layered cortex in higher vertebrates, the polarized optic tectum in birds, or the retina. The molecular events controlling the generation or maintenance of neural progenitor pools remain largely hypothetical.

The embryonic midbrain-hindbrain domain (MH) is characterized by the maintenance of a zone of delayed differentiation at the midbrain-hindbrain boundary (MHB). This zone, called 'intervening zone' (IZ), separates midbrain from anterior hindbrain neuronal clusters and has been described in all vertebrates (Bally-Cuif et al., 1993; Geling et al., 2003; Vaage, 1969). Its functional importance is attested by genetic ablation experiments. For instance, in mouse embryos lacking the function of the two bHLH E(spl)-like transcription factors Hes1 and Hes3, premature differentiation of the IZ occurs, leading to the lack of several MH neuronal populations, and to the collapse of MH structures (Hirata et al., 2001). These defects may primarily result from a disruption of the isthmic organizer, an inducing cell population located at the MHB and involved in MH maintenance (Hirata et al., 2001; Martinez, 2001; Rhinn and Brand, 2001; Wurst and Bally-Cuif, 2001). Recent results in zebrafish have permitted dissection of the mechanisms of IZ formation in more detail. There, expression of the *hairy/E(spl)* gene *her5* (Muller et al., 1996) precisely delineates the IZ at all embryonic stages (Geling et al., 2003). At the onset of neurogenesis (tail-bud stage), *her5* expression separates the early midbrain ventrocaudal proneural cluster (vcc) from the anterior hindbrain proneural clusters of rhombomere 2 (presumptive motorneurons –r2MN– and lateral

neurons –r2LN–). In the absence of Her5 function, ectopic neurogenesis occurs in the medial (future basal) part of the IZ, as revealed by the ectopic expression of the proneural genes *neurogenin1* (*ngn1*) and *coe2* and the later differentiation of neurons across the basal MHB, bridging the vcc and r2MN (Geling et al., 2003; Geling et al., 2004). Conversely, forced expression of *ngn1* within the MH domain leads to a partial downregulation of MHB markers' expression (Geling et al., 2003). These results have two implications. First, they confirm that the IZ is necessary to maintain MHB integrity. Second, they demonstrate that the IZ is composed of at least two domains along the mediolateral axis, which differ in their requirement for Her5 function: the medial IZ domain (MIZ), which crucially depends on Her5 for neurogenesis inhibition, and the lateral (future alar) IZ domain (LIZ), which forms even in the absence of Her5. Within the MIZ, Her5 acts as a prepattern factor that prevents the formation of a proneural cluster, and inhibits expression of *ngn1* and *coe2* upstream of Notch signaling (Geling et al., 2004).

Our study of Her5 function did not address the formation of the LIZ, in spite of its crucial role in controlling midbrain and anterior hindbrain alar neurogenesis. To now approach this issue, we reasoned that other Hairy/E(spl) factors might be expressed within this domain and act redundantly with Her5. Because there are examples of physically linked *E(spl)* genes in *Drosophila* (*E(spl)* complex) (Klambt et al., 1989; Knust et al., 1992) and zebrafish (*her1* and *her7*) (Henry et al., 2002), and because linked genes are more likely to share spatiotemporal characteristics of expression, we searched for new *Hairy/E(spl)* genes in the vicinity of the *her5* locus. Sequencing a *her5*-containing PAC revealed a new *her*-like gene, *him*, adjacent to *her5* and in opposite orientation (hence *him* for *her5* image), identically expressed across the IZ. We report here that Him is the hypothetical factor cooperating with Her5 to control LIZ formation in vivo, and that Him also crucially contributes to MIZ formation. Together, our results unravel the genetic combination preventing neurogenesis across the MHB.

Materials and methods

Cloning and phylogenic analysis of *him*

Systematic sequencing of genomic DNA surrounding known *her* genes was performed using PAC clones obtained from RZPD. A new ORF was detected close to the *her5* gene locus in PAC BUSMP706H15152Q2. 5′ RACE experiments were done to identify full-length cDNA, according to the manufacturer's recommendations (Invitrogen). The newly cloned gene, *him*, corresponds to ENSDARG00000002707 now predicted by The Welcome Trust Sanger Institute, with the exception that in the prediction the first exon is missed and the last exon is truncated.

The phylogenetic tree of zebrafish Her family was done using the phylodendrone software (www.es.embnet.org/Doc/phylodendron/treeprint-form.html). To construct the phylogenetic tree, the VectorNTI software and full-length sequences were used. The accession numbers of compared proteins are: Her5: NP_571152, Her1: NP_571153, Her7: NP_571684, Her4: NP_571165, Her2: NP_571164, Her3: NP_571155, Her9: NP_571948 and Her6: NP_571154. Proteins predicted by The Wellcome Trust Sanger Institute are: Her11 (ENSDARP00000012990), Her13 (ENSDARP0000008307), Hes6 (ENSDARP00000021078) and Her12 (ENSDARP00000038100) (http:www.ensembl.org, release from 08-02-2004).

Zebrafish strains and transgenic lines

Embryos obtained from natural spawning of AB wild-type or transgenic fish, her5PAC::egfp (Tallafuss and Bally-Cuif, 2003) and –8.4ngn1::egfp (Blader et al., 2003), were raised and staged according to Kimmel et al. (Kimmel et al., 1995). *no isthmus* (*noi*^{tu29a}), *acerebellar* (*ace*^{ti282a}) (Brand et al., 1996) and *knypek* (*b404, kny*^{m119}) (Solnica-Krezel et al., 1996; Topczewski et al., 2001) mutants were obtained by pairwise mating of heterozygous adult carriers, as described previously.

Protein expression interference assays

Morpholino antisense oligonucleotides (*her5*MO^{ATG}) were purchased from Gene-Tools, Inc. (Oregon, USA). The morpholino was dissolved to a stock concentration of 5 mM in H_2O and injected into one-cell stage embryos at 1 mM. *him*MOs lead to non-specific cell death (not shown). Thus, *Grip*NA antisense oligonucleotides preventing *him* translation, specific for the *him* ATG region (*himGrip*NA^{ATG}) or acceptor site of the second *him* exon (*himGrip*NA^{SPL}), were purchased from Active Motif (Belgium). *Grip*NAs were dissolved to stock solution of 1 mM in H_2O and injected into one-cell stage embryos at 0.5 mM. At this dose, the effect of *himGrip*NAs on *ngn1* expression was maximal. Sequences of antisence oligonucleotides were as follows: *her5*MO^{ATG}: 5′-TTGGTTCGCTCATTTTGTGTATTCC-3′; *himGrip*NA^{ATG}: 5′-ATTCGGTGTGCTCTTCAT-3′ and *himGrip*NA^{SPL}: 5′-TACTCACAGTGTCTGCAG-3′. All injection experiments were repeated at least three times.

In situ hybridization and immunohistochemistry

Probe synthesis, in situ hybridization and immunohistochemistry were carried out as previously described (Hammerschmidt et al., 1996). The following in situ antisense RNA probes were used: *her5* (Muller et al., 1996), *him* (this paper), *ngn1* (Korzh et al., 1998), *pax2.1* (Lun and Brand, 1998) and *egfp* (Clontech). Primary antibodies used for immunohistochemistry were rabbit anti-GFP (ams biotechnology Europe, TP401) used at a final dilution of 1/500 and mouse anti-human neural protein HuC/HuD (MoBiTec A-21271) (1/300). They were revealed by using FITC-conjugated goat anti-rabbit secondary antibody (Jackson ImmunoResearch Laboratories, 111-095-003) or Cy3-conjugated goat anti-mouse secondary antibody (Jackson ImmunoResearch Laboratories, 115-165-044) (1/200), as appropriate. Embryos were scored and photographed under a Zeiss SV 11 stereomicroscope or a Zeiss Axioplan photomicroscope.

RNA injections

knypek capped RNA was synthesized using Ambion mMessage mMachine kit following the recommended procedure. Capped RNA was injected at the concentration of 60 ng/μl into the embryos at the one-cell stage.

Protein interaction assays

For two-hybrid assays, The MATCHMAKER GAL4 Two-Hybrid System 3 (Clontech) was used following procedures described by the manufacturer. The 'bait' and 'AD' plasmids were constructed by fusing in-frame the complete ORFs of *her5*, *him* and *ngn1* to either pGBKT7 (encoding the GAL4 DNA-binding domain) or pGADT7 (encoding the GAL4 activation domain). The relative stringency of Her5 homodimerization versus its heterodimerization with Him was quantified by β-galactosidase assay according to the manufacturer's recommendation (Clontech). The β-galactosidase activity was quantified according to Lazo et al. (Lazo et al., 1978).

Co-immunoprecipitation and western blot analysis

Transformed yeast cells expressing the two proteins of interest were lysed in 0.5 ml of lysis buffer (50 mM Tris-HCl pH 8, 150 mM NaCl, 0.1% NP40, 0.1 mM DTT, 0.1 mg/ml pepstatin A, 0.03 mM leupeptin, 145 mM benzamidine, 0.37 mg/ml aprotinin, 1 mM

phenylmethylsulfonyl fluoride) with 0.25 g of glass beads (425-600 μl, Sigma) for one hour at 4°C with shaking. The extracts were then centrifuged at 15 000 ***g*** for 10 minutes at 4°C to eliminate cell debris, and the supernatant was collected. For each immunoprecipitation, 0.4 ml aliquots of lysate were precleaned by incubation with 150 μl of pre-immune rabbit serum and 100 μl of 1:1 slurry of Protein A Sepharose™ CL-4B (Amersham Bioscience AB) for 30 minutes at 4°C. Precleaned extracts were immunoprecipitated with 10 μl of rabbit anti-HA antibody (dilution 1/1000) (Sigma) and 100 μl of 1:1 slurry of Protein A Sepharose CL-4B (Amersham Bioscience AB) for 30 minutes at 4°C. The sepharose beads were washed three times with 1 ml of lysis buffer. The precipitates were fractionated on SDS-PAGE and subsequent western blot analysis was performed according to standard protocols, by using mouse anti-c-Myc antibodies (1/1000) (Sigma). The primary antibodies were revealed using HRP-coupled secondary antibodies (Jackson Laboratories) diluted to 1/200 and enhanced chemiluminescence (Amersham Bioscience AB).

Quantification of *him* mRNA in the *her5*PAC::*egfp* line

Total RNA was isolated from *her5*PAC::*egfp* embryos and WT siblings at the five-somite stage and reverse-transcribed before real-time PCR amplification. Real-time PCR was done by using LightCycler FastStart DNA Master SYBR Green I kit (Roche, Germany) and Light Cycler Instrument (Roche, Germany). Quantitative values were obtained from the threshold cycle number at which the increase in the signal associated with exponential growth of the PCR products begins to be detected using the LightCycler Software, according to the manufacturer's recommendations. The precise amount of total RNA added to each reaction mix (based on optical density) and its quality (lack of extensive degradation) are both difficult to assess precisely. We therefore also quantified the transcript of the *pax6* gene as the endogenous RNA control, and both samples were normalized to the basis of *pax6* content (*R*-value on the graph). The nucleotide sequences of the specific primers used are shown in Table 1. The thermal cycling conditions comprised an initial denaturation step at 95°C for 10 minutes and 65 cycles at 95°C for 15 seconds, 55°C for 10 seconds and 72°C for 15 seconds. The quantifications were performed in triplicate on a pool of 50 embryos for each line and results represent the mean value±s.e.m.

Table 1. Sequences of primers used in real-time PCR

Gene	Oligonucleotide	Sequence*	Amplicon size (bp)
him	forward primer	5′-GTTATATCTCCTGCGGGT-3′	163
	reverse primer	5′-GGGATAAGAGGAAGCCTTT-3′	
otx1	forward primer	5′-GATACCCAGCAACACCG-3′	136
	reverse primer	5′-ATCTTCAGTGCCACCT-3′	
pax6	forward primer	5′-TTTGCCTGGGAGATTC-3′	167
	reverse primer	5′-CTCTGCCCGTTGAGCATTCT-3′	

*Primers were chosen with the assistance of LightCycler Probe Design software.

Results

A new *hairy/E(spl)* gene, *him*, is physically linked to *her5* in a head-to-head orientation

We searched for genes physically linked to *her5* by sequencing a *her5*-containing PAC (Tallafuss and Bally-Cuif, 2003). This revealed the presence of an open reading frame encoding a new Hairy/E(spl) factor located 3.3 kb upstream of *her5* and in a head-to-head orientation (Fig. 1A). RT-PCR experiments demonstrated the presence of the corresponding transcript in embryos (not shown), and blasting against the zebrafish genome (release from 08-02-04) confirmed the association of this gene with *her5*. We named this new gene *him* (for '*h*er5 im*a*ge') (GenBank accession number AY705671). The genomic structure of *him* was determined by aligning cDNA and genomic sequences and shows several alterations compared to the zebrafish genome prediction, notably the presence of an additional 5′ coding exon (true exon 1) as well as a different position and size of the last exon (exon 4), coding for 195 amino acids instead of the 22 predicted (Fig. 1A).

The head-to-head association of the gene pair him-her5 is reminiscent of the genomic organization of *her7-her1* (Henry et al., 2002). Further analysis of the zebrafish genome suggests at least another additional gene pair, *her4* and a new predicted *her* gene that we named *her12* (ENSDARG00000028110) (Fig. 1B). Therefore, we propose that a paired organization might be a conserved feature among zebrafish *her* genes.

The Him protein, translated from our full-length cDNA sequence, consists of 297 amino acids and exhibits all structural features of an Hairy/E(Spl) bHLH factor acting as transcriptional repressor (Davis and Turner, 2001): a conserved proline residue in the basic domain, an 'orange' domain (Dawson et al., 1995) and a WRPW tetrapeptide in the C-terminus (Fisher et al., 1996) (Fig. 1C). Within the zebrafish Her family, Him shows the highest similarity to Her1 with 28.6% identical and 35.2% conserved amino acid (aa) residues. Similarity between Him and Her5 is slightly weaker (20.1% identical and 29.2% conserved aa residues) (Fig. 1B, red lines, and Fig. 1C). Comparison restricted to the functional bHLH domain reveals 66% identity to Her1 and 50% identity to Her5.

him expression within the presumptive midbrain-hindbrain is identical to *her5* and marks the intervening zone

We analyzed *him* expression by RT-PCR and in situ hybridization. *him*, like *her5*, is maternally expressed (Fig. 2A). Early zygotic *him* expression is ubiquitous (data not shown) but rapidly resolves in a first, transient, profile within the presumptive dorsal endoderm and mesoderm (Fig. 2B) at 30% epiboly: *him* is expressed in deep scattered cells of the dorsal embryonic margin and in the deep layer of the dorsal mesendoderm (Fig. 2B and 2B′, red arrows). From mid-gastrulation onwards (70% epiboly), *him* expression in the presumptive endo- and mesoderm becomes undetectable (Fig. 2C). At that stage, *him* becomes transcribed in the anterior neural plate, in a V-shaped domain interrupted at the midline (Fig. 2C, red arrowhead). Expression in the lateral aspects of this domain is slightly broader and stronger than medially. At the three-somite stage, this expression fuses medially and, by anatomical landmarks, is clearly located within the presumptive MH domain (Fig. 2E,F). *him* expression is maintained at the MHB later on until 36 hpf (Fig. 2H,I). Starting at late gastrulation, *him* is also expressed in the presomitic mesoderm (Fig. 2D-F, blue arrows). Expression in this territory is detectable until late somitogenesis (Fig. 2H).

To determine whether and to what extent *him* and *her5* share expressing cells within the presumptive MH, we compared their expression profiles by double ISH. At three somites (Fig. 2F), observation at high resolution of double-stained embryos showed that the MH expression of *him* and *her5* are exactly identical. Thus, *him* expression, like *her5*, precisely delineates

the MH primordium (Tallafuss and Bally-Cuif, 2003). Like *her5* (Geling et al., 2003), it is also a permanent marker of the IZ, separating the early midbrain proneural cluster vcc from rhombomere 2 presumptive motor- and sensory neurons at late gastrulation (Fig. 2J). *him* expression is detected in this domain slightly earlier than *her5* (not shown).

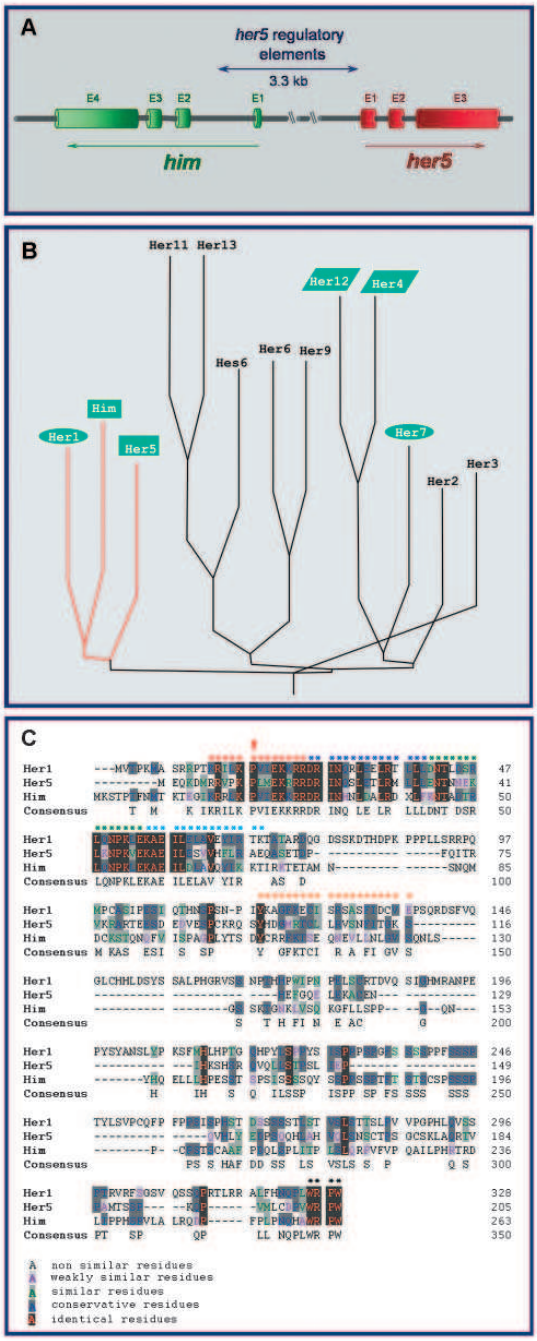

Taken together, our data suggest a more complex picture than expected from the genomic organization of *him* and *her5*. *him* and *her5* share expression within the MH domain, but differ elsewhere in *her5*-specific versus *him*-specific domains (pharyngeal precursors versus presomitic mesoderm at late gastrulation, respectively). In the neural plate however, Him is, together with Her5, the earliest marker of the MH and IZ, prompting us to analyze its function in this domain in more detail, in relation to MH patterning and Her5 activity.

Like Her5, and in contrast to most MH factors, Him does not control patterning events within the MH region

Refined regionalization and maintenance of the MH domain at somitogenesis stages depends on a positive cross-regulatory loop involving Fgf8 and Pax2.1 (Brand et al., 1996; Lun and Brand, 1998; Reifers et al., 1998; Tallafuss and Bally-Cuif, 2003). To determine whether *him* was part of this loop, we analyzed its expression in *ace/fgf8* and *noi/pax2.1* mutants (Brand et al., 1996; Lun and Brand, 1998; Reifers et al., 1998). Expression of *him* in *ace* mutant embryos is initiated normally (data not shown) but, from mid-somitogenesis stages onwards, gradually narrows to persist at the MHB only in a dorsal patch (Fig. 3A,B). At 24 hpf *him* expression in *ace* is undetectable (data not shown). Similarly, in *noi* mutants, a downregulation of *him* expression can be observed from mid-segmentation stages onwards. In contrast to *ace*, *him* expression in *noi* later remains restricted to the ventral MHB (Fig. 3C,D), like *her5* (Lun and Brand, 1998; Reifers et al., 1998). Together, these observations demonstrate that the maintenance of *him* expression is, like that of other MH genes and within a similar time-window, under control of the MH regulatory loop.

Because Him is one of the earliest selective markers of the MH primordium, we asked in turn whether Him activity was involved in controlling aspects of MH regionalization. Loss of Him function, performed by injection of an antisense *Grip*NA oligonucleotide specific for the ATG region of *him* (*him Grip*NA^{ATG}) into one-celled embryos (see below for results demonstrating the functionality and specificity of this *Grip*NA), however affected neither the expression of MH

Fig. 1. Sequence analysis and phylogeny of the new bHLH transcription factor Him. (A) Genomic organization of the *him/her5* locus. The coding region is interrupted by three introns, the bHLH domain being encoded by exons E2 and E3. Note that the first exon of *him* is within the domain identified as necessary for MH expression of *her5* (Tallafuss and Bally-Cuif, 2003).
(B) Phylogenetic tree of the zebrafish Her family, showing relationship between known and predicted Her proteins. The alignment used for tree construction was obtained using the VectorNTI software, and is based on full-length sequences. Paired genes are boxed in blue, and individual pairs are marked with the same symbol (oval, rectangle or diamond). Accession numbers for the proteins used in this tree are: Her5 (NP_571152), Her1(NP_571153), Her7(NP_571684), Her4(NP_571165), Her2(NP_571164), Her3(NP_571155), Her9(NP_571948) and Her6(NP_571154). Proteins predicted by The Wellcome Trust Sanger Institute (http:www.ensembl.org) are: Her11, Her12, Her13 and Hes6. (C) Sequence alignment of Her1, Her5 and Him. Basic domains are overlaid with red asterisks, Helix 1 domains with dark blue, loop domains with green, Helix 2 domains with light blue, orange domains (H3/H4) with orange stars and WRPW tetrapeptides

patterning markers (e.g. *pax2.1*, *eng2*, *eng3*), nor that of IsO activity markers (e.g. *wnt1*, *fgf8*) at the 3- and 15-somite stages (data not shown).

Thus, although *him* expression depends on the MH maintenance loop, Him activity itself does not appear to impinge on this loop to influence MH patterning, like that of Her5.

Him activity is crucial for the formation of the medial IZ at early neurogenesis stages

We demonstrated previously that Her5 is crucially necessary to prevent neurogenesis across the MIZ (Geling et al., 2003). Because of the similar expression of *him*, and its encoding a related Hairy/E(Spl) factor, we explored a potential involvement of Him in IZ formation. At early neurogenesis stages, the IZ is also the major site of *pax2.1* expression, which we used as landmark in future experiments (see Fig. 4D).

We tested a requirement for Him in IZ formation in loss-of-function experiments where *him* mRNA translation was blocked by specific antisense *Grip*NAs. Two *Grip*NAs were used: *himGrip*NA^{ATG} (as above), and a second *Grip*NA targeting the acceptor splice site of him exon2 (*himGrip*NA^{SPL}). Undistinguishable phenotypes (see below) were obtained with the two *Grip*NAs, but not with a control *Grip*NA of unrelated sequence, indicating that the phenotypes observed are a specific consequence of Him dysfunction. Specifically, *himGrip*NAs-injected embryos assayed at the three-somite stage for *ngn1* expression displayed a complete lack of the MIZ, with bridging of the vcc and r2MN clusters by ectopic *ngn1*-expressing cells (76% of cases, *n*=21 for *himGrip*NA^{ATG}, 83% of cases, *n*=24 for *himGrip*NA^{SPL}) (Fig. 4B,C, compare to 4D). This phenotype is followed by the development of ectopic differentiated neurons across the basal MHB at later stages (data not shown). It is in all respects

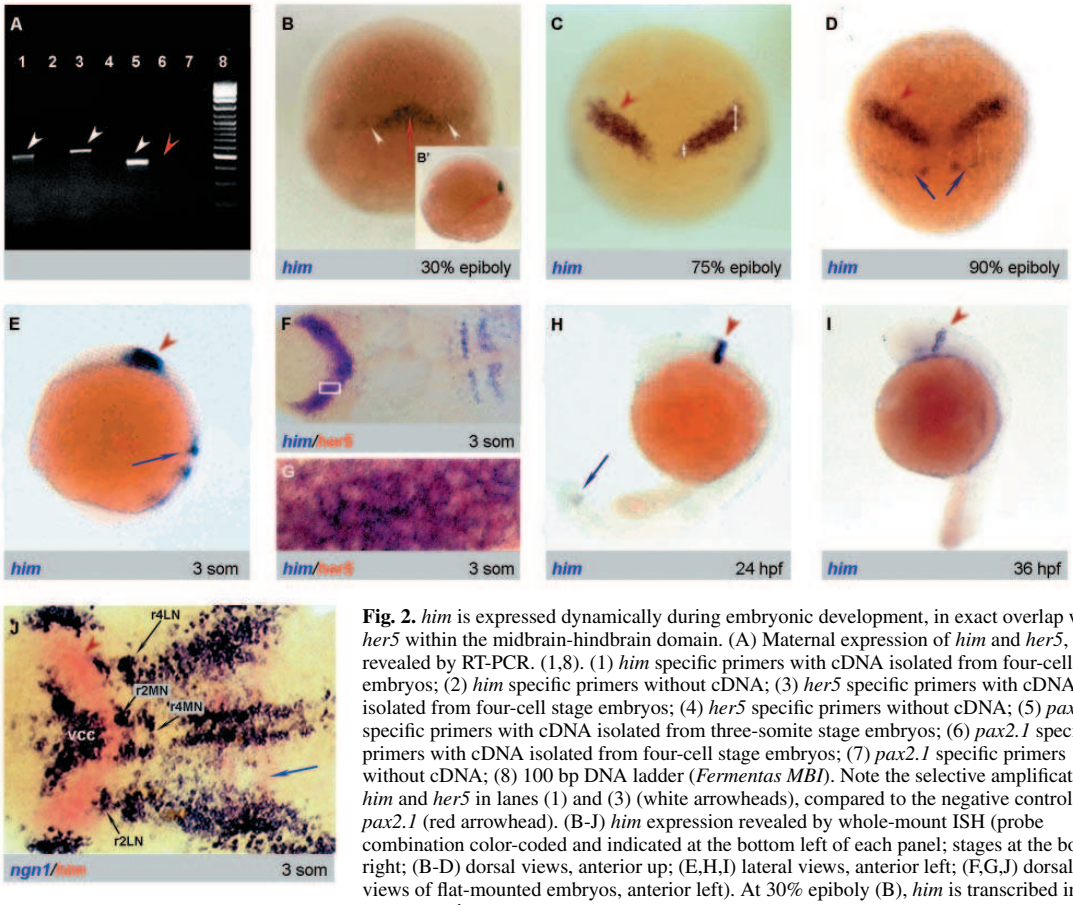

Fig. 2. *him* is expressed dynamically during embryonic development, in exact overlap with *her5* within the midbrain-hindbrain domain. (A) Maternal expression of *him* and *her5*, revealed by RT-PCR. (1,8). (1) *him* specific primers with cDNA isolated from four-cell stage embryos; (2) *him* specific primers without cDNA; (3) *her5* specific primers with cDNA isolated from four-cell stage embryos; (4) *her5* specific primers without cDNA; (5) *pax2.1* specific primers with cDNA isolated from three-somite stage embryos; (6) *pax2.1* specific primers with cDNA isolated from four-cell stage embryos; (7) *pax2.1* specific primers without cDNA; (8) 100 bp DNA ladder (*Fermentas MBI*). Note the selective amplification of *him* and *her5* in lanes (1) and (3) (white arrowheads), compared to the negative control *pax2.1* (red arrowhead). (B-J) *him* expression revealed by whole-mount ISH (probe combination color-coded and indicated at the bottom left of each panel; stages at the bottom right; (B-D) dorsal views, anterior up; (E,H,I) lateral views, anterior left; (F,G,J) dorsal views of flat-mounted embryos, anterior left). At 30% epiboly (B), *him* is transcribed in the deep layer of the mesoderm (red arrows, see sagittal view in B′) and in scattered cells of the dorsal embryonic margin (white arrowheads). *him* expression within the MH domain (red arrowheads) is initiated at 75% epiboly (C) (note the difference in expression in medial and lateral parts of the IZ is indicated with white arrows) and maintained until 36 hpf (I). Note in F (and see higher magnification of the boxed area in G) that *him* and *her5* expression in this domain are exactly coincident. *him* expression in the presomitic mesoderm starts at 90% epiboly (D) (blue arrows) and is maintained until 24 hpf (H). *him* and *ngn1* are complementarily expressed in the MH region (J). Red arrowheads indicate *him* expression at the MHB and blue arrows expression in the presomitic mesoderm. IZ, intervening zone; vcc, ventrocaudal cluster, r2M, presumptive motorneurons of rhombomere 2; r2L, presumptive lateral neurons of rhombomere 2; r4M, presumptive motorneurons of rhombomere 4; r4L, presumptive lateral of rhombomere 4.

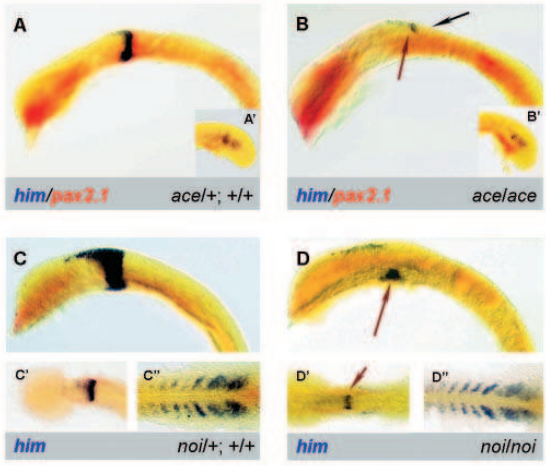

Fig. 3. *him* expression is controlled by Pax2.1 and Fgf8 during the MH maintenance loop. (A,B) *him* (blue) and *pax2.1* (red) expression in *ace* mutants (B) and WT siblings (A) at the 21-somite stage (all embryos deyolked, lateral view, anterior left). Note that both genes are coincidentally switched off at the MHB, except for a common dorsal patch (arrows), while *him* expression in the presomitic mesoderm is intact (A′,B′, insets). (C,D) *him* expression (blue) in *noi* mutants (D) and WT siblings (C) at the 17-somite stage (C,D: deyolked embryos, lateral views, anterior left; C′-D″: dorsal views of flat-mounted heads (C′,D′) and tails (C″,D″). *him* expression at the MHB is restricted to a ventral patch in *noi* (arrow), while presomitic expression is unaffected (C″,D″).

similar to that triggered by loss of Her5 function in *her5*MO^{ATG} morphants (Fig. 4A) (Geling et al., 2003). Thus, loss-of-function of either Her5 or Him results in the same failure to form and maintain the MIZ.

Him and Her5 are independently required for medial IZ formation

The above results are compatible with a simple model where Him and/or Her5 would act in a common regulatory cascade, one factor positively regulating expression of the other gene. Thus, loss of Him function would cause loss of *her5* expression, or the reverse. Alternatively, Him and Her5 might be independently necessary for MIZ formation. To address this question, we studied *him* and *her5* expression in embryos where Her5 or Him activity, respectively, was blocked. We observed that *him* expression was unchanged in Her5 morphants, in both the MH region and the presomitic mesoderm, under conditions where *ngn1* expression was strongly induced in place of the MIZ (Fig. 4E,F, and data not shown). Thus *him* expression is not under immediate control of Her5. Likewise, injection of *Grip*NA^{ATG} into wild-type embryos did not produce alterations in *her5* transcription, although the MIZ was lost (Fig. 4I compared to 4K, and data not shown). Furthermore, injection of *Grip*NA^{ATG} did not affect the production of the fusion Her5-GFP protein, driven under control of all *her5* regulatory elements in *her5PAC::egfp* transgenics (Tallafuss and Bally-Cuif, 2003) (Fig. 4J,L). Thus, Him does not influence *her5* transcription or translation.

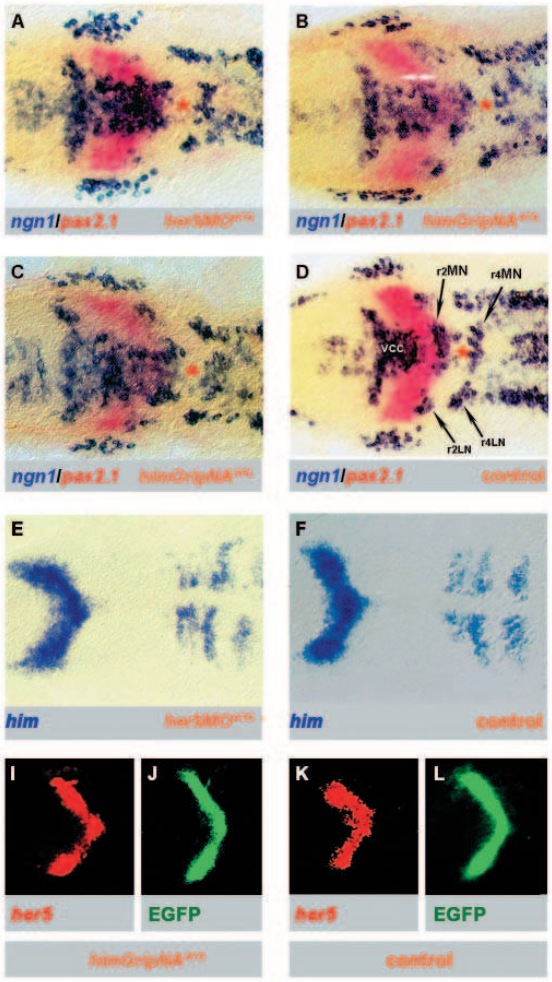

Fig. 4. The activity of both Him and Her5 is necessary to prevent neurogenesis across the medial IZ in vivo. (A-D) The inhibition of either Him or Her5 function triggers ectopic neurogenesis in place of the MIZ (dorsal views of the MH region in flat-mounted embryos at the four-somite stage, anterior to the left). Embryos are probed for *ngn1* (blue) and *pax2.1* (red) expression following injection of *her5*MO^{ATG}(A), *himGrip*NA^{ATG} (B), *himGrip*NA^{SPL} (C) (orange labels), compared to a non-injected WT control embryo (D). Note that the vcc and r2MN are bridged by ectopic *ngn1*-positive cells (double arrows) after blocking Her5 or Him activity, while other undifferentiated areas are not affected (e.g. area between r2MN and r4MN, asterisk. (G-L) *him* and *her5* expression are not successive and interdependent steps of the anti-neurogenic cascade acting in the MIZ (dorsal views of the MH area in flat-mounted embryos at the three-somite stage, anterior to the left, used markers are color-coded). (G,H) *him* expression in wild-type embryos (H) or after injection with *her5*MO^{ATG} (G). Note that *him* expression is not modified. (I-L) Expression of *her5* (I,K) and GFP (J,L) in *her5PAC::egfp* embryos injected (K,L) or not (I,J) with *himGrip*NA^{ATG}. Note that *her5* and GFP expression are unaffected. vcc: ventro-caudal cluster, r2MN: prospective motorneurons of rhombomere 2, r4MN: prospective motorneurons of rhombomere 4.

We conclude that Him and Her5 do not act in a simple cascade of cross-regulation of expression. Rather, the two genes are expressed independently of each other and are both essential to MIZ formation.

The crucial determinant of MIZ formation is the total dose of Him + Her5 inhibitory activities

Several hypotheses could account for the above results. First, Him and Her5 might both be required for MIZ formation because they need to heterodimerize with each other to be active. Alternatively, these factors do not have unique essential activities, but rather are required to reach together a threshold level of Hairy/E(spl) activity necessary to prevent proneural gene expression. Finally, both factors might exert distinct and/or complementary functions necessary for MIZ formation.

To unravel the relevance of each hypothesis in vivo, we first tested whether Him and Her5 could interact in a yeast two-hybrid system. bHLH factors have the capacity to dimerize via their HLH domain, however their affinity for hetero- versus homodimerization cannot be a priori predicted, and some instances of DNA binding as oligomers have also been reported (Firulli et al., 2000; Iso et al., 2001; Wainwright and Ish-Horowicz, 1992). We observed that Her5 can homodimerize as well as bind Ngn1, while Him and Ngn1 failed to interact. In addition, heterodimers of Him and Her5 were produced. Whether Him is also able to homodimerize could not be tested due to unexplained toxicity of the him-expressing constructs (Table 2). All these interactions were confirmed by coimmunoprecipitation (Fig. 5A). Moreover, the affinity for heterodimerization between Him and Her5, based on beta-galactosidase activity (Lazo et al., 1978), appeared six-fold higher than the affinity of Her5 for homodimerization (Fig. 5B), suggesting that the Him-Her5 configuration predominates in vivo if the amount of proteins is equal. Thus, the requirement for Him and Her5 for MIZ formation in vivo might indeed be explained by the necessity for these factors to heterodimerize.

Our finding that Her5 can homodimerize, however, as well as reports of functional bHLH oligomers (Firulli et al., 2000; Iso et al., 2001; Wainwright and Ish-Horowicz, 1992), suggest that Her5 and/or Him alone could permit MIZ formation, provided the dose of this factor is sufficient. To test this hypothesis we studied neurogenesis in *her5PAC::egfp* transgenic embryos (Tallafuss and Bally-Cuif, 2003), where Him is in excess. This transgenic line was obtained by recombination of *egfp* into the second exon of *her5* in a *her5*-containing PAC. Thus, in this transgene *her5* is not functional. However, because of the small genetic distance separating the *her5* and *him* locus, and because the entire recombinant PAC was used for germ line transformation (Tallafuss and Bally-Cuif, 2003), these transgenics carry an additional copy of *him* together with the *her5-egfp* fusion (see Fig. 5C for a scheme of the transgene). Real-time PCR confirmed a 1.5-fold increase in the amount of *him* messenger in embryos heterozygous for the *her5PAC::egfp* transgene, while the amount of *otx1* mRNA, used as a control, was unchanged (Fig. 5D). Because *him* regulatory elements are also contained within the recombined PAC, additional *him* transcripts produced from the transgene display the endogenous *him* profile, restricted to the IZ within the neural plate (not shown). Therefore, *her5PAC::egfp* transgenics provide an ideal background to measure MIZ formation in a context where *her5* expression is normal but the dose of Him is increased across the IZ. Most interestingly, we observed that *her5PAC::egfp* transgenic embryos where Her5 activity was blocked by *her5*MO^{ATG} formed a normal MIZ (Fig. 5E, compare to Fig. 4D). In all cases, we verified that Her5 activity was completely abolished, by monitoring the lack of EGFP protein expression (data not shown). Thus Him, when present in sufficient amount (in a minimum of three doses, as in *her5PAC::egfp/+* heterozygote embryos), is capable of replacing Her5 activity to prevent neurogenesis across the MIZ.

We conclude from these observations that the crucial component of MIZ formation and maintenance is a threshold level of 'Him + Her5' inhibitory activity. In the normal embryo, this level is probably achieved by Her5-Him heterodimers, although a possible contribution of homodimers and/or oligomers from each factor separately cannot be excluded.

Table 2. Possible interactions of the proteins relevant to IZ formation, revealed in a yeast two-hybrid assay

	pGBKT7		
pGADT7	Her5	Him	T-antigen
Her5	+	+	+
Ngn1	+	–	+
p53	+	+	+
Lam	–	–	–

The assay was performed with full-length Her5, Him and Ngn1 proteins expressed from pGBKT7 and pGADT7 expression vectors. p53 expressed from pGADT7 and T-antigen expressed from pGBKT7 were used as positive controls. Lam protein from pGADT7 was used as a negative control for interactions.

+, interaction between the proteins tested, revealed by activation of *ade*, *his* and *mel* genes.

–, absence of interaction.

Formation of the lateral IZ also relies on the level of 'Him + Her5 activity' but with a lower threshold than the medial IZ

The LIZ is preserved in both *her5* and *him* single knockdown embryos, suggesting that it might require other factors than Him and Her5 for its formation. Alternatively, the LIZ might primarily differ from the MIZ in requiring a lower threshold of 'Him + Her5' activity, the endogenous level of one factor alone (two doses) being sufficient to block neurogenesis in this location. To address these hypotheses we assayed for lateral *ngn1* expression in double knockdown embryos obtained by the co-injection of *her5*MO^{ATG} and *himGrip*NA^{ATG}. Strikingly, we observed that the simultaneous interference with both Her5 and Him activities results in ectopic *ngn1* expression in place of the entire IZ, i.e. including the LIZ (88% of cases, *n*=25) (Fig. 6A,A′ compared to 6D,D′), in striking contrast to single knockdowns (0% of cases for *her5* knockdowns, *n*=21, 0% of cases for *him* knockdowns, *n*=24) (Fig. 6B,C).

To confirm these results we analyzed *b404* mutants (Topczewski et al., 2001), which we found to carry a deletion encompassing the *her5* and *him* locus in addition to *knypek* (*kny*). As expected, expression of both *him* and *her5* in these mutants is completely absent at all stages (Fig. 7A-D). Mutations in zebrafish *kny* impair gastrulation movements of convergence and extension that normally narrow the embryonic body and elongate it from head to tail, resulting in shorter and broader embryos (see Fig. 7B,D) (Henry et al.,

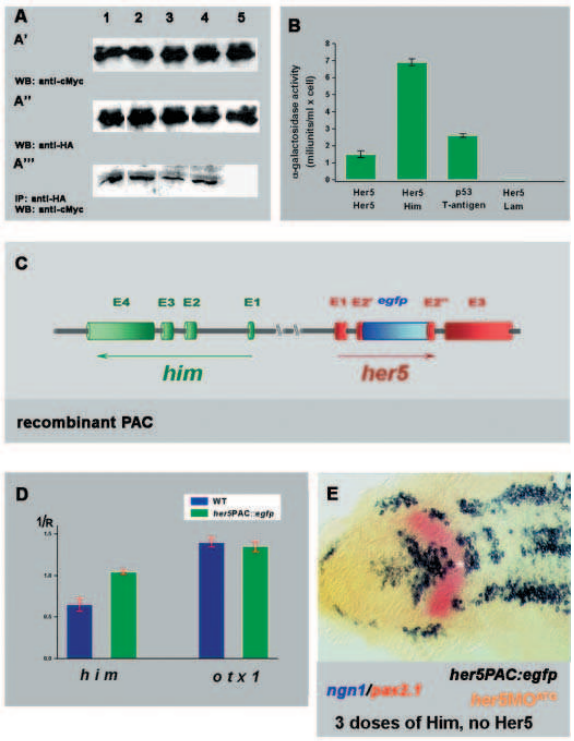

Fig. 5. The crucial determinant of medial IZ formation is the level of Him + Her5 inhibitory activity, probably achieved in vivo by Him/Her5 heterodimers but replaceable by a higher level of either factor alone. (A) Co-immunoprecipitation assays reveal possible interactions between the bHLH transcription factors important to prevent/promote neurogenesis at the MHB. Crude protein extracts were isolated from yeasts transformed with the following constructs combinations: (1) *her5*pGBKT/ + *her5*pGADT7, (2) *her5*pGBKT7 + *ngn1*pGADT7, (3) *him*pGBKT7 + *her5*pGADT7, (4) *T-antigen* pGBKT7 + *p53*pGADT7; (5) *her5*pGADT7 + *lam*pGADT7. Isolated extracts were either probed with anti-cMyc antibodies (A′) and anti-HA antibodies (A″) or immunoprecipitated with anti-HA antibodies and then probed with anti-cMyc antibodies (A‴). (B) Stringency of Her5 homodimerization and Her5/Him heterodimerization, based on beta-galactosidase activity of yeast cells expressing appropriate construct combinations (Lazo et al., 1978). Note that the interaction between Him and Her5 is significantly stronger than Her5 homodimerization. (C-E) A higher dose of Him alone can compensate for the loss of Her5 activity and maintain the MIZ. (C) Schematic representation of the transgene integrated to generate *her5PAC::egfp* embryos (Tallafuss and Bally-Cuif, 2003): the *egfp* cDNA (blue cylinder) is inserted into the *her5* region coding for the bHLH domain, resulting in a dysfunctional protein unable to bind both DNA and other bHLH factors. However, the *him* gene, contained in the PAC, is intact. (D) Quantification of *him* and *otx1* (control) mRNAs in *her5PAC::egfp* transgenic compared to wild-type embryos using real-time RT-PCR. We do not know the number of recombined PAC copies integrated into the genome in our transgenic lines; however, note that the amount of *him* mRNA is 1.5-fold higher in the *her5*PAC::*egfp* transgenic embryo than in wild-type siblings. The change in threshold-crossing cycle (1/*R*) is shown for each mRNA relative to that for *pax6* (assumed as a housekeeping gene) (a decrease in threshold-crossing corresponds to increase in mRNA level). The increase in *him* expression in the transgenic line is significant ($P<0.02$ by Student's *t*-test). Standard deviations are indicated with red lines. (E) Blocking Her5 activity (by injecting *her5*MO^{ATG}) in *her5PAC::egfp* transgenic embryos fails to trigger ectopic expression of *ngn1* across the MIZ (white asterisk) (flat-mounted embryo at three somites, anterior left, used markers color-coded).

2000; Topczewski et al., 2001). In addition to this phenotype, assaying *b404* mutants for neurogenesis revealed ectopic *ngn1*-positive cells in place of both the MIZ (Fig. 7F, asterisk) and LIZ (Fig. 7F, arrow, enlarged in F′), a phenotype never observed in control siblings (Fig. 7E, enlarged in E′) or in embryos for a null point mutation in the *knypek* gene (*kny*^{m119} allele, not shown) (Solnica-Krezel et al., 1996). The number of *ngn1*-positive cells in the lateral aspect of the MH domain (white box in Fig. 7E-G) is increased by 40% in *b404* embryos compared to control siblings (n=13 mutants and 10 wild-type embryos), while other populations of neuronal precursors, such as trigeminal ganglia neurons, are unaffected (black box in Fig. 7E-G), further supporting the specificity of this phenotype. Further, this phenotype was maintained upon rescuing Kny function in *b404* homozygous embryos injected with *kny* mRNA at the one-cell stage (Fig. 7H,H′).

The above results demonstrate that ectopic neurogenesis in *b404* is selective of the IZ and unrelated to the lack of Kny activity itself. It remains possible however that the *b404* deletion encompasses other genes than *him* and *her5* that contribute to this phenotype. To address this issue, we rescued Him activity in *b404* homozygotes (Fig. 7J) by crossing them into the transgenic *her5PAC::egfp* background. *b404/b404;her5PAC::egfp* embryos display a normal expression of *him* in time and space (Fig. 7J), but no expression of *her5* (not shown). We observed that, under these conditions, the LIZ was preserved (Fig. 7I, white box, enlarged in I′). Thus, restoring Him activity is sufficient to rescue formation of the LIZ in *b404* mutants, strongly arguing that the neurogenic phenotype in the lateral MH of these mutants results from the lack of Her5 and Him function. In addition, these results demonstrate that one dose of Him activity provides a level of inhibition sufficient for LIZ formation. In contrast, loss of the MIZ was maintained in *b404/b404;her5PAC::egfp* embryos (Fig. 7I), in keeping with our finding that MIZ formation requires more than one or two copies of *him* or *her5* (Fig. 4A-C, 5E).

Him and Her5 are equally potent neurogenesis inhibitors in the lateral IZ

We demonstrated above that the total amount of Him + Her5 inhibitory activity is the crucial determinant for IZ formation, and that increased levels of Him could compensate for loss of Her5 both in the medial and lateral IZ. These experiments however did not address the relative contribution of Her5 to the total inhibitory activity required for IZ formation. To determine whether Him and Her5 contribute equally to this activity, we analyzed LIZ formation in *b404*/+; *kny*^{m119}/+ embryos where the function of either Her5 (Fig. 7K) or Him (Fig. 7L) was abolished. This background, obtained by crossing *b404*/+ with *kny*^{m119}/+ heterozygote adults, allows immediate identification of the embryos carrying one single copy of each gene *him* and *her5*, since such embryos display the *knypek* phenotype. Blocking the activity of Him or Her5 *b404*/+; *kny*^{m119}/+

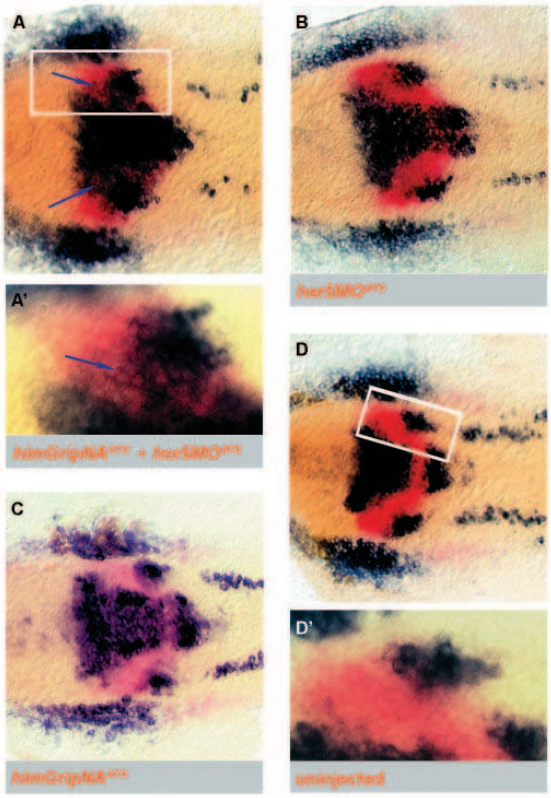

Fig. 6. The activity of both Her5 and Him is necessary to prevent neurogenesis in the lateral IZ. Dorsal views of flat-mounted –8.4*ngn1*::*egfp* transgenic embryos (Blader et al., 2003) probed at the three-somite stage for *egfp* expression (blue) after injection of 1 mM *her5*MO^{ATG} + 0.25 mM *himGrip*NA^{ATG} (A), 1 mM *her5*MO^{ATG} (B), 0.25 mM *himGrip*NA^{ATG} (C), compared to an uninjected control (D). A′ and D′ are enlargements of the boxed areas in A and D, respectively. The IZ is indicated by *pax2.1* expression (red staining). Note that the LIZ is undergoing ectopic neurogenesis only in the embryo injected with both *her5*MO^{ATG} and *himGrip*NA^{ATG} (blue arrows).

embryos leaves only one functional copy of either *her5* or *him*, respectively. Assaying for *ngn1* expression revealed that the LIZ forms normally in such embryos (Fig. 7K,K′ and 7L,L′ compared to 7M,M′, white arrowhead) (while, as expected, the MIZ is lost, Fig. 7K, and 7L, compared to 7M, white arrow). These results are in agreement with an equal potency of Him and Her5 to inhibit lateral neurogenesis at the MHB and, like for the MIZ, we propose that a crucial determinant of LIZ formation is the threshold of Him + Her5 activities rather than the specific presence of both factors.

Discussion

Maintaining a progenitor pool at the embryonic MHB is crucial to MH growth and IsO maintenance, and we report here a new molecular player and its associated mechanism preventing neurogenesis in this territory. Looking for genes physically linked to *her5*, we unraveled a previously unknown, paired and divergently transcribed *hairy/E(spl)* gene, *him*, which shares with *her5* expression across the IZ. We demonstrate that blocking either Her5 or Him function results in the same failure to form and maintain the MIZ, and that interfering concomitantly with the function of both factors prevents formation of the LIZ. In both domains, we demonstrate that sufficient levels of one factor alone are sufficient to compensate for the lack of the other. Together, our results are most compatible with a model where the molecular basis of IZ formation is the total Him + Her5 inhibitory activity, at different thresholds along the mediolateral axis. They highlight a new mechanism, relying on paired Hairy/E(spl) factors, for the maintenance of a non-differentiating signaling boundary during embryonic development.

him and *her5* are a new co-functional gene pair

him and *her5* are located 3 kb apart in a head-to-head, in a manner reminiscent of the *her7/her1* gene pair (Henry et al., 2002). Our search through the zebrafish genome revealed an additional similarly organized pair of *her* genes, *her4/her12*, located on chromosome fragment ctg10516. ESTs BM023698 and AL716753 match with 100% to the cDNA sequence deducted from *ENSDARG00000028110*, suggesting that *her12* is a real transcribed gene. Thus, our results suggest that a paired and divergently transcribed configuration is a frequent organization of zebrafish *her* genes. Our search through other vertebrate genomes, however, including mouse and *Fugu rubripes* (*Fugu* genome, The Welcome Trust Sanger Institute, release 08-02-04), failed to reveal a similar organization of *hairy/E(spl)*-like genes in these species, suggesting that the molecular process(es) generating *her* pairs took place along the lineage leading to zebrafish.

Our results do not suggest a simple evolutionary model leading to the generation of zebrafish *her* pairs. Indeed, the six *her* genes involved belong in sequence to two groups of orthologs (group 1: *him/her5/her1* versus group 2: *her7/her4/her12*), but only the *her7/her1* pair contains one gene from each group. Thus the situation is not comparable to *dlx* gene pairs, interpreted to result from a tandem duplication followed by a cluster duplication. Because *her4* and *her12* have very similar coding sequences, it is possible that these two genes underwent a recent event of gene conversion, facilitated by the formation of intrachromosomal hairpins (Hickey et al., 1991). We failed to detect indications supporting gene conversion within the *him/her5* gene pair, but other recombination events might have occurred (D. Chourrout, J.N. and L.B.-C., unpublished observations).

Linked genes sharing sequence similarity have been reported for a variety of genetic functions in several organisms.(Akam, 1989; Alonso and Cabrera, 1988; Bober et al., 1994; Coleman et al., 1987; Kmita and Duboule, 2003; Knust et al., 1992; Stein et al., 1996). Duplication events resulting in linked arrays of related genes generate copies that often share cis-acting regulatory sequences. Whether *him* and *her5* expression across the IZ are coregulated remains to be directly demonstrated but is highly likely, given that the enhancer driving MH expression of *her5* extends into the *him* locus (Tallafuss and Bally-Cuif, 2003). In addition, *him* and *her5* differ in some aspects of their expression profiles (in the shield and presomitic mesoderm, versus presumptive pharyngeal endoderm, respectively). The

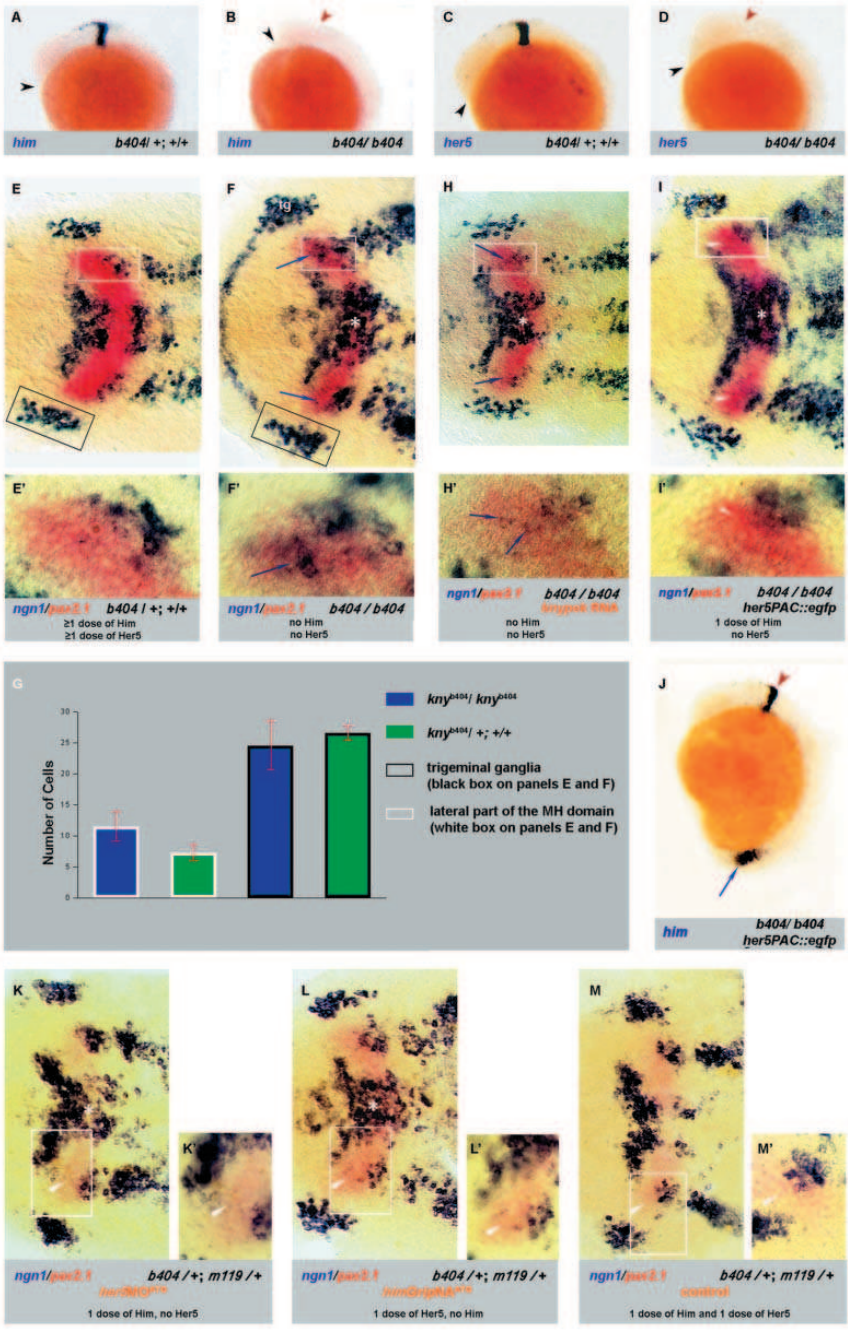

Fig. 7. Ectopic neurogenesis in both the medial and lateral IZ in *b404* deletion mutants results from the deletion of *him* and *her5*. (A-D) *b404* mutants lack *her5* and *him* expression. Lateral views of whole-mount embryos assayed for *him* or *her5* expression at the 17-somite stage (anterior left, probes indicated bottom left, genotype bottom right). The position of the MHB in mutant embryos is indicated with a red arrowhead. The position of the head, reflecting the delayed convergence and extension problems in the mutant embryo, is indicated with a black arrowhead. (E-G) Ectopic neurogenesis across the LIZ revealed by *ngn1* expression (blue) in *b404* mutants (F,F′) compared to non-mutant siblings (E,E′). In *b404* embryos, ectopic *ngn1*-positive cells are present both in the lateral (blue arrow) and medial (asterisk) IZ (E′ and F′ are high magnification of the areas boxed in white in E and F, respectively). (G) The number of *ngn1*-positive cells in the future alar MH (area indicated with white box in E and F) is 40% higher in mutant embryos compared to WT siblings, while other neural plate areas are not affected (e.g. trigeminal ganglia, area boxed in black in E and F). (H) Reintroducing Knypek function in *b404* mutants does not alter the IZ neurogenesis phenotype. Expression of *ngn1* (blue) in three-somite *b404* mutants where Kny function has been restored by *kny* RNA injection (dorsal views of flat-mounted embryos, anterior left, A′ is a high magnification of the area boxed in A). Note that ectopic *ngn1* expression both across the MIZ (asterisk) and LIZ (blue arrows) is not altered compared to uninjected *b404* mutants (Fig. 7F). (I-J) Restoring Him function at endogenous levels in *b404* mutants is sufficient to rescue the LIZ. (J) Crossing the *b404* mutation into the *her5*PAC::*egfp* background generates *b404*/*b404*;*her5PAC::egfp* embryos where *him* expression is recovered with endogenous levels and expression pattern (lateral view of a 17-somite embryo, anterior left). (I,I′) Expression of *ngn1* (blue) in three-somite *b404*/*b404*;*her5PAC::egfp* embryos (dorsal views of flat-mounted embryos, anterior left, I′ is a high magnification of the area boxed in I). Note that no ectopic neurogenesis is detectable any longer across the LIZ (white arrowheads), while the MIZ remains bridged by ectopic *ngn1*-positive cells (asterisk). (K-M). Him and Her5 equally contribute to the total inhibitory activity and one copy of either Him or Her5 is sufficient for formation of the LIZ. Formation of the LIZ in the *b404/+; m119/+* embryos is indistinguishable in Him morphants (K,K′), Her5 morphants (L,L′) and uninjected embryos (M,M′) (white arrowheads). Note that after blocking either Him or Her5 activity ectopic neurogenesis occurs in the MIZ (white asterisk). K′,L′ and M′ are enlargements of boxed area in K, L and M respectively (25 embryos was analyzed for *b404/+; m119/+* injected with *her5*MO^{ATG}, 27 for *b404/+; m119/+* injected with *him*Grip^{ATG} and 20 uninjected *b404/+; m119/+*).

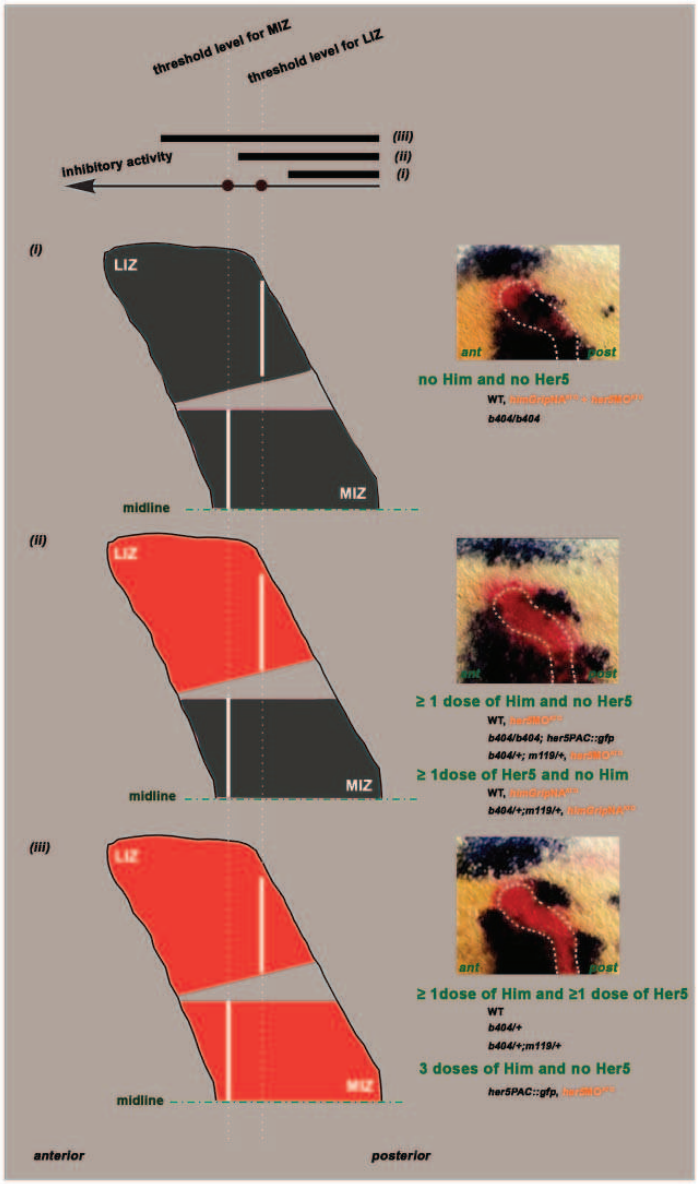

Fig. 8. Models for IZ formation based on dose dependence for Him + Her5 inhibitory activity. In each panel, a half IZ is represented and color-coded (red: MIZ or LIZ, light grey: intermediate field, dark grey: *ngn1*-positive areas), and the level of Him + Her5 inhibitory activity is indicated by black horizontal bars. The threshold required for *ngn1* inhibition within the LIZ is lower than the MIZ threshold (white bars). Thus, if Him + Her5 activity is below the LIZ threshold level, ectopic neurogenesis will occur both laterally and medially, and the MIZ and LIZ are lost (i). This situation corresponds to the absence of activity of both Her5 and Him. When Him + Her5 activity reaches the LIZ threshold level (one dose of Her5 or Him is sufficient), *ngn1* expression is prevented laterally but not medially, and the LIZ forms but not the MIZ (ii). Finally, if Him + Her5 activity is above the MIZ threshold (⩾1 dose of Him and ⩾1 dose of Her5 or three doses of Him), the whole IZ is formed properly (normal development of wild-type embryos, (iii). The persisting absence of *ngn1* expression within the intermediate field located between the MIZ and LIZ (light grey triangle) could result from additional inhibitor(s) expressed along the AP axis, in register with longitudinal non-differentiation stripes of the rhombomere and spinal cord. Flat-mounted embryos at three-somite stage, with *ngn1* expression in dark and *pax 2.1* in red, corresponding to each situation are shown adjacent to the scheme. The combinations of inhibitory factors producing the appropriate level of inhibitory activity for each situation are listed (green letters), as well as the genetic ways to obtain this particular inhibitory activity (black letters for genotype and orange for interfering agents).

regulatory elements controlling endodermal expression of *her5* are located closer to the *her5* ATG than the MH expression elements (Tallafuss and Bally-Cuif, 2003). Thus expression of the *him/her5* pair may be controlled by a combination of proximal and gene-specific elements (accounting for the differential expression sites of the two genes) and distal and probably common elements (driving IZ expression). It is possible that the proximal elements are new modifications in the evolution of the gene pair, extending genetic functions by the acquisition of new expression domains (Ohta, 2000). It will be interesting to determine whether such cis-regulatory organization is involved in generating different expression sites within other gene pairs.

The combined activities of Her5 and Him determine LIZ formation

We previously identified Her5 as the first determinant of MIZ formation in zebrafish (Geling et al., 2003). However, although *her5* expression covers the whole IZ, and ectopic *her5* expression can inhibit *ngn1* in the lateral MH area, we failed to implicate Her5 alone in LIZ formation in vivo. A main advance of our present work is to provide an interpretation for this finding, by identifying a new Hairy/E(spl) factor, Him, as the partner for Her5 in LIZ formation. Our arguments rely on the phenotype of embryos where the functions of Her5 and Him are concomitantly blocked in a non-genetic interference approach, and of embryos carrying the *b404* deletion, where both *him* and *her5* genes are absent. In both cases, ectopic *ngn1*-positive cells replace the LIZ. This phenotype is not found by blocking the function of either Him or Her5 alone, and is rescued by selectively reintroducing endogenous levels and profile of Him function into the *b404* background, arguing for its specificity. Further, we show that one copy of either *him* or *her5* (as in *b404/+*;*kny*^{m119}/+ heterozygote embryos where Her5 or Him function is blocked) similarly preserves the LIZ, demonstrating that Him and Her5 are equally potent at inhibiting *ngn1* expression in that location. Thus, our results identify Him and Her5 as truly redundant factors that play

equivalent roles, and are together the only determinant, in LIZ formation.

The molecular cascade downstream of Him remains unknown. Because Him is sufficient for LIZ formation in the absence of Her5, we can exclude a mechanism where Him would primarily promote Her5 activity. Rather, because of the similar sequences of Him and Her5, it is more likely that both factors act together on common targets controlling neurogenesis. Within the MIZ, Her5 and Him (J.N. and L.B.-C., unpublished) act upstream of Notch to inhibit expression of *ngn1* and *coe2*, but not other early MH proneural genes such as *asha*, *ashb* and *ato3* (Geling et al., 2003). It will be important to determine whether the molecular cascade(s) and mechanisms downstream of Her5 and Him are conserved in the MIZ and LIZ. Compared to the MIZ, the LIZ exhibits an additional block, still molecularly unknown, that prevents neurogenesis downstream of Ngn1 activity (Geling et al., 2003). Whether Him and Her5 also take part in this second block remains to be tested.

A unified model for IZ formation along the entire mediolateral extent of the neural plate

The absence of Her5 leads to disappearance of the entire MIZ and its replacement by *ngn1*-expressing cells, which later differentiate into Hu-, HNK1- and acetylated-tubulin-positive neurons (Geling et al., 2003). Surprisingly, our results now demonstrate that Him plays an equally important role in MIZ formation, since an exactly identical phenotype is triggered by lack of Him activity (this paper, and data not shown). We further rule out an interdependent regulation of *him* and *her5* expression (Fig. 4E-L). Thus, another important implication of our work is that MIZ formation relies on prepatterning by both Him and Her5.

A priori, the finding that loss of Him or Her5 function result in identical phenotypes can have three different molecular interpretations: first, Him and Her5 might act in distinct pathways that converge on and are both necessary for neurogenesis control at the MIZ; second, the activities of Him and Her5 might be interdependent; third, Him and Her5 might have equivalent functions, a minimal dose of 'Him + Her5' activity being required for MIZ formation. The first two mechanisms are unlikely, given the observation that increased levels of Him alone to three doses (as in *her5PAC::egfp* /+ heterozygote transgenic embryos injected with *her5*MO, Fig. 5E) can compensate for the lack of Her5 function within the MIZ. We do not have genetic means of assessing whether a high dose of Her5 alone would also suffice for MIZ formation. However, our findings that Him and Her5 are equally potent to prevent lateral neurogenesis strongly suggest that this is the case. Thus, we propose that the crucial determinant of MIZ formation, is a total level of 'Him + Her5' inhibitory activity. Hence, above a threshold of Him + Her5, *ngn1* expression is prevented medially and the MIZ is formed, while *ngn1* expression is induced below this threshold (Fig. 8). As discussed above, our results indicate that three doses of one factor alone is the minimum level of inhibitory activity required for MIZ formation. Interestingly, however, two doses are sufficient when both Him and Her5 are present, as in *b404*/+ heterozygote embryos. This result might be related to the higher propensity of Him and Her5 to hetero- than homo-dimerize, or to an increased activity of heterodimers versus homodimers or oligomers. Because the same factors Him and Her5 account for LIZ formation, and can functionally replace each other in this domain as well, a parsimonious interpretation of our findings is to implicate the same dose-dependent mechanism within the LIZ, albeit with a lower threshold level (Fig. 8). The LIZ minimal level of inhibition would be achieved with one dose of Him or Her5 alone. Together, our results thus lead to a unified model where the maintenance of a pool of progenitor cells at the MHB is orchestrated by a variable dose-dependency to the Him/Her5 pair.

Even in the absence of Him and Her5, we failed to induce *ngn1* expression within a small intermediate field located between the MIZ and LIZ (see Fig. 7F, and grey triangle in Fig. 8). In this domain, an additional (as yet unknown) factor might increase the total inhibitory activity and/or prevent neurogenesis in addition to Him and Her5. We failed to recover additional IZ-expressed *E(spl)* genes following our search through the zebrafish genome and expression studies (J.N., C.L. and L.B.-C., unpublished). Because the intermediate field is aligned with the longitudinal domains of non-differentiation in the hindbrain and spinal cord, it is perhaps more likely that this factor is expressed along the AP axis of the neural plate, like other known neurogenesis inhibitors (Bally-Cuif and Hammerschmidt, 2003).

An interesting open question remains to identify the cues controlling the differential sensitivity of the MIZ versus LIZ to Him + Her5, and their functional significance. The MIZ and LIZ differ in their proliferation rates: the MIZ exhibits more cells in M phase than the LIZ at late gastrulation, based on anti-phosphoH3 immunostaining (Geling et al., 2003). It will be crucial to investigate the possible relationship between MIZ and LIZ cell cycle properties and their response to Him + Her5. Also, several morphogens acting in this region are expressed following a mediolateral gradient. For instance, *wnt1* is expressed in a spatio-temporal pattern similar to *her5* and *him* at late gastrulation, thus with initially higher levels laterally than medially, and might enhance cell sensitivity to neurogenesis inhibitors. This might be related to the delay of dorsal differentiation proposed to result from the gradient of Wnt signaling from the spinal cord roof plate (Megason and McMahon, 2002). Conversely Shh signaling from the ventral midline and specifically active at the MHB (Carl and Wittbrodt, 1999; Koster et al., 1997) could increase 'neurogenic competence'. These hypotheses will be important to test experimentally to gain insight into the prepatterning of IZ formation.

Biological significance of a redundant process for IZ formation

Redundant factors are generally viewed as 'safety' locks, and the biological significance of the Him/Her5 couple might be to secure IZ formation. This case of redundancy is more extreme than observed for Her1/Her7, where the disruption of each gene alone produced distinct (although moderate) somitic defects, indicating partially different activities (Henry et al., 2002). The embryonic MHB progenitor pool serves several vital functions. It generates the large majority of MH neurons and glia, as demonstrated in lineage tracing experiments (Tallafuss and Bally-Cuif, 2003) and genetic or surgical ablation (Cowan and Finger, 1982; Hirata et al., 2001). MH neurons form crucial integration centers involved

in visual, auditory and motor control and social behavior. By its long-lasting proliferative activity, the IZ also permits the expansion of MH tissue over time. Although the relative importance of MH derivatives varies between species, most vertebrates are characterized by highly developed visual, auditory or locomotor functions, which are paired with enlarged mesencephalic derivatives or cerebellum. Finally, and importantly, the IZ coincides in space with the isthmic organizer, necessary for patterning the entire MH domain and for the subdivision of mid-versus hindbrain structures (Bally-Cuif et al., 2000; Liu and Joyner, 2001; Rhinn and Brand, 2001). In the mouse, IZ formation also relies on the two redundant bHLH factors Hes1 and Hes3 (Hirata et al., 2001). In that case however *Hes1* and *Hes3* are not genetically linked and their expression profiles are clearly distinct, overlapping only at the MHB (Allen and Lobe, 1999; Lobe, 1997), suggesting that mouse and zebrafish have independently evolved a strategy for the redundant expression and function of Hairy/E(spl) factors at the MHB. A dose dependency and the spatial details of IZ formation in the mouse have not been explored. The fact that one dose of each factor Him and Her5 suffices to maintain the MIZ in zebrafish, while two doses of each single factor do not, probably explains the maintenance of the two genes *him* and *her5* in zebrafish. Whether Hes1 and Hes3, or Him and Her5, exert in addition other and perhaps distinct activities at the MHB remains to be explored.

The IZ is not an isolated case of maintenance of a non-differentiation zone at embryonic signaling boundaries. Such events have been reported, e.g. at the *Drosophila* wing margin, along the dorsal and ventral midlines of the neural tube (Alexandre and Wassef, 2003), as well as between rhombomeres (Cheng et al., 2004). Like the IZ, these boundaries are involved in the progressive building and patterning of their adjacent territories, and the maintenance of their integrity necessitates their remaining undifferentiated. This process is achieved by Notch signaling at the wing margin and inter-rhombomeric boundaries, and Shh signaling along the neural tube ventral midline, while the factors involved along the dorsal midline probably involve Wnt and BMP signaling. Our work demonstrates that a distinct molecular mechanism accounts for non-differentiation at the MHB, namely the differential response of MHB cells to the combined inhibitory activity of two twin and co-regulated Hairy/E(spl)-like factors, independently of Notch. Our findings add to the panel of identified developmental strategies used to build and maintain signaling centers.

Note added in proof

him is identical to *her11*, which has been recently reported for its role in zebrafish somitogenesis (Sieger et al., 2004). The gene referred to as *her11* in the present manuscript (Fig. 1B, ENSDARP00000012990), named before publication by Sieger et al., is a different coding sequence and corresponds to *her13* of Sieger et al. The gene referred to as *her13* in the present manuscript (Fig. 1B, ENSDARP0000008307) is a new gene, not reported by Sieger et al. We suggest that the latter gene be renamed *her16* and that the nomenclature of Sieger et al. be used for all other genes in future work.

We are grateful to U. Strähle, M. Wassef and W. Wurst for their critical reading of the manuscript, and to K. Imai, M. Wahl and L.B.-C. lab members for discussions and suggestions throughout this work. We thank A. Folchert and B. Tannhäuser for expert technical assistance, and the GSF fish facility staff for fish care. We acknowledge M. Brand (*pax2.1*), J. A. Campos-Ortega (*her5*) and U. Strähle (*ngn1*) for gifts of probes and constructs, and D. Meyer for comparison of *him* sequences prior to publication. Work in L.B.-C. laboratory is supported by a VolkswagenStiftung 'junior research group' grant.

References

Akam, M. (1989). Hox and HOM: homologous gene clusters in insects and vertebrates. *Cell* **57**, 347-349.

Alexandre, P. and Wassef, M. (2003). The isthmic organizer links anteroposterior and dorsoventral patterning in the mid/hindbrain by generating roof plate structures. *Development* **130**, 5331-5338.

Allen, T. and Lobe, C. G. (1999). A comparison of Notch, Hes and Grg expression during murine embryonic and post-natal development. *Cell Mol. Biol. (Noisy-le-grand)* **45**, 687-708.

Alonso, M. C. and Cabrera, C. V. (1988). The achaete-scute gene complex of Drosophila melanogaster comprises four homologous genes. *EMBO J.* **7**, 2585-2591.

Bally-Cuif, L. and Hammerschmidt, M. (2003). Induction and patterning of neuronal development, and its connection to cell cycle control. *Curr. Opin. Neurobiol.* **13**, 16-25.

Bally-Cuif, L., Goridis, C. and Santoni, M. J. (1993). The mouse NCAM gene displays a biphasic expression pattern during neural tube development. *Development* **117**, 543-552.

Bally-Cuif, L., Goutel, C., Wassef, M., Wurst, W. and Rosa, F. (2000). Coregulation of anterior and posterior mesendodermal development by a hairy-related transcriptional repressor. *Genes Dev.* **14**, 1664-1677.

Blader, P., Plessy, C. and Strahle, U. (2003). Multiple regulatory elements with spatially and temporally distinct activities control neurogenin1 expression in primary neurons of the zebrafish embryo. *Mech. Dev.* **120**, 211-218.

Bober, E., Baum, C., Braun, T. and Arnold, H. H. (1994). A novel NK-related mouse homeobox gene: expression in central and peripheral nervous structures during embryonic development. *Dev. Biol.* **162**, 288-303.

Brand, M., Heisenberg, C. P., Jiang, Y. J., Beuchle, D., Lun, K., Furutani-Seiki, M., Granato, M., Haffter, P., Hammerschmidt, M., Kane, D. A. et al. (1996). Mutations in zebrafish genes affecting the formation of the boundary between midbrain and hindbrain. *Development* **123**, 179-190.

Carl, M. and Wittbrodt, J. (1999). Graded interference with FGF signalling reveals its dorsoventral asymmetry at the mid-hindbrain boundary. *Development* **126**, 5659-5667.

Cheng, Y. C., Amoyel, M., Qiu, X., Jiang, Y. J., Xu, Q. and Wilkinson, D. G. (2004). Notch activation regulates the segregation and differentiation of rhombomere boundary cells in the zebrafish hindbrain. *Dev. Cell* **6**, 539-550.

Coleman, K. G., Poole, S. J., Weir, M. P., Soeller, W. C. and Kornberg, T. (1987). The invected gene of Drosophila: sequence analysis and expression studies reveal a close kinship to the engrailed gene. *Genes Dev.* **1**, 19-28.

Cowan, W. and Finger, T. (1982). Regeneration and regulation in the developing central nervous system, with special reference to the reconstitution of the optic tectum of the chick following removal of the mesencephalic alar plate. *Curr. Top. Neurobiol.* **11**, 377-415.

Davis, R. L. and Turner, D. L. (2001). Vertebrate hairy and Enhancer of split related proteins: transcriptional repressors regulating cellular differentiation and embryonic patterning. *Oncogene* **20**, 8342-8357.

Dawson, S. R., Turner, D. L., Weintraub, H. and Parkhurst, S. M. (1995). Specificity for the hairy/enhancer of split basic helix-loop-helix (bHLH) proteins maps outside the bHLH domain and suggests two separable modes of transcriptional repression. *Mol. Cell. Biol.* **15**, 6923-6931.

Firulli, B. A., Hadzic, D. B., McDaid, J. R. and Firulli, A. B. (2000). The basic helix-loop-helix transcription factors dHAND and eHAND exhibit dimerization characteristics that suggest complex regulation of function. *J. Biol. Chem.* **275**, 33567-33573.

Fisher, A. L., Ohsako, S. and Caudy, M. (1996). The WRPW motif of the hairy-related basic helix-loop-helix repressor proteins acts as a 4-amino-acid transcription repression and protein-protein interaction domain. *Mol. Cell. Biol.* **16**, 2670-2677.

Geling, A., Itoh, M., Tallafuss, A., Chapouton, P., Tannhauser, B., Kuwada, J. Y., Chitnis, A. B. and Bally-Cuif, L. (2003). bHLH

transcription factor Her5 links patterning to regional inhibition of neurogenesis at the midbrain-hindbrain boundary. *Development* **130**, 1591-1604.

Geling, A., Plessy, C., Rastegar, S., Strahle, U. and Bally-Cuif, L. (2004). Her5 acts as a prepattern factor that blocks neurogenin1 and coe2 expression upstream of Notch to inhibit neurogenesis at the midbrain-hindbrain boundary. *Development* **131**, 1993-2006.

Hammerschmidt, M., Pelegri, F., Mullins, M. C., Kane, D. A., van Eeden, F. J., Granato, M., Brand, M., Furutani-Seiki, M., Haffter, P., Heisenberg, C. P. et al. (1996). dino and mercedes, two genes regulating dorsal development in the zebrafish embryo. *Development* **123**, 95-102.

Henry, C. A., Hall, L. A., Burr Hille, M., Solnica-Krezel, L. and Cooper, M. S. (2000). Somites in zebrafish doubly mutant for knypek and trilobite form without internal mesenchymal cells or compaction. *Curr Biol* **10**, 1063-1066.

Henry, C. A., Urban, M. K., Dill, K. K., Merlie, J. P., Page, M. F., Kimmel, C. B. and Amacher, S. L. (2002). Two linked hairy/Enhancer of split-related zebrafish genes, her1 and her7, function together to refine alternating somite boundaries. *Development* **129**, 3693-3704.

Hickey, D. A., Bally-Cuif, L., Abukashawa, S., Payant, V. and Benkel, B. F. (1991). Concerted evolution of duplicated protein-coding genes in Drosophila. *Proc. Natl. Acad. Sci. USA* **88**, 1611-1615.

Hirata, H., Tomita, K., Bessho, Y. and Kageyama, R. (2001). Hes1 and Hes3 regulate maintenance of the isthmic organizer and development of the mid/hindbrain. *EMBO J.* **20**, 4454-4466.

Iso, T., Sartorelli, V., Poizat, C., Iezzi, S., Wu, H. Y., Chung, G., Kedes, L. and Hamamori, Y. (2001). HERP, a novel heterodimer partner of HES/E(spl) in Notch signaling. *Mol. Cell. Biol.* **21**, 6080-6089.

Kimmel, C. B., Ballard, W. W., Kimmel, S. R., Ullmann, B. and Schilling, T. F. (1995). Stages of embryonic development of the zebrafish. *Dev. Dyn.* **203**, 253-310.

Klambt, C., Knust, E., Tietze, K. and Campos-Ortega, J. A. (1989). Closely related transcripts encoded by the neurogenic gene complex enhancer of split of Drosophila melanogaster. *EMBO J.* **8**, 203-210.

Kmita, M. and Duboule, D. (2003). Organizing axes in time and space; 25 years of colinear tinkering. *Science* **301**, 331-333.

Knust, E., Schrons, H., Grawe, F. and Campos-Ortega, J. A. (1992). Seven genes of the Enhancer of split complex of Drosophila melanogaster encode helix-loop-helix proteins. *Genetics* **132**, 505-518.

Korzh, V., Sleptsova, I., Liao, J., He, J. and Gong, Z. (1998). Expression of zebrafish bHLH genes ngn1 and nrd defines distinct stages of neural differentiation. *Dev. Dyn.* **213**, 92-104.

Koster, R., Stick, R., Loosli, F. and Wittbrodt, J. (1997). Medaka spalt acts as a target gene of hedgehog signaling. *Development* **124**, 3147-3156.

Lazo, P. S., Ochoa, A. G. and Gascon, S. (1978). alpha-Galactosidase (melibiase) from Saccharomyces carlsbergensis: structrual and kinetic properties. *Arch. Biochem. Biophys.* **191**, 316-324.

Liu, A. and Joyner, A. L. (2001). Early anterior/posterior patterning of the midbrain and cerebellum. *Annu. Rev. Neurosci.* **24**, 869-896.

Lobe, C. G. (1997). Expression of the helix-loop-helix factor, Hes3, during embryo development suggests a role in early midbrain-hindbrain patterning. *Mech. Dev.* **62**, 227-237.

Lun, K. and Brand, M. (1998). A series of no isthmus (noi) alleles of the zebrafish pax2.1 gene reveals multiple signaling events in development of the midbrain-hindbrain boundary. *Development* **125**, 3049-3062.

Martinez, S. (2001). The isthmic organizer and brain regionalization. *Int. J. Dev. Biol.* **45**, 367-371.

Megason, S. G. and McMahon, A. P. (2002). A mitogen gradient of dorsal midline Wnts organizes growth in the CNS. *Development* **129**, 2087-2098.

Muller, M., v Weizsacker, E. and Campos-Ortega, J. A. (1996). Expression domains of a zebrafish homologue of the Drosophila pair-rule gene hairy correspond to primordia of alternating somites. *Development* **122**, 2071-2078.

Ohta, T. (2000). Evolution of gene families. *Gene* **259**, 45-52.

Reifers, F., Bohli, H., Walsh, E. C., Crossley, P. H., Stainier, D. Y. and Brand, M. (1998). Fgf8 is mutated in zebrafish acerebellar (ace) mutants and is required for maintenance of midbrain-hindbrain boundary development and somitogenesis. *Development* **125**, 2381-2395.

Rhinn, M. and Brand, M. (2001). The midbrain–hindbrain boundary organizer. *Curr. Opin. Neurobiol.* **11**, 34-42.

Sieger, D., Tautz, D. and Gajewski, M. (2004). her11 is involved in the somitogenesis clock in zebrafish. *Dev. Genes Evol.* **214**, 393-406.

Solnica-Krezel, L., Stemple, D. L., Mountcastle-Shah, E., Rangini, Z., Neuhauss, S. C., Malicki, J., Schier, A. F., Stainier, D. Y., Zwartkruis, F., Abdelilah, S. et al. (1996). Mutations affecting cell fates and cellular rearrangements during gastrulation in zebrafish. *Development* **123**, 67-80.

Stein, S., Niss, K. and Kessel, M. (1996). Differential activation of the clustered homeobox genes CNOT2 and CNOT1 during notogenesis in the chick. *Dev. Biol.* **180**, 519-533.

Tallafuss, A. and Bally-Cuif, L. (2003). Tracing of her5 progeny in zebrafish transgenics reveals the dynamics of midbrain-hindbrain neurogenesis and maintenance. *Development* **130**, 4307-4323.

Topczewski, J., Sepich, D. S., Myers, D. C., Walker, C., Amores, A., Lele, Z., Hammerschmidt, M., Postlethwait, J. and Solnica-Krezel, L. (2001). The zebrafish glypican knypek controls cell polarity during gastrulation movements of convergent extension. *Dev. Cell.* **1**, 251-264.

Vaage, S. (1969). The segmentation of the primitive neural tube in chick embryos (Gallus domesticus). A morphological, histochemical and autoradiographical investigation. *Ergeb. Anat. Entwicklungsgesch* **41**, 3-87.

Wainwright, S. M. and Ish-Horowicz, D. (1992). Point mutations in the Drosophila hairy gene demonstrate in vivo requirements for basic, helix-loop-helix, and WRPW domains. *Mol. Cell. Biol.* **12**, 2475-2483.

Wurst, W. and Bally-Cuif, L. (2001). Neural plate patterning: upstream and downstream of the isthmic organizer. *Nat. Rev. Neurosci.* **2**, 99-108.

Appendix B

Article in *Methods*

The zebrafish as a model system for assessing the reinforcing properties of drugs of abuse

Jovica Ninković and Laure Bally-Cuif

Methods, *in press*

The zebrafish as a model system for assessing the reinforcing properties of drugs of abuse

Jovica Ninković * and Laure Bally-Cuif *

Zebrafish Neurogenetics Junior Research Group, Institute of Virology, Technical University Munich, Trogerstrasse 4b, D-81675, Munich, Germany and GSF-National Research Center for Environment and Health, Department Zebrafish Neurogenetics, Institute of Developmental Genetics, Ingolstaedter Landstrasse 1, D-85764, Neuherberg, Germany

Abstract

Recent reports make use of the zebrafish to study complex behavior such as addiction, anxiety, or learning and memory. We have invested in establishing reliable tests and their appropriate controls to measure these behavioral parameters in the zebrafish adult. Our assays are robust enough to permit the detection of dominant mutations affecting drug-induced reward, and therefore can be used in forward genetic screens. We provide the reader with the technical details of these tests, as well as with their appropriate and crucial -although often overlooked- control assays. In particular, our results make it possible to use the zebrafish as a promising model to identify new genetic components of the reward pathway.

Key words: zebrafish, addiction, conditioned place preference (CPP), aversion, learning and memory, D-amphetamine, behavior.

Introduction

Behavioral disorders are among the most widespread and costly brain diseases in modern societies[24]. However, our understanding of the molecular networks underlying these disorders is still limited, preventing adequate therapies. A number of animal models have been used to investigate the role of different brain structures in disease development, but the identification of the

* authors for correspondence at:
Email addresses: ninkovic@gsf.de (Jovica Ninković), bally@gsf.de (Laure Bally-Cuif).

genes involved has been difficult, both because of the complexity of the disorders, which involve environmental factors, and because of limited candidate genes. The candidate gene approach, used mainly in rodents, has two main disadvantages: *(i)* it requires that the genes of interest are known and very well characterized and *(ii)* the production of adequate sample size is costly. On the contrary, forward genetics methods where the genome is mutagenized, the resulting phenotypes characterized and the affected gene subsequently cloned give an opportunity to detect both new and known factors controlling the behavior of interest. Forward genetics has been successfully employed in several large-scale screens[25][14], aimed to reveal genes controlling early development of zebrafish. Researchers have used either embryos or juveniles and utilized the main advantages of the zebrafish: *(i)* Its good balance between simplicity and complexity of organic systems. For example the fish nervous system is simpler than in rodents, but still able to control a variety of complex behaviors like learning, addiction, aggression, locomotion, etc. *(ii)* Its powerful genetics. Mutations can be induced with high frequency and rapidly cloned thanks to comprehensive genetic maps [31][17]. *(iii)* Its relatively short generation time and large progeny sizes, facilitating large-scale screens and *(iv)* Its relatively simple and cheap breading conditions. Compared to the assays designed for embryos and juveniles, the use of adult fish in large-scale screens appears to be cumbersome. It requires extra breading, extended housing and increased time for mutation recovery. Additionally, adult fish are very sensitive to handling-induced stress[26][22] and great care has to be taken when behavioral assays are performed[26]. Nevertheless, it is obvious that adult animals have to be used when the behavior of interest requires the full functionality of a mature nervous system. Recently, considerable efforts have been placed into the development of robust, rapid and reproducible assays for adult zebrafish behavior, which can be used in large-scale screens and Table 1. summarizes the behavioral assays currently published.

This review will highlight three assays addressing complex behavior in the adult zebrafish: *(i)* addiction(reward), *(ii)* basal level of aversion (a likely measurement of anxiety) and *(iii)* learning and memory. It summarizes the results of several years of investigations in our laboratory, to eventually achieve tests and controls sufficiently robust to permit their use in large-scale genetic screens. We will detail our experimental protocols, insist on important pitfalls, and demonstrate that our tests are suitable for large-scale screens for dominant modifiers of the reward response.

Measuring addiction in zebrafish using the conditioned place preference paradigm

Addiction is characterized by the uncontrollable and chronically relapsing compulsion to take drugs in spite of their dramatically negative effect on normal brain function. Addiction was studied in animal models, mainly rodents, using two experimental protocols: the Conditioned Place Preference (CPP) paradigm and different protocols of drug self-administration. In the CPP paradigm, the primary motivational properties of a drug serve as a conditioning stimulus that is repeatedly paired with a set of environmental cues. During the course of conditioning, these cues acquire secondary motivational properties.

There are a number of excellent reviews on CPP *(Carr* et al.*, 1989[10]; Hoffman, 1989[19]; Schechter and Calcagnetti, 1993[29]; Bardo* et al.*, 1995[3]; Bozarth, 1987[6]; van der Kooy, 1987[36]; White* et al.*, 1987[37]; Calcagnetti* et al.*, 1995[8]; Tzschentke, 1998[34])* and the reader is referred to these publications for detailed discussions and considerations of basic methodological issues of the CPP paradigm.

In this article, we will focus on the methodology we have developed to use CPP in large-scale ENU-screens, aimed at recovering mutations affecting the molecular pathway(s) of drug-induced reward in zebrafish adults. We will point out the crucial aspects of CPP experiment design and the necessary specific controls, such as the assessment of the animal's stress, learning capacity and memory. To validate the zebrafish as a model system in addiction studies, we further analyzed the conservation of the neurotransmitter pathways underlying addiction in *Teleostei* and mammals. We focused on the cholinergic system[26], a known modulator of dopaminergic transmission in mammals, and our key results will be reviewed here. Finally, we will present the strategy, the organization and the first results of pilot ENU-screens using the CPP test that we conducted to look for genetic modifiers of the reward response.

General experimental procedure

Most CPP experiments reported in this chapter use the general procedure schematized in Fig 1A, performed in an isolated room (below referred to as Behavior room). We used 3- to 6-month-old adult zebrafish weighing 0.5 to 1 g. The fish were moved to the behavior room under maintenance conditions and feeding schedule identical to the fish facility at least two days before each assay. Thus, we kept environmental variance at a minimum for all behavioral assays. The testing apparatus is a 3-liter, rectangular tank containing 2 liters of water and placed in an isolated cabinet with top illumination (we have used four bulbs (100W each) (scheme of the cabinet with experimental tank, bulbs

and camera position available upon request). The water level was kept to 10 cm from the tank bottom to minimize stress. Distinct visual cues divide the experimental tank into two halves: a dark half colored in brown and a light half colored in white with two "frightening" black spots placed at the bottom of the tank (for more details about tank design see section *Biased vs unbiased visual cues*). After an initial introduction into the testing apparatus, each fish was separately accommodated to the new environment for two whole days (days 1 and 2 on Fig 1A.) and was afterwards recorded in one 15-minute trial on day 3 (Fig 1A.) using either the Noldus Ethovision v.2.3 system (Noldus Information Technology, Netherlands, http://www.noldus.com) or Videotrack software (Viewpoint, France, http://viewpoint.fr), typical tracking images are illustrated in Fig. 2G. The importance of the accommodation phase and the optimal measuring interval will be discussed in sections *Habituation* and *Optimal measuring interval*. The preferred compartment was defined as the compartment in which a fish spends most of its time during the measurement on day 3, and the place preference (PP) is calculated as the percentage of time that the fish spends in the preferred compartment. On day 4, each fish was weighed and then received an optimal dose (see section *Dose response*) of D-amphetamine (40 μg of D-amphetamine (Sigma-Aldrich A0922, Germany) and 3 μg methylene-blue as a tracer per gram of fish in 110 mM NaCl) by intraperitoneal injection. Immediately afterwards, the fish was confined to the non-preferred compartment for 45 minutes (day 4, Fig 1A.). The restriction to this compartment was achieved using a transparent slider. Thus, visual contact with the preferred compartment remained, and the difference between the conditioning and recording conditions was minimized. A transparent slider was used to minimize differences between the tanks used for recording and conditioning. The experimental tank and conditions were otherwise identical to the ones used for place preference determination, and each fish was tested separately. After 45 minutes, the fish was removed from the experimental tank and kept in a 1.5-liter tank on a color-neutral background (blue on Fig 1A). The choice of such a background is important since the duration of D-amphetamine action on the fish CNS, its metabolism, or the activity of D-amphetamine metabolites are not known. On day 5 (Fig 1A.), the fish was injected intraperitoneally with a saline solution (3 μg of methylene-blue per gram of fish in 110 mM NaCl), then restricted for 45 minutes into the preferred compartment. Between each injection session, the experimental tank was cleaned with 70 % ethanol and rinsed with fish facility water. Since olfactory stimuli are extremely important to fish, this procedure is necessary when large numbers of subjects are tested in the same boxes. Otherwise, a fish may be responding to the olfactory cues left by earlier animals rather then making a place preference discrimination based on its own conditioning experience. The D-amphetamine treatment was repeated on days 6 and 8 and the saline treatment on day 7 (see section *Drug application*), always at the same time of the day. Place preference was then measured again on day 9. The efficiency of conditioning was estimated as the change in place preference before and

after treatment, relative to the place preference before treatment, as follows: % of change = 100×(PP-CPP)/PP, where % of change is the relative change in place preference, PP is the place preference before treatment and CPP is the place preference after treatment.

Using the procedure described above, most AB fish tested (90 %, n>20) initially showed preference for the dark compartment of the experimental tank (see Fig 6A, the center of the Gauss distribution of the time spent in the brown compartment for a population of AB fish is at 60.5 % .

In the conditions described above, D-amphetamine conditioning on the animal results in a rapid and robust change in place preference, never observed with saline (Fig 1B).

Establishment of the experimental set-up to measure the reinforcing properties of D-amphetamine

The reproducibility and reliability of CPP experiments in measuring the reinforcing properties of drugs of abuse in laboratory animals depends on several important variables, discussed below.

Experimental tank design
-Biased vs unbiased visual cues-

Most CPP studies employ two- or three-compartment conditioning boxes. A conditioning apparatus can be designed such that animals do not show a significant place preference to one of the compartments upon initial exposure to the experimental tank (unbiased design). Alternatively, visual cues can be chosen such that the animals show unconditioned place preference for one side of the tank over the other (biased design). The biased tank design has often been criticized because it can be misleading in cases where the drug has a strong anxiolytic component. However, it will allow detecting several behavioral states (the initial aversive state of the animal, the response to the anxiolytic action of drugs, reward) that can be discriminated with appropriate controls.

To be able to use the same experimental tank to address both the initial aversion state of the animal and the reinforcing properties of the drugs, we opted for the biased tank design. There, one has to set-up the environmental cues such that the animals clearly prefer one compartment, but that the aversion to the initially non-preferred compartment can be overcome by the rewarding effect. To address this issue we analyzed initial place preference and drug-induced place preference as a function of different environmental cues, i.e. different colors of the walls and bottom of the experimental tank (see Fig 2A). We found that a strong contrast between the visual cues (Fig 2A, upper de-

sign) results in a very coherent place preference: 90 % of the fish tested (n=11) spent more than 80 % of their time in the darker compartment(Fig 2B), but the optimal dose of 40 μg/g of D-amphetamine (see below) was in 82 % of cases insufficient to induce a reversal in place preference (Fig 2B,D). Therefore, we reduced the contrast between the initially preferred and non-preferred compartments by designing the experimental tank shown on Fig 2A, bottom. The darker side has a light brown color and the bright compartment a white bottom with two black spots. In this tank, the majority of naive AB fish (95 %, n=12) spent between 55 and 75 % of their time in the darker compartment (Fig 2C and Fig 6A). Upon D-amphetamine treatment, 83 % of the fish tested reverted their place preference (Fig 2C), leading to a positive change in place preference in 95 % of cases (Fig. 2D, 6E). Note also, that the variance in the change in place preference is dramatically larger for the population of fish tested in the black-white tank compared to the brown-white one (Fig. 2D, red bars), indicating a more coherent and more robust conditioning obtained in the latter case.

Habituation

The clear place preference displayed for one side of the test apparatus during the preconditioning trials might include a fear of novelty, which will decrease over consecutive days independently from any effect of the drug on the reward pathway.

To address the effect of habituation on place preference, we monitored the place preference of AB fish in 15-min measurements over 5 consecutive days (one trial per day). The fish were kept in the testing apparatus during the entire experiment. We observed that the time spent in the initially preferred compartment significantly decreases until day 3 (Fig 2E) and then remain stable $\pm$ 4 % for an individual fish at 55-70 % over 10 days (not shown). Thus, we took the percentage of time spent in the preferred compartment at day 3 as a basis in all further measurements. The mean value of change in place preference induced with 40 μg/g of D-amphetamine is 24.2 $\pm$ 2.8 % for AB fish (Fig 2D and 6E) which clearly can not be accounted for the spontaneous decrease of place preference after day 3 (4 %, see above). Furthermore, amphetamine injected fish are compared with saline injected fish, the behavior of which incorporates the possible spontaneous decrease in place preference after day 3.

We conclude that the difference between the place preference measured on day 3 and day 9 (Fig 1A.) is a consequence of the conditioning developed upon D-amphetamine administration.

Optimal measuring interval

Practically, a short test is best. However, it should reproducibly highlight the fish preference.

To determine the minimal measuring interval, we recorded 5 AB fish on day 3 for one hour. We next compared the PP value obtained for one hour with that for the first 2, 5, 10, and 15 minutes of the measurement. This analysis revealed that the fish should be measured at least for the first 15 minutes to get a representative value of the place preference (Fig 2F and not shown).

Drug administration

The number of conditioning sessions (stimulus-response pairing) is an important parameter influencing the intensity of a conditioned response. To determine the dependence of CPP on the number of conditioning sessions, three different groups of fish were submitted to respectively one, two or three 30-minutes conditioning sessions. In the case of two and three conditioning trials, respectively one or two intervening injections of saline solution were performed. Increasing the number of conditioning trials resulted in a linear increasing of CPP outcome (Fig 3A). Thus, CPP experiments have to involve a number of conditioning sessions. Experiments employing two conditioning sessions per day have been performed in rodents by several authors [5][35][9] and gave results indistinguishable from those obtained with one conditioning per day with the same total number of conditioning sessions. However, when several conditioning sessions per day are conducted, one has to make sure that the drug effect from the previous session does not carry over to the next session, particularly when counterbalancing injection schemes are used.

For this reason, and since the pharmacokinetics of D-amphetamine in zebrafish are not known, we decided to use one conditioning sessions per day and, except otherwise indicated, three D-amphetamine conditioning sessions counterbalanced with two saline injections.

Dose-response analysis

In rodents, psychostimulants induce reward in a dose-dependent manner, but doses above a threshold induce a stereotypic freezing behavior. Thus, we used spectrum of doses to determine the optimal dose in zebrafish.

The influence of the dose of drug on the magnitude of CPP is shown on Figure 3 (Red squares and line on B and C). Doses below 5 μg/g failed to induce a change in place preference and these doses are not shown on the graphic. Doses between 5 and 80 μg/g induce a reproducible CPP following a Gaussian distribution. Maximal CPP is observed at a dose of 62.3 μg/g according to the Gauss fit (Fig. 3B). Doses above this value induce CPP with progressively

reduced magnitude, most likely due to immobilization and stress of the animal and/or death (see Fig. 3C, black curve), as reported in mammals[34]. These data suggest that conditioning is sensitive to D-amphetamine dosage and that there is a significant difference between the threshold response and the maximum response using this conditioning protocol. Therefore, dose selection is one of the key points in designing conditioning experiments.

We selected a dose of 40 μg/g, which triggers robust CPP with reasonably low mortality.

Specificity of CPP to measure reinforcing

The habituation of the fish to the testing set-up before the experiments, and the control experiments showing that saline injections fail to modify place preference, permit to conclude that the CPP obtained results from the positive reinforcing properties of D-amphetamine in the wild-type adult zebrafish. However, in cases where CPP will not be modified, additional controls are needed before concluding to the absence of positive reinforcing properties of the drug used. Indeed, at least three parameters unrelated to reinforcing *per se* might artificially bias the CPP response: *(i)* the degree of aversion to the initially non-preferred compartment, which may interfere with conditioning, *(ii)* the capacity of the animal tested to learn and remember which compartment was associated with the drug, and *(iii)* the capacity of the animal tested to appreciate the visual cues identifying the drug-paired compartment. To rule out an involvement of these factors in the cases where a low CPP is detected, we have developed appropriate set-ups to estimate the basal levels of aversion and cognitive capacities of adult zebrafish. For vision tests on zebrafish adults, the reader is referred to excellent recent publications [23][2].

Basal levels of aversion

The aversion of each fish for the non-preferred compartment was calculated as the difference in the time spent in the preferred versus non-preferred compartment as follows: $Av = PP - ta$, where Av represents the aversion, PP is the percentage of time spent in the preferred compartment and ta is the percentage of time in the non-preferred compartment. Thus, a high difference between PP and ta is interpreted as a high level of aversion for the non-preferred compartment, measured using the tank in Fig. 1A (bottom) after two days of habituation. The basal levels of aversion for commonly used zebrafish strains are shown on Fig 4A. Note that there are no significant differences between the strains tested. Nevertheless, these subtle differences in the basal levels of aversion could influence CPP and induce misleading results when two populations with different Av value are compared. Thus, it is necessary to either

normalize drug-induced CPP to the initial aversion state or show that the CPP and the level of Av are not correlated.

Learning and memory test

Learning and memory tests were conducted in a T-maze, modified from Darland and Dowling [12]. The experimental tank was composed of one long (46 cm) and two equally short (30 cm) arms. All arms were 6 cm wide and 15 cm deep with a water level of at least 10 cm. One of the two short arms has an opening into a deep (20 cm) square tank (23 cm x 23 cm) with black walls and artificial grass to offer a favorable habitat for the zebrafish (Fig 4B). Most fish tested spent the majority of their time in this compartment once they found it. Two days before testing, a group of 10 fish was restricted, with a transparent slider, to the long arm of the T-maze for one hour per day to accommodate to the testing environment. After accommodation, each fish was placed alone at the beginning of the long arm and the time needed to find the deep compartment was recorded. After reaching the deep compartment, the fish received there its daily feeding. Each fish was tested once a day. Between the testing phases, the fish were kept separately in a 1.5-liter tank on a color-neutral background. We considered that a fish has learned the task when its time to find the target compartment varied of less than 10 % upon consecutive trials. Analyses conducted on wild-type fish from the AB strain showed that AB fish need 6 trials to learn the task (Fig 4C). Cases where low CPP are associated with a significant lengthening from this baseline learning value have to be interpreted with caution.

Detection of dominant modifiers of D-amphetamine induced reward

Before using the tests described above in screening for mutants, it is crucial to prove that they are robust enough to detect behavioral alterations. Thus, we tested whether we could detect behavioral changes in the existing mutant $ache^{sb55}$. Zebrafish $ache^{sb55}$ mutants harbor a point mutation in the acetylcholinesterase (AChE)-encoding gene, resulting in the production of a non-functional AChE enzyme[4]. Because AChE is the only ACh-degrading enzyme in zebrafish, $ache^{sb55}/ache^{sb55}$ homozygous embryos are completely deficient in ACh hydrolysis and die of progressive paralysis at early larval stages[4]. Heterozygotes reach adulthood without obvious locomotor or any morphological defects. We found that ACh level in brain extracts obtained from $ache^{sb55}/+$ heterohygotes is 1.4-fold increased compared to their WT siblings or AB fish (Fig 5A) (n=9, $p \leq 0.02$) as a consequence of reduced AChE activity[26]. These results suggest that $ache^{sb55}/+$ fish are a valuable genetic model to test the effects of increased brain levels of ACh, and thus an appro-

priate model to evaluate our tests since the ACh system modulates addiction in mammals. To address the impact of changed cholinergic transmission on D-amphetamine-induced reward we compared the CPP of $ache^{sb55}$/+ heterozygotes and their WT siblings (Fig 5B). The mean CPP in $ache^{sb55}$/+ heterozygotes is 14 %, against 24 % in their WT siblings. To determine wether this reduction of CPP is significant, we compared the two populations using independent Student t-test, where arcsine-transformed CPP values were used as raw data. The arcsine transformation is used to correct the skew possibly generated by using percentages as raw data for statistical analyses, especially when these percentages are outside the range 30 - 70 %. This transformation tends to increase the spread of data and therefore more rigorous statistical analyses can be performed. We have used the usual arcsine transformation: CPP'=arcsine$\sqrt{CPP}$ (For more details, see Hogg and Craig,[20]). As shown in Fig 5C,D-amphetamine-induced CPP is significantly lower in $ache^{sb55}$/+ heterozygotes than in their WT siblings ($p \leq 0.05$) or in control AB fish even after performing arcsine transformation. Comparison of the dose-response curves for WT and $ache^{sb55}$/+ fish confirmed that the dose of D-amphetamine administrated (40 μg/g) was also triggering the most robust rewarding effect tolerable for a reasonable survival rate in $ache^{sb55}$/+ fish (Fig 5D)(each point $\geq$15 fish) and that $ache^{sb55}$/+ fish respond with lower CPP than WT fish over the whole range of doses tested. We further verified that alterations in the aversion and cognitive capacities of $ache^{sb55}$/+ fish could not account for this lowered CPP response [26]. We conclude that the cholinergic system strongly modulates addictive behavior in zebrafish.

These results have two main implications. First, they show that the rewarding potential of D-amphetamine, as well as the importance of the cholinergic system in modulating this effect, are conserved between mammals and teleosts. This validates the zebrafish as a reliable model to give insight into the molecular neurobiology of drug-induced reward in vertebrates. Second, they show that our methodology can be used to reveal dominant modifiers of drug addiction in genetic screens.

Genetic screens for the detection of dominant modifiers of D-amphetamine-induced reward in adult zebrafish

Using the technology described above we performed a pilot genetic screen aiming at recovering dominant modifiers of D-amphetamine-induced reward in zebrafish. This screen was performed in the F_1 (phase I) and/or F_2 (phase II) generations and together cover more than 1000 genomes, with the recovery of 26 potential mutations(unpublished).

The next crucial step to recover gene affected by ENU-mutagenesis is the positional cloning of the mutation[17], which can be performed only if the

mutant phenotype can be detected in a polymorphic background. Thus, we addressed the applicability of our experimental procedure to genetic backgrounds different from AB.

We analyzed the initial place preference (Fig 6A-D) and the CPP (generated as described above)(Fig 6E-H) for several fish strains. The center of the Gauss distribution in PP analysis showed that there is a clear initial place preference to one of the two compartments of the experimental tank for all strains tested (Fig 6A-D), allowing us to conduct our biased test design CPP. However, there are significant differences between strains, which should be taken into account, especially when the basal levels of aversion are analyzed.

In all strains, the CPP output after conditioning with D-amphetamine is significantly different from the CPP induced with saline solution (Fig 6E-H and not shown), indicating that D-amphetamine induces a reward that is detectable in our experimental set-up for all strains analyzed. However, there are obvious differences in the magnitude of CPP between the strains (red bars on Fig 6E-H), indicating that the conditions optimized for AB fish are not necessarily the best for all other fish strains and we would like to stress an absolute requirement for the optimization of experimental variables for each strain used. In spite of these differences however, we were able to recover the phenotype of our first mutant in at least one mixed genetic background (AB/Tü used for mapping (Fig. 7)). We conclude that the phenotyping necessary for positional cloning can be conducted at least when AB and Tü strains are used as genetically polymorphic strains.

Concluding remarks

Our understanding of the mechanisms controlling complex disorders like addiction will greatly benefit from the identification of new modifiers of the pathways involved, and an obviously promising approach is to use the zebrafish in large-scale screens designed to recover mutations affecting these modifiers.

In this article we have described a rapid, robust and reproducible assay to address the reinforcing properties of psychostimulant D-amphetamine by measuring CPP in adult zebrafish. In our test conditions, D-amphetamine administration induced CPP in about 95 % of naive AB fish, while saline failed to do so. Additionally, we showed that our assay can be successfully applied to fish strains like Tü or ABO permitting the recovery and positional cloning of detected mutations.

Since the CPP paradigm is also sensitive to processes affecting aversion or learning, we also developed reliable assays to address the basal level of aversion and learning and memory in adult zebrafish. Combining with additional tests for vision defects these procedures enable us to distinguish between addiction-related phenotypes and other phenotypes not connected to reward *per se*.

Although CPP is a powerful measure of the rewarding properties of drugs, this technique should be used with caution. In particular, special attention should be paid to the following: *(i)* drug-injected fish should always be compared with saline-injected fish to exclude an influence of forced habituation or novelty-seeking behavior, *(ii)* handling stress should be minimized and constant across all treatment conditions, *(iii)* the initial basal levels of aversion, vision, locomotor activity and learning and memory should be checked, and *(iv)* a correlation between the level of drug received in the brain and the behavioral response should be made. When all these precautions are observed, the CPP technique can clearly highlight drug-induced reward from and unrelated artefacts.

Taking together the power of CPP and the ease with which zebrafish can be used for drug or mutant screens, the forward genetic method that we present here should open the way to fruitful systematic searches for genetic or pharmacological modifiers of drug-induced reward.

References

[1] O. V. Anichtchik, J. Kaslin, N. Peitsaro, M. Scheinin, and P. Panula. Neurochemical and behavioural changes in zebrafish danio rerio after systemic administration of 6-hydroxydopamine and 1-methyl-4-phenyl-1,2,3,6-tetrahydropyridine. *J Neurochem*, 88(2):443–53, 2004. 0022-3042 Journal Article.

[2] H. Baier. Zebrafish on the move: towards a behavior-genetic analysis of vertebrate vision. *Current Opinion in Neurobiology*, 10(4):451–455, 2000.

[3] M. T. Bardo, J. K. Rowlett, and M. J. Harris. Conditioned place preference using opiate and stimulant drugs: a meta-analysis. *Neurosci Biobehav Rev*, 19(1):39–51, 1995. 0149-7634 Journal Article Meta-Analysis.

[4] M. Behra, X. Cousin, C. Bertrand, J. L. Vonesch, D. Biellmann, A. Chatonnet, and U. Strahle. Acetylcholinesterase is required for neuronal and muscular development in the zebrafish embryo. *Nat Neurosci*, 5(2):111–8, 2002. 1097-6256 Journal Article.

[5] C. A. Bolanos, G. M. Garmsen, M. A. Clair, and S. A. McDougall. Effects of the kappa-opioid receptor agonist u-50,488 on morphine-induced place preference conditioning in the developing rat. *Eur J Pharmacol*, 317(1):1–8, 1996. 0014-2999 Journal Article.

[6] M.A. Bozarth. *Conditioned place preference: a parametric analysis using systemic heroin injections*. Methods of Assessing the Reinforcing Properties of Abused Drugs. Springer Verlag, New York, 1987.

[7] S. Bretaud, S. Lee, and S. Guo. Sensitivity of zebrafish to environmental toxins implicated in parkinson's disease. *Neurotoxicol Teratol*, 26(6):857–64, 2004. 0892-0362 Journal Article.

[8] D. J. Calcagnetti, B. J. Keck, L. A. Quatrella, and M. D. Schechter. Blockade of cocaine-induced conditioned place preference: relevance to cocaine abuse therapeutics. *Life Sci*, 56(7):475–83, 1995. 0024-3205 Journal Article Review Review, Tutorial.

[9] D. J. Calcagnetti and M. D. Schechter. Reducing the time needed to conduct conditioned place preference testing. *Prog Neuropsychopharmacol Biol Psychiatry*, 16(6):969–76, 1992. 0278-5846 Journal Article.

[10] G.D. Carr, H.C. Fibiger, and A.G. Phillips. *Conditioned place preference as a measure of drug reward*. The Neuropharmacogical Basis of Reward. Clarendon Press, Oxford, 1989.

[11] 3rd Carvan, M. J., E. Loucks, D. N. Weber, and F. E. Williams. Ethanol effects on the developing zebrafish: neurobehavior and skeletal morphogenesis. *Neurotoxicol Teratol*, 26(6):757–68, 2004. 0892-0362 Journal Article.

[12] T. Darland and J. E. Dowling. Behavioral screening for cocaine sensitivity in mutagenized zebrafish. *Proc Natl Acad Sci U S A*, 98(20):11691–6, 2001. 0027-8424 Journal Article.

[13] C. A. Dlugos and R. A. Rabin. Ethanol effects on three strains of zebrafish: model system for genetic investigations. *Pharmacol Biochem Behav*, 74(2):471–80, 2003. 0091-3057 Journal Article.

[14] W. Driever, L. Solnica-Krezel, A. F. Schier, S. C. Neuhauss, J. Malicki, D. L. Stemple, D. Y. Stainier, F. Zwartkruis, S. Abdelilah, Z. Rangini, J. Belak, and C. Boggs. A genetic screen for mutations affecting embryogenesis in zebrafish. *Development*, 123:37–46. 0950-1991 Year = 1996.

[15] R. E. Engeszer, M. J. Ryan, and D. M. Parichy. Learned social preference in zebrafish. *Curr Biol*, 14(10):881–4, 2004. 0960-9822 Journal Article.

[16] R. Gerlai, M. Lahav, S. Guo, and A. Rosenthal. Drinks like a fish: zebra fish (danio rerio) as a behavior genetic model to study alcohol effects. *Pharmacol Biochem Behav*, 67(4):773–82, 2000. 0091-3057 Journal Article.

[17] P. Haffter, M. Granato, M. Brand, M. C. Mullins, M. Hammerschmidt, D. A. Kane, J. Odenthal, F. J. van Eeden, Y. J. Jiang, C. P. Heisenberg, R. N. Kelsh, M. Furutani-Seiki, E. Vogelsang, D. Beuchle, U. Schach, C. Fabian, and C. Nusslein-Volhard. The identification of genes with unique and essential functions in the development of the zebrafish, danio rerio. *Development*, 123:1–36, 1996. 0950-1991 Journal Article.

[18] D. Hall and M. D. Suboski. Visual and olfactory stimuli in learned release of alarm reactions by zebra danio fish (brachydanio rerio). *Neurobiol Learn Mem*, 63(3):229–40, 1995. 1074-7427 Journal Article.

[19] D. C. Hoffman. The use of place conditioning in studying the neuropharmacology of drug reinforcement. *Brain Res Bull*, 23(4-5):373–87, 1989. 0361-9230 Journal Article.

[20] Robert Vincent Hogg. *Introduction to mathematical statistics*. Prentice Hall, Englewood Cliffs, N.J., 5. edition, 1995. Robert V. Hogg, Allen T. Craig.

[21] E. D. Levin and E. Chen. Nicotinic involvement in memory function in zebrafish. *Neurotoxicol Teratol*, 26(6):731–5, 2004. 0892-0362 Journal Article.

[22] B. Lockwood, S. Bjerke, K. Kobayashi, and S. Guo. Acute effects of alcohol on larval zebrafish: a genetic system for large-scale screening. *Pharmacol Biochem Behav*, 77(3):647–54, 2004. 0091-3057 Journal Article.

[23] V. Y. Makhankov, O. Rinner, and S. C. F. Neuhauss. An inexpensive device for non-invasive electroretinography in small aquatic vertebrates. *Journal of Neuroscience Methods*, 135(1-2):205–210, 2004.

[24] T. L. Mark, G. E. Woody, T. Juday, and H. D. Kleber. The economic costs of heroin addiction in the united states. *Drug Alcohol Depend*, 61(2):195–206, 2001. 0376-8716 Journal Article.

[25] M. C. Mullins, M. Hammerschmidt, P. Haffter, and C. Nusslein-Volhard. Large-scale mutagenesis in the zebrafish: in search of genes controlling development in a vertebrate. *Curr Biol*, 4(3):189–202. 0960-9822 Year = 1994.

[26] J. Ninkovic, A. Folchert, V. Y. Makhankov, S. C. F. Neuhauss, S. Sillaber, and L. Bally-Cuif. Genetic identification of ache as a positive modulator of addiction to the psychostimulant d-amphetamine in zebrafish. *submited*, 2005.

[27] G. Pradel, M. Schachner, and R. Schmidt. Inhibition of memory consolidation by antibodies against cell adhesion molecules after active avoidance conditioning in zebrafish. *J Neurobiol*, 39(2):197–206, 1999. 0022-3034 Journal Article.

[28] G. Pradel, R. Schmidt, and M. Schachner. Involvement of l1.1 in memory consolidation after active avoidance conditioning in zebrafish. *J Neurobiol*, 43(4):389–403, 2000. 0022-3034 Journal Article.

[29] M. D. Schechter and D. J. Calcagnetti. Trends in place preference conditioning with a cross-indexed bibliography; 1957-1991. *Neurosci Biobehav Rev*, 17(1):21–41, 1993. 0149-7634 Bibliography Journal Article Review.

[30] E. L. Serra, C. C. Medalha, and R. Mattioli. Natural preference of zebrafish (danio rerio) for a dark environment. *Braz J Med Biol Res*, 32(12):1551–3, 1999. 0100-879x Journal Article.

[31] L. Solnica-Krezel, A. F. Schier, and W. Driever. Efficient recovery of enu-induced mutations from the zebrafish germline. *Genetics*, 136(4):1401–20, 1994. 0016-6731 Journal Article.

[32] H. A. Swain, C. Sigstad, and F. M. Scalzo. Effects of dizocilpine (mk-801) on circling behavior, swimming activity, and place preference in zebrafish (danio rerio). *Neurotoxicol Teratol*, 26(6):725–9, 2004. 0892-0362 Journal Article.

[33] E. R. Turnell, K. D. Mann, G. G. Rosenthal, and G. Gerlach. Mate choice in zebrafish (danio rerio) analyzed with video-stimulus techniques. *Biol Bull*, 205(2):225–6, 2003. 0006-3185 Journal Article.

[34] T. M. Tzschentke. Measuring reward with the conditioned place preference paradigm: a comprehensive review of drug effects, recent progress and new issues. *Prog Neurobiol*, 56(6):613–72, 1998. 0301-0082 Journal Article Review.

[35] T. M. Tzschentke and W. J. Schmidt. Interactions of mk-801 and gyki 52466 with morphine and amphetamine in place preference conditioning and behavioural sensitization. *Behav Brain Res*, 84(1-2):99–107, 1997. 0166-4328 Journal Article.

[36] D. van der Kooy. *Place conditioning: a simple and effective method for assessing the motivational properties of drugs.* Methods of Assessing the Reinforcing Properties of Abused Drugs. Springer Verlag, New York, 1987.

[37] N.M. White, C. Messier, and G.D. Carr. *Operationalizing and measuring the organizing influence of drugs on behavior.* Methods of Assessing the Reinforcing Properties of Abused Drugs. Springer Verlag, New York, 1987.

[38] F. E. Williams, D. White, and W. S. Messer. A simple spatial alternation task for assessing memory function in zebrafish. *Behav Processes*, 58(3):125–132, 2002. 0376-6357 Journal article.

[39] D. Wright, L. B. Rimmer, V. L. Pritchard, J. Krause, and R. K. Butlin. Inter and intra-population variation in shoaling and boldness in the zebrafish (danio rerio). *Naturwissenschaften*, 90(8):374–7, 2003. 0028-1042 Journal Article.

Acknowledgements
We are grateful to S. Hölter, K. Imai, R. Kster, S. Neuhauss, F. Rosa, I. Sillaber, U. Straehle and all our laboratory members for input and support, and to B. Chatterjee and H. Sirowej (Labmed, Dortmund) for help in measuring brain levels of amphetamine in injected fish. We acknowledge funding from a VWStiftung junior group grant and from the EU 6th Framework (contract N LSHC-CT-2003-503466) to LBC.

Legends to Figures

Figure1. Conditioning in the adult zebrafish
A: Flow-chart of the experimental protocol. See explanations in the text. Abbreviations: A-initially non preferred compartment; S-transparent slider; P-initially preferred compartment.**B**: D-amphetamine induces conditioning in adult zebrafish. The mean value of the "change in place preference" for 20 fish is shown after 3 conditioning sessions with saline (left) and D-amphetamine (right). The "change in place preference" (Y axis) is measured as the difference in time spent in the preferred (non-amphetamine-paired) compartment before (PP on day 3) and after drug exposure (CPP on day 9), in percentage of PP.Note that D-amphetamine induces significantly higher change in place preference than saline.

Figure2. Establishment of the experimental set-up to measure D-amphetamine-induced reward in zebrafish adults.
A: Design of the experimental apparatuses used to measure place preference in adult zebrafish. All dimensions are given in centimeters. **B-D**: Dependence of the place preference and conditioned place preference on the tank design. Time in the preferred compartment before (filled symbols) and after D-amphetamine application (open symbols) for N different AB fish is shown for the black-white box (B) and the brown-white box (C). Note that the fish always prefer the darker side but that the percentage of time spent in the black compartment is significantly higher and more coherent than that in the brown compartment. When the brown-white design was used, D-amphetamine was able to reduce the time spent in the preferred compartment for all fish tested (D, stippled bars), with in most cases (75 %) a reversal of the place preference (C). In the case of the black-white design, a reduction in the time spent in the preferred compartment was achieved in only 5 cases out of 10 fish tested (D, gray bars) and a reversal was obtained only with two fish (B). The average change in place preference for the two groups tested (red bars on D) indicate that the use of the brown-white design permits both a higher change and less individual variations (see error bars) than the black-white design. The "change in place preference" (Y axis) is measured as the difference in time spent in the preferred (non-amphetamine-paired) compartment before and after drug exposure, in percentage of PP. **E**: Habituation curve. Percentage of the time spent in the brown compartment versus in the white compartment (see Fig 2A, bottom) in 15-minute measuring intervals over 5 consecutive days (one trial per day). Each bar represents the average of 5 AB fish. The percentage of time spent in the preferred compartment significantly decreases until day 3 and then remains stable at 55-70 %. The percentage of time in the preferred compartment at day 3 (PP after habituation, later referred to as PP) is taken as a basis in all further measurements. **F**: Representative measuring interval.

The percentage of time spent in the preferred compartment for 5 different AB fish after 2 days of accommodation to the experimental apparatus was determined for 4 consecutive 15-minute intervals. Note that the place preference determined for the first 15-minute interval (gray bars) does not significantly differ from the average value for four intervals (i.e. one hour)(stippled bars). Therefore, the first 15-minute interval (but not shorter intervals, see text) fully represents the fish place preference. **G**: Video-recorded routes followed by 3 different AB fish at day 3 (before the drug, upper panels) and at day 10 (after the drug, lower panels).

Figure3. The D-amphetamine administration protocol is a crucial parameter for successful conditioning. **A**: The change in place preference is a linear function of the number of D-amphetamine injections within the range of values used in our experiments. Each point is an average value of N fish tested (see graphic). **B**: CPP (percentage of change in PP, Y axis, left, red curve) and brain amphetamine levels measured by HPLC on brain extracts(MedLab, Dueseldorf, Germany)(Y axis, right, dashed black curve) as a function of the dose of amphetamine injected (X axis). Each measurement of brain amphetamine levels is averaged for 3 fish. Note that the level of amphetamine received in the brain is a linear function of the dose injected within the range of values used in our experiments. Note also that it keeps increasing linearly above the threshold dose inducing maximum CPP, confirming that the decreased CPP above this dose is due to a toxic effect of amphetamine rather than its elimination from the zebrafish organism. **C**: CPP (percentage of change in PP, Y axis, left, red curve) and mortality (percentage of fish dying during the procedure, Y axis, right, dashed black curve) as a function of the dose of amphetamine injected (X axis). Each point is based on the test of at least 15 fish. Our experimental conditions produce a dose/CPP response curve following a Gaussian distribution similar to that observed in mammals[34], where doses above a certain threshold (here 50 μg/g) induce a toxic response.

Figure4. Experimental set-up to measure the aversion and learning and memory of adult zebrafish.
A: The aversion of different zebrafish strains for the non-preferred compartment is given as the difference in the percentage of the time spent in the preferred versus non-preferred compartment of the tank after two days of habituation (Aversion, Av, Y axis). Bars represent an average result for N fish (see bars). **B**: Scheme of the T-maze used to address cognitive ability of zebrafish. All dimensions are given in centimeters. **C**: Learning capacity of wild-type fish (AB strain). The time needed to reach the deep chamber target (gray in B)(Y axis) is given as a function of the trial number (one trial per fish per day). Each point is the average of at least 30 fish, with error bars

indicated. The fish decrease their time upon trial (starting from high values, $\geq$100 s), thus progressively learn to find the target and reach a plateau at comparably low values (20 s) after enough trials. The trial number at the beginning of the plateau (after which point the time needed to find the target varies of less than 10 % upon consecutive trials) gives information about the capacity of the fish to learn.

Figure5. Lowered D-amphetamine-induced CPP in *ache*^{sb55}/+ heterozygotes detected in the CPP experimental set-up. A: Altered brain levels of acetylcholine (ACh) in *ache*^{sb55}/+ heterozygotes (left) compared to their wild-type siblings (+/+, middle) or AB controls (right, determined using Amplex Red Acetylcholine/Acetylcholinesterase Assay Kit (Molecular Probes, Eugen, USA) according to the manufacturer's instructions). Each value is an average of N fish (see bars). The brain levels of ACh are increased by 40 % in *ache*^{sb55}/+ heterozygotes compared to their wild-type siblings, which do not differ from AB controls. **B-C**: Amphetamine-induced CPP in *ache*^{sb55}/+ heterozygotes (left) compared to their wild-type siblings (+/+, middle) and AB controls (right) before (**B**) and after arcsine (**C**) transformation. The change in PP (Y axis) shown on B is measured as in Fig 2F, and each value is an average of N fish (see bars). Amphetamine-induced CPP is significantly decreased (1.6 times) in *ache*^{sb55}/+ heterozygotes compared to their wild-type siblings, which do not differ from AB controls. **D**: Compared dose-response curve in *ache*^{sb55}/+ heterozygotes (dashed line) and AB controls (red line). The CPP (percentage of change in PP, Y axis) is represented as a function of the dose of amphetamine injected (X axis). Each point is the average of at least 15 fish. *ache*^{sb55}/+ heterozygotes respond to amphetamine following a Gaussian curve of smaller amplitude than that of wild-type fish but with the same center position 65.3 for wild-type fish versus 62.3 for *ache*^{sb55}/+ fish. Thus, the dose of 40 μg/g amphetamine selected as optimal for wild-type fish is also optimal in *ache*^{sb55}/+ heterozygotes, which respond with lower CPP than wild-type to the complete range of amphetamine doses tested.

Figure6. Strain-induced variations in the place preference (PP) and conditioned place preference (CPP). A-D: Place preference for the most widely used zebrafish strains. Distribution of the percentage of time in the brown compartment of the experimental apparatus (see Fig 2A, bottom panel) is shown for four different strains: AB strain bred in our fish facility since over 20 generations (A), ABO background derived from ABO strain and crossed to our AB background for 2 generations (B), Tü background (C) and AB/Tü background obtained by crossing AB fish into the Tü background (D). Distribution for all four strains fits the Gauss model (equation: $y=y_0 + \frac{1}{w\sqrt{\pi/2}} \cdot Ae^{-2\cdot(\frac{x-xc}{w})^2}$) and the center of the curve is highlighted in red. Although,

based on the center of the Gauss distribution, there is a tendency for fish to prefer the darker environment, note that Tü fish do not show preference to the brown compartment ($y_c = 46\,\%$). Thus, it appears necessary to specifically design the best experimental apparatus for each strain used in order to address addiction as well as aversion. **E-G**: CPP induced by the intra-peritoneal administration of $40\,\mu$g/g of D-amphetamine paired with the non-preferred compartment for three different fish strains (same as in A-C). The "change in place preference" (Y axis) is measured as the difference in time spent in the preferred (non-amphetamine-paired) compartment before and after drug exposure, in percentage of PP. Each bar represents an individual fish to give an impression of the variability in the response, while red bars are an average for 20 fish. The majority of amphetamine-injected fish significantly reduce their place preference to choose the amphetamine-paired compartment after drug exposure for all strains, although strain variations are noticeable. **H**: Saline (110 mM NaCl) does not induce CPP. AB fish were injected with saline only, alternatively paired with non-preferred and preferred compartments. Fish injected with saline do not change their PP.

Figure7. The transmission of a mutant phenotype follows a Mendelian distribution for dominant mutation in the polymorphic AB/Tü background. The proportion of mutant phenotypes in the F_2 (left N=25) and F_3 (right N=98) generations is showed for the dne^{3265} mutant recovered in screen I (unpublished). Note that this proportion does not significantly change despite the change in genetic background. We counted a fish as WT when its "percentage of change" was higher than 5 % and as mutant when it was null or negative D-amphetamine administration. If the percentage of change was between 0 and 5 %, the fish were not considered for further analysis.

Tables

Complex behavior	Paradigm	Reference
Addiction	Conditioned place preference	Gerlai *et al.*, 2000[16] Ninkovic *et al.*, 2005[26]
Anxiety/ Exploratory behavior	Locomotor activity	Gerlai *et al.*, 2000[16]
	Group preference	Gerlai *et al.*, 2000[16]
	Place preference	Serra *et al.*, 1999[30] Ninkovic *et al.*, 2005[26]
	Light/dark preference test	Gerlai *et al.*, 2000[16]
	Time in enriched chamber of T-maze	Swain *et al.*, 2004[32]
	Exit latency test	Serra *et al.*, 1999[30]
Aggression	Mirror image test	Gerlai *et al.*, 2000[16]
	Pigment response	Gerlai *et al.*, 2000[16]
	Startle reaction	Dlugos and Rabin, 2003[13]
Memory	T-Maze	Darland and Dowling, 2001[12] Swain *et al.*, 2004[32] Ninkovic *et al.*, 2005[26]
	Spatial alternation learning and memory	Williams *et al.*, 2002[38] Carvan *et al.*, 2004[11]
	Delayed spatial alternation	Levin and Chen, 2004[21]
	Active avoidance conditioning	Pradel *et al.*, 1999;[27] Pradel *et al.*, 2000[28]
	Learned alarm reactions	Hall and Suboski, 1995[18]
Locomotor activity	Number of lines crossed	Gerlai *et al.*, 2000[16] Bretaud *et al.*, 2004[7] Swain *et al.*, 2004 [32]
	Total distance moved	Anichtchik *et al.*, 2004[1]
	Mean velocity	Anichtchik *et al.*, 2004[1]
	Turning angle	Anichtchik *et al.*, 2004[1]
Social preference	Group preference	Gerlai et al., 2000 [16]
	Shoaling	Wright *et al.*, 2003[39] Engeszer *et al.*, 2004[15]
	Nearest neighbor distance	Dlugos and Rabin, 2003[13]
	Area occupied	Dlugos and Rabin, 2003[13]
Mate choice	Video-stimulus techniques	Turnell *et al.*, 2003[33]
Boldness/ Antipredatory behavior	Predator simulation	Gerlai *et al.*, 2000[16] Wright *et al.*, 2003[39]

Table 1
Behavioral paradigms addressing complex behavior in zebrafish

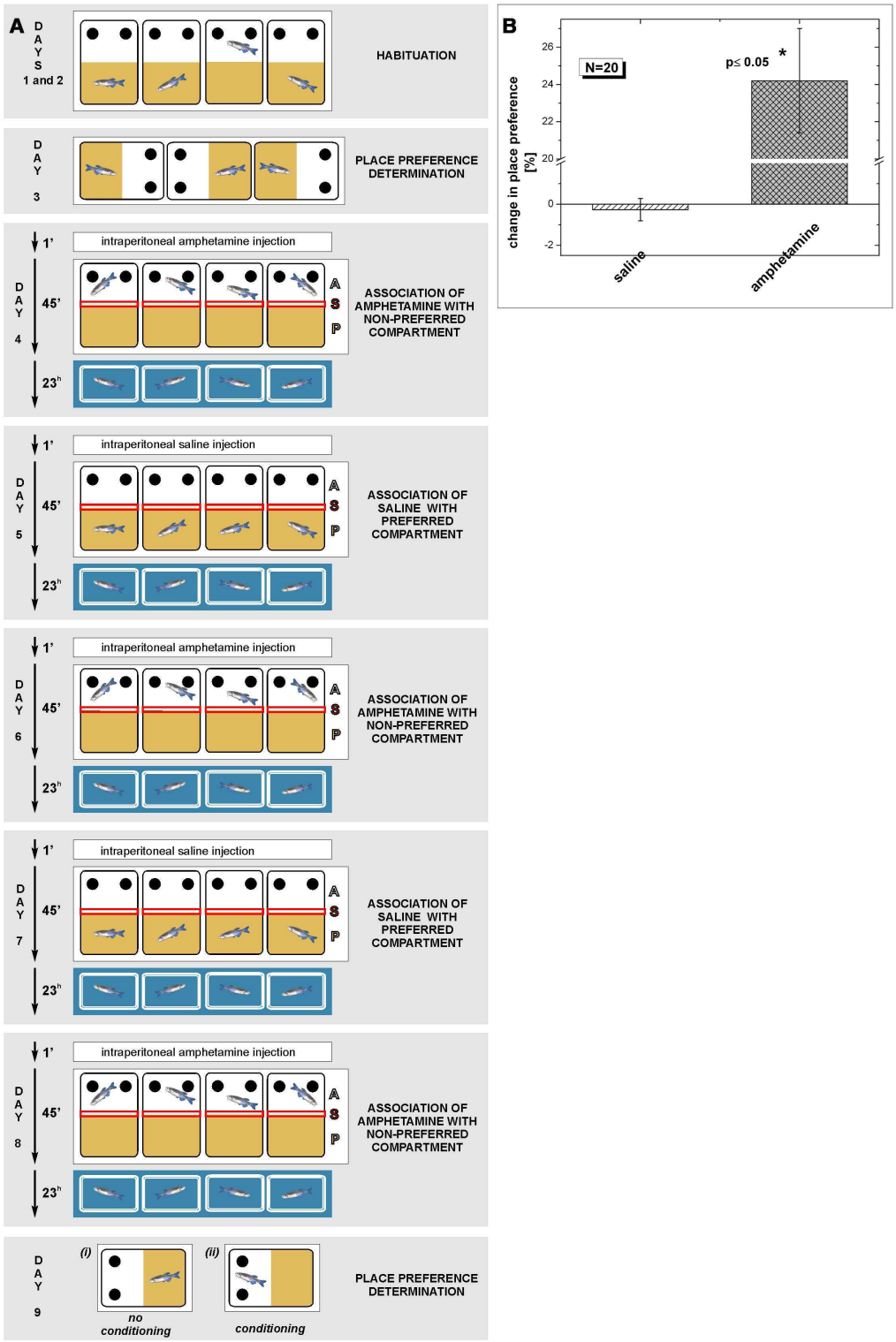

Ninkovic and Bally-Cuif, Fig1

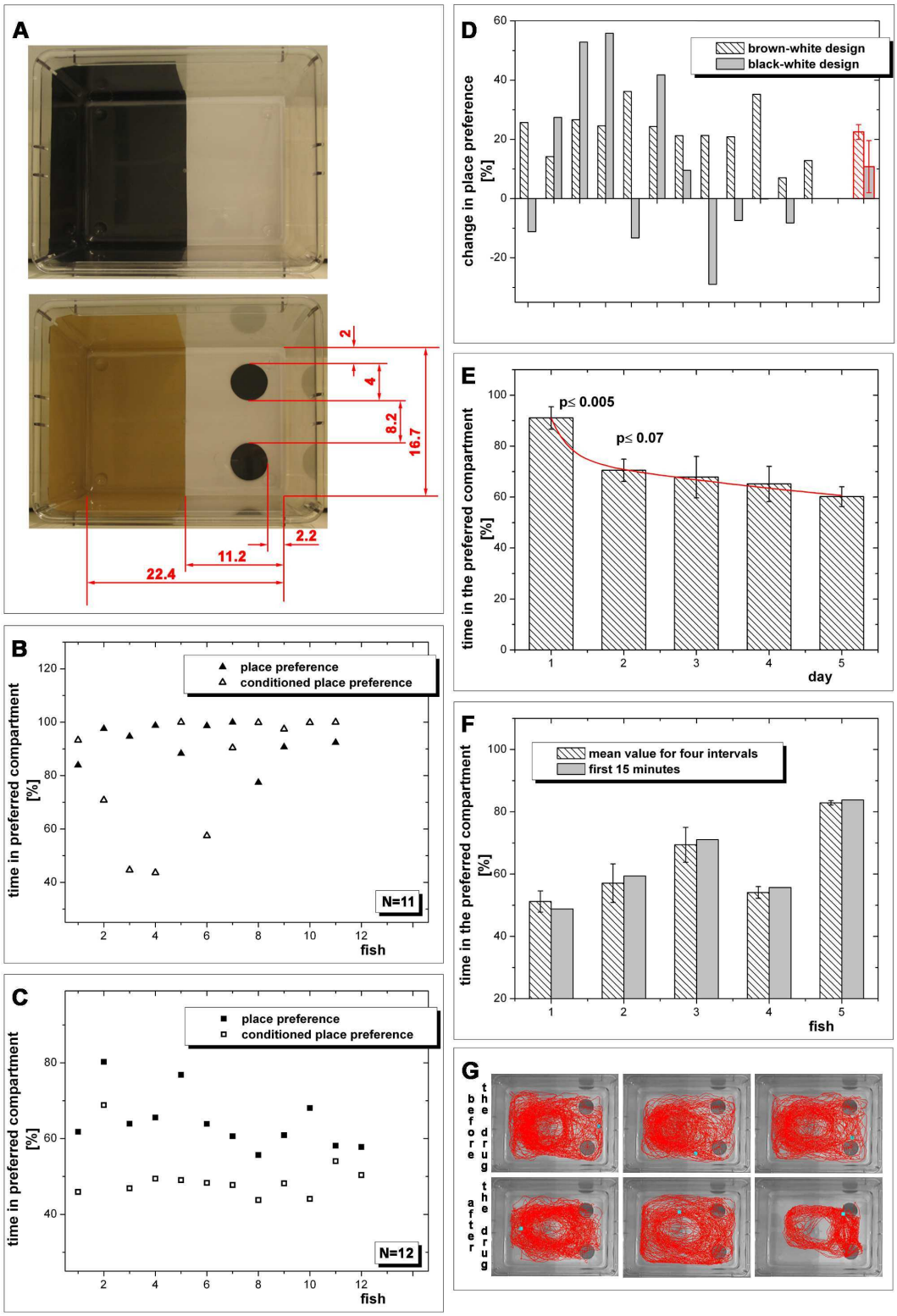

Ninkovic and Bally-Cuif, Fig2

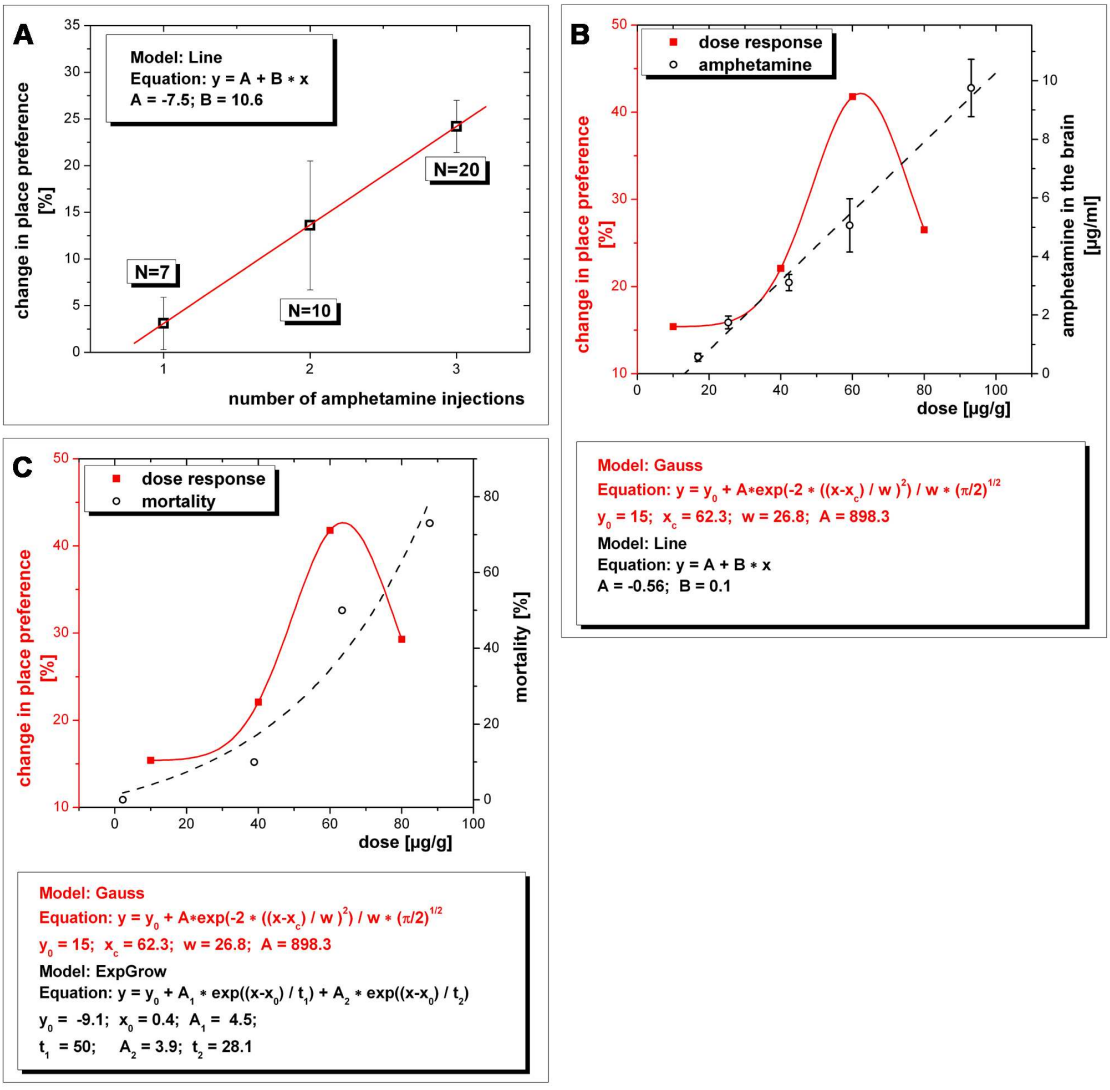

Ninkovic and Bally-Cuif, Fig3

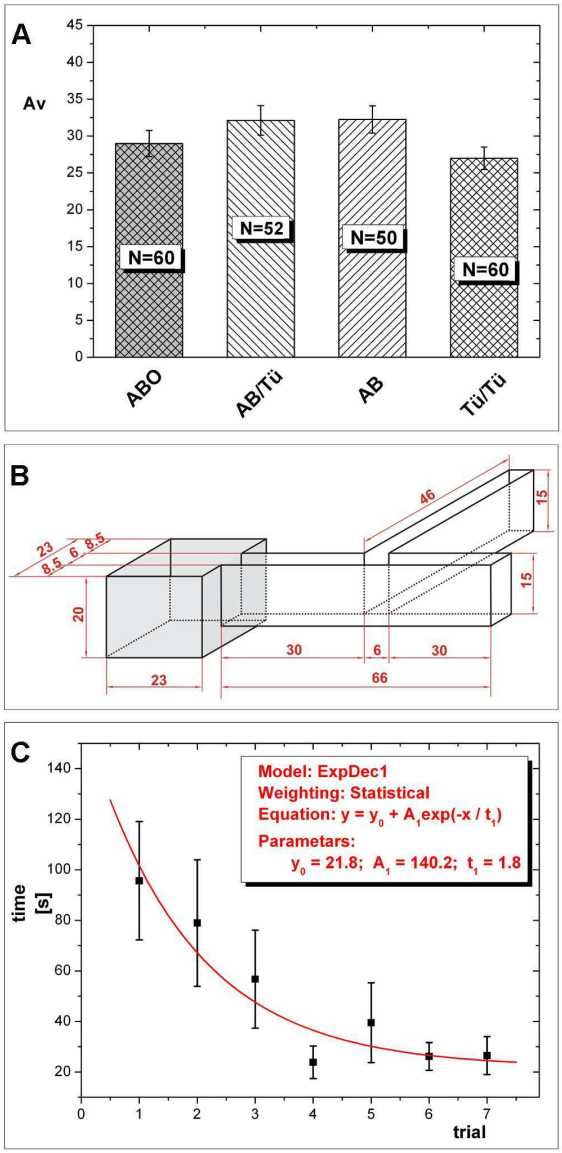

Ninkovic and Bally-Cuif, Fig4

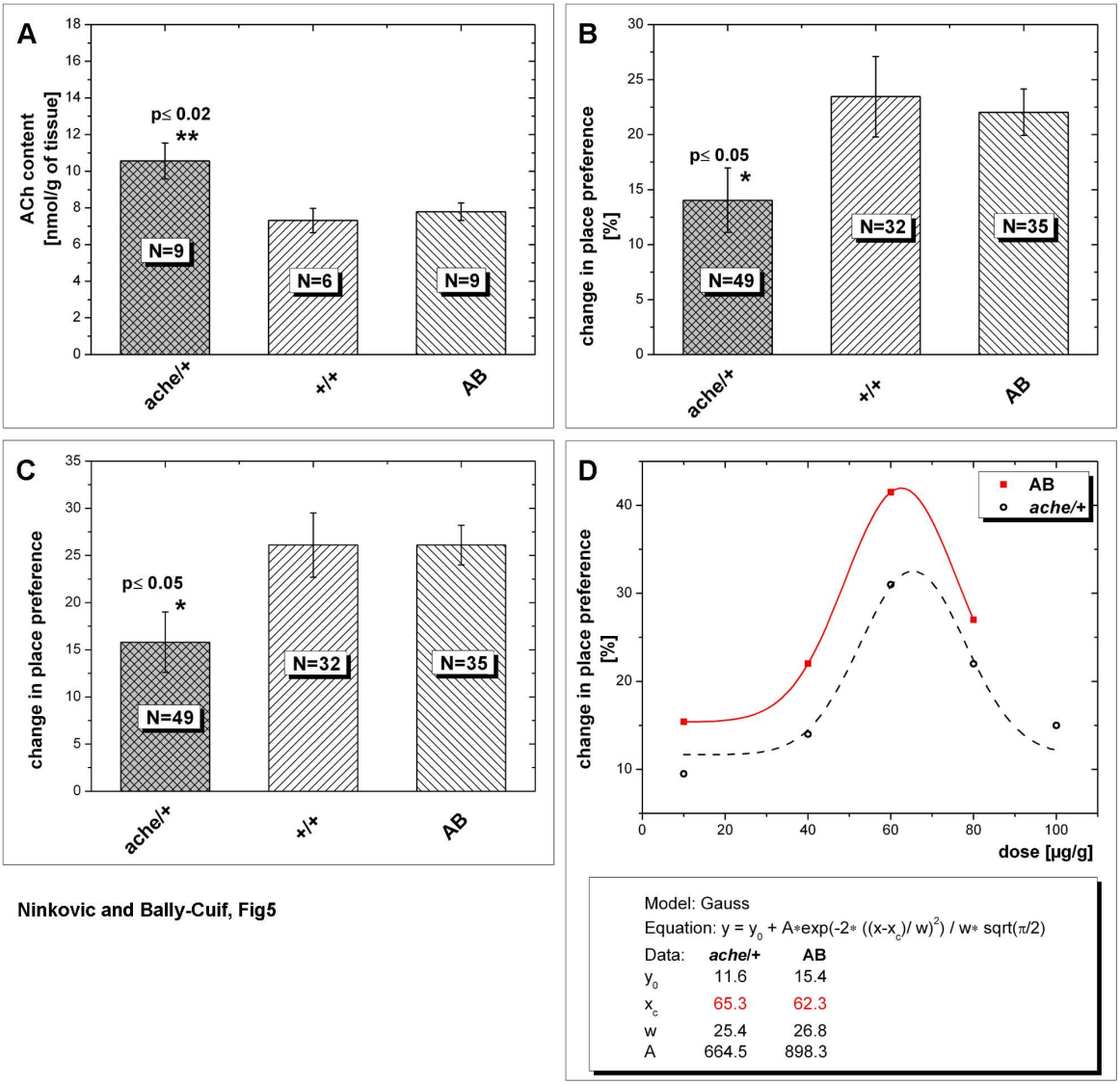

Ninkovic and Bally-Cuif, Fig5

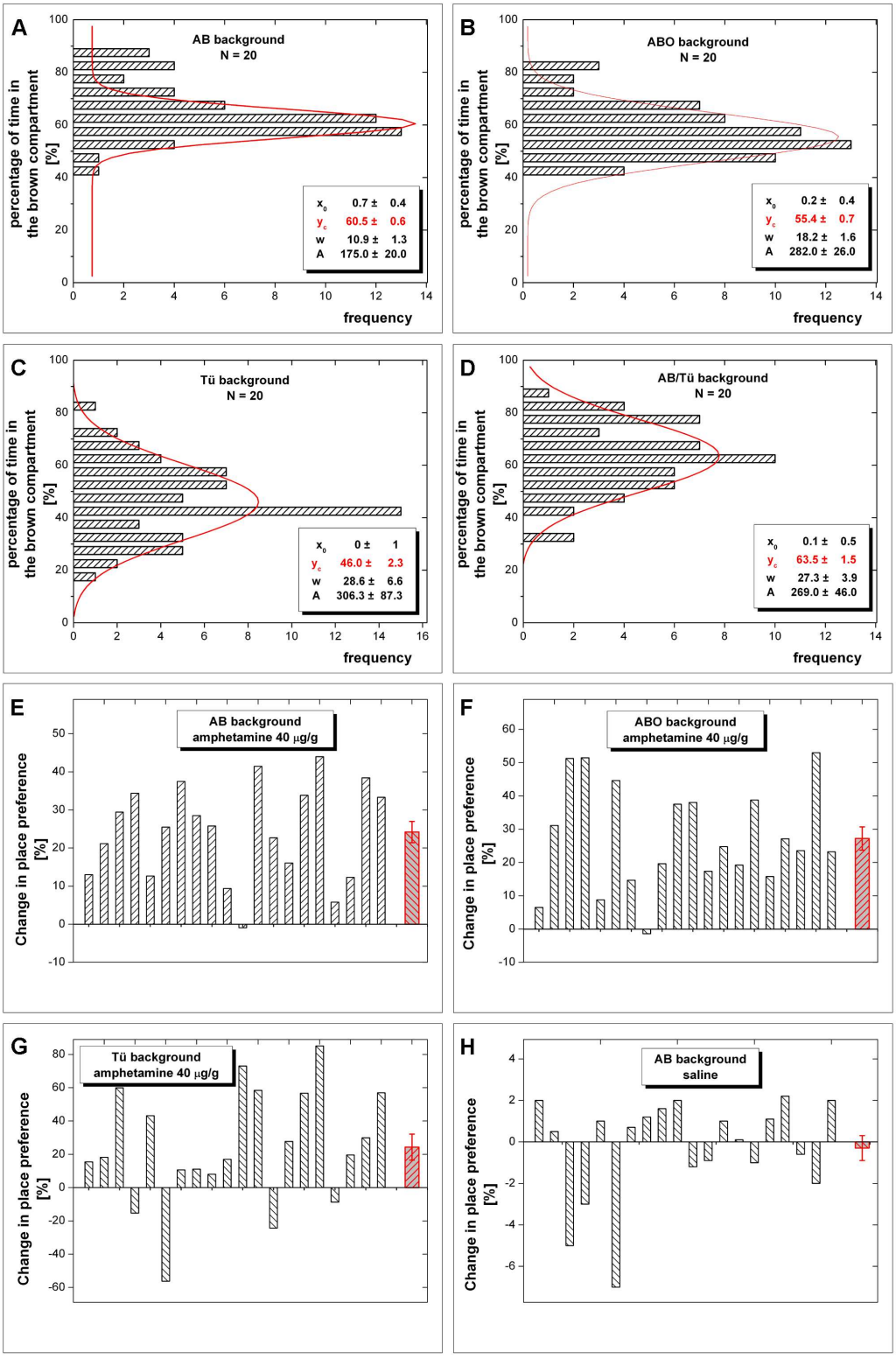

Ninkovic and Bally-Cuif, Fig6

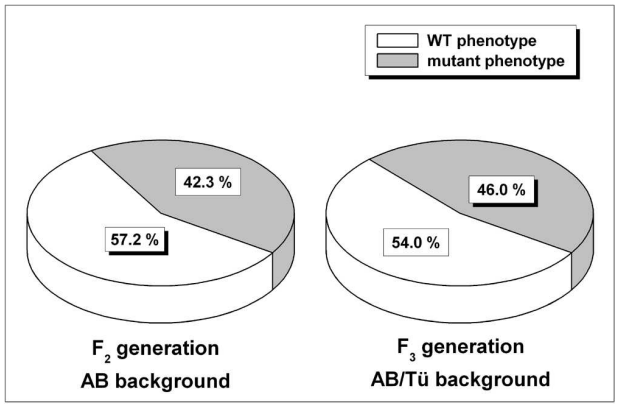

Ninkovic and Bally-Cuif, Fig7

Appendix C

Article in *Journal of Neurobiology*

Genetic identification of AChE as a positive modulator of addiction to the psychostimulant D-amphetamine in zebrafish

Jovica Ninković, Anja Folchert, Yuri V. Makhankov, Stephan C.F. Neuhauss, Inge Silaber, Uwe Straehle and Laure Bally-Cuif

Journal of Neurobiology, *in press*

Genetic identification of AChE as a positive modulator of addiction to the psychostimulant D-amphetamine in zebrafish

Running title: AChE and amphetamine-induced reward in zebrafish

Jovica Ninkovic[1], Anja Folchert[1], Yuri V. Makhankov[2], Stephan C.F. Neuhauss[2], Inge Sillaber[3], Uwe Straehle[4] and Laure Bally-Cuif[1,*]

[1] Zebrafish Neurogenetics Junior Research group, Institute of Virology, Technical University-Munich, Trogerstrasse 4b, D-81675, Munich, Germany and GSF-National Research Center for Environment and Health, Department Zebrafish Neurogenetics, Institute of Developmental Genetics, Ingolstaedter Landstrasse 1, D-85764 Neuherberg, Germany; [2] Brain Research Institute, University of Zurich and ETH Zurich, Winterthurerstrasse 190, CH-8057 Zurich, Switzerland; [3] MPI for Psychiatry, Kraepelinstrasse 2-8, D-80804 Muenchen Germany; [4] University of Heidelberg and Institute of Toxicology and Genetics, Forschungszentrum Karlsruhe, Postfach 3640, D-76021 Karlsruhe, Germany

* **author for correspondence at** email: bally@gsf.de; tel: (49).89.3187.3562; fax: (49).89.3187.3099; GSF-National Research Center for Environment and Health, Department Zebrafish Neurogenetics, Institute of Developmental Genetics, Ingolstaedter Landstrasse 1, D-85764 Neuherberg, Germany

Acknowledgements

We are grateful to T. Becker, C. Goridis, S. Hölter and C. Stigloher for their critical reading of the manuscript, to S. Hölter, K. Imai, R. Köster, F. Rosa and all our laboratory members for input and support, and to B. Chatterjee and H. Sirowej (Labmed, Dortmund) for help in measuring brain levels of amphetamine in injected fish. We acknowledge funding from a VWStiftung junior group grant to LBC and from the EU 6th Framework to LBC, US and SCFN (contract N° LSHC-CT-2003-503466). Additional support from the ETH commision (0-20941-01) to YVM and the Schweizer Nationalfonds (PP00A-68868) are appreciated.

Abstract

Addiction is a complex maladaptive behavior involving alterations in several neurotransmitter networks. In mammals, psychostimulants trigger elevated extracellular levels of dopamine, which can be modulated by central cholinergic transmission. Which elements of the cholinergic system might be targeted for drug addiction therapies remains unknown. The rewarding properties of drugs of abuse are central for the development of addictive behavior and are most commonly measured by means of the conditioned place preference (CPP) paradigm. We demonstrate here that adult zebrafish show robust CPP induced by the psychostimulant D-amphetamine. We further show that this behavior is dramatically reduced upon genetic impairment of acetylcholinesterase (AChE) function in *ache*/+ mutants, without involvement of concomitant defects in exploratory activity, learning and visual performance. Our observations demonstrate that the cholinergic system modulates drug-induced reward in zebrafish, and identify genetically AChE as a promising target for systemic therapies against addiction to psychostimulants. More generally, they validate the zebrafish model to study the effect of developmental mutations on the molecular neurobiology of addiction in vertebrates.

Keywords: zebrafish, reward, acetylcholinesterase, amphetamine, conditioned place preference, behavior.

Introduction

Addiction, the uncontrollable compulsion to take drugs in spite of their negative effect on normal brain function, is a widespread and costly brain disorder in modern societies. Yet, its neural mechanisms remain incompletely understood, and pharmacological treatments, if available, are in most cases ineffective.

The mesocorticolimbic dopamine (DA) system, originating in the midbrain Ventral Tegmental Area (VTA) and innervating the Nucleus Accumbens (NAc) in the ventral striatum, was directly implicated in the rewarding effects of most drugs of abuse in higher vertebrates (Everitt and Wolf, 2002; Laakso et al., 2002; White, 2002; Wise, 2002). Indeed, psychostimulants increase extracellular levels of DA in the NAc, e.g. by blocking the DA transporter (Amara and Sonders, 1998; Jones et al., 1998; Gainetdinov et al., 2002; Saal et al., 2003), thereby affecting the homeostasis of the brain reward system. However, addiction is an intricately complex dysfunction of the reward pathway and likely involves a plethora of neurotransmitter responses, themselves dependent on parameters that can vary upon drug administration, such as progressive neuroadaptative mechanisms. To date, additional monoamine systems (norepinephrine, serotonin) and modulatory pathways (acetylcholine -ACh-, GABA, glutamate) have been proposed to contribute to the manifestation of the addictive state, by sharing molecular components with the DA system, by influencing the activity of VTA or NAc neurons (Gaspar et al., 2003; Auclair et al., 2004; Kelley, 2004), or by as yet unresolved mechanisms.

Recent emphasis was placed on the cholinergic system. In several instances, blocking muscarinic cholinergic transmission in rodents increases response to psychostimulants in the self-administration or conditioned place preference (CPP) tests (Gerber et al., 2001; Ichikawa et al., 2002), paradigms classically applied to evaluate addictive behavior. The NAc is densely innervated by cholinergic interneurons; the activity of these neurons is decreased by DA release (Alcantara et al., 2003) and their ablation increases the sensitivity to psychostimulants and the reinforcing effects of cocaine

(Hikida et al., 2001). Further, other components of the cholinergic system, like M5 muscarinic receptors on VTA DA neurons or nicotinic ACh receptors on DA terminals in the striatum, are implicated in the regulation of addictive behavior (see (Tzschentke, 1998). While most studies agree that cholinergic activity can modulate DA transmission, thereby the propensity for addiction, a reliable pharmacological target of this system for drug addiction therapy has to be determined. Using pharmacological inhibitors, (Hikida et al., 2003) suggested that inhibiting acetylcholinesterase (AChE) activity, which terminates ACh action at the synapse, can block cocaine- and morphine-induced CPP in the mouse. Thus AChE inhibitors might be promising therapeutic agents, although their specificity and range of efficiency remain to be determined.

Here we address the relevance and generality of AChE inhibition on drug-induced behavior. The zebrafish, often proposed as an alternative to mammalian models, is increasingly used as a new genetic system in social behavior studies, because of its amenability to large-scale genetic screens (Gerlai et al., 2000; Darland and Dowling, 2001; Guo, 2004; Lockwood et al., 2004). We demonstrate that adult zebrafish show a clear CPP induced by a widely used psychostimulant, D-amphetamine, and that this effect is significantly attenuated upon genetic impairment of AChE activity in *ache*^{sb55}/+ mutants (Behra et al., 2002). Our results provide the first genetic demonstration that AChE is a promising target for therapeutic approaches to addiction, and validate the zebrafish to study the consequences of developmental mutations and the neuronal pathways underlying this condition in vertebrates. The experimental paradigms developed here are the first sufficiently robust to use the excellent genetic model zebrafish to conclusively screen for mutations affecting reward.

Methods

Animal care and maintenance

Adult zebrafish were kept in the fish facility, as previously described (Kimmel et al., 1995). At least two days before each assay, the fish were moved to an

isolated room under maintenance conditions and feeding schedule identical to the fish facility (14hr/10hr day/light cycle, two feedings per day at 8:00 am and 2:00 pm –except in the case of learning tests, see below-, water temperature 28°C). Thus, we kept environmental variance at a minimum for all behavioral assays. The AB strain was bred in our fish facility since more than 20 generations. *ache*^{sb55}/+ (Behra et al., 2002), initially on ABO background, were crossed for at least three generations to our AB strain before all experiments. They were identified in random brother-sister crossing giving rise to 25% *ache*^{sb55}/*ache*^{sb55} immobile embryos, as described (Behra et al., 2002). All experiments reported in this paper were done on 3 to 6 months-old females (however we observed no difference in the behavior of males compared to females) (not shown). Care was taken to always test the same fish at the same time of the day over the successive days of each experiment.

Place preference determination

The testing apparatus is a 3-liter, rectangular tank containing 2 liters of water and placed in an isolated cabinet with top illumination. The water level was kept to 10 cm from the tank bottom to minimize stress. Distinct visual cues divide the experimental tank into two halves: a dark half colored in brown and a light half colored in white with two frightening, black circles placed at the bottom of the tank. After an initial introduction in the testing apparatus, each fish was separately accommodated to the new environment for two entire days (days 1 and 2) and was afterwards recorded in one 15-minute trial on day 3 using Noldus Ethovision v.2.3 system (Noldus Information Technology, Netherlands). The preferred compartment was defined as the compartment in which a fish spends most time on day 3, and the basal level of place preference (PPi), serving as a basis for all further comparisons, is calculated as the percentage of time that the fish spends in the preferred compartment during the 15-minute recording on day 3. PPi levels between *ache*^{sb55}/+ and their wild-type siblings were measured in the set-up described above and compared using independent samples Student t-test; all graphics were generated using Origin v.7 (OriginLab, Northampton, USA).

D-amphetamine-induced conditioned place preference

After place preference determination (day 3), each fish was weighed (typically, weights varied between 0.5 and 3g per fish) then intraperitoneally injected with D-amphetamine (40 µg of D-amphetamine (Sigma-Aldrich A0922, Germany) and methylene-blue as a tracer (3 µg per gram of fish in 110 mM NaCl, if not otherwise indicated) and immediately confined to the non-preferred compartment for 45 minutes (day 4). Restriction to this compartment was achieved using a transparent slider such that visual contact with the preferred compartment was possible, to minimize the difference between the conditioning and the measuring tank. The experimental tank and conditions were otherwise identical to the ones used for place preference determination, and each fish was tested alone. After 45 minutes, the fish was removed from the experimental tank and kept in a 1.5-liter tank on a color-neutral background. On day 5, the fish was injected intraperitoneally with a saline solution (3 µg of methylene-blue per gram of fish in 110 mM NaCl), then restricted for 45 minutes into the preferred compartment. Between each injection session, the experimental tank was cleaned with 70 % ethanol and rinsed with fish facility water. The D-amphetamine treatment was repeated on days 6 and 8 and the saline treatment on day 7. Place preference was then measured again on day 9. Repeating the saline treatment on day 9, followed by measurement of place preference on day 10, lead to identical results (not shown). Unless otherwise specified, conditioning was estimated as the change in place preference before and after treatment, relative to the place preference before treatment, as follows: % of change = 100 x (PPi-PPf)/PPi, where % of change is the relative change in place preference, PPi is the percentage of time spent in the initially preferred compartment (measured at day 3, see above), and PPf the percentage of time spent in this same compartment after treatment (measured at day 9 or 10). For percentages outside the range 30-70%-, the calculation of % of change was followed by arcsine transformation (as recommended in (Hogg, 1995)) (Fig.1C, 2C). In all experiments, a comparison with scoring the percentage of change in absolute values (PPi-PPf) was performed, leading to identical conclusions (see Supplemental Figures 1B, 2, and see Figure 3B,C). The significance of all comparisons was established using independent samples Student t-test and all graphics were generated using Origin v.7 (OriginLab, Northampton, USA).

All manipulations were performed according to authorization N°AkZ 209.1/211-2531-20/02 from the Government of Upper Bavaria and the German Institute for Drug Control (Bundesopiumstelle).

Learning and memory tests

Learning and memory tests were conducted in a T-maze, following a procedure modified from Darland and Dowling (Darland and Dowling, 2001). The experimental tank was composed of one long (46cm) and two equally short (30 cm) arms. All arms were 6 cm wide and 15 cm deep with a water level of at least 10 cm. One of the two short arms is opening into a deep (20 cm) square tank (23cm x 23 cm) with black walls and artificial grass to offer a favorable habitat for the zebrafish. Most of the fish tested spent the majority of their time in this compartment once they found it. Two days before testing, a group of 10 fish was restricted with the transparent slider to the long arm of the T-maze for one hour per day to accommodate to the testing environment. After accommodation, each fish was placed alone at the beginning of the long arm and the time needed to find the deep compartment was recorded. After reaching the deep compartment, the fish got there their daily feeding. Each fish was tested once a day. We considered that a fish has learned the task when its time to find the target compartment varies of less than 10 % upon consecutive trials. The learning ability of fish with different genotypes were compared using independent samples t-test and all graphics were generated using Origin v.7 (OriginLab, Northampton, USA).

Brain D-amphetamine level

The brains were removed on ice, weighed and homogenized in 100 µl of plasma-spiegel solution (0.12 % H_3PO_4, pH 3.5 adjusted with 6M NaOH). Amphetamine extraction and determination of amphetamine concentration were carried out according to an HPLC protocol developed by Labmed (Dortmund, Germany).

Acetylcholinesterase (AChE) and Acetylcholine (ACh) assays

The brains were removed on ice and weighed. Achetylcholinesterase activity of brain extracts was determinated according to Ellman et al. (Ellman et al.,

1961) and measured as the amount of ACh that is broken down by AChE per gram of brain tissue per time unit. ACh concentration in brain extracts was measured with the Amplex Red Acetylcholine/Acetylcholinesterase Assay Kit (Molecular Probes, Eugen, USA) according to the manufacturer's instructions.

Electroretinography (ERG)

ERGs were performed on adult zebrafish as previously described (Makhankov et al., 2004). Briefly, the recording electrode was positioned on the surface of the cornea. A chlorodized silver wire was fixed on the opposite nostril as a reference electrode. To ensure oxygenation of the animal, MESAB medium (Sigma–Aldrich, Buchs, Switzerland) was flushed by gravity forces over the gills by a plastic tube inserted into the mouth. The fish were dark-adapted for at least 30 min before mounting the electrode under dim red light. Before exposure to light, they were adapted in complete darkness for at least 15 min. A 1-sec light stimulus was chosen with an interstimulus interval of 10 sec. Illumination was increased in 1.0 log unit steps over the range from −5 log unit (0.5 cd/m^2) to −1 log unit (5 000 cd/m^2). Unattenuated light intensity was measured at the diffuser surface of the light guide over the fish head by a light meter (Tekronix J17, Texas Instruments, USA). ERG responses were averaged 3-7 times depending on the signal-to-noise ratio. Statistical analysis was performed using SPSS v.11 (SPSS Inc., Chicago, USA).

Results

Amphetamine-conditioned place preference in zebrafish

Amphetamine can trigger a conditioned change in place preference in higher vertebrates, but has only been tested in teleosts (goldfish) in an associative paradigm (Lett and Grant, 1989). Thus we first invested in setting-up a reliable amphetamine-conditioned CPP test in zebrafish. Our test is based on remembering the association of the rewarding effect of amphetamine with an initially non-preferred environment, recognizable by visual cues. To establish the ideal visual parameters, we built on previous reports demonstrating place preference (PP) of adult zebrafish for one side of

a two-color tank (Serra et al., 1999; Gerlai et al., 2000; Darland and Dowling, 2001).

Reliability and robustness of a CPP test implies to meet a number of requirements. First, before being confronted with the drug, the animal has to habituate to the test conditions until its place preference to one side of the tank becomes stable. This level (PP after habituation, or PPi) is the only reliable base to measure changes in PP following administration of the drug. Second, a two-color compartment has to be developed where PPi is not excessive so as to permit reversal upon administration of an optimal dose of drug. In higher vertebrates, conditions where PPi to one side approaches 55-65% work best (Tzschentke, 1998). Third, the dose of drug has to be determined as the best compromise between a high response and an acceptable rate of animal survival, as determined on a dose/response-survival curve. In addition, to make sure that the drug acts via its impairment of brain function, one has to ascertain that the level of drug received in the brain is in proportion of the dose administered.

Because previous studies did not agree on the preference of zebrafish adults for brightness or darkness (Serra et al., 1999; Gerlai et al., 2000; Darland and Dowling, 2001), we first had to find appropriate conditions yielding reliable results. We thus designed a number of two-color 3-liter tanks and tested more than 20 wild-type adults in each. We selected a light brown versus white contrast (Fig.1A), where a test on 50 wild-type adults demonstrated that more than 95% of these fish spend between 55 and 70% of their time in the brown side following two days of habituation (on days 1 and 2) (not shown). We further observed that the percentage of time spent in this preferred compartment remained stable after day 3 (Fig.1B). We thus measured PP at day 3 as PPi and started our conditioning procedure at day 4. In such conditions, more than 90% of the animals tested significantly reverted their place preference following three intra-peritoneal administrations of 10 μg amphetamine per gram of body weight (on days 3, 5 and 7), each time paired with 45 minutes in the non-preferred compartment and separated by daily injections of saline (on days 4 and 6) paired with the preferred compartment (Supplemental Figure 1A top panel). Control fish injected every day with a

saline solution alternatively paired with the white and brown compartments failed to revert their place preference (Supplemental Figure 1A bottom panel).

Next, we determined the optimal dose of drug permitting robust CPP at acceptable toxicity. In a dose-response study, we observed that doses of amphetamine below 5 μg/g did not lead to a reproducible change in place preference, while doses above 50 μg/g progressively reduced this change due to immobilization and stress of the animal and/or death (Fig.1D, each point > 15 fish). Similar observations have been reported in mammals (Tzschentke, 1998). Thus, we selected a dose of 40 μg/g, which triggers robust change in place preference but low mortality (Fig.1D). We further verified that at this value, the dose of amphetamine received in the brain, measured by gas-HPLC on brain extracts within 10 minutes after injection, was a linear function of the dose injected (Fig.1E, each point = 3 fish). In these conditions and using the experimental paradigm described above, 95% of wild-type fish significantly revert their place preference when administered with 40 μg/g amphetamine (n=22) (Fig.1C), while 97% of control fish (i.e. injected only with a saline solution) fail to do so (n=21) ($p<0.001$) (Fig.1C) (see also Supplemental Figure 1).

Reduced amphetamine-induced CPP in zebrafish AChE mutants

In mammals, lowered brain ACh signaling has been associated with an increased propensity to get addicted to psychostimulants (Gerber et al., 2001; Ichikawa et al., 2002). To determine whether the cholinergic system was involved in a similar regulatory pathway in zebrafish, we measured the sensitivity of zebrafish with genetically impaired ACh metabolism towards the rewarding effects of amphetamine. Zebrafish *ache*^{sb55} mutants harbor a point mutation in the AChE-encoding gene, resulting in the production of a non-functional AChE enzyme (Behra et al., 2002). Because AChE is the only ACh-degrading enzyme in zebrafish, *ache*^{sb55}/*ache*^{sb55} homozygous embryos are completely deficient in ACh hydrolysis and die of progressive paralysis at early larval stages (Behra et al., 2002). *ache*^{sb55}/+ heterozygotes, however, reach adulthood without obvious locomotor or any morphological defects (not shown) (n>50). We found that AChE activity was decreased by nearly 50% in

the brain of *ache*^{sb55}/+ heterozygotes compared to their wild-type siblings or our AB control strain (Fig.2A) (n=9, p<=0.05), resulting in a 1.4-fold increase in their level of brain ACh (Fig.2B) (n=9, p<=0.02). Immunohistochemical analyses failed to reveal defects in the location and organization of dopaminergic, serotonergic and cholinesterase-positive brain neuronal clusters in *ache*^{sb55}/+ heterozygotes, suggesting that, in spite of their perturbed levels of AChE and ACh, these fish do not suffer from grossly abnormal neuroanatomy (not shown). These results suggest that *ache*^{sb55}/+ mutants are a valuable genetic model to test the effects of increased brain levels of ACh.

To measure the impact of lowered AChE activity on drug-induced effects, we assessed the behavior of *ache*^{sb55}/+ adults upon administration of 40 μg/g amphetamine in the conditions described above. We found that *ache*^{sb55}/+ heterozygotes exhibit a significantly lowered change in place preference compared to their wild-type siblings: while the average change in siblings in 24%, it is 14% in *ache*^{sb55}/+, representing a 46% reduction in the response (Fig.2C, red crossed bar) (n=49, p<=0.05) (see also Supplemental Figure 2). Again, siblings do not differ from controls of the wild-type AB strain (Fig.2C, red stippled bars), and *ache*^{sb55}/+ fish injected with saline, like AB fish, fail to modify their place preference (Fig.2C, black bars). A dose-response curve confirmed that the dose of amphetamine administered (40 μg/g) was also triggering the most robust rewarding effects tolerable for a reasonable survival rate in *ache*^{sb55}/+ fish (Fig.2D) (each point >= 15 fish; note that *ache*^{sb55}/+ fish respond with a significantly lower CPP than their siblings over a range of doses reaching at least 60 μg/g). We conclude that the cholinergic system strongly modulates addictive behavior in zebrafish.

Genetic impairment of AChE function is not associated with an abnormally high initial place preference, with lowered memory or with vision defects

Three parameters unrelated to reward per se might artificially bias the CPP response: (i) the initial level of place preference (a high PPi may interfere with conditioning), (ii) the capacity of the animal tested to learn and remember which compartment was associated with the drug, and (iii) the capacity of the

animal tested to appreciate the visual cues identifying the drug-paired compartment. To rule out an involvement of these factors on the lowered CPP response of *ache*^{sb55}/+ heterozygotes, we assessed their basal level of place preference, memory and visual performance.

We used the PP test to measure the PPi of *ache*^{sb55}/+ heterozygotes, as described above: after two days of habituation, the percentage of time spent in the preferred compartment was recorded. Although, like wild-type fish, most *ache*^{sb55}/+ heterozygotes still prefer the brown side (not shown), we found that their preference for this compartment is significantly decreased compared to that of their wild-type siblings or AB controls (Fig.3A) (n=54, p<=0.05). Thus, *ache*^{sb55}/+ fish display a relative greater initial preference for the conditioning compartment, making it unlikely that their reduced change in place preference following amphetamine administration is due to their difference in PPi compared to wild-type fish. In support of this interpretation, we further verified that, for both *ache*$^{sb55/+}$ and wild-type fish, the absolute change in place preference following amphetamine administration is unrelated to the initial PPi level (Fig.3B,C): the correlation factor between the absolute change in place preference and PPi in a linear regression analysis is below 0.2 for both genotypes. These results further support our conclusion that the lowered change in place preference of *ache*$^{sb55/+}$ fish upon amphetamine injection is not related to their basal preference levels.

We next assessed the learning capacities of *ache*^{sb55}/+ heterozygotes. We built a simple T-maze assay where the fish have to reach a deep chamber, after which performance they receive a food treat (see Materials and Methods for details). One trial was performed per fish per day. We observed that the time taken to find the chamber decreased upon trials in both *ache*^{sb55}/+ heterozygotes and wild-type siblings, showing that both populations were capable of learning (Fig.3D, and Supplemental Movie 1 on-line). We considered the learning phase to be over when the time needed to find the compartment changed less than 10% upon consecutive trials. We observed that *ache*^{sb55}/+ fish need less trials to reach this point than their wild-type siblings or AB fish (Fig.3D, arrow and arrowhead, and Fig.3E) (n=20, p<=0.005), while the time needed to reach the chamber in the initial trial and after learning are comparable in all cases (Fig.3D, see time for trial 3 in

ache^{sb55}/+, for trial 6 in wild-type, and see Supplemental Movies 2 and 3 online). The location of the chamber was memorized for over two weeks after a pause in testing in both genotypes (not shown). We conclude that, in this test, *ache*^{sb55}/+ fish learn faster than controls. Thus, their reduced CPP is unlikely to result from an inability to learn and remember.

Finally, we assessed the visual performance of *ache*^{sb55}/+ fish by electroretinography (ERG). The ERG b-wave was used to evaluate physiological function in vivo. A 2-way repeated measure ANOVA indicated that the b-wave amplitude of *ache*^{sb55}/+ heterozygotes was not significantly different from their wild-type siblings (Fig.3F,G) (2-way ANOVA, n=3 each, $F(df=2)<1$, $p<0.7$). These ERG tests together with the T-maze assay suggest that vision defects are unlikely to account for the reduced CPP in *ache*^{sb55}/+.

Discussion

The zebrafish behavioral repertoire is complex and is increasingly studied for the modeling of parameters such as anxiety, addiction and social interactions (Engeszer et al., 2004). To date, two studies, focusing respectively on ethanol and cocaine, used zebrafish adults to approach the neurogenetics of drug addiction (Gerlai et al., 2000; Darland and Dowling, 2001). Importantly, in contrast to these early works, we failed to reproduce efficient drug administration by dissolving drugs in water (Darland and Dowling, 2001): in such cases, in our hands, the amount of drug reaching the brain was undetectable (as measured by HPLC, see Materials and Methods) (not shown). Rather, we successfully used intraperitoneal injections. We also found that a habituation phase of at least two days to the test conditions was necessary to obtain reliable assessment of PP and CPP. Finally, our method eliminates scoring behaviors unrelated to the reward pathway per se but rather reflecting changes in the stress status of the tested individual, or impaired drug uptake or transport to the brain. It was crucial, for instance, to verify the amount of drug received by the brain for each subject showing atypical behavior, and to verify the normality of other parameters involved such as memory and vision. In a CPP test using the so-called “biased” place

conditioning procedure (i.e. with a preexisting bias for one area of the test arena, as we used here), anxiety might also affect place reversal. Here we rule out the influence of such a phenomenon by demonstrating that the PPi of *ache*^{sb55}/+ mutants is not greater than that of their siblings (Fig.3A), thus should permit conditioning. Finally, because *ache*$^{sb55/+}$ and wild-type fish differ in their initial place preference level (PPi), verifying that the PPi value does not influence CPP is another important control (Fig.3B,C). Together, the reliability of our set-up was instrumental in detecting psychostimulant-induced differences in the CPP paradigm between different genetic backgrounds such as *ache*^{sb55}/+ heterozygotes and wild-type. This success demonstrates that zebrafish adults can be used to screen for the effect of developmental mutations on adult reward-related behavior and therefore to identify dominant modulators of behavior related to addiction, as we here identify AChE.

Another major result of our study is the implication of the cholinergic system in the modulation of the rewarding properties of amphetamine, of place preference and of cognitive capacities in zebrafish. Because this parallels the situation in mammals, our results provide the first validation of the zebrafish model for studying the neurotransmitter and molecular pathways that underlie the process of addiction in vertebrates. This result is of high significance given the demonstrated amenability of the zebrafish system to genetic screens and the molecular mapping of mutations, at a level to date remaining far from reach in other vertebrate models. In a parallel ENU mutant screen (J.N. and L.B-C., unpublished), the procedure described in this paper allowed scoring, in less than 5 months, 1128 mutagenized zebrafish genomes and recovering 26 mutants potentially affected in their response to the rewarding effects of amphetamine. Such a forward genetic approach will provide crucial and unbiased information not only on the molecular biology of drug addiction but also on the neuronal and molecular networks underlying natural reward learning and memory in vertebrates.

A number of molecular components of the zebrafish cholinergic system have been identified (Zirger et al., 2003; Williams and Messer, 2004), but, outside choline acetyltransferase (ChAT, the ACh synthesizing enzyme) and AChE (Clemente et al., 2004; Mueller et al., 2004), their spatial distribution in the adult brain has not been established. The latter reports agree on the

presence of ChAT immunoreactive nuclei and fibers in the diencephalon and on AChE activity in most of the forebrain, while Mueller et al. (Mueller et al., 2004) describe in addition an intense cholinergic innervation and cell bodies in the subpallium (striatum). Because the *ache* mutation is likely to affect ACh amounts at all brain levels, our results do not permit to point to the specific cholinergic pathways and developmental time points involved in modulating reward, exploratory activity or learning in zebrafish. These results do not necessarily contrast with previous targeted studies performed in mammals where, although the cholinergic system was initially locally perturbed e.g. by targeted neuron ablation, a widespread adaptative regulation of cholinergic transmission was noted (Kitabatake et al., 2003). In our model however, because the genetic impairment of AChE function is operating since the earliest developmental stages, a permanent increase in cholinergic activity is operating to modulate behavior. This may suggest a role for desensitization of AChR rather than an acute inhibition of AChE. In mammals, DA terminals projecting to the NAc harbor nAChR that are highly prone to desensitization. These have been invoked in explaining the gradual decrease of DA release that follows the stabilization of high NAc ACh levels by AChE inhibitors (Zhou et al., 2001). A zebrafish functional equivalent to the NAc remains to be identified, but it is possible that a similar mechanism is at play in the zebrafish subpallium. In addition, in mammals, desensitization of the mAChR present on DA cell bodies projecting to the NAc might also limit the reinforcing effect of amphetamine triggered by ACh on these neurons (Fiorillo and Williams, 2000; Fink-Jensen et al., 2003). It will be important to determine whether DA neurons of the posterior tuberculum, the likely zebrafish equivalent of the mammalian VTA (Rink and Wullimann, 2001), receive cholinergic innervation via mAChR. The action of cholinergic input on exploratory behavior and learning processes in mammals is believed to rely on different control centers such as the dorsal hippocampus and amygdala, and the ascending basal cholinergic forebrain system, respectively (File et al., 2000; Degroot and Treit, 2002). Recent results suggest that the goldfish medial pallium might contain neurons functionally homologous to the amygdala in an avoidance learning paradigm (Portavella et al., 2004). Direct equivalents of all these centers in zebrafish remain to be identified by projection tracing followed by

experimental perturbation and behavioral tests as described in this paper. Obviously, our current knowledge of the functionality of the zebrafish adult CNS remains fragmentary, making behavioral phenotypes still more difficult to interpret than in higher vertebrates. The present paper, by providing the reliable tools to assess a behavioral function in zebrafish, precisely sets the stage to link the neuroanatomical and neurotransmitter networks with their function in this species.

Although psychostimulants and the modulating effect of the cholinergic system generally affect both reward and locomotor activity, instances of dissociations between these two effects in given paradigms have also been reported ((Tzschentke, 1998), and refs therein). Strikingly, in our conditions, amphetamine does not modify zebrafish swimming speed (not shown). It is possible that amphetamine is ineffective on locomotor activity in zebrafish, or that our experimental conditions do not permit to measure this response.

Although the central modulatory role of ACh in the CNS and in particular in the control of central DA transmission is well documented, a universal and directly accessible target of this system for drug addiction therapy has been lacking. Local microinfusions of AChE inhibitors into the hippocampus have been demonstrated to reduce anxiety and to improve memory in mammalian animal models (Degroot et al., 2001; Degroot and Parent, 2001; Degroot and Treit, 2002; Degroot and Treit, 2003), but their effect on addiction has not been tested, and their practicality in humans is questionable. We demonstrate here that lowering the central activity of AChE by 2 fold is sufficient to reduce the rewarding effect of amphetamine. Further, the group of *ache*^{sb55}/+ heterozygotes includes a proportion of fish where amphetamine-induced CPP was not only lowered but completely abolished (not shown). In line with our study, a recent report pointed to the pharmacological inhibition of AChE activity by intraperitoneal injection of donepezil in the mouse as a potential means of decreasing the addictive response elicited by cocaine and morphine (Hikida et al., 2003). It is likely that such injections also globally affect AChE levels, like in zebrafish *ache*$^{sb55/+}$ mutants, further suggesting that targeting AChE at the organismal level might be effective over a broad range of drugs. Importantly, *ache*^{sb55}/+ zebrafish survive the general modification of AChE and ACh levels over their entire life

span without deleterious effects in our housing conditions. In particular, in mixed families of *ache*^{sb55}/+ and +/+ siblings raised together from the first days onwards, the ratio of *ache*^{sb55}/+ adults, as well as their size and reproduction rate, was never biased (not shown). Together, our findings suggests that a treatment moderately lowering AChE activity could be envisaged in a systemic manner over an extended period of the individual's life with a significant improvement of his resistance to addiction. The zebrafish model itself might be used to select anti-AChE compounds that exhibit minimal side effects (Behra et al., 2004).

Conclusion

Our results show that the rewarding potential of amphetamine has been conserved through vertebrate evolution. They also demonstrate that higher central cholinergic activity in zebrafish is associated with decreased sensitivity towards the addictive properties of amphetamine, increased exploratory activity and faster learning, demonstrating that the importance of the cholinergic system in modulating these behaviors has also been evolutionarily conserved. Importantly, our results also provide the first genetic arguments supporting manipulations of AChE activity as a promising avenue towards limiting addiction behavior to psychostimulants. Together, and given the ease to produce mutants in zebrafish, our findings set the stage to make the zebrafish a highly attractive model to study these behavioral processes at the neuroanatomical and molecular levels, and in particular to give insight into the molecular neurobiology of drug-induced reward in vertebrates.

References

Alcantara A, Chen V, Herring B, Mendenhall J, Berlanga M. 2003. LOcalization of dopamine D2 receptors on cholinergic interneurons of the dorsal striatum and nucleus accumbens of the rat. Brain Res. 986:22-29.

Amara S, Sonders M. 1998. Neurotransmitter transporters as molecular targets for addictive drugs. Drug and Alcohol Dependence 51:87-96.

Auclair A, Drouin C, Cotecchia S, Glowinski J, Tassin J-P. 2004. 5-HT2A and alpha1b-adrenergic receptors entirely mediate dopamine release, locomotor response and behavioral sensitization to opiates and psychostimulants. Eur. J. Neurosc. 20:3073-3084.

Behra M, Cousin X, Bertrand C, Vonesch JL, Biellmann D, Chatonnet A, Strahle U. 2002. Acetylcholinesterase is required for neuronal and muscular development in the zebrafish embryo. Nat Neurosci 5:111-118.

Behra M, Etard C, Cousin X, Straehle U. 2004. The use of zebrafish mutants to identify secondary target effects of acetycholinesterase inhibitors. Toxicol. Sci. 77:325-333.

Clemente D, Porteros A, Weruaga E, Alonso J, Arenzana F, Aijon J, Arevalo R. 2004. Cholinergic elements in the zebrafish central nervous system: histochemical and immunohistochemical analysis. J. Comp. Neurol. 474:75-107.

Darland T, Dowling JE. 2001. Behavioral screening for cocaine sensitivity in mutagenized zebrafish. Proc Natl Acad Sci U S A 98:11691-11696.

Degroot A, Kashluba S, Treit D. 2001. Septal GABAergic and hippocampal cholinergic systems modulate anxiety in the plus-maze and shock-probe tests. Pharmacol Biochem Behav 69:391-399.

Degroot A, Parent MB. 2001. Infusions of physostigmine into the hippocampus or the entorhinal cortex attenuate avoidance retention deficits produced by intra-septal infusions of the GABA agonist muscimol. Brain Res 920:10-18.

Degroot A, Treit D. 2002. Dorsal and ventral hippocampal cholinergic systems modulate anxiety in the plus-maze and shock-probe tests. Brain Res 949:60-70.

Degroot A, Treit D. 2002. Dorsal and ventral hippocampal cholinergic systems modulate anxiety in the plus-maze and shock-probe tests. Brain Res. 949:60-70.

Degroot A, Treit D. 2003. Septal GABAergic and hippocampal cholinergic systems interact in the modulation of anxiety. Neuroscience 117:493-501.

Dowling J. 1987. The retina: an approachable part of the brain.

Ellman C, Courtney D, Andres V, Featherstone R. 1961. A new and rapid colorimetric determination of acetylcholinesterase activity-. Biochem. Pharmacol. 7:8895.

Engeszer RE, Ryan MJ, Parichy DM. 2004. Learned social preference in zebrafish. Curr Biol 14:881-884.

Everitt B, Wolf M. 2002. Psychomotor stimulant addiction: a neural systems perspective. J. neurosc. 22:3312-3320.

File SE, Kenny PJ, Cheeta S. 2000. The role of the dorsal hippocampal serotonergic and cholinergic systems in the modulation of anxiety. Pharmacol Biochem Behav 66:65-72.

Fink-Jensen A, Fedorova I, Wortwein G, Woldbye D, Rasmussen T, Thomsen M, Bolwig T, Knitowski K, McKinzie D, Yamada M, Wess J, Basile A. 2003. Role for M5 muscarinic acetylcholine receptors in cocaine addiction. J. Neurosc. Res. 74:91-96.

Fiorillo CD, Williams JT. 2000. Cholinergic inhibition of ventral midbrain dopamine neurons. J Neurosci 20:7855-7860.

Gainetdinov R, Sotnikova T, Caron M. 2002. Monoamine transporter pharmacology and mutant mice. Trends Pharma. Sci. 23:367-373.

Gaspar P, Cases O, Maroteaux L. 2003. The developmental role of serotonin: news from mouse molecular genetics. Nat Rev Neurosci 4:1002-1012.

Gerber D, Sotnikova T, Gainetdinov R, Huang S, Caron M, Tonegawa S. 2001. Hyperactivity, elevated dopaminergic transmission, and response to

amphetamine in M1 muscarinic acetylcholine receptor-deficient mice. Proc. Natl. Acad. Sci. USA 98:14312-15317.
Gerlai R, Lahav M, Guo S, Rosenthal A. 2000. Drinks like a fish: zebra fish (Danio rerio) as a behavior genetic model to study alcohol effects. Pharmacol Biochem Behav 67:773-782.
Guo S. 2004. Linking genes to brain, behavior and neurological diseases: what can we learn from zebrafish? Genes, Brain and Behavior 3:63-74.
Hikida T, Kaneko S, Isobe T, Kitabatake Y, Watanabe D, Pastan I, Nakanishi S. 2001. Increased sensitivity to cocaine by cholinergic cell ablation in the nucleus accumbens. Proc. Natl. Acad. Sci. USA 23:13351-13354.
Hikida T, Kitabatake Y, Pastan I, Nakanishi S. 2003. Acetylcholine enhancement in the nucleus accumbens prevents addictive behaviors of cocaine and morphine. Proc. Natl. Acad. Sci. USA 100:6169-6173.
Hogg R. 1995. Introduction to mathematical statistics. Prentice Hall, Englewood Cliffs, N.J. 5th edition, Robert V. Hogg and Allen T. Craig Eds.
Ichikawa J, Chung Y, Li Z, Dai J, Meltzer H. 2002. Cholinergic modulation of basal and amphetamine-induced dopamine release in rat medial prefrontal cortex and nucleus accumbens. Brain Res. 958:176-184.
Jones S, Gainetdinov R, Wightman R, Caron M. 1998. Mechanisms of amphetamine action revealed in mice lacking the dopamine transporter. J. Neurosc. 18:1979-1986.
Kelley A. 2004. Memory and addiction: shared neural circuitry and molecular mechanisms. Neuron 44:161-179.
Kitabatake Y, Hikida T, Watanabe D, Pastan I, Nakanishi S. 2003. Impairment of reward-related learning by cholinergic cell ablation in the striatum. Proc Natl Acad Sci U S A 100:7965-7970.
Laakso A, Mohn A, Gainetdinov R, Caron M. 2002. Experimental genetic approaches to addiction. Neuron 36:213-228.
Lett BT, Grant VL. 1989. The hedonic effects of amphetamine and pentobarbital in goldfish. Pharm. Biochem. Behavior 32:355-356.
Lockwood B, Bjerke S, Kobayashi K, Guo S. 2004. Acute effects of alcohol on larval zebrafish: a genetic system for large-scale screening. Pharma. Biochem. Behav. 77:647-654.
Makhankov YV, Rinner O, Neuhauss SC. 2004. An inexpensive device for non-invasive electroretinography in small aquatic vertebrates. J Neurosci Methods 135:205-210.
Mueller T, Vernier P, Wullimann M. 2004. The adult central nervous cholinergic system of a neurogenetic model animal, the zebrafish Danio rerio. Brain Res. 1011:156-169.
Portavella M, Torres B, Salas C, Papini M. 2004. Lesios of the medial pallium, but not the lateral pallium, disrupt spaced-trial avoidance learning in goldfish (Carassius auratus). Neurosci Lett 362:75-78.
Rink E, Wullimann MF. 2001. The teleostean (zebrafish) dopaminergic system ascending to the subpallium (striatum) is located in the basal diencephalon (posterior tuberculum). Brain Res 889:316-330.
Saal D, Dong Y, Bonci A, Malenka R. 2003. Drugs of abuse and stress trigger a common synaptic adaptation in dopamine neurons. Neuron 37:577-582.
Serra E, Medalha C, Mattioli R. 1999. Natural preference of zebrafish (Danio rerio) for a dark environment. Braz. J. Med. Biol. Res. 32:1551-1553.
Tzschentke T. 1998. Measuring reward with the conditioned place preference paradigm: a comprehensive review of drug effects, recent progress and new issues. Prog. Neurobiol. 56:613-672.
White F. 2002. A behavioral/systems approach to the neuroscience of drug addiction. J. Neurosc. 22:3303-3305.

Williams F, Messer WJ. 2004. Muscarinic acetylcholine receptors in the brain of the zebrafish (Danio rerio) measured by radioligand binding techniques. Comp. Biochem. Psysiol. 137:349-353.

Wise R. 2002. Brain reward circuitry: insights from unsented incentives. Neuron 36:229-240.

Zhou F-M, Liang Y, Dani J. 2001. Endogenous nicotinic cholinergic activity regulates dopamine release in the striatum. Nat. Neurosc. 4:1224-1229.

Zirger J, Beattie C, McKay D, Thomas Boyd R. 2003. Cloning and expression of zebrafish neuronal nicotinic acetylcholine receptors. Gene Expr. Patterns 3:747-754.

Legends to Figures

Figure 1. Establishment of reliable test conditions to measure D-amphetamine-induced reward in zebrafish adults. A: Place Preference measurement set-up (left panel, viewed from top) and representative video-recorded route followed by a wild-type fish in this set-up at day 3 (right panel, example with 58% of the time spent in the brown compartment). **B**: Habituation curve. Percentage of time spent in the brown versus the white compartment (see A) in 15-minute measurements over 5 consecutive days (one trial per day). Each bar represents the average of 5 fish, with standard errors indicated. The variations in the preference of fish for the brown side between consecutive days were compared using independent samples Student t-test. Note that the time spent in the preferred compartment significantly decreases until day 3, after which time it remains stable at a value of 55-70% (until at least day 10, not shown). This initial decrease might reflect increased exploratory activity of the fish as it gets used to the test tank. The percentage of time spent in the preferred compartment at day 3 (PP after habituation, later referred to as PPi) is taken as a basis in all subsequent measurements. **C**: Change in place preference induced by the intra-peritoneal administration of 40 μg/g of D-amphetamine (left) paired with the non-preferred compartment, compared to the administration of saline (right) in identical conditions. The “change in place preference” (Y axis) is measured as the relative difference in time spent in the preferred (non-amphetamine-paired) compartment before (PPi) and after (PPf) drug exposure (in percentage of PPi). This change was compared between N amphetamine-treated and control fish using independent samples Student t-test followed by arcsine transformation (see Materials and Methods), standard errors are indicated (see Supplemental Figure 1A, middle and bottom panels, for a survey of the response of individual fish). Note that amphetamine-injected fish significantly revert their place preference to choose the amphetamine-paired compartment after drug exposure, while fish injected with saline do not revert their preference. Identical conclusions are reached when scoring the absolute difference between PPi and PPf (see Supplemental Figure 1B). **D**: Change in

place preference (Y axis, left, red curve) and mortality (percentage of fish dying during the procedure, Y axis, right, dotted black curve) as a function of the dose of amphetamine injected (X axis, saline injections indicated as the zero dose). Each point is based on the test of at least 15 fish, with standard errors indicated; statistical significance between the responses at different doses was calculated using independent samples Student t-test (see values on the graph and table below). Our experimental conditions produce a dose/change response curve following a Gaussian distribution similar to that observed in mammals (Tzschentke, 1998), where doses above a certain threshold (here 50 μg/g) induce a toxic response. **E**: Change in place preference (Y axis, left, red curve, same as in D) and brain amphetamine levels (Y axis, right, dotted black curve) as a function of the dose of amphetamine injected (X axis). Each measurement of brain amphetamine levels is averaged from 3 fish, with standard errors indicated; statistical significance between the levels of amphetamine in the brain at consecutives doses injected was calculated using independent samples Student t-test (see values in black on the graph). Note that the level of amphetamine received in the brain is a linear function of the dose injected within the range of values used in our experiments. Note also that it keeps increasing linearly above the threshold dose inducing maximum CPP, confirming that the decreased CPP above this dose is due to a toxic effect of amphetamine rather than its elimination from the zebrafish organism.

Figure 2. Lowered amphetamine-induced CPP in *ache*^{sb55}/+ heterozygotes. In all cases, fish with different genotypes were compared using independent samples Student t-test, and standard errors are indicated. **A**,**B**: Altered brain levels of AChE activity (A) and ACh (B) in *ache*^{sb55}/+ heterozygotes (left) compared to their wild-type siblings (+/+, middle) or AB controls (right). Each value is an average of N fish. Brain levels of AChE are reduced by nearly 50% (A) and brain levels of ACh are increased by 40% (B) in *ache*^{sb55}/+ heterozygotes compared to their wild-type siblings, which do not differ from AB controls. **C**: Change in place preference induced by 40μg/g amphetamine in *ache*^{sb55}/+ heterozygotes (red, left), their wild-type siblings

(+/+, red, middle) and AB controls (red, right), also compared to the effect of saline injections in *ache*$^{sb55/+}$ (black, right) and AB (black, left). The change in place preference (Y axis) is measured and statistically evaluated as in Fig.1C, and each value is an average of N fish. Amphetamine-induced change in place preference is significantly decreased (1.6 times) in *ache*^{sb55}/+ heterozygotes compared to their wild-type siblings, which do not differ from AB controls, and saline injections have no effect. Identical conclusions are reached when scoring the change in place preference in absolute values (Supplemental Figure 2). **D**: Compared dose-response curve in *ache*^{sb55}/+ heterozygotes (dotted line) and AB controls (red line). The percentage of change in PP (Y axis) is represented as a function of the dose of amphetamine injected (X axis). Each point is the average of at least 15 fish, statistical significance between the responses of the two genotypes at a given dose was calculated using independent samples Student t-test (standard errors indicated, see significance values on the table below the graph). *ache*^{sb55}/+ heterozygotes respond to amphetamine following a Gaussian curve of similar amplitude than that of wild-type fish but shifted towards lower Y values (centre position for wild-type fish: 65.3; for *ache*^{sb55}/+ fish: 62.3). Thus, the dose of 40 μg/g amphetamine selected as optimal for wild-type fish is also optimal in *ache*^{sb55}/+ heterozygotes, which respond with lower CPP than wild-type to the complete range of amphetamine doses tested.

Figure 3. Lower PPi, increased learning potential and unaltered vision in *ache*^{sb55}/+ adults. In all cases, fish with different genotypes were compared using independent samples Student t-test, and standard errors are indicated. **A**: Preference of *ache*^{sb55}/+ heterozygotes (left) for one compartment of the test tank, compared to that of their wild-type siblings (middle) or AB controls. The percentage of time spent in the preferred versus non-preferred compartment of the tank after two days of habituation is measured (PPi). Bars represent an average result for N fish. Note that PPi is significantly smaller ($p<=0.05$) in *ache*^{sb55}/+ fish. **B,C:** Correlation between the percentage of time spent in the initially preferred compartment before conditioning (PPi, X axis) and the absolute change in place preference after conditioning (PPf minus

PPi, Y axis) in wild-type (B) and *ache*^{sb55}/+ (C) fish. Each dot represents an individual fish. A linear regression analysis shows that the correlation factor between the absolute change in PP and PPi is below 0.2 for both genotypes (r=0.17, N=31, p<=0.3 for AB and r=0.19, N=33, p<=0.3 for *ache*^{sb55}/+), indicating that these values are not linked. **D,E**: Learning capacity of *ache*^{sb55}/+ heterozygotes compared to their wild-type siblings (+/+) and AB controls (AB). D: Time needed to reach a deep chamber target (Y axis) as a function of the trial number (one trial per fish per day). Each point is the average of at least 30 fish, with standard error indicated. Both *ache*^{sb55}/+ and +/+ fish decrease their time upon trial, thus progressively learn to find the target (see supplementary movies online). Note also that they start from comparably high values (> 100 s) and reach a plateau at comparably low values (20 s) after enough trials. Thus our results are not biased by a differential speed of swimming. However, *ache*^{sb55}/+ heterozygotes reach this plateau after trial 3 (arrow) while +/+ siblings need 6 trials (arrowhead). E: Compared number of trials required to learn the position of the target chamber (Y axis) in the different genotypes, each bar is the average of N fish (see bars). We considered that one fish has learned when its time to find the target varies of less than 10% upon consecutive trials; the first trial of this plateau is then considered as “learning trial”. Note that *ache*^{sb55}/+ heterozygotes (left) learn in significantly less trials than their wild-type siblings (middle) or control fish (right) (p<=0.05). **F,G**: Functionality of the retinal network of *ache*^{sb55}/+ fish compared to their wild-type siblings (+/+), measured by electroretinography. Typically, the evoked response consists of an initial negative deflection (a-wave) followed by a large, positive component (b-wave) after applying a light stimulus (Dowling, 1987). F: Amplitude of the electric response for a stimulation of 5000 cd/m^2 (top) and 0.5 cd/m^2 (bottom) in one fish of each genotype (color-coded). Note that the curves are similar in both genotypes. A range of stimulation values were tested between these extremes and showed a similar response in *ache*^{sb55}/+ and +/+ fish. G: Compared amplitude of the b-wave response in *ache*^{sb55}/+ fish compared to their wild-type siblings (+/+).

Supplemental Figure 1. Comparison of CPP scoring methods in relative (A) and absolute (B) differences between the time spent in the initially prefered compartment before and after conditioning. CPP was conditioned by the intra-peritoneal administration into wild-type adults of 0 (saline), 10 or 40 μg/g of D-amphetamine, as indicated, paired with the non-preferred compartment. In **A**, the "change in place preference" (Y axis) is measured as the difference in time spent in the initially preferred compartment before (PPi) and after (PPf) drug exposure, in percentage of PPi. Each black and white bar represents an individual fish to give an impression of the variability in the response, while red bars are an average for N fish. Statistical significance between the mean values between the different injections is calculated using independent samples Student t-test, with standard errors indicated. Note that the scales of the Y axes differ for the different doses injected. In **B**, absolute differences are scored to evaluate the change in place preference (PPi minus PPf). Each bar is an average for N fish, and the significance of the differences between these PP values are calculated using independent samples Student t-test (standard errors indicated). Note that an identical conclusion is reached with both "relative" (**A**) and "absolute" (**B**) calculation schemes: amphetamine-injected fish significantly revert their place preference to choose the amphetamine-paired compartment after drug exposure, while fish injected with saline do not revert their PP.

Supplemental Figure 2. Change in place preference in *ache*^{sb55}/+ versus wild-type fish upon administration of amphetamine (red bars) or saline (black bars), calculated in absolute values. The change in place preference is calculated as in Supplemental Figure 1B, as PPi minus PPf. Each bar is an average for N fish, the statistical significance between the mean values of saline- versus amphetamine-injected fish is calculated using independent samples Student t-test, and standard errors are indicated. Upon amphetamine administration, *ache*^{sb55}/+ fish change their place preference significantly less than wild-type fish. Like wild-type fish, their place preference remains unaffected by saline injections.

Supplemental movies online. Learning capacity of *ache*/+ versus +/+ sibling fish in the T-maze set-up. The fish are always placed at the beginning of the long arm (begin) and have to reach the deep chamber (target), where they receive a food treat. **Movie 1: Learning of +/+ fish.** The paths followed by typical +/+ experimental fish were recorded on day 1 (trial 1) (before training), day 3 (trial 3) and day 6 (trial 6). Note that, although the time needed to reach the target decreases between days 1 and 3, the fish still explore all arms of the maze on day 3. On day 6, when the learning phase is over, the fish go directly to the target. **Movie 2: Behavior of *ache*/+ versus their +/+ siblings on day 1.** Note that *ache*/+ and +/+ fish need the same time to reach the target compartment on day 1. **Movie 3: Behavior of *ache*/+ versus their +/+ siblings at the end of the learning period (day 3 for *ache*/+, day 6 for +/+).** As described on Fig. 3B,C, *ache*/+ fish learn in 3 trials, while their siblings need 6 trials. At the end of their respective learning phases, however, both fish genotypes take the same time to find the target.

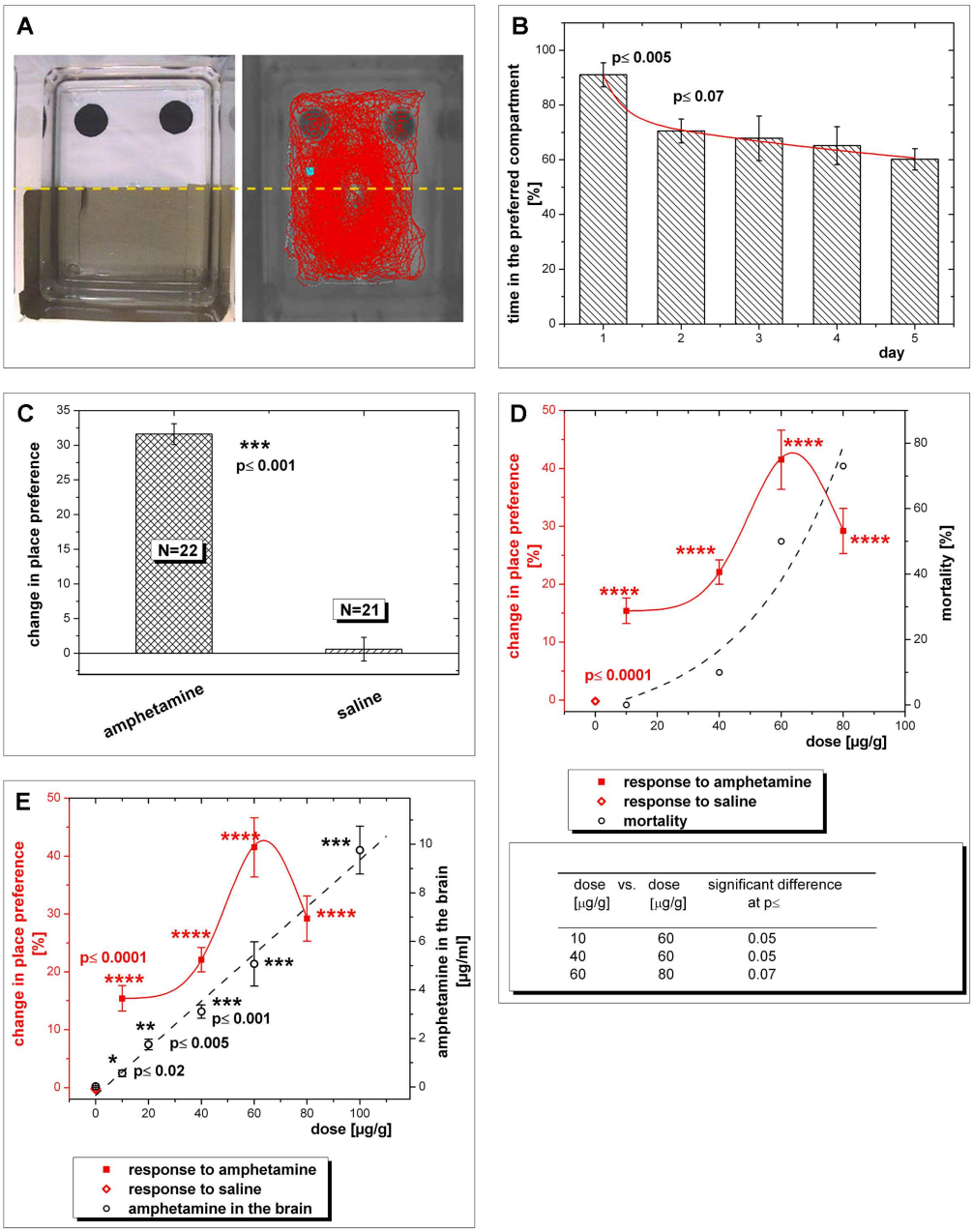

Ninkovic et al., Figure 1

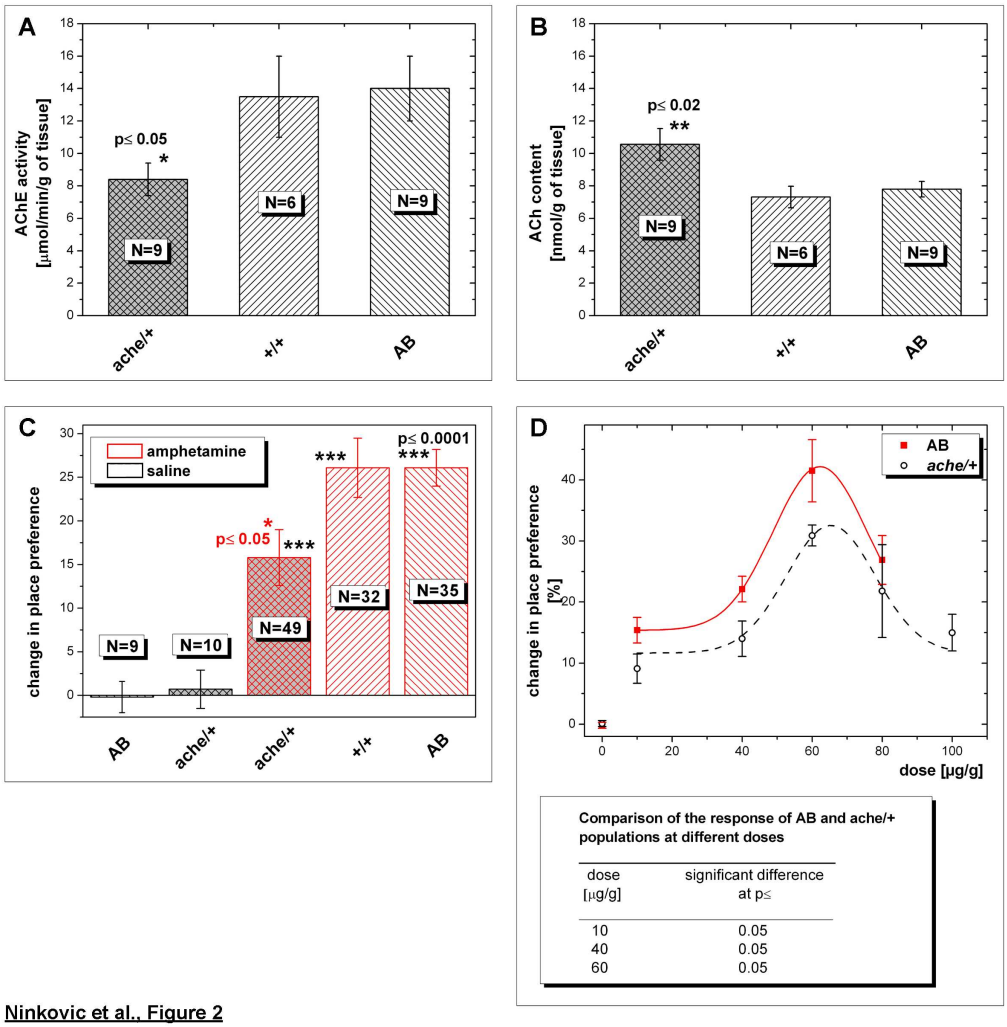

Ninkovic et al., Figure 2

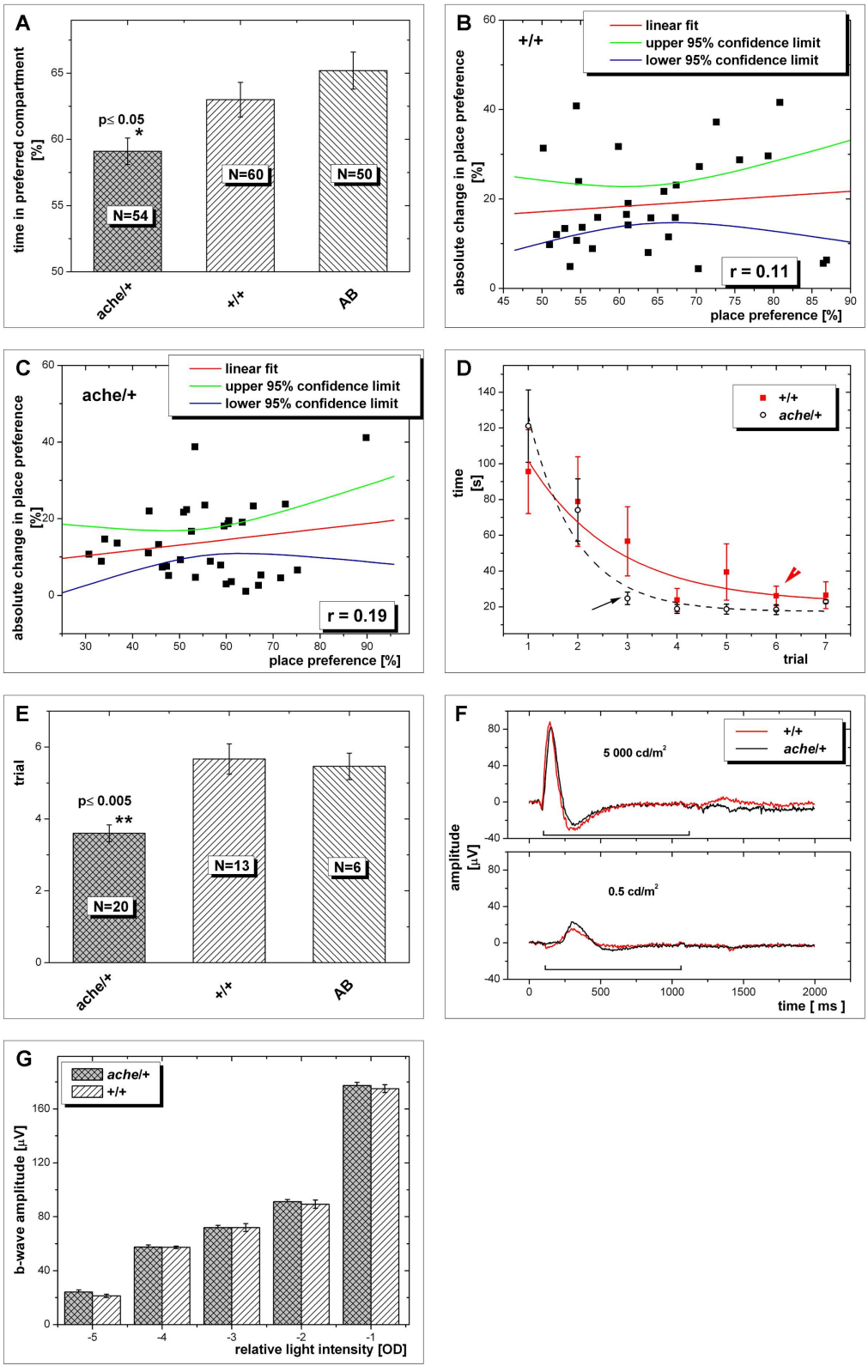

Ninkovic et al., Figure 3

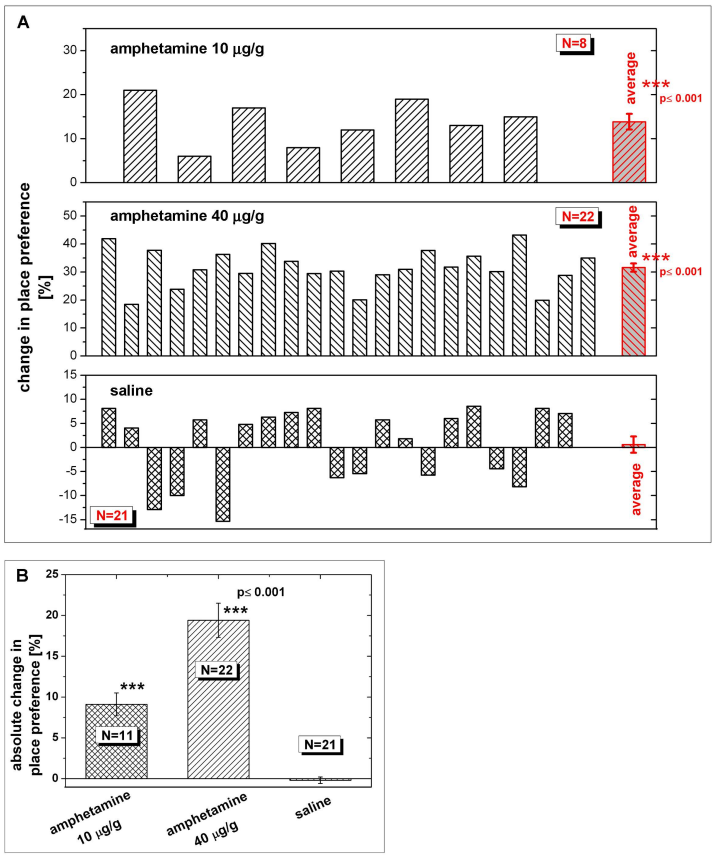

Ninkovic et al., Supplementary Figure 1.

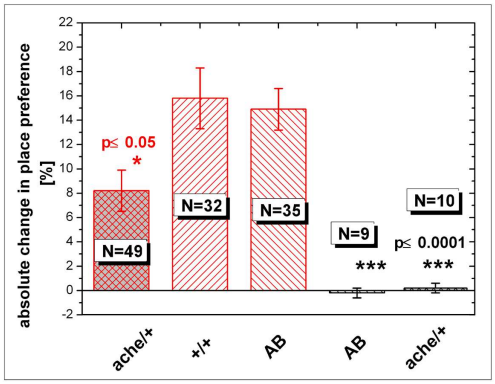

Ninkovic et al., Supplementary Figure 2.

Appendix D

The large-scale genetic screen

-experiment details-

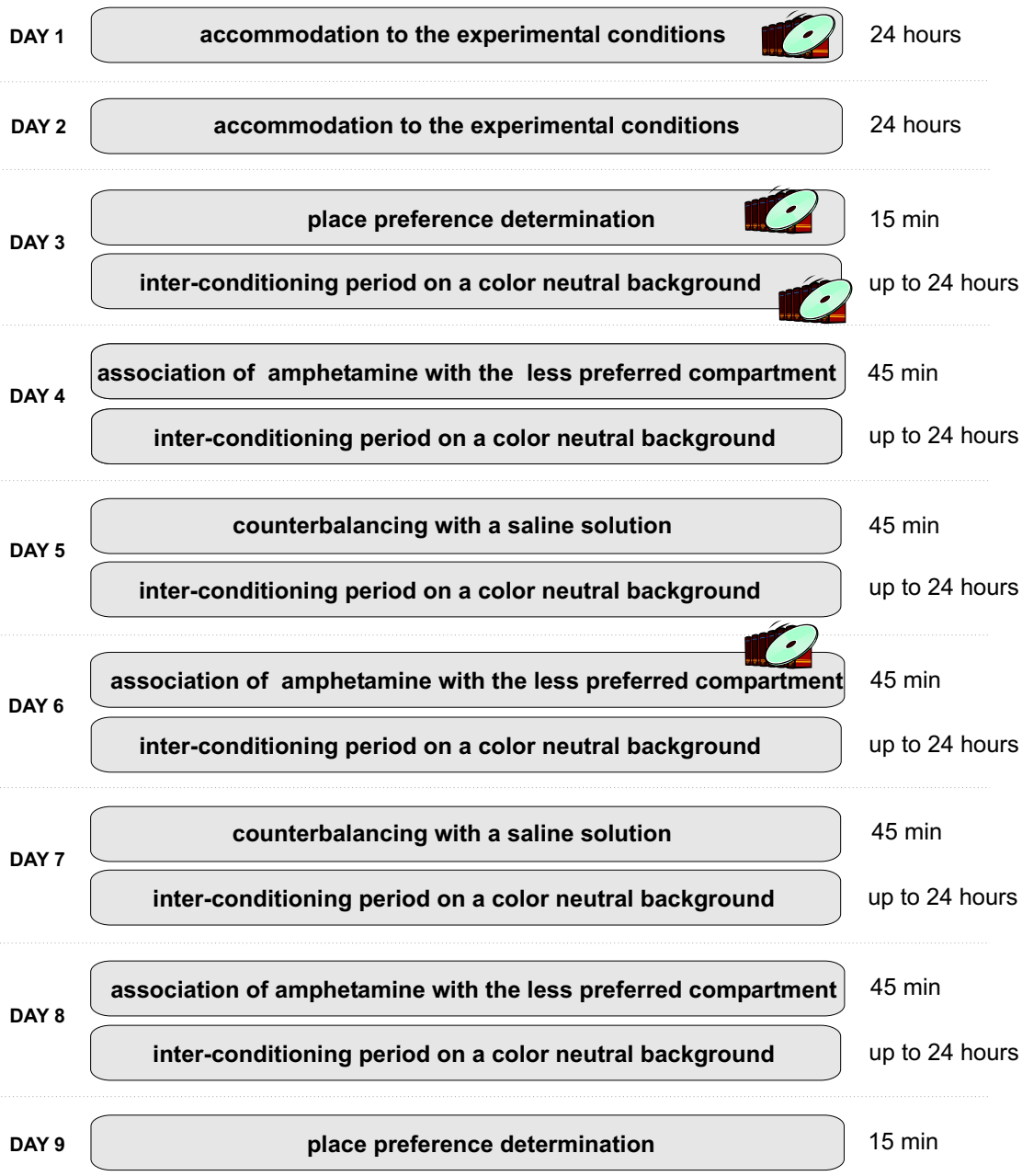

Figure D.1: **Experimental protocol used to score for addiction to D - amphetamine in mutagenized fish populations.**

Figure D.2: **Organization of two genetic screens aimed to recover dominant modifiers of addiction to D - amphetamine.** The adult male AB or Tü fish are mutagenized by incubating in water containing ENU once a week for four weeks. Mutagenized fish are kept for one month before the first cross to AB female fish to produce F_1 generation. This delay should allow the spermatogonial cells that are mutagenized at premeiotic stage to develop to mature sperm. The use of sperm that received ENU-treatment at premeiotic stages is necessary to prevent mosaicism in progeny. All fish in F_1 generation carry one mutagenized genome, but with mutations in different gene loci, because mutagenized males are crossed with non-mutagenized females to produce F_1 generation. Existence of one mutagenized genome allows screening for dominant phenotypes, as I did in ScreenI. To increase the density of mutations and the efficiency of screening, F_2 generation is produced by brother-sister crossing in F_1 generation. Therefore, each fish in F_2 generation carries two mutagenized genomes. This generation was screened in screen II, asn the families where 50 % of tested fish does not develop addiction to D - amphetamine are scored as families carrying mutation, as expected for dominant mutations.

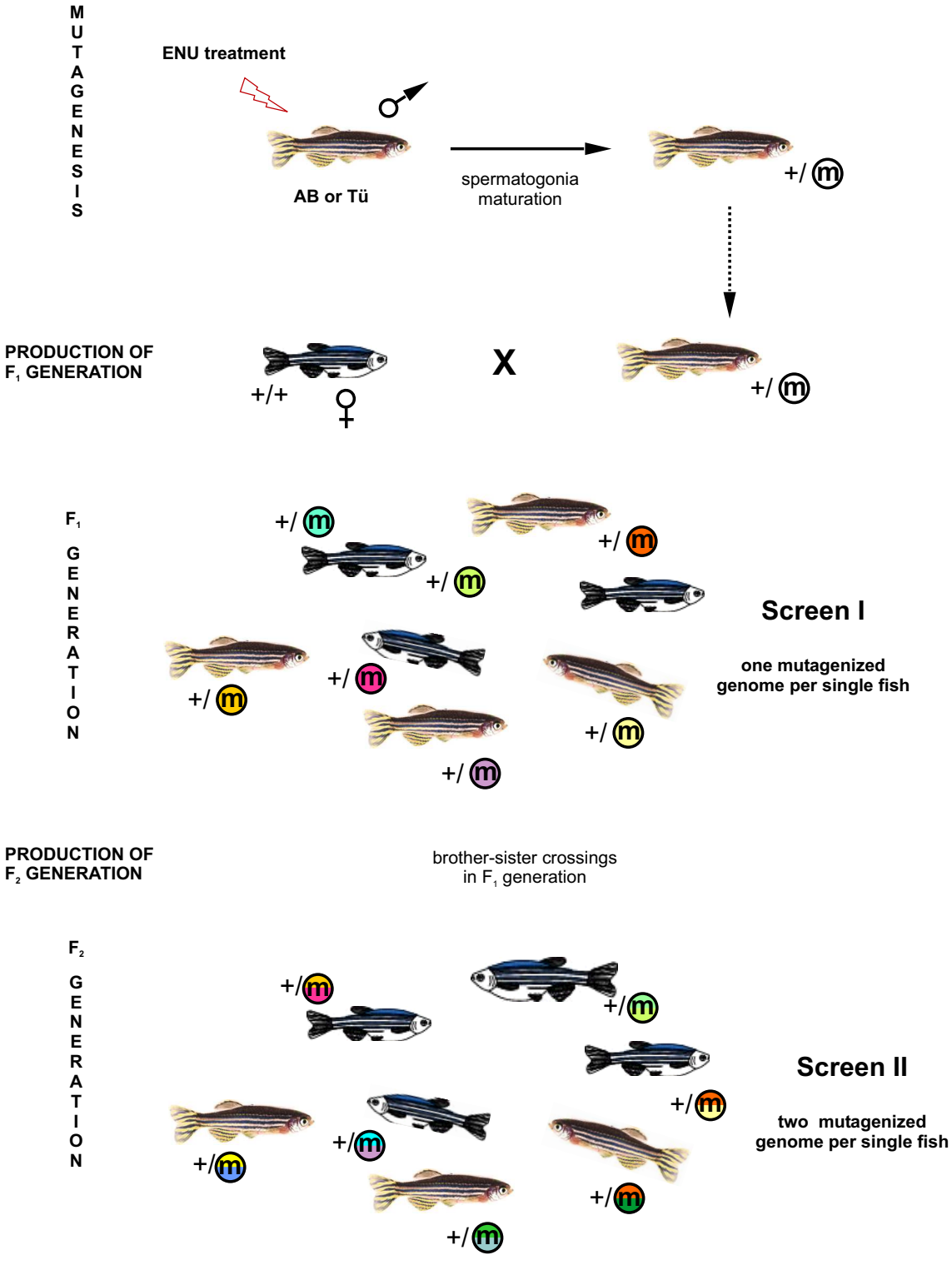
MUTAGENESIS
ENU treatment
AB or Tü
spermatogonia maturation
+/ⓜ
PRODUCTION OF F1 GENERATION
+/+
X
+/ⓜ
F1 GENERATION
Screen I
one mutagenized genome per single fish
PRODUCTION OF F2 GENERATION
brother-sister crossings in F1 generation
F2 GENERATION
Screen II
two mutagenized genome per single fish
ⓜ mutagenized genome. Each color represents a different combination of mutations with approximately 30 mutations per fish at the dose of ENU used

Acknowledgments

I feel it my profound privilege to express my sincere thanks and gratitude to my supervisor Prof. Dr. Wolfgang Wurst for giving me an opportunity to accomplish this work within Zebrafish Neurogenetics Group at Institute of Developmental Biology, GSF-Research Center in Neuherberg.

Now, as I meet the finale of my endeavour, the search for a suitable word to thank is still not over as it is beyond my expression for my esteemed supervisor, Dr. Laure Bally-Cuif. Her valuable guidance, creative suggestions, constructive criticism and constant encouragement during my PhD are not only praiseworthy but also unforgettable. Her analytical perusal of the manuscript is highly acknowledged. Laure, it was indeed a pleasure for me to work under your excellent guidance. Thanks a lot for always having time for my JUST one second, just one question...

I would also like to take this opportunity to thank to all members of the Zebrafish Neurogenetics group for lively and stimulating atmosphere. To many names for a list and too high risk of forgetting something important to say. Instead, I just put this little cartoon, hooping that everyone will find herself(him)self.

Nevertheless, I have to say thanks to Anja, Birgit and Christian for helping me to go through nightmare called Tü screen and even have some fun in Tübingen. In addition, I would like to thank Christian for finding time to read and discuss this manuscript and *ache* paper.
OK, I started...I simply like to talk. So,
Prisca and Birgit thanks for all confocal secrets,
Dendrogram, Cladogram, phenogram, eurogram, curvogram, CONFUSEgram.....thanks Christoph,
Silvia thanks for all beautiful ISH, minis, maxis, PCRs, pictures, ... You can now change the tape on the last pipetman!!!!
Birgitt and Stina I will miss you a lot for coffee breaks. I am just over the corridor. I will be back.....
Steffi thanks for talking every morning while injecting, giving me sometimes injector number 4 (although it could be more often, but that is the life), allowing me to work on your bench over the weekend... Can you imagine that I finish? Crazy, isn't it?
Steffi M. and Katharine for understanding and encouragement during my writing phase.

Finally, I am thankful to Gianfranco, Alex and Andrea for a lot of useful advises during the time when I started at the bench.

Special thanks to Dr. Kenji Imai for his input and discussions that invaluably contributed in shaping my work.

I also want to thank
Dr. Frédéric Rosa for many ideas in the behavioral field,
Dr. Reinhard Köster and his group for help with confocal microscope and useful discussions,
Dr. Chatterjee for trying to make a good PhD student of me and help in measuring brain levels of amphetamine,
Aleksandra and Sabit for support and giving me chance to speak Serbian.
A sincere thankfulness I have to express to Dr. Inge Sillaber and Dr. Sabine Hölter for invaluable help to survive in the behavioral field.

Many thanks to REBECCA, Vera, Anni, Heike and Ivone for making my fish happy and healthy.

To the end the deepest THANK YOU is reserved for my family.
Mama i tata, hvala vam za razumevanje i bezrezervnu podrsku tokom svih ovih godina. Kazu da je svako dete dragulj ogromne vrednosti. Samo ga treba znati izbrusiti i pažljivo čuvati. Vi ste taj posao odradili na najbolji moguci način. Neizmerno sam vam na tome zahvalan. Toplina koju sam poneo iz naše kuće mi je pomogla i još uvek mi pomaže da nadjem svoj put i u životu vidim sve ono što je lepo i sve što treba čuvati. Ne želim da vam kažm još jednom hvala, jer ono sta ja osećam prema vama se ne može iskazati ni da mi dozvole da proširim doktorat na još dvesta strana.....
Za tebe imam samo jednu rečenicu. Hvala ti što si uvek bio MOJ BRAT. Kažu da bracu i rodjake nemožemo birati. Ja sam izgleda imao sreće. A tebe sam ja izabrao. Hvala za sve ove godine, hvala za sve rezumevanje naročito za vreme mučnog perioda pisanja. Opet bi mi trebalo jedno stotinjak stranica da izrazim svu svoju zahvalnost. Umesto toga ja jednostavno kazem JVVVJŽŽŽSCCC.

Curriculum Vitae

Name: Jovica Ninkovic

Born: 10th November 1976 Glamoc, Bosnia and Herzegovina Sex: Male Institution where working with status and address: PhD student, Zebrafish Neurogenetics Junior Research Group of the TUM GSF-Research Center for Environment and Health Institute of Developmental Genetics Ingolsteadter Landstrasse 1 D.85764 Neuherberg Germany Phone: +49.89.3187.2944 Fax: +49.89.3187.3099 E-mail: ninkovic@gsf.de